ECAP法で作製した超微細粒合金の組織安定性とホール・ペッチの関係

（研究課題番号：０９６５０７６４）

平成９年度～平成10年度科学研究費補助金［基盤研究(C)(2)］
研究成果報告書

平成11年３月

研究代表者　古　川　　稔
（福岡教育大学教育学部助教授）

はしがき

金属材料の結晶粒を微細化すれば、変形に際して比較的低温でかつ高ひずみ速度で大きな伸びを得ることができ、また使用に当たってはホール・ペッチの関係により高強度が期待される。しかし、従来の微細粒材料はメカニカルアロイング法、イナートガス凝集凝着法、すべり摩耗法などにより作製されていたため、多孔性およびバルク状試料が得にくいなどの欠点が存在した。しかし、1986年に強ひずみを課して金属材料を大変形させる方法が考案され、1991年にサブミクロン結晶粒をもち空隙のないバルク状試料を作製することに応用され始めた。その作製法は、材料を入口と出口の径が同じで途中に角度のついたパイプの中を繰り返し高圧で通す(Equal-Channel Angular Pressing: ECAP)方法である。著者らは、ECAP法によるサブミクロン結晶粒Al-3%Mg固溶体合金の焼鈍による組織変化についてはすでに報告している。また、その装置の開発と改良を行っているところである。この方法により作製したサブミクロン結晶粒径組織の高温での安定性とそれに伴う強度の関係を解明することは、これらの材料を実際に加工し実用材料として用いる際に大きな役割を果たすことになる。

本研究では、ECAP法により作製したサブミクロン結晶粒径の純Al、Al-Mg、Al-Zr、Al-Sc、Al-Mg-Sc、Al-Mg-Li-Zr合金について、熱処理により組織を段階的に粗大化させ、その組織安定性を電子顕微鏡により調べた。また、サブミクロン粒径範囲までホール・ペッチの関係が成り立つかを、硬度試験および圧縮試験により調べることを目的とした。さらに、高温において引張試験を行い超塑性特性を調べた。

得られた結果の概要は以下のようである。

1．ECAP後の粒径と加熱後の組織安定性

ECAPした微細結晶粒径をもつ合金を用いて、熱処理後に組織(とくに結晶粒径)がいかに変化するかを、室温から773Kの範囲の各温度で1時間等温焼鈍を行い、電子顕微鏡により観察した。

(1) 純Alを室温で4パスECAPすることにより1.2μmの微細粒が得られ、微細粒は473Kまで安定しており、それ以上573Kまでは微細粒と粗大粒の混在組織、623K以上では粗大粒のみであった。

(2) Al-3%Mg合金を室温で6パスECAPすることにより0.3μmの微細粒が得られ、微細粒の熱的安定性は純Alと同様に473Kまで保たれ、それ以上573Kまでは微細粒と粗大粒の混在組織、623K以上では粗大粒のみであった。

(3) Al-0.2%Zr合金を室温で8パスECAPすることにより0.7μmの微細粒が得られ、微細粒の熱的安定性は573Kまで保たれた。Zrを含む合金が純AlやAl-Mg合金より高温まで微細粒の熱的安定性を保つ原因は微細な$L1_2$規則粒子Al_3Zrの存在によるものである。

(4) Al-0.2%Sc合金を室温で8パスECAPすることにより0.7μmの微細粒が得られ、微細粒の熱的安定性はAl-0.2%Zr合金よりも高い673Kまで保たれた。この原

因は微細な規則粒子Al_3Scの存在によるものであり、Al_3ScはAl_3Zrよりもより高温までAl合金に対する再結晶抑制効果が顕著であることを示している。

(5) Al-3%Mg-0.2%Sc合金を室温で8パスECAPすることにより0.2μmの微細粒が得られ、微細粒は673Kまでほぼ安定に保たれた。723Kでも1～2μm程度の微細粒であった。

(6) Al-5.5%Mg-2.2%Li-0.12%Zr合金を673Kで8パスECAPした後さらに473Kで4パスECAPすることにより1.2μmの微細粒が得られ、微細粒は673Kまで安定に保たれた。

2．ホール・ペッチの関係

室温から723Kの各温度で1時間等温焼鈍を行い、結晶粒径を段階的に変化させ、硬度測定および圧縮試験による降伏応力の測定により、サブミクロン粒径の範囲までホール・ペッチの関係が成り立つかを調べた。

(1) Al-3%Mg合金では、結晶粒径0.2～100μmの範囲で$Hv=46+35d^{-1/2}$（ここでHvはビッカース硬度、dは結晶粒径）のホール・ペッチの関係が成り立った。

(2) Al-5.5%Mg-2.2%Li-0.12%Zr合金では、結晶粒径2～60μmの範囲で$Hv=75+27d^{-1/2}$のホール・ペッチの関係が成り立った。

3．超塑性特性

室温から723Kまでの範囲の各温度で引張試験を行い、強度の評価を行うとともに、変形後の組織を電子顕微鏡により観察した。

(1) ECAPしたAl-3%Mg-0.2%Sc合金では、673K, $3.3\times10^{-2}s^{-1}$の条件で1030%の超塑性伸びを示した。

(2) ECAPしたAl-5.5%Mg-2.2%Li-0.12%Zr合金では、623K, $10^{-2}s^{-1}$の条件で1200%以上の超塑性伸びを示した。

(3) 破断部の結晶粒はつかみ部に比べて大きくなっており、高温での引張試験中に応力誘起により粒成長が起こっていることがわかった。

(4) $10^{-2}s^{-1}$の変形速度は大量生産が可能な変形速度であり、実際の加工にきわめて有望であることがわかった。

研究組織

研究代表者：古　川　　稔（福岡教育大学・教育学部・助教授）

研究経費

平成９年度	３，５００千円
平成10年度	５００千円
計	４，０００千円

研究発表

(1)学会誌等

1. M.Furukawa, Z.Horita, M.Nemoto, R.Z.Valiev and T.G.Langdon
Microstructural Characteriatics of an Ultrafine Grain Metal Processed with Equal-Channel Angular Pressing.
Materials Characterization, Elsevier Science Inc., Vol.37 (1996), pp.277-283, 1997年5月.

2. Z.Horita, D.J.Smith, M.Furukawa, M.Nemoto, R.Z.Valiev and T.G.Langdon
Evolution of Grain Boundary Structure in Submicrometer-Grained Al-Mg Alloy.
Materials Characterization, Elsevier Science Inc., Vol.37 (1996), pp.285-294, 1997年5月.

3. M.Furukawa, Z.Horita, M.Nemoto, R.Z.Valiev and T.G.Langdon
Recrystallization in Ultrafine-Grained Materials with Non-Equilibrium Grain Boundaries.
Proceedings of ReX'96, The Third International Conference on Recrystallization and Related Phenomena, ReX'96 International Advisory Board and Organizing Committee, (1997), pp.149-160, 1997年9月.

4. M.Furukawa, Y.Iwahashi, Z.Horita, M.Nemoto, N.K.Tsenev, R.Z.Valiev and T.G.Langdon
Structural Evolution and the Hall-Petch Relationship in an Al-Mg-Li-Zr Alloy with Ultra-Fine Grain Size.
Acta Metallurgica et Materialia, Elsevier Science Ltd, Vol.45, No.11, pp.4751-4757, 1997 年11月.

5. M.Furukawa, Y.Ma, Z.Horita, M.Nemoto, R.Z.Valiev and T.G.Langdon
Microstructural Characteristics and Superplastic Ductility in a Zn-22% Al Alloy with Submicrometer Grain Size.
Materials Science and Engineering A, Elsevier Science, Vol.A241(1998), No.1-2, pp.122-128, 1998年1月.

6. M.Furukawa, P.B.Berbon, Z.Horita, M.Nemoto, N.K.Tsenev, R.Z.Valiev and T.G.Langdon
Age Hardening and the Potential for Superplasticity in a Fine-Grained Al-Mg-Li-Zr Alloy.
Metallurgical and Materials Transactions A, The Minerals, Metals and Materials Society, and ASM International, Vol.29A, January 1998, pp.169-177, 1998年1月.

7. M.Furukawa, Y.Ma, Z.Horita, M.Nemoto, R.Z.Valiev and T.G.Langdon
Fabrication and Properties of a Submicrometer-Grained Zn-22% Al Alloy.
Proceedings of International Conference on Thermomechanical Processing of Steels and Other Materials, Thermec'97, pp.1875-1881, 1998年2月.

8. Z.Horita, D.J.Smith, M.Furukawa, M.Nemoto, R.Z.Valiev and T.G.Langdon

Characterization of Ultra-Fine Grained Materials Produced by Tosion Straining. Proceedings of International Conference on Thermomechanical Processing of Steels and Other Materials, Thermec'97, pp.1937-1943, 1998年2月.

9. P.B.Berbon, N.K.Tsenev, R.Z.Valiev, M.Furukawa, Z.Horita, M.Nemoto and T.G.Langdon
Superplasticity in Alloys Processed by Equal-Channel Angular Pressing.
Superplasticity and Superplastic Forming 1998, The Minerals, Metals and Materials Society, 1998, pp.127-134, 1998年2月.

10. M.Furukawa, Z.Horita, M.Nemoto and T.G.Langdon
Microstructural Evolution in Pure Aluminum During Equal-Channel Angular Pressing.
Modeling the Mechanical Response of Structural Materials, The Minerals, Metals and Materials Society, 1997, pp.165-172, 1998年2月.

11. P.B.Berbon, M.Furukawa, Z.Horita, M.Nemoto, N.K.Tsenev, R.Z.Valiev and T.G.Langdon
Application of Equal-Channel Angular Pressing for Producing Superplastic Aluminum Alloys.
Modeling the Mechanical Response of Structural Materials, The Minerals, Metals and Materials Society, 1997, pp.173-180, 1998年2月.

12. 小村章吾、宇都宮淳、堀田善治、根本實、古川稔、P.B.Berbon、T.G.Langdon
拘束強ひずみ加工で作製した超微細粒組織
日本金属学会会報(まてりあ)、日本金属学会、第37巻、第5号、376ページ、1998年5月.

13. T.G.Langdon, M.Furukawa, Z.Horita and M.Nemoto
Using Intense Plastic Strainng for High-Strain-Rate Superplasticity.
Journal of Materials (JOM), The Minerals, Metals and Materials Society, Vol.50, No.6, June 1998, pp.41-45, 1998年6月.

14. M.Furukawa, Z.Horita, M.Nemoto, R.Z.Valiev and T.G.Langdon
Factors Influencing the Flow and Hardness of Materials with Ultrafine Grain Sizes.
Philosophical Magazine A, Taylor & Francis Ltd., Vol.78, No.1, July 1998, pp.203-215, 1998年6月.

15. S.Komura, P.B.Berbon, M.Furukawa, Z.Horita, M.Nemoto and T.G.Langdon
High Strain Rate Superplastisity in an Al-Mg Alloy Containing Scandium.
Scripta Metallurgica et Materialia, Vol.38, No.12,1998, pp.1851-1856, 1998年6月.

16. H.Hasegawa, S.Komura, Z.Horita, M.Furukawa M.Nemoto and T.G.Langdon
Grain Refinement and Potential for Superplasticity in Al Alloys Containing Small Particles.
Proceedings of the Third Pacific Rim International Conference on Advanced Materials and Processing (PRICM-3), The Minerals, Metals and Materials Society,

1998, pp.1873-1878, 1998年7月.

17. K.Oh-ishi, Z.Horita, M.Furukawa, M.Nemoto and T.G.Langdon
Optimizing the Rotation Conditions for Grain Refinement in Equal-Channel Angular Pressing.
Metallurgical and Materials Transactions A, The Minerals, Metals and Materials Society, and ASM International, Vol.29A, July 1998, pp.2011-2013, 1998年7月.

18. P.B.Berbon, M.Furukawa, Z.Horita, M.Nemoto, N.K.Tsenev, R.Z.Valiev and T.G.Langdon
Optimizing the Processing of a Commercial Al-Based Alloy for High Strain Rate Superplasticity.
Proceedings of the Third International Symposium on Microstructures and Mechanical Properties of New Engineering Materials (IMSP'97), Mie University Press, pp.81-88, 1998年9月.

19. P.B.Berbon, N.K.Tsenev, R.Z.Valiev, M.Furukawa, Z.Horita, M.Nemoto and T.G.Langdon
Fabrication of Bulk Ultrafine-Grained Materials Through Intense Plastic Straining.
Metallurgical and Materials Transactions A, The Minerals, Metals and Materials Society, and ASM International, Vol.29A, September 1998, pp.2237-2243, 1998年9月.

20. Y.Iwahashi, M.Furukawa, Z.Horita, M.Nemoto and T.G.Langdon
Microstructural Characteristics of Ultrafine-Grained Aluminum Produced Using Equal-Channel Angular Pressing.
Metallurgical and Materials Transactions, The Minerals, Metals and Materials Society, and ASM International, Vol.29A, September 1998, pp.2245-2252, 1998年9月.

21. 堀田善治、古川稔、根本實、T.G.Langdon
新しい組織制御法としてのEqual-Channel Angular Pressing (ECAP)
日本金属学会会報（まてりあ）、日本金属学会、第37巻、第9号、767-774ページ、1998年9月.

22. P.B.Berbon, M.Furukawa, Z.Horita, M.Nemoto, N.K.Tsenev, R.Z.Valiev and T.G.Langdon
Requirements for Achieving High Strain Rate Superplasticity in Cast Aluminum Alloys.
Philosophical Magazine Letters, Taylor & Francis Ltd., Vol.78, No.4, pp.313-318, 1998年10月.

23. P.B.Berbon, M.Furukawa, Z.Horita, M.Nemoto, N.K.Tsenev, R.Z.Valiev and T.G.Langdon
Processing of Aluminum Alloys for High Strain Rate Superplasticity.
Hot Deformation of Aluminum Alloys II, The Minerals, Metals and Materials Society, 1998, pp.111-124, 1998年10月.

24. S.Komura, P.B.Berbon, A.Utsunomiya, M.Furukawa, Z.Horita, M.Nemoto and T.G.Langdon
Superplasticity in an Ultrafine-Grained Al-Mg-Sc Alloy Produced by Equal-Channel Angular Pressing.
Hot Deformation of Aluminum Alloys II, The Minerals, Metals and Materials Society, 1998, pp.125-138, 1998年10月.

(2)口頭発表

1. 岩橋芳憲、長谷川秀明、堀田善治、藤波隆善、根本實、古川稔、T.G.Langdon
拘束強ひずみ加工法による結晶粒微細化と超塑性特性
第92回軽金属学会春期大会、東北大学工学部、1997年5月18日

2. Z.Horita, D.J.Smith, M.Furukawa, M.Nemoto, R.Z.Valiev and T.G.Langdon
Characterization of Ultra-Fine Grained Materials Produced by Tosion Straining.
International Conference on Thermomechanical Processing of Steels and Other Materials (Thermec'97), University of Wollongong, Wollongong, Australia, 1997年7月9日.

3. M.Furukawa, Y.Ma, Z.Horita, M.Nemoto, R.Z.Valiev and T.G.Langdon
Fabrication and Properties of a Submicrometer-Grained Zn-22% Al Alloy.
International Conference on Thermomechanical Processing of Steels and Other Materials (Thermec'97), University of Wollongong, Wollongong, Australia, 1997年7月9日.

4. P.B.Berbon, M.Furukawa, Z.Horita, M.Nemoto, N.K.Tsenev, R.Z.Valiev and T.G.Langdon
Optimizing the Processing of a Commercial Al-Based Alloy for High Strain Rate Superplasticity.
The Third International Symposium on Microstructures and Mechanical Properties of New Engineering Materials, 三重大学, 1997年8月9日.

5. J.Wang, P.B.Berbon, Z.Horita, M.Furukawa, M.Nemoto and T.G.Langdon
Superplastic Behavior of Aluminum-Based Materials Processed by Equal-Channel Angular Pressing.
The Third International Symposium on Microstructures and Mechanical Properties of New Engineering Materials, 三重大学, 1997年8月9日.

6. P.B.Berbon, N.K.Tsenev, R.Z.Valiev, M.Furukawa, Z.Horita, M.Nemoto an T.G.Langdon
High Strain Rate Superplasticity in Fine-Grained Commercial Al Alloys Processed by Equal-Channel Angular Pressing.
The NATO Meeting, Prague, Poland, 1997年9月8日.

7. P.B.Berbon, N.K.Tsenev, R.Z.Valiev, M.Furukawa, Z.Horita, M.Nemoto and T.G.Langdon
Fabrication of Bulk Ultrafine-Grained Materials Through Intense Plastic Straining.

The TMS Fall Meeting'98, Indianapolis, USA, 1997年9月8日.

8. Y.Iwahashi, M.Furukawa, Z.Horita, M.Nemoto and T.G.Langdon
Microstructural Characteristics of Ultrafine-Grained Aluminum Produced Using Equal-Channel Angular Pressing.
The TMS Fall Meeting'98, Indianapolis, USA, 1997年9月8日.

9. P.B.Berbon、古川稔、N.K.Tsenev、R.Z.Valiev、堀田善治、根本實、T.G. Langdon
ECAP法で作製したAl合金の超塑性
第121回日本金属学会秋期大会、東北大学川内北キャンパス、1997年9月25日.

10. 長崎昭、古川稔
チルキャストしたAl-Zn-Mg-Zr合金の二段時効
日本産業技術教育学会第10回九州支部大会、宮崎大学教育学部、1997年10月25日.

11. 西山誠司、前田裕蔵、古川稔
銅合金における各種硬さ試験機の換算表と実験値の比較
第10回日本産業技術教育学会九州支部大会、宮崎大学教育学部、1997年10月25日.

12. 前田裕蔵、荒木治司、古川稔
強加工したAl合金のビッカース硬度と降伏応力の関係
第10回日本産業技術教育学会九州支部大会、宮崎大学教育学部、1997年10月25日.

13. P.B.Berbon, N.K.Tsenev, R.Z.Valiev, M.Furukawa, Z.Horita, M.Nemoto and T.G.Langdon
Superplasticity in Alloys Processed by Equal-Channel Angular Pressing.
The 127th TMS Annual Meeting, San Antonio, USA, 1998年2月16日.

14. M.Furukawa, Z.Horita, M.Nemoto and T.G.Langdon
Microstructural Evolution in Pure Aluminum During Equal-Channel Angular Pressing.
The 127th TMS Annual Meeting, San Antonio, USA, 1998年2月17日.

15. P.B.Berbon, M.Furukawa, Z.Horita, M.Nemoto, N.K.Tsenev, R.Z.Valiev and T.G.Langdon
Application of Equal-Channel Angular Pressing for Producing Superplastic Aluminum Alloys.
The 127th TMS Annual Meeting, San Antonio, USA, 1998年2月17日.

16. 古川稔、大石敬一郎、堀田善治、根本實、T.G.Langdon
ECAP法におけるせん断変形モデルとその組織
第122回日本金属学会春季大会、工学院大学新宿校舎、1998年3月27日.

17. 大石敬一郎、岩橋芳憲、古川稔、堀田善治、根本實、T.G.Langdon
ECAP法における結晶粒微細化の最適条件
第122回日本金属学会春季大会、工学院大学新宿校舎、1998年3月27日.

The TMS Fall Meeting'98, Indianapolis, USA, 1997年9月8日.

8. Y.Iwahashi, M.Furukawa, Z.Horita, M.Nemoto and T.G.Langdon
Microstructural Characteristics of Ultrafine-Grained Aluminum Produced Using Equal-Channel Angular Pressing.
The TMS Fall Meeting'98, Indianapolis, USA, 1997年9月8日.

9. P.B.Berbon、古川稔、N.K.Tsenev、R.Z.Valiev、堀田善治、根本實、T.G. Langdon
ECAP法で作製したAl合金の超塑性
第121回日本金属学会秋期大会、東北大学川内北キャンパス、1997年9月25日.

10. 長崎昭、古川稔
チルキャストしたAl-Zn-Mg-Zr合金の二段時効
日本産業技術教育学会第10回九州支部大会、宮崎大学教育学部、1997年10月25日.

11. 西山誠司、前田裕蔵、古川稔
銅合金における各種硬さ試験機の換算表と実験値の比較
第10回日本産業技術教育学会九州支部大会、宮崎大学教育学部、1997年10月25日.

12. 前田裕蔵、荒木治司、古川稔
強加工したAl合金のビッカース硬度と降伏応力の関係
第10回日本産業技術教育学会九州支部大会、宮崎大学教育学部、1997年10月25日.

13. P.B.Berbon, N.K.Tsenev, R.Z.Valiev, M.Furukawa, Z.Horita, M.Nemoto and T.G.Langdon
Superplasticity in Alloys Processed by Equal-Channel Angular Pressing.
The 127th TMS Annual Meeting, San Antonio, USA, 1998年2月16日.

14. M.Furukawa, Z.Horita, M.Nemoto and T.G.Langdon
Microstructural Evolution in Pure Aluminum During Equal-Channel Angular Pressing.
The 127th TMS Annual Meeting, San Antonio, USA, 1998年2月17日.

15. P.B.Berbon, M.Furukawa, Z.Horita, M.Nemoto, N.K.Tsenev, R.Z.Valiev and T.G.Langdon
Application of Equal-Channel Angular Pressing for Producing Superplastic Aluminum Alloys.
The 127th TMS Annual Meeting, San Antonio, USA, 1998年2月17日.

16. 古川稔、大石敬一郎、堀田善治、根本實、T.G.Langdon
ECAP法におけるせん断変形モデルとその組織
第122回日本金属学会春季大会、工学院大学新宿校舎、1998年3月27日.

17. 大石敬一郎、岩橋芳憲、古川稔、堀田善治、根本實、T.G.Langdon
ECAP法における結晶粒微細化の最適条件
第122回日本金属学会春季大会、工学院大学新宿校舎、1998年3月27日.

18. 小村章吾、P.B.Berbon、宇都宮淳、古川稔、堀田善治、根本實、T.G.Langdon
ECAP法による超塑性Al-3%Mg-0.2%Sc合金の作製
第122回日本金属学会春季大会、工学院大学新宿校舎、1998年3月27日.

19. 中嶋清孝、古川稔、堀田善治、藤波隆善、根本實
ECAP法で作成した微細粒Al-Cu系合金の時効挙動
第94回軽金属学会春季大会、長岡技術科学大学、1998年5月15日.

20. 山下晃弘、小村章吾、宇都宮淳、古川稔、堀田善治、根本實
Sc添加Al-3%Mg合金のECAP法による微細組織制御
平成10年度日本金属学会九州支部大会、熊本大学工学部、1998年6月12日.

21. 宇都宮淳、小村章吾、山下晃弘、古川稔、堀田善治、根本實、P.B.Berbon、T.G.Langdon
ECAP法で結晶粒微細化したAl合金の超塑性
平成10年度日本金属学会九州支部大会、熊本大学工学部、1998年6月12日.

22. H.Hasegawa, S.Komura, Z.Horita, M.Furukawa, M.Nemoto and T.G.Langdon
Grain Refinement and Potential for Superplasticity in Alloys Containing Small Particles.
Third Pacific Rim International Conference on Advanced Materials and Processing (PRICM-3), Hilton Hawaiian Village Hotel, Honolulu, Hawaii, USA, 1998年7月14日.

23. M.Nemoto, Z.Horita, M.Furukawa and T.G.Langdon
Microstructural Evolution for Superplasticity Using Equal-Channel Angular Pressing.
International Conference on Towards Innovation in Superplasticity II (JIMIS 9), 神戸国際会議センター、神戸, 1998年9月21日.

24. Z.Horita, S.Komura, P.B.Berbon, A.Utsunomiya, M.Furukawa, M.Nemoto and T.G.Langdon
Superplasticity of Ultrafine-Grained Aliminum Alloys Processed by Equal-Channel Angular Pressing.
International Conference on Towards Innovation in Superplasticity II (JIMIS 9), 神戸国際会議センター、神戸, 1998年9月22日.

25. M.Furukawa, K.Oh-ishi, S.Komura, A.Yamashita, Z.Horita, M.Nemoto and T.G.Langdon
Optimazation of Microstructure for Superplasticity Using Equal-Channel Angular Pressing.
International Conference on Towards Innovation in Superplasticity II (JIMIS 9), 神戸国際会議センター、神戸, 1998年9月22日.

26. 古川稔、大石敬一郎、堀田善治、根本實、T.G.Langdon
ECAP法による微細組織に及ぼすプレス速度の影響
第123回日本金属学会秋期大会、愛媛大学城北キャンパス、松山、1998年9月28日.

27. 堀田善治、D.J.Smith、大石敬一郎、古川稔、根本實、T.G.Langdon
強ひずみ加工で作製した微細結晶粒の粒界構造
第123回日本金属学会秋期大会、愛媛大学城北キャンパス、松山、1998年9月28日.

28. 山下晃弘、小村章吾、宇都宮淳、古川稔、藤波隆善、堀田善治、根本實
ECAP法により作製したAl-3Mg-0.2Sc合金の微細粒組織と熱的安定性
第123回日本金属学会秋期大会、愛媛大学城北キャンパス、松山、1998年9月29日.

29. 宇都宮淳、小村章吾、山下晃弘、古川稔、堀田善治、根本實、P.B.Berbon、T.G.Langdon
ECAP法で作製したAl-0.2ScとAl-3Mg-0.2Scの超塑性挙動
第123回日本金属学会秋期大会、愛媛大学城北キャンパス、松山、1998年9月29日.

30. P.B.Berbon, M.Furukawa, Z.Horita, M.Nemoto, N.K.Tsenev, R.Z.Valiev and T.G.Langdon
Processing of Aluminum Alloys for High Strain Rate Superplasticity.
The TMS Fall Meeting'98, O'Hale Hilton Hotel, Chicago, USA, 1998年10月12日.

31. S.Komura, P.B.Berbon, A.Utsunomiya, M.Furukawa, Z.Horita, M.Nemoto and T.G.Langdon
Superplasticity in an Ultrafine-Grained Al-Mg-Sc Alloy Produced by Equal-Channel Angular Pressing.
The TMS Fall Meeting'98, O'Hale Hilton Hotel, Chicago, USA, 1998年10月12日.

32. 井旭偉、森田靖敏、古川稔
Li, Mg, Znを含むAl合金の熱処理中の脱元素
第11回日本産業技術教育学会九州支部大会、大分大学教育学部、大分、1998年10月24日.

33. 前田裕蔵、西山誠司、古川稔
銅合金における硬度と降伏応力の関係
第11回日本産業技術教育学会九州支部大会、大分大学教育学部、大分、1998年10月24日.

34. Z.Horita, M.Furukawa, M.Nemoto and T.G.Langdon
Microstructural Control for High Strain Rate Superplasticity Using Equal-Channel Angular Pressing.
International Conference of Plasticity '99, Cancun, Mexico, 1999年1月.

ELSEVIER

Microstructural Characteristics of an Ultrafine Grain Metal Processed with Equal-Channel Angular Pressing

Minoru Furukawa,* Zenji Horita,† Minoru Nemoto,† Ruslan Z. Valiev,‡ and Terence G. Langdon§

**Department of Technology, Fukuoka University of Education, Munakata, Fukuoka 811-41, Japan; †Department of Materials Science and Engineering, Faculty of Engineering, Kyushu University, Fukuoka 812-81, Japan; ‡Institute of Physics of Advanced Materials, Ufa State Aviation Technical University, Ufa 450000, Russia; and §Departments of Materials Science and Mechanical Engineering, University of Southern California, Los Angeles, CA 90089-1453*

Equal-channel angular pressing is a procedure for producing a fully dense material with an ultrafine grain size, typically in the submicrometer or nanometer range, by subjecting the material to a very high plastic strain. This paper describes the principle of equal-channel angular pressing and illustrates the capability of the technique by reference to a series of detailed experiments conducted on an Al-3%Mg solid solution alloy in which the grain size was successfully reduced by equal-channel angular pressing from an initial size of ~500μm in the hot-rolled condition to a final size of ~0.2μm..

INTRODUCTION

Superplastic metallic alloys are capable of exhibiting very high tensile elongations, often >1000%, when tested at elevated temperatures [1]. However, experimental evidence suggests that a decrease in grain size into the submicrometer or nanometer range will make it possible to achieve superplastic elongations at faster strain rates or at lower testing temperatures or both. Each of these effects is potentially beneficial for the utilization of these materials in industrial forming operations because it would decrease the total forming time while simultaneously minimizing the extent of tool wear.

The fabrication of ultrafine-grained (UFG) materials was initially demonstrated by using a gas condensation technique [2]; subsequently other procedures, such as high energy ball milling [3] and sliding wear [4], were developed. Nevertheless, without exception, all of these techniques have the disadvantage that it is difficult, if not impossible, to fabricate large, fully dense structures. An alternative procedure is also available for the fabrication of UFG microstructures by subjecting the material to a very high plastic strain, using a process such as equal-channel angular (ECA) pressing [5–8]. The procedure of ECA pressing has the capability of producing large, fully dense UFG samples suitable for use in forming operations.

Recently, experiments were undertaken to evaluate the microstructural characteristics of an Al-3%Mg solid solution alloy subjected to ECA pressing. The present paper is an overview of some of the experimental results obtained in this program.

PRINCIPLE OF ECA PRESSING

The principle of ECA pressing is illustrated by the section through the pressing die represented schematically in Fig. 1. Two chan-

MATERIALS CHARACTERIZATION 37:277–283 (1996)

655 Avenue of the Americas, New York, NY 10010

S1044-5803/96/$15.00
PII S1044-5803(96)00131-3

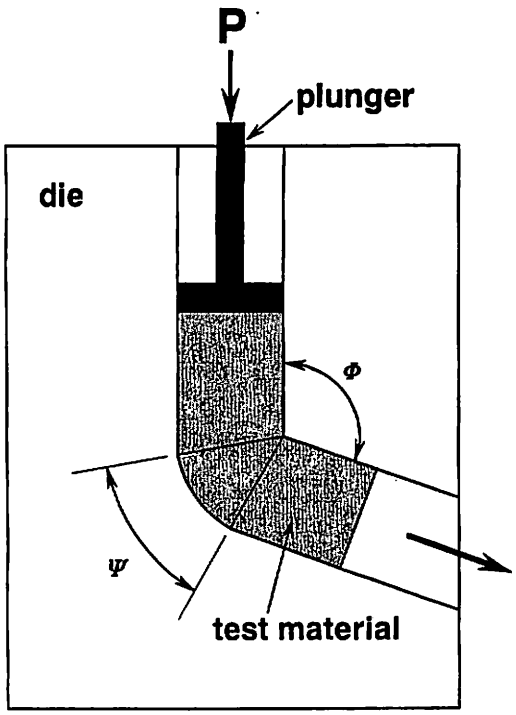

FIG. 1. Schematic representation of a die for ECA pressing.

nels of equal cross section intersect at an angle ϕ, and an angle ψ is subtended by the arc of curvature at the outer point of contact between the two channels. The test material is cut to fit within the die, and it is pressed through the die with the use of a plunger and a load, P. It can be shown that the strain, ε< accumulated in the material by a single passage through the die is given by [9]

$$\varepsilon = \left[\frac{2\cot\left(\frac{\phi}{2}+\frac{\psi}{2}\right)+\psi\,\mathrm{cosec}\left(\frac{\phi}{2}+\frac{\psi}{2}\right)}{\sqrt{3}}\right]. \quad (1)$$

In practice, the pressings may be repeated several times to attain the required level of strain. Typically, materials are subjected to ECA pressing to plastic strains of as much as ~4–8.

MICROSTRUCTURE OF AN Al-Mg ALLOY AFTER ECA PRESSING

Experiments were conducted with the use of a hot-rolled Al-3%Mg solid solution alloy having an initial grain size of ~500μm. Samples were subjected to ECA pressing at room temperature to an equivalent true plastic strain of ~4, and they were then rolled at room temperature to a final thickness of ~1mm. A detailed description of the microstructural stability of this alloy is given elsewhere [10–13].

In the rolled condition, after ECA pressing but without subsequent annealing, there was a heterogeneous microstructure containing areas of equiaxed and elongated grains. Examples are shown in Fig. 2 at three different magnifications, including a selected area diffraction pattern taken at the lowest

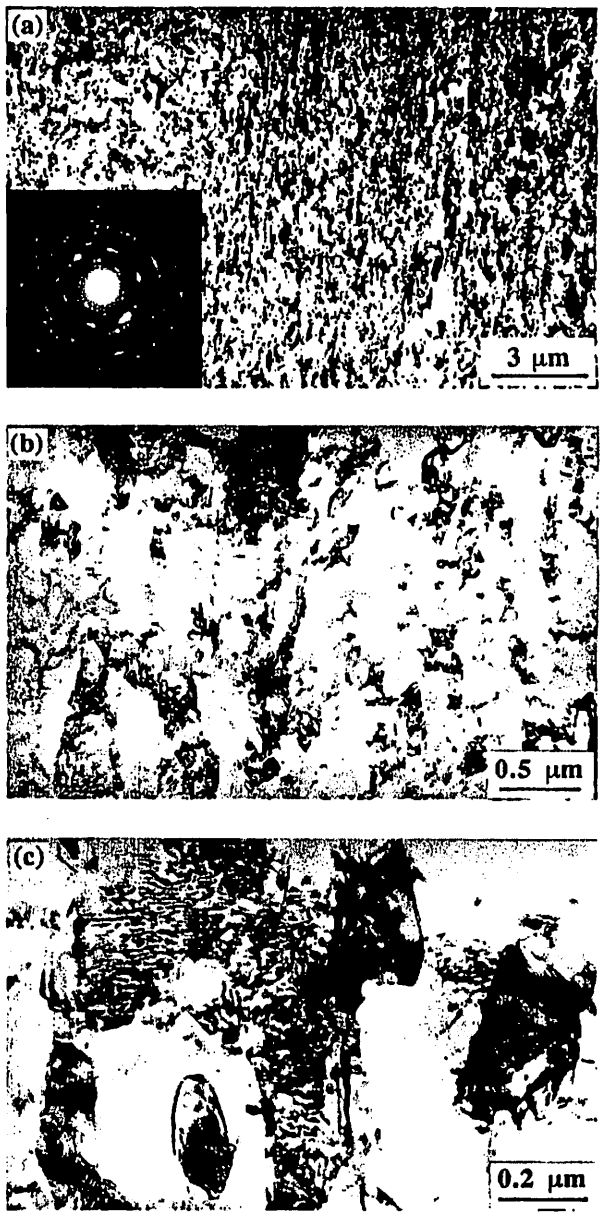

FIG. 2. Microstructures at three different magnifications of an Al-3%Mg alloy after ECA pressing.

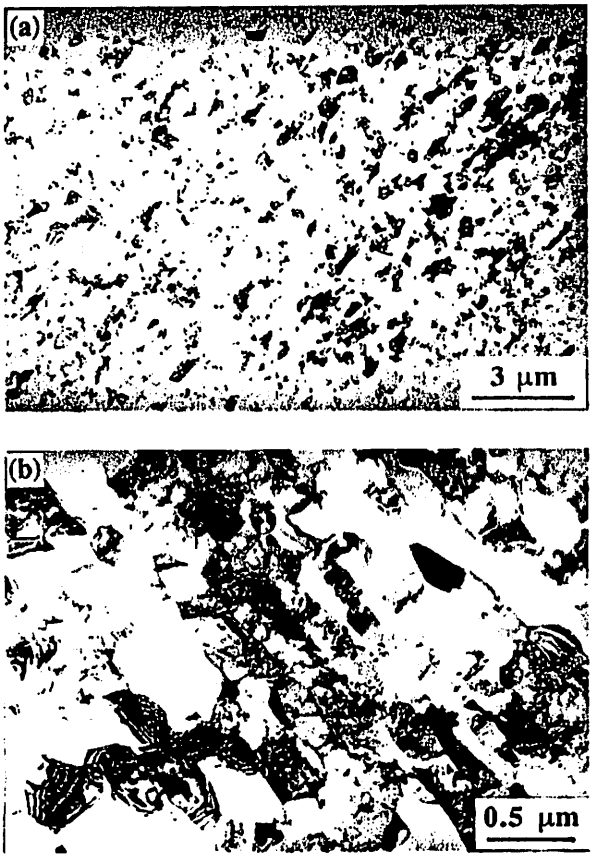

FIG. 3. Microstructures at two different magnifications after annealing for 1 h at 443K.

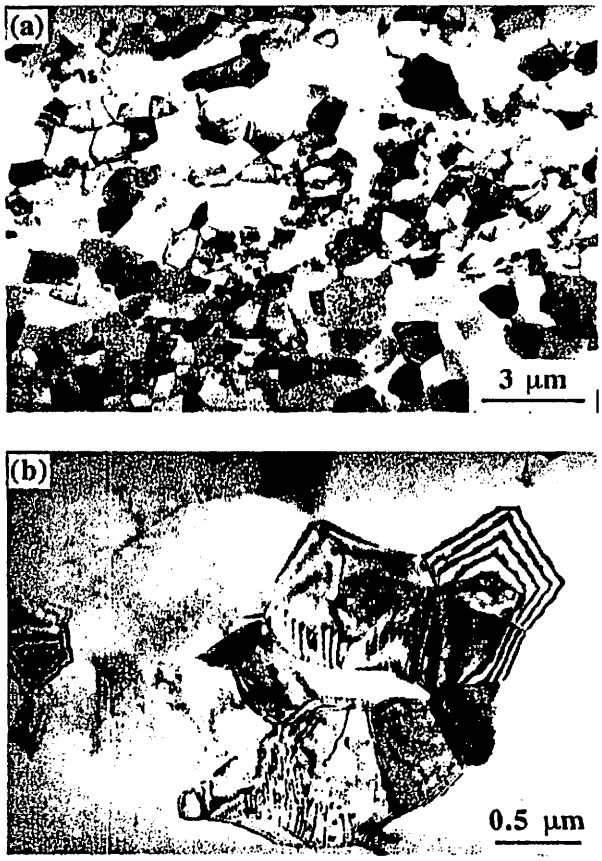

FIG. 4. Microstructures at two different magnifications after annealing for 1 h at 503K.

magnification, using a diameter of 1.9μm. In this as-fabricated condition, inspection showed that many of the grain boundaries were poorly delineated, and it was concluded that the boundaries were in a high-energy nonequilibrium configuration [14]. The mean linear intercept grain size was estimated as ~0.2μm. Thus, it is demonstrated that ECA pressing was successful in reducing the grain size of this alloy by more than three orders of magnitude.

Static annealing of the samples led to grain growth and an evolution in the microstructure into a more equilibrated configuration. Figure 3 shows examples after annealing for 1 h in a silicone oil bath at a temperature of 443K. At this annealing temperature, a comparison of Figs. 2(b) and 3(b) shows that grain growth is very limited. However, there was a very marked changed in the appearance of the microstructure when the annealing was conducted for 1 h at a temperature of 503K, as shown by the microstructures in Fig. 4. Close examination revealed that the structure was divisible into regions of unrecrystallized grains and adjacent regions where recrystallization appeared to be essentially complete. This duality in microstructure was especially apparent after annealing for 1 h at 533K, as shown in Fig. 5 in which can be seen a clear mixture of fairly large (~2μm) and very small (~0.5μm) grains. At even higher annealing temperatures, the material was in a fully recrystallized condition, and the grains were relatively uniform and separated by high-angle grain boundaries having an equilibrium structure. An example is shown in Fig. 6 after annealing for 1 h in an argon atmosphere at 563K.

QUANTITATIVE MEASUREMENTS OF THE GRAIN CONFIGURATION

After ECA pressing, samples were annealed for 1 h at each of a series of temperatures, with a maximum of 803K. After each anneal-

FIG. 5. Microstructure after annealing for 1 h at 533K.

ing treatment, measurements were taken to determine the mean linear intercept grain size. Figure 7 is a plot of the grain size against the annealing temperature, and it is apparent that the grain size is initially fairly stable up to ~450K; but, at higher temperatures, the average grain size is >100μm. A similar trend, but covering a series of temperatures with a maximum of only 673K, was noted earlier for an Al-1.5%Mg alloy into which a UFG microstructure was introduced by torsion straining under high pressure [15].

The Vickers microhardness was measured for each sample after static annealing, using a diamond pyramidal indentor. Figure 8

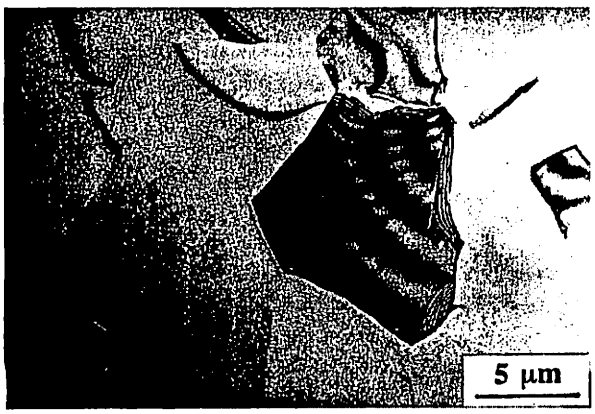

FIG. 6. Microstructure after annealing for 1 h at 563K.

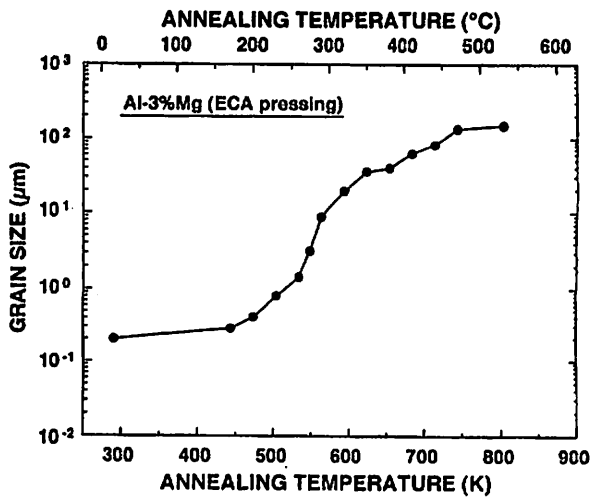

FIG. 7. Grain size versus annealing temperature, showing growth from ~0.2μm to >100μm.

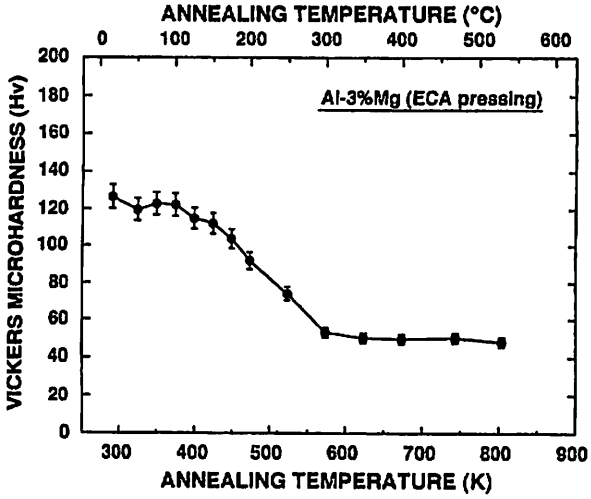

FIG. 8. Vickers microhardness versus annealing temperature.

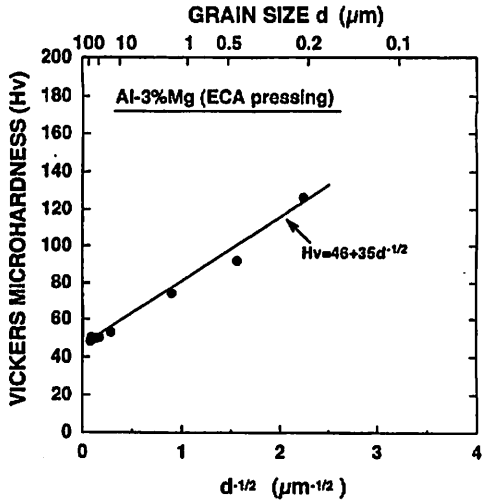

FIG. 9. Demonstration of the validity of the Hall-Petch relation over the entire range of grain sizes.

shows the variation in microhardness, Hv (in kg mm^{-2}), with annealing temperature up to a maximum of 803K, where the error bar on each experimental point represents the total range of individual values recorded for Hv in seven separate measurements. This plot shows a gradual decrease in the values of Hv with increasing annealing temperature to a maximum of ~550K and a subsequent leveling at even higher annealing temperatures. There is no evidence in Fig. 8 to support the trend, reported earlier for a UFG Al-1.5%Mg alloy processed by torsion straining [15] and samples of nanocrystalline Pd produced by inert gas condensation and compaction [16], of an initial increase in microhardness at the lowest annealing temperatures followed by a subsequent decrease.

The well-established Hall-Petch equation relates the yield stress of a material, σ_y, to the grain size, d, through the expression

$$\sigma_y = \sigma_o + k_y d^{-1/2}, \tag{2}$$

where σ_o is the friction stress and k_y is a constant of yielding. In the absence of appreciable work hardening, the hardness, Hv, is proportional to the yield stress through an expression of the form

$$Hv \simeq 3\sigma_y; \tag{3}$$

so Eq. (2) may be written as

$$Hv = H_o + k_H d^{-1/2}, \tag{4}$$

where H_o and k_H are appropriate constants.

To check the validity of Eq. (4), Fig. 9 shows a plot of Hv against $d^{-1/2}$. It is apparent that the Hall-Petch relation is obeyed in this UFG material down to the initial grain size of ~0.2μm, with values of the constants in Eq. (4) of $H_o \simeq 46Hv$ and $k_H \simeq 35Hv\mu m^{1/2}$.

It is usual to express the occurrence of grain growth through a relation of the form

$$d^2 - d_o^2 = k_g t^n, \tag{5}$$

where d and d_o represent the instantaneous and initial grain sizes, respectively, k_g is a

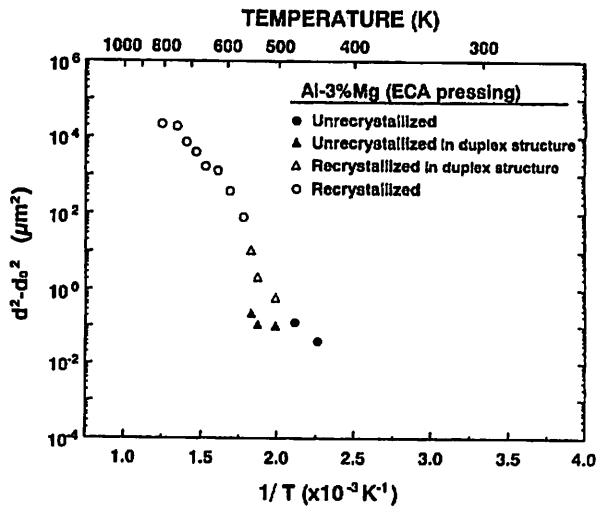

FIG. 10. Demonstration of the use of the grain growth relation given in Eq. (5).

constant, t is the time, and n is a constant usually taken as equal to unity.

The value of k_g is usually given by a relation of the form

$$k_g = A\exp(-Q/RT), \quad (6)$$

where Q is the appropriate activation energy for grain growth, R is the gas constant, and A is a constant.

Figure 10 shows the experimental data plotted as $(d^2 - d_o^2)$ versus $1/T$, where T is the absolute temperature of annealing and d_o was taken as the smallest grain size immediately after ECA pressing (0.2μm). As a result of the duplex structure clearly evident in Fig. 5, the data points are identified separately as measurements taken within the unrecrystallized and recrystallized regions.

From the slope of the points within the recrystallized region in Fig. 10, Q is estimated as ~90kJmol^{-1}, which is close to the value of ~86kJmol^{-1} expected for grain boundary diffusion in pure aluminum [17]. In the unrecrystallized condition, the slope in Fig. 10 is very much lower and leads to a value of Q of the order of ~25kJmol^{-1}. This low value of Q is consistent with the suggestion that nonequilibrium grain boundaries in UFG structures are associated with very high atomic mobility [18, 19].

SUMMARY

Equal-channel angular pressing is a powerful tool for the processing of materials with ultrafine grain structures within the submicrometer and nanometer range. Experiments on an Al-3%Mg solid solution alloy demonstrate the feasibility of using ECA pressing to reduce the average grain size from ~500μm initially after hot rolling to a final value of ~0.2μm. Microstructural examination after ECA pressing shows that the grain boundaries are in a high-energy nonequilibrium configuration. Static annealing experiments lead to grain growth, and there is a simultaneous microstructural evolution into a more equilibrated condition. At high annealing temperatures (>720K), the grain boundaries have an equilibrium structure and the average grain size is >100μm.

This work was supported in part by the Light Metal Educational Foundation of Japan and in part by the National Science Foundation of the United States under Grants No. INT-9404693 and DMR-9115443.

References

1. A. H. Chokshi, A. K. Mukherjee, and T. G. Langdon, Superplasticity in advanced materials. *Mater. Sci. Eng.* R10:237–274 (1993).
2. H. Gleiter, Materials with ultra-fine grain sizes. In *Deformation of Polycrystals: Mechanisms and Microstructures*, N. Hansen, A. Horsewell, T. Leffers, and H. Lilholt, eds., Risø National Laboratory, Roskilde, Denmark, pp. 15–21 (1981).
3. C. C. Koch and Y. S. Cho, Nanocrystals by high energy ball milling. *Nanostruct. Mater.* 1:207–212 (1992).
4. D. A. Rigney, Sliding wear of metals. *Annu. Rev. Mater. Sci.* 18:141–163 (1988).
5. V. M. Segal, V. I. Reznikov, A. E. Drobyshevskiy, and V. I. Kopylov, Plastic working of metals by simple shear. *Izv. Akad. Nauk SSSR Metally* 1:115–123 (1981).
6. R. Z. Valiev, N. A. Krasilnikov, and N. K. Tsenev, Plastic deformation of alloys with submicron-grained structure. *Mater. Sci. Eng.* A137:35–40 (1991).
7. N. A. Akhmadeev, N. P. Kobelev, R. R. Mulyukov, Ya. M. Soifer, and R. Z. Valiev, The effect of heat treatment on the elastic and dissipative properties of copper with the submicrocrystalline structure. *Acta Metall. Mater.* 41:1041–1046 (1993).
8. V. M. Segal, Materials processing by simple shear. *Mater. Sci. Eng.* A197:157–164 (1995).
9. Y. Iwahashi, J. Wang, Z. Horita, M. Nemoto, and T. G. Langdon, Principle of equal-channel angular pressing for the processing of ultra-fine grained materials. *Scr. Mater.* 35:143–146 (1996).
10. J. Wang, Z. Horita, M. Furukawa, M. Nemoto, N. K Tsenev, R. Z. Valiev, Y. Ma, and T. G. Langdon, An investigation of ductility and microstructural evolution in an Al-3%Mg alloy with submicror grain size. *J. Mater. Res.* 8:2810–2818 (1993).
11. J. Wang, Y. Iwahashi, Z. Horita, M. Furukawa, M Nemoto, R. Z. Valiev, and T. G. Landgon, An investigation of microstructural stability in an Al-Mg alloy with submicrometer grain size. *Acta Mater* 44:2973–2982 (1996).
12. J. Wang, M. Furukawa, Z. Horita, M. Nemoto, R. Z Valiev, and T. G. Langdon, Enhanced grain growth

in an Al-Mg alloy with ultrafine grain size. *Mater. Sci. Eng.* AZ16:41–46 (1996).

13. M. Furukawa, Z. Horita, M. Nemoto, R. Z. Valiev, and T. G. Langdon, Microhardness measurements and the Hall-Petch relationship in an Al-Mg alloy with submicrometer grain size. *Acta Mater.* 44:4619–4629 (1996).
14. A. A. Nazarov, A. E. Romanov, and R. Z. Valiev, On the structure, stress fields and energy of non-equilibrium grain boundaries. *Acta Metall. Mater.* 41:1033–1040 (1993).
15. R. Z. Valiev, F. Chmelik, F. Bordeaux, G. Kapelski, and B. Baudelet, The Hall-Petch relation in submicro-grained Al-1.5%Mg alloy. *Scr. Metall. Mater.* 27:855–860 (1992).
16. J. R. Weertman and P. G. Saunders, Plastic deformation of nanocrystalline metals. *Solid State Phenom.* 35–36:249–262 (1994).
17. F. A. Mohamed and T. G. Langdon, Deformation mechanism maps based on grain size. *Metall. Trans.* 5:2339–2345 (1974).
18. R. Z. Valiev, E. V. Kozlov, Yu. F. Ivanov, J. Lian, A. A. Nazarov, and B. Baudelet, Deformation behaviour of ultra-fine-grained copper. *Acta Metall. Mater.* 42:2467–2475 (1994).
19. J. Lian, R. Z. Valiev, and B. Baudelet, On the enhanced grain growth in ultrafine grained metals. *Acta Metall. Mater.* 43:4165–4170 (1995).

Received June 1996; accepted September 1996.

ELSEVIER

Evolution of Grain Boundary Structure in Submicrometer-Grained Al-Mg Alloy

Zenji Horita,* David J. Smith,† Minoru Furukawa,‡ Minoru Nemoto,* Ruslan Z. Valiev,§ and Terence G. Langdon‖

**Department of Materials Science and Engineering, Faculty of Engineering 36, Kyushu University, Fukuoka 812-81, Japan; †Center for Solid State Science and Department of Physics and Astronomy, Arizona State University, Tempe, Arizona 85287; ‡Department of Technology, Fukuoka University of Education, Munakata, Fukuoka 811-41, Japan; §Institute of Physics of Advanced Materials, Ufa State Aviation Technical University, Ufa 450000, Russia; and ‖Departments of Materials Science and Mechanical Engineering, University of Southern California, Los Angeles, California 90089-1453*

This paper presents high-resolution electron microscopy studies of grain boundary structures in a submicrometer-grained Al-3%Mg solid solution alloy produced by an intense plastic straining technique. The studies include the effect of static annealing on the grain boundary structure. Many grain boundaries are in a high-energy nonequilibrium state in the as-strained sample. The nonequilibrium character is retained on some grain boundaries in samples annealed at temperatures below the onset of significant grain growth. The effect of electron irradiation on the grain boundary structure also is examined. © Elsevier Science Inc., 1996

INTRODUCTION

Grain size refinement is an important procedure not only to improve the yield strength at lower temperatures without reducing ductility, but also to facilitate the advent of superplasticity at faster strain rates. The refinement is feasible by using an intense plastic straining technique where plastic strain of the order of several hundreds of percent is imposed under quasi-hydrostatic pressure [1–5]. With this technique, it is possible to reduce grain sizes to the submicrometer level or, occasionally, to the nanometer level [6]. The advantage of the technique over other grain-size refining techniques is that a large quantity of the submicrometer-grained (SMG) material may be produced without introducing residual porosity.

The microstructures of SMG materials produced by the intense plastic straining technique are generally characterized by highly deformed grains and poorly defined grain boundaries [4, 7]. High-resolution electron microscopy has confirmed the presence of regular or irregular arrangements of facets and steps at grain boundaries as well as the presence of a region adjacent to some grain boundaries containing significant distortion or even missing lattice fringes [8]. It has been concluded that the grain boundaries of SMG materials are in a high-energy and nonequilibrium state. Static annealing experiments of the SMG samples have led to a significant reduction of dislocations within the grains and the development of well-defined grain boundaries before significant grain growth takes place [9]. However, preliminary observations using high-resolution electron microscopy, have revealed that the grain boundaries still retain a nonequilibrium character [10]. In this study, high-resolution electron microscopy observations are further conducted to examine the evolution of grain boundary structure accompanying static annealing, and more evidence is provided

MATERIALS CHARACTERIZATION 37:285–294 (1996)

655 Avenue of the Americas, New York, NY 10010

1044-5803/96/$15.00
PII S1044-5803(96)00178-7

to support the earlier conclusions from the high-resolution electron microscopy studies.

EXPERIMENTAL PROCEDURES

A total strain of ~7 was imposed at room temperature on an Al-3%Mg solid solution alloy with an initial grain size of ~500μm by using a torsion straining technique [4, 8, 11]. The strained alloy was in the form of disks with diameters of ~15mm and thicknesses of ~0.3mm. These disks were reduced to thicknesses of ~150–250μm by polishing on both surfaces, and then small disks, having diameters of 3mm, were punched out.

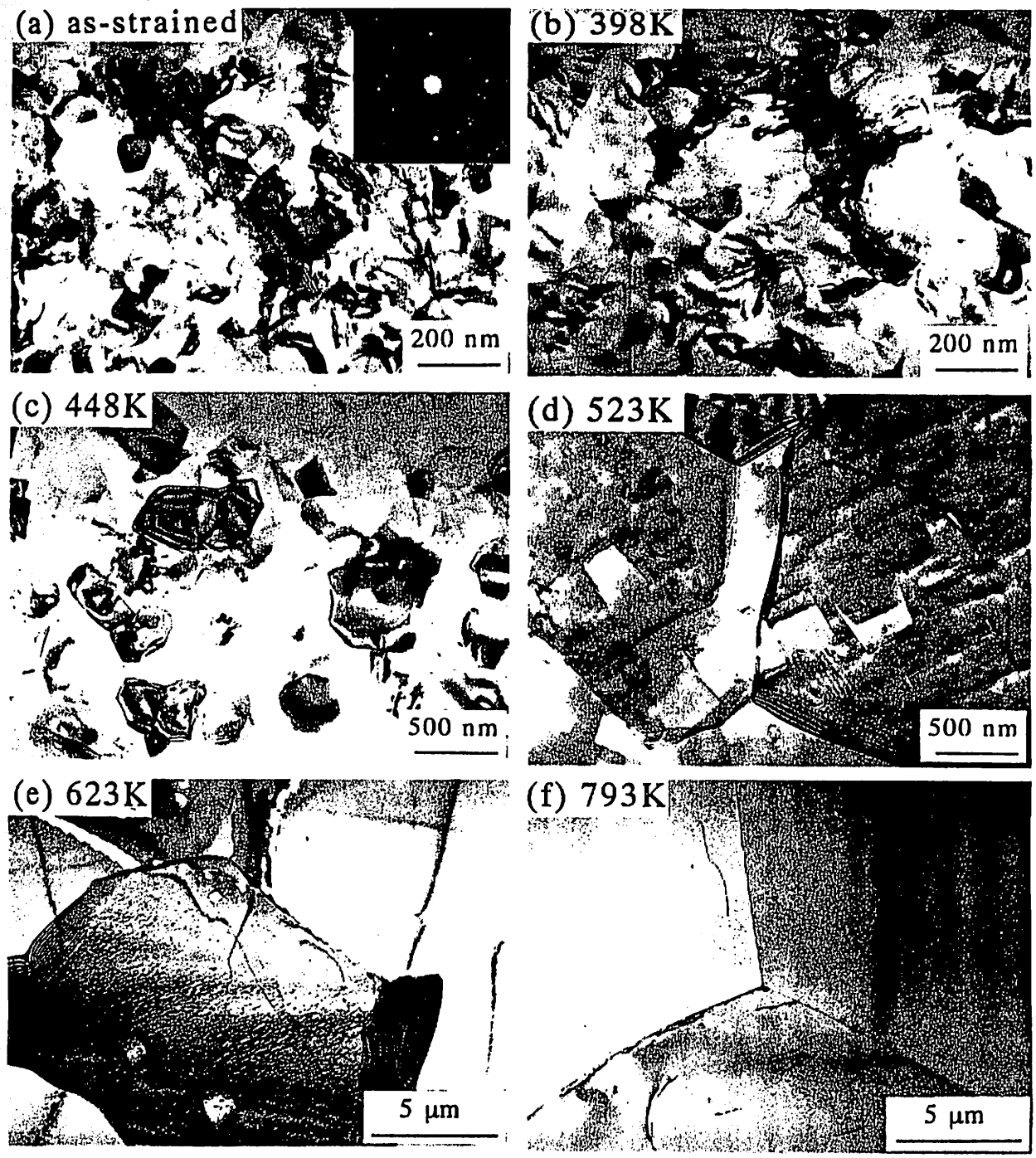

FIG. 1. Microstructures (a) in as-strained condition and after annealing at (b) 398K, (c) 448K, (d) 523K, (e) 623K, and (f) 793K for 1 h.

Some of the small disks were annealed at temperatures up to 793K for 1 h in an argon atmosphere.

The disks were thinned for transmission electron microscopy with a twin-jet polisher, using a solution of 10%$HClO_4$, 20%$C_3H_8O_3$, and 70%C_2H_5OH at a temperature of 278K. The thinned specimens were examined by using a JEM-1000D high-voltage electron microscope operating at 1000kV and a JEM-4000EX high-resolution electron microscope operating at 400kV. The former microscope was used for observations of grains and grain boundary configurations at lower magnifications; the latter microscope was used for atomic structure observations at and near the grain boundaries in the as-strained samples and those annealed at 448K, which correspond to the onset of significant grain growth. Lattice images were taken at the optimum defocus condition, typically at a magnification of 500,000 times. Since the grain sizes were less than 1μm, individual grains were not tilted during observation but a sufficient number of grains oriented close to <110> was found for lattice imaging.

RESULTS

EVOLUTION OF GRAIN CONFIGURATION

Figure 1 shows the microstructure of the sample in the as-strained condition with a selected area electron diffraction (SAED) pattern taken from a 0.55μm diameter region (Fig. 1(a)) and in the annealed conditions at temperatures up to 793K (Fig. 1(b–f)), thereby demonstrating an evolution of the SMG structure with respect to annealing temperature. In the as-strained condition, some grain boundaries are visible, and these boundaries appear to be mostly curved or wavy. There are also some grain boundaries that are poorly defined. The contrast within the grains is not uniform but often changes in a complex way. All of these observations suggest that the grains and the grain boundaries are in a nonequilibrium state. However, the SAED pattern with many diffracted beams around rings indicates that there are many small grains with multiple orientations in the selected field of view. As the annealing temperature is increased, the grain boundaries become straight and well defined. The observations thus suggest that there is a reduction in both the nonequilibrium character of the grain boundaries and the level of the internal stress within the grains.

The average grain sizes measured from the micrographs are plotted in Fig. 2 with respect to annealing temperature. Significant grain growth begins to occur at a temperature of about 450K.

AS-STRAINED STRUCTURE

Figure 3 shows the lattice image of the region containing a grain boundary in the as-strained sample. Facets and steps are visible on the grain boundary with the facets formed parallel to (111) in the grain on the left, but there is no regularity in the formation of the facets. Close observation reveals that there is distortion of the (111) lattice fringes over a few layers near the boundary.

A grain boundary in the as-strained sample is also shown in Fig. 4(a–d), the parts corresponding to the images recorded after every few minutes at a current density of 5.5mA/m^2. Moiré fringes are visible on the grain boundary because the lattice fringes

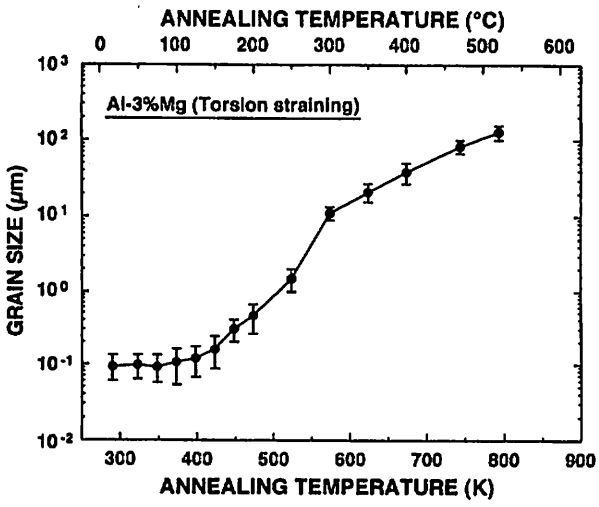

FIG. 2. Average grain size versus annealing temperature.

of the two adjacent grains are superimposed. Because the specimen is not tilted and thus the specimen surface is perpendicular to the beam direction, the presence of moiré fringes indicates that the grain boundary plane is inclined to the surface normal. The width of the moiré fringe zone becomes small along the grain boundary from the bottom left to the top right, and the zone eventually disappears near the triple point. The inclination angle is then diminished along the grain boundary, and the boundary plane is perpendicular to the surface at the triple point. Inspection of Fig. 4(a–d) shows that the zone width decreases with the observation of images in parts (a) to (d), and thus it demonstrates that the grain boundary tended to be perpendicular to the specimen surface after exposure to high-energy electrons. The portion of the grain boundary near the triple point, which was perpendicular to the specimen surface at the initial stage of the observation, became smooth and straight and increased its length during observation of the four images.

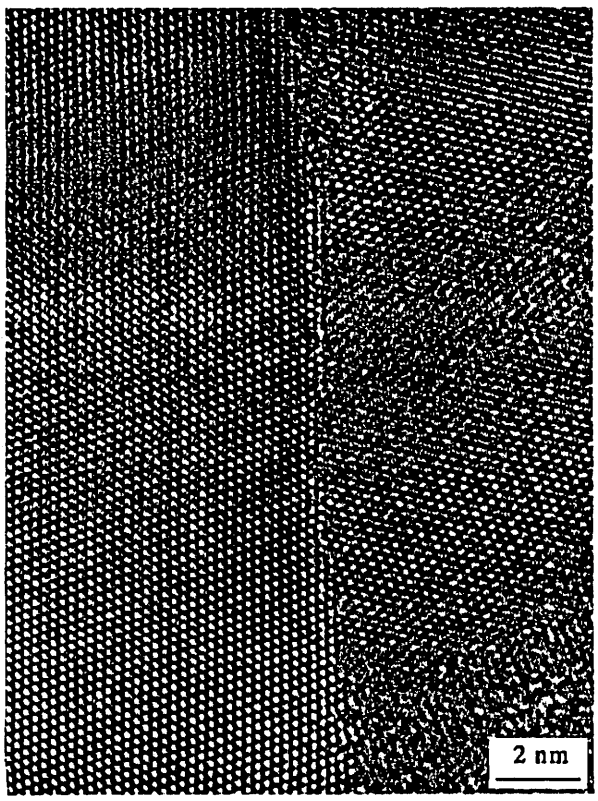

FIG. 3. Grain boundary lattice image in as-strained condition.

In Fig. 4(c,d), planar defects are visible on {111}, as indicated by arrows, but there are no such defects in Fig. 4(a,b). The defects were formed because of the exposure to high-energy electrons. The critical voltage for defect formation has been reported as ~170kV [12], which is well below 400kV, the accelerating voltage adopted in the present observation.

Figure 5 shows a general view of grains taken after the series of images in Fig. 4: the region corresponding to Fig. 4 is indicated by a square. Most of the boundaries in the micrograph are curved or wavy. There are also many boundaries that are inclined to the surface normal with the inclination angle changing.

ANNEALED STRUCTURE

Figure 6 is a higher magnification image of a grain in the sample annealed at 448K for 1 h. The grain boundaries marked A, B, C, and D are smooth and straight without inclination to the surface normal, and thus the boundaries appear to be in a more stable condition than those shown in Fig. 5. However, the boundaries at E and F are inclined to the surface normal and have a zigzag nature. Thus, complete equilibrium has not been reached in the grain of Fig. 6. The region indicated by a square on grain boundary D is further magnified in Fig. 7. The portion of the grain boundary near the triple point exhibits a stepwise arrangement of facets but, with increasing distance from the triple point, the boundary becomes smooth and straight. This difference in the grain boundary configuration is more clearly demonstrated with the lattice images shown in Fig. 8, in which parts (a) and (b) correspond to the images near and away from the triple point, respectively.

Figure 9 is another image of grains and grain boundaries in the sample annealed at 448K for 1 h. The grain boundaries marked B, C, and D are smooth, but they are curved and bowed out between two neighboring triple points. The grain boundaries marked A and E take an irregular or zigzag nature. Thus, the grains shown in Fig. 9 have not

reached complete equilibrium, similar to the grain shown in Fig. 6. The lattice images of the grain boundaries marked A, B, and C at the portions indicated by arrows are shown in parts (a), (b), and (c), respectively, of Fig. 10.

In Fig. 10(a), the grain boundary at the portions marked A and B is parallel to (111) in the grain with two-dimensional lattice fringes. Between the two portions, ledges are formed on the boundary, but there is no regularity in the formation of the ledges. Close observation reveals that there is distortion of the lattice fringes adjacent to the boundary, and the distortion extends to about two layers of (111), corresponding to

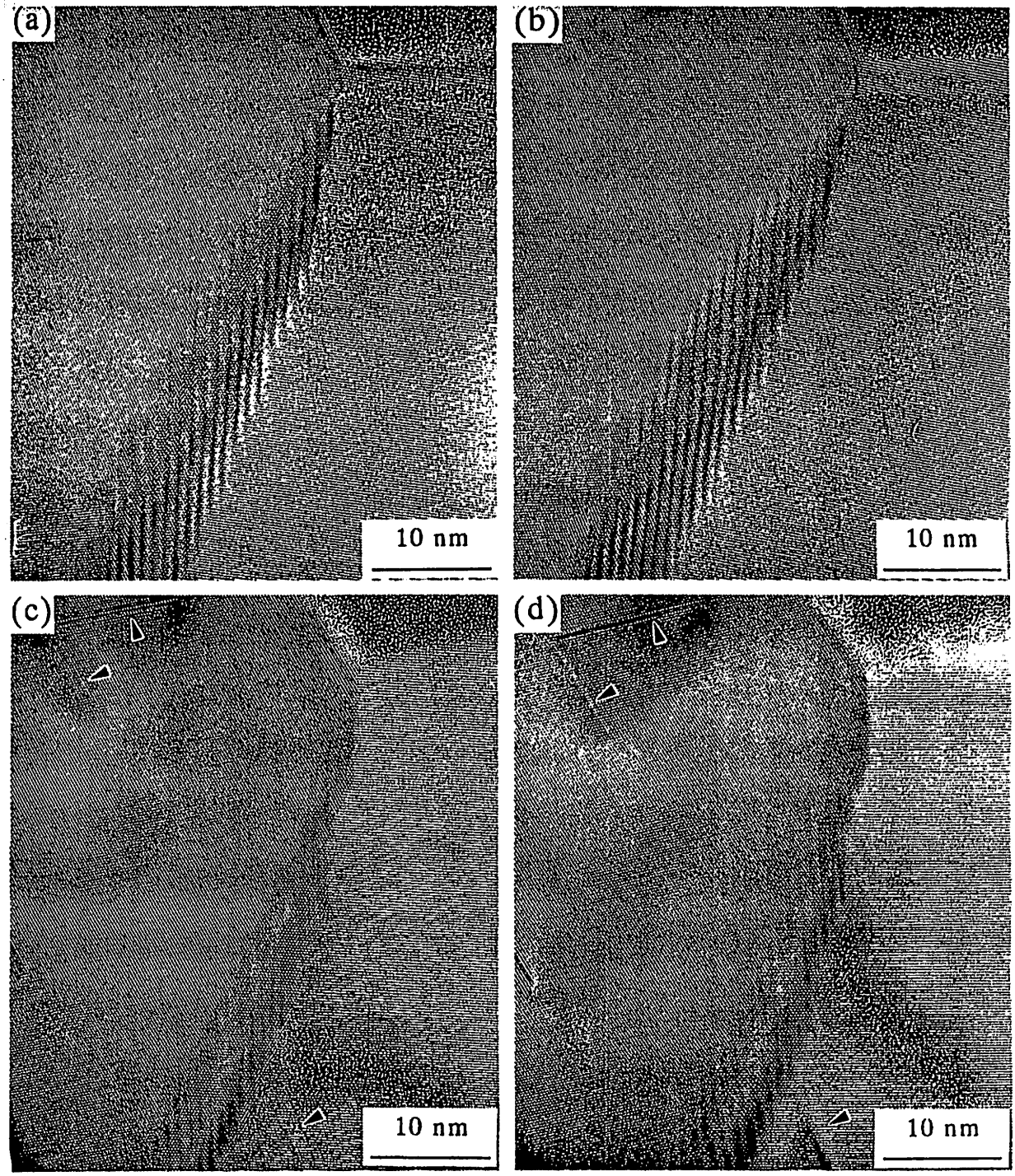

FIG. 4. Images recorded from (a) to (d) after every few minutes at current density 5.5mA/m², showing change in grain boundary configuration during observation.

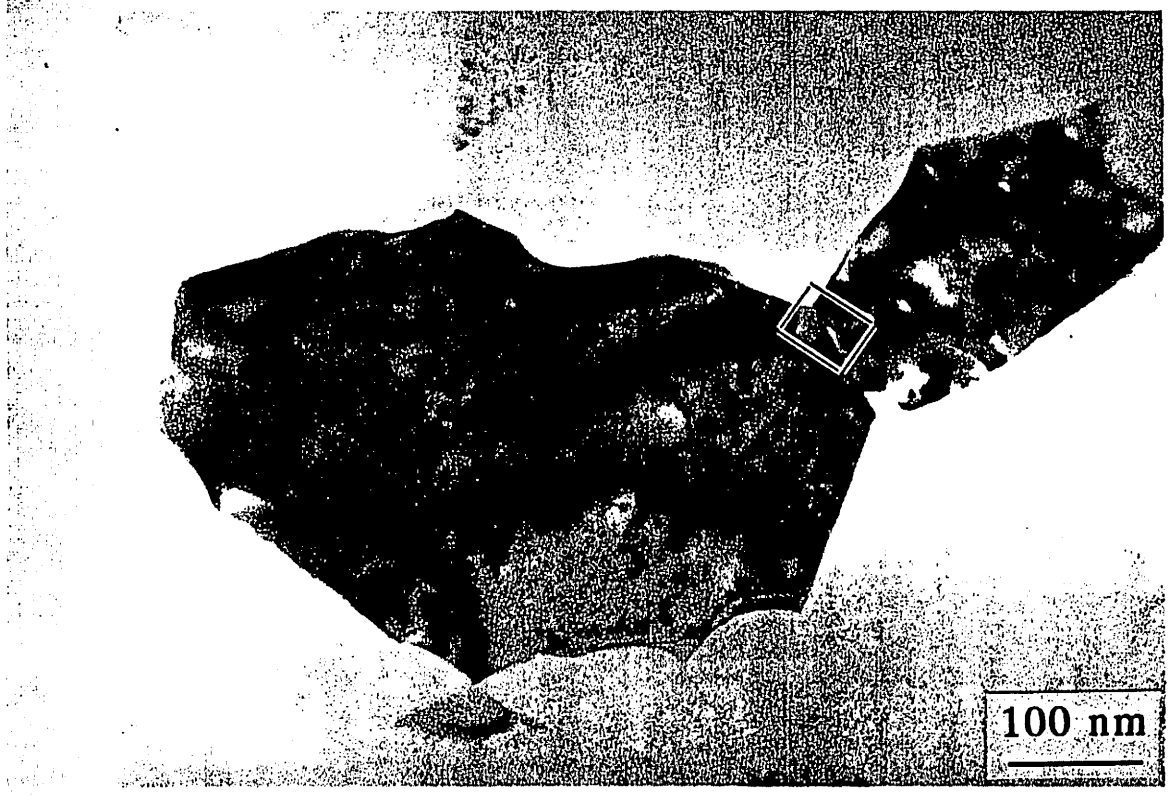

FIG. 5. General view of grains taken after images in Fig. 4(a–d). Region indicated by square corresponds to Fig. 4.

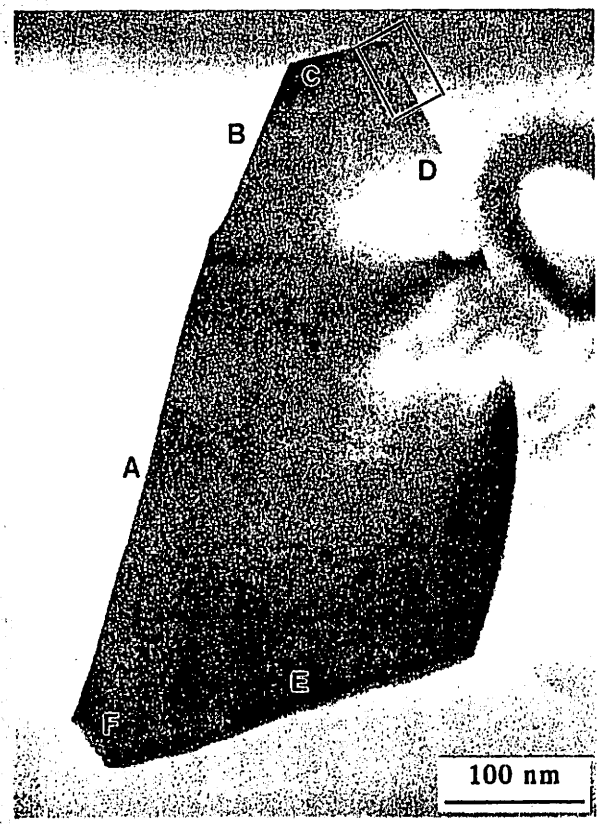

FIG. 6. High-magnification view of grain after annealing at 448K for 1 h. Region indicated by square on grain boundary D is enlarged in Fig. 7.

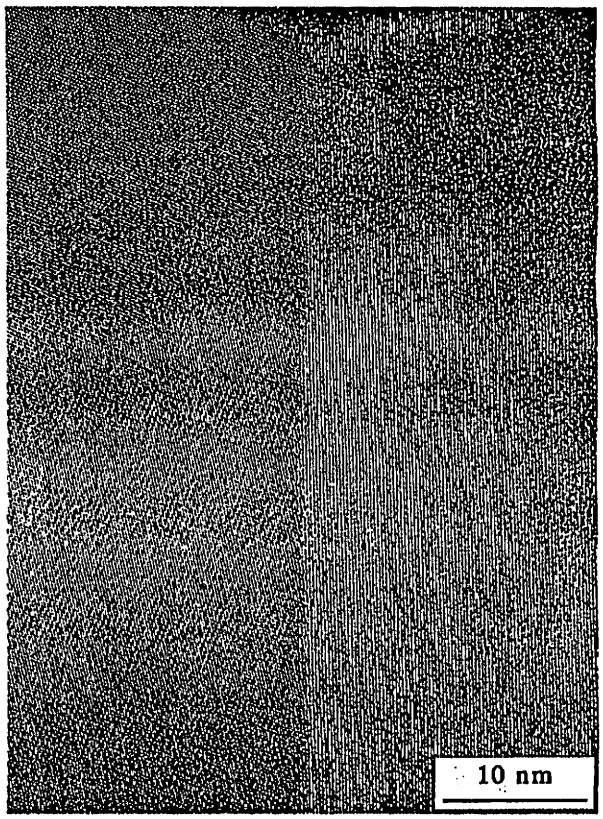

FIG. 7. Enlargement of region indicated by square on grain boundary D in Fig. 6.

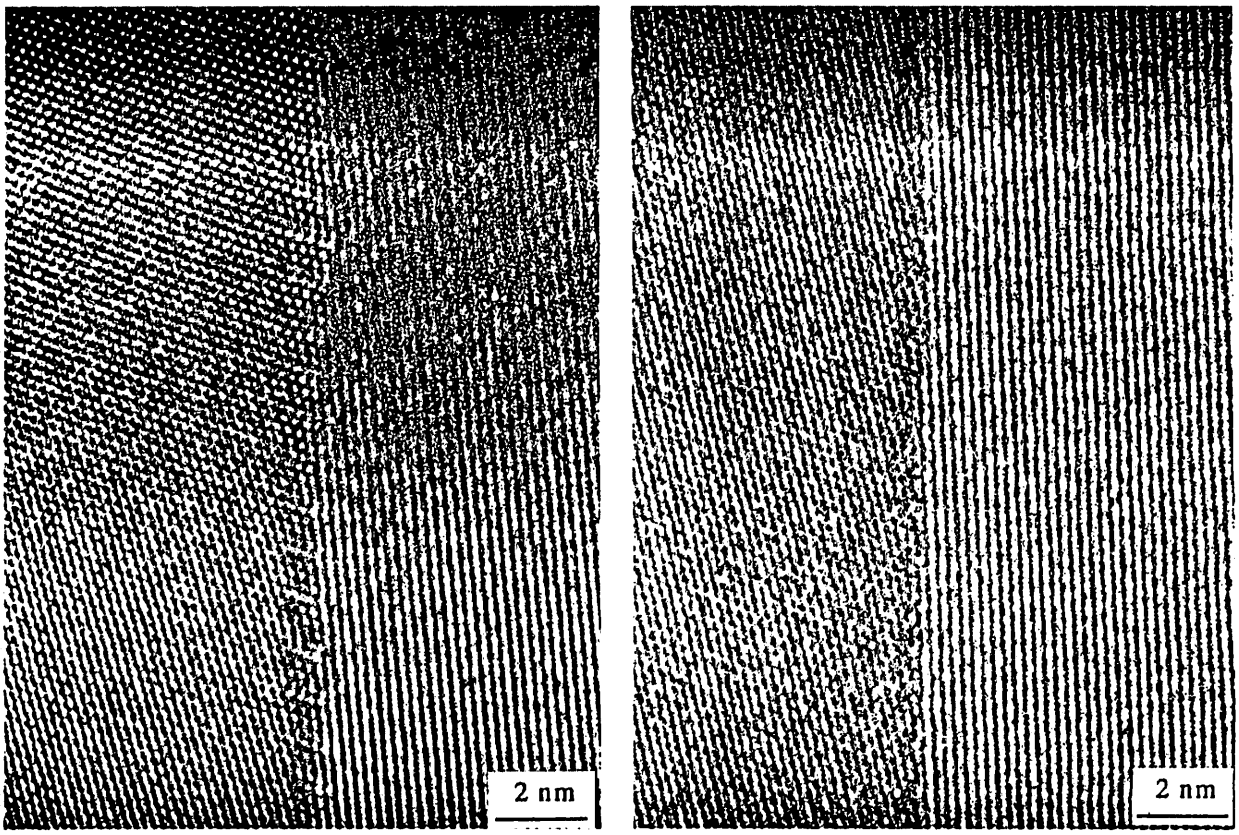

FIG. 8. Grain boundary lattice images (a) near and (b) away from triple point shown in Fig. 7.

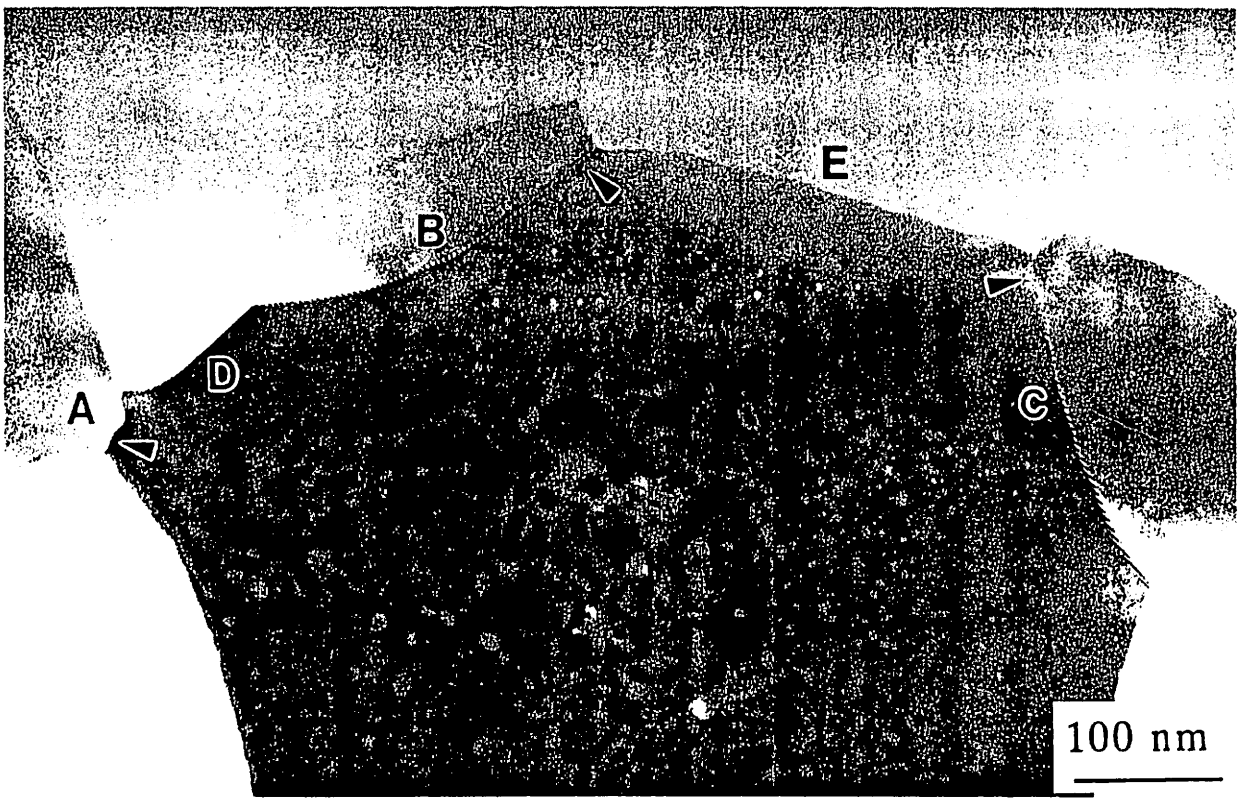

FIG. 9. High-magnification view of grain after annealing at 448K for 1 h. Grain boundary portions indicated by arrows on grain boundaries A, B, and C are enlarged in parts (a), (b), and (c), respectively, of Fig. 10.

~0.3nm, in the grain with two-dimensional lattice fringes. The grain boundary in Fig. 10(a) appears to be in a high-energy state despite the fact that the sample was annealed at 448K.

The lattice image in Fig. 10(b) reveals that the (111) lattice fringes in the grain on the right meet with those in the grain on the

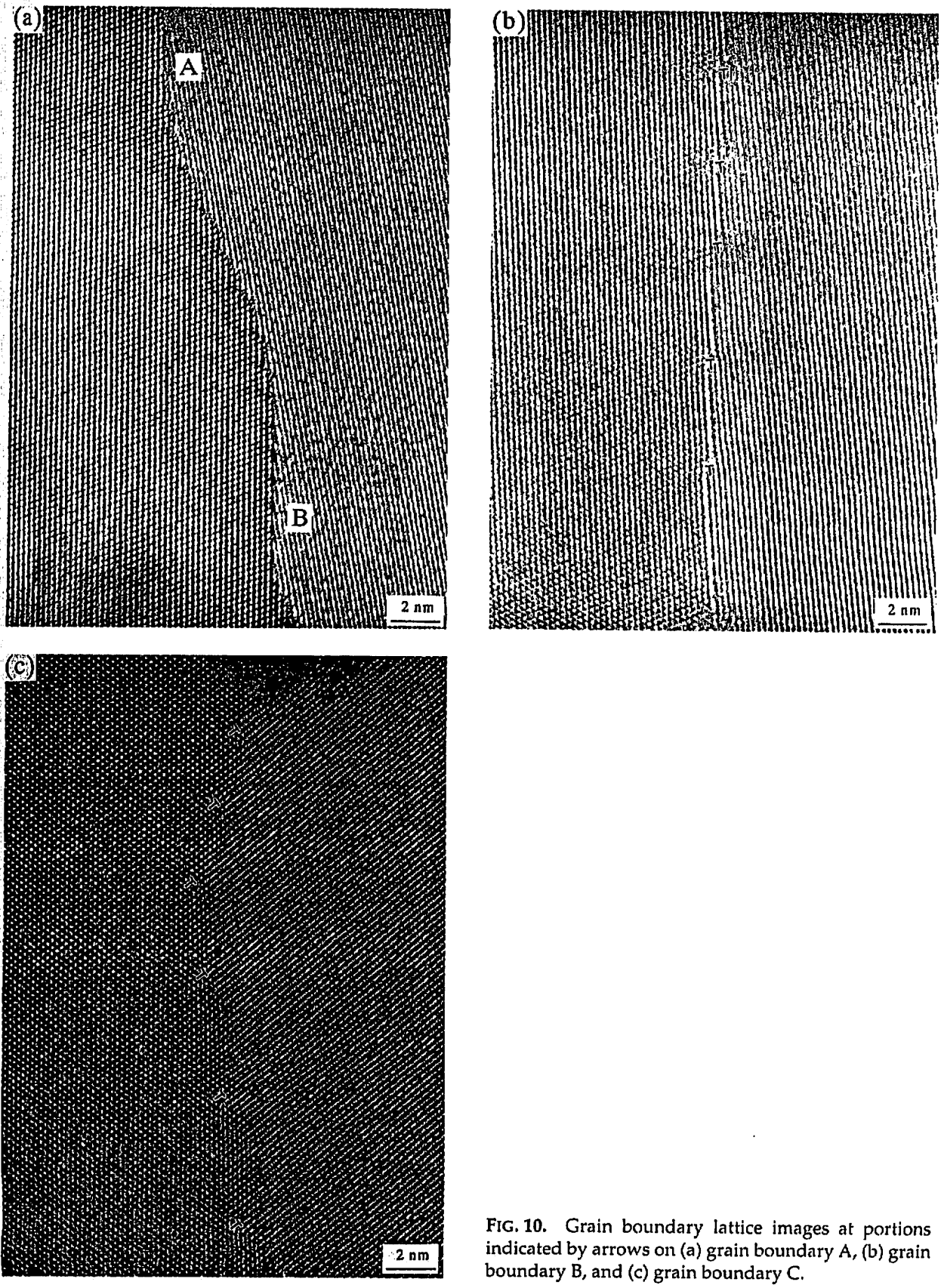

FIG. 10. Grain boundary lattice images at portions indicated by arrows on (a) grain boundary A, (b) grain boundary B, and (c) grain boundary C.

left at an angle of 3°. The grain boundary consists of an array of dislocations due to the terminations of (111) lattice fringes in the grain on the right at the points marked T. The grain boundary appears to be a low-angle grain boundary, but there must be a rotation of one grain with respect to the other about the axis perpendicular to the (111) lattice fringes of each grain because the one-dimensional fringes appear only in the grain on the left. The formation of a regular arrangement of facets and steps suggests that the grain boundary is in a high-energy state.

In Fig. 10(c), the (111) lattice fringes in the grain on the right meet with those in the grain on the left at an angle of 5°, and there are dislocations resulting from the terminations of (111) lattice fringes in the grain on the right at the points marked T. As in Fig. 10(b), grain rotation occurs about the axis perpendicular to the (111) lattice fringes of each grain. However, the grain boundary is not straight, unlike the boundary in Fig. 10(b). Thus, the grain boundary again appears to be in a high-energy state.

DISCUSSION

ELECTRON-IRRADIATION EFFECT

The formation of the planar defects shown in Fig. 4(c,d) demonstrates that the effect of electron irradiation is significant. However, examination of Fig. 4(a–d) reveals that the grain boundary structure tends to an equilibrium condition during electron irradiation. This indicates that the nonequilibrium character of the grain boundary structure observed at the initial stage of observation, as in Fig. 4(a), represents the image inherent or closer to the as-strained SMG structure. It also appears that the electron-irradiation effect should be rather minor when image observations are made quickly. Thus, whenever a nonequilibrium character of the grain boundary structure is observed, it is due not to electron irradiation but to the inherent nature of the SMG structures.

IMPORTANCE OF HIGH-RESOLUTION ELECTRON MICROSCOPY

The lower-magnification images shown in Fig. 1 reveal that the grain boundaries become smooth and well defined as the annealing temperature is increased. There are many smooth and well-defined grain boundaries visible in Fig. 1(c) of the sample annealed at 448K, corresponding to the onset of significant grain growth. However, the sample also contains some grain boundaries with a zigzag nature or bowed out between two neighboring grains. The present high-resolution electron microscopy observations have confirmed that the grain boundaries with a zigzag nature always exhibit nonequilibrium structures, but even those with a smooth and well-defined nature occasionally exhibit nonequilibrium structures when they are observed at a magnification at the atomic level, using high-resolution electron microscopy. It is therefore emphasized that high-resolution electron microscopy observations are important in evaluating the equilibrium nature of the grain boundary.

CONCLUSIONS

The grain boundaries in an as-strained SMG sample were generally curved, wavy, or inclined to the specimen surface normal and were in a high-energy nonequilibrium state. For the sample annealed at 448K for 1 h, corresponding to an onset of significant grain growth, there were many grain boundaries that were smooth and well defined. However, such grain boundaries did not always exhibit equilibrium structures when observed at a magnification at the atomic level.

Prolonged electron irradiation led to the formation of planar defects on {111} planes within the grains. However, during the electron irradiation, the grain boundaries changed to a more equilibrium condition, becoming smooth and, when inclined to the surface normal, becoming perpendicular to the surface. Thus, the nonequilibrium nature of the grain boundaries observed by

high-resolution electron microscopy represents the inherent structure of the boundaries in SMG materials.

This work was supported by the Light Metal Educational Foundation of Japan, the Grant-in-Aid for Scientific Research from the Ministry of Education, Science, Culture, and Sports of Japan, the National Science Foundation of the United States under Grants No. INT-9404693 and No. DMR-9115443. The Center for High Resolution Electron Microscopy at Arizona State University is supported by the National Science Foundation under Grant No. DMR-9314326.

References

1. V. M. Segal, V. I. Reznikov, A. E. Drobyshevskiy, and V. I. Koylov: Plastic working of metals by simple shear. *Izv. Akad. Nauk SSSR Metally* 1:115–123 (1981); English translation in *Russ. Metall. (Metally)* 1:99–105 (1981).
2. N. A. Smirnova, V. I. Levit, V. I. Pilyugin, R. I. Kuznetsov, L. S. Davydova, and V. A. Sazonova: Evolution of structure of f.c.c single crystals during strong plastic deformation. *Fiz. Met. Metalloved.* 61:1170–1177 (1986); English translation in *Phys. Met. Metall.* 61:127–134 (1986).
3. R. Sh. Musalimov and R. Z. Valiev: Dilatometric analysis of aluminum alloy with submicrometer grained structure. *Scr. Metall. Mater.* 27:1685–1690 (1992).
4. R. Z. Valiev, A. V. Korznikov, and R. R. Mulyukov: Structure and properties of ultra-fine grained materials produced by severe plastic deformation. *Mater. Sci. Eng.* A168:141–148 (1993).
5. V. M. Segal: Materials processing by simple shear. *Mater. Sci. Eng.* A197:157–164 (1995).
6. R. Z. Valiev and R. Sh. Musalimov: High-resolution transmission electron microscopy of nanocrystalline materials. *Phys. Met. Metall.* 78:666–670 (1994).
7. J. Wang, Z. Horita, M. Furukawa, M. Nemoto, N. K. Tsenev, R. Z. Valiev, Y. Ma, and T. G. Langdon: An investigation of ductility and microstructural evolution in an Al-3%Mg alloy with submicron grain size. *J. Mater. Res.* 8:2810–2818 (1993).
8. Z. Horita, D. J. Smith, M. Furukawa, M. Nemoto, R. Z. Valiev, and T. G. Langdon: Investigation of grain boundaries in submicrometer-grained Al-Mg solid solution alloys using high-resolution electron microscopy. *J. Mater. Res.* 11:1880–1890 (1996).
9. J. Wang, Y. Iwahashi, Z. Horita, M. Furukawa, M. Nemoto, R. Z. Valiev, and T. G. Langdon: An investigation of microstructural stability in an Al-Mg alloy with submicrometer grain size. *Acta Mater.* 44:2973–2982 (1996).
10. Z. Horita, D. J. Smith, M. Furukawa, M. Nemoto, R. Z. Valiev, and T. G. Langdon: Effect of annealing on grain boundary structure in submicrometer-grained Al-3%Mg alloy observed by high-resolution electron microscopy. *Ann. Chim.* 21:417–425 (1996).
11. R. Z. Valiev, N. A. Krasilnikov, and N. K. Tsenev: Plastic deformation of alloys with submicron-grained structure. *Mater. Sci. Eng.* A137:35–40 (1991).
12. A. Wolfenden, Near threshold electron damage in aluminum: purity effects. *Radiat. Eff.* 21:197–199 (1974).

Received June 1996; accepted June 1996.

Proceedings of ReX'96, the Third International Conference on Recrystallization and Related Phenomena
Edited by Terry R. McNelley
ReX'96 International Advisory Board and Organizing Committee, 1997

RECRYSTALLIZATION IN ULTRAFINE-GRAINED MATERIALS WITH NON-EQUILIBRIUM GRAIN BOUNDARIES

Minoru Furukawa*, Zenji Horita, Minoru Nemoto****
Ruslan Z. Valiev*** and Terence G. Langdon******

*Department of Technology, Fukuoka University of Education, Munakata, Fukuoka 811-41, Japan

**Department of Materials Science and Engineering, Faculty of Engineering, Kyushu University, Fukuoka 812-81, Japan

***Institute of Physics of Advanced Materials, Ufa State Aviation Technical University, Ufa 450000, Russia

****Departments of Materials Science and Mechanical Engineering, University of Southern California, Los Angeles, CA 90089-1453, U.S.A.

ABSTRACT

It is now established that an ultrafine grain size may be achieved by subjecting a material to intense plastic straining through procedures such as equal-channel angular pressing and torsion straining. However, the grain boundaries in these materials are often in a high energy non-equilibrium configuration. This paper describes experiments conducted to examine the role of microstructural evolution in an Al-3% Mg solid solution alloy after the introduction of an ultrafine grain size. The results show that grain evolution occurs with two distinct activation energies depending upon whether the material is in an unrecrystallized or recrystallized condition.

INTRODUCTION

There is considerable current interest in the development of materials with ultrafine grain sizes in the submicrometer or nanometer range. These materials have a potential for numerous industrial applications including superplastic forming at relatively high strain rates [1]. Several techniques are now available for fabricating materials with ultrafine grain sizes but the use of intense plastic straining provides the opportunity of attaining large bulk samples without the presence of any residual porosity. This paper reviews some recent observations on the structure and microstructural stability of an ultrafine-grained Al-Mg alloy where it was possible to achieve grain sizes as small as ~90 nm.

TECHNIQUES FOR INTENSE PLASTIC STRAINING

Two techniques were used to produce samples having an ultrafine grain size: these techniques are illustrated schematically in Fig. 1. Figure 1(a) depicts the process of equal-channel angular (ECA) pressing [2], in which a polycrystalline material is pressed, under a load P, through a die consisting of two channels of equal cross-section intersecting at an angle of Φ and subtending an angle of Ψ at the outer arc of curvature where the two channels intersect. The test material, shown shaded in Fig. 1(a), is machined so that it fits tightly within the die, and the die is designed so that repetitive pressings of a single sample can be used to attain a high level of strain. It can be shown that a total strain of ε_N is accumulated after N separate pressings through the die, where ε_N is given by [3]

$$\varepsilon_N = \frac{N}{\sqrt{3}}\left[2\cot\left(\frac{\Phi}{2}+\frac{\Psi}{2}\right)+\Psi\,\mathrm{cosec}\left(\frac{\Phi}{2}+\frac{\Psi}{2}\right)\right] \qquad (1)$$

Figure 1(b) illustrates the principle of torsion straining [4], where a small sample in the form of a disk, typically having a diameter of ~15 mm, is subjected to intense plastic deformation by torsion straining under a high pressure. For this procedure, the imposed strain is equal to $\ln(\phi r/\ell)$, where ϕ is the angle of rotation in radians and r and ℓ are the diameter and thickness of the disk, respectively.

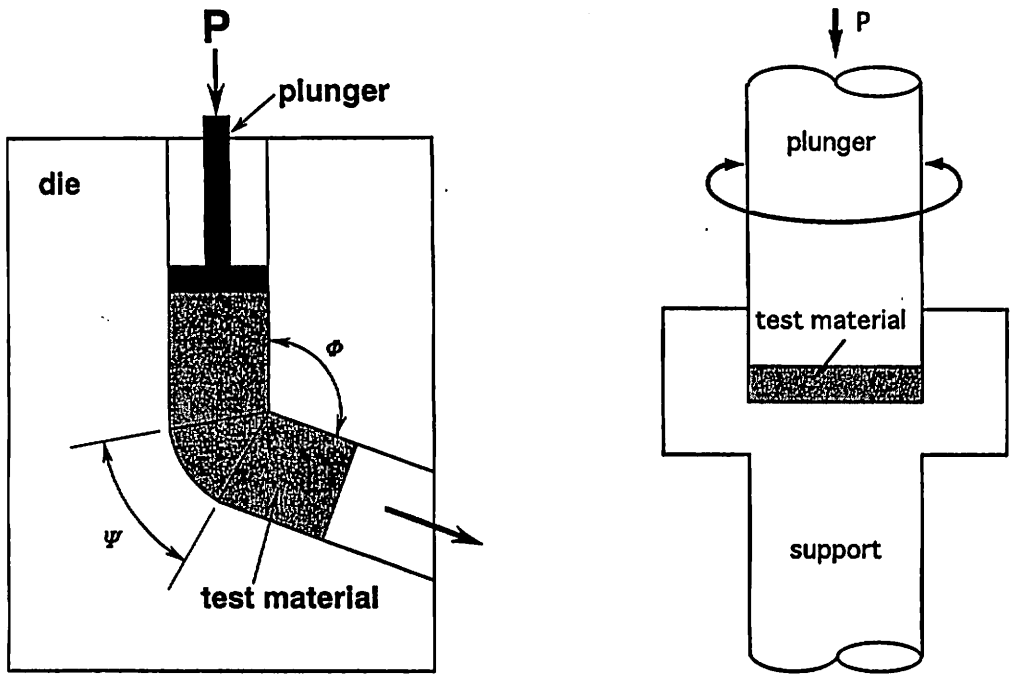

Fig. 1 Schematic illustration of the procedures of (a) equal-channel angular (ECA) pressing and (b) torsion straining under high pressure.

AS-FABRICATED MATERIAL

The experiments were conducted using a hot-rolled Al-3% Mg solid solution alloy with an initial grain size of ~500 μm. Samples of the alloy were subjected to ECA pressing or torsion straining at room temperature to total strains in the range from ~4 to ~7. Full details are given elsewhere of the procedures employed for ECA pressing [5] and torsion straining [6].

Figure 2 shows an example of the microstructure in the Al-Mg alloy after ECA pressing, together with selected area electron diffraction patterns taken from regions A, B and C using a diameter of 1.9 μm [7]. Inspection showed that the microstructure after ECA pressing was very heterogeneous, with areas of reasonably equiaxed grains (as at A) and areas of elongated grains (as at C) separated by transition regions (as at B). It is apparent from inspection of the selected area electron diffraction patterns that there are large misorientations between the individual grains and the pronounced azimuth spreading is evidence for the presence of large internal stresses in the as-fabricated material. Detailed measurements gave an average grain size of ~0.2 μm: further information on the microstructural measurements were given earlier [8].

Figure 3 shows the typical microstructure achieved after torsion straining, plus selected area electron diffraction patterns taken from areas A, B and C using a diameter of 1.3 μm [7]. For these conditions, the as-fabricated microstructure was reasonably uniform and there were large misorientations across the grain boundaries. The average grain size of the microstructure shown in Fig. 3 is ~90 nm.

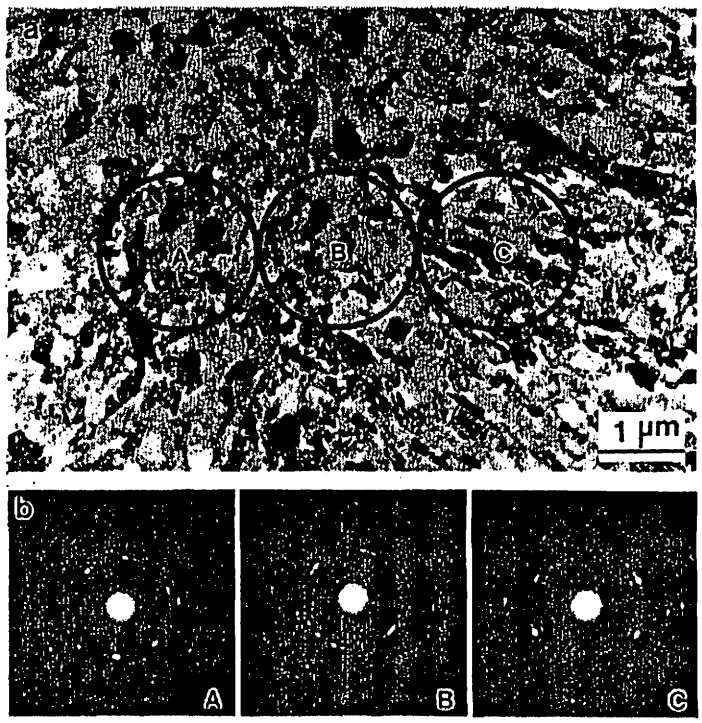

Fig. 2 As-fabricated condition after ECA pressing: (a) microstructure and (b) selected area electron diffraction patterns from regions A, B and C.

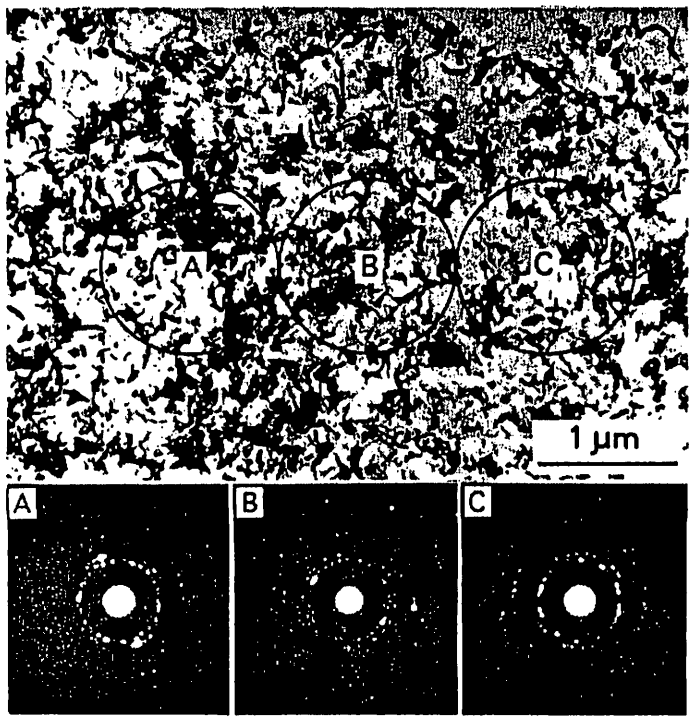

Fig. 3 As-fabricated condition after torsion straining: (a) microstructure and (b) selected area electron diffraction patterns from regions A, B and C.

Detailed microstructural inspection of the Al-3% Mg alloy subjected to intense plastic straining by ECA pressing revealed that many of the grain boundaries are poorly defined and appear essentially as diffuse transition zones between highly deformed grains [8]. These observations suggest that the grain boundaries are in a non-equilibrium configuration. Therefore, to investigate the grain boundary structure in more detail, extensive observations were conducted with high resolution electron microscopy and using Al-Mg alloys prepared with the torsion straining technique: full details of these observations are given elsewhere [6].

Figure 4 shows a transmission electron micrograph of a typical grain in the Al-3% Mg alloy after torsion straining to a strain of ~7: the selected area electron diffraction pattern corresponds to a [110] grain orientation. The grain boundaries surrounding this grain appear to be curved or wavy along their lengths and there is evidence for corrugations of the boundaries in the regions labelled A and B. These corrugations are more evident in the higher magnification micrographs shown in Figs 5 (a) and (b), representing boundary regions A and B in Fig. 4, respectively. In Fig. 5, there are two-dimensional lattice fringes corresponding to the [011] orientation on the left and one-dimensional lattice fringes from the (200) systematic reflections on the right. In Fig. 5(a), the grain boundary exhibits a periodic and stepwise arrangement of facets parallel to (100), with each facet consisting of four or five layers of (111) planes. Close inspection of Fig. 5(a) revealed a region adjacent to the grain boundary, having a thickness of ~5 nm, where there was significant lattice distortion and evidence for the presence of dislocations: some examples of terminated lattice fringes are designated by the letter T on the

Fig. 4 A typical grain in the as-fabricated condition after torsion straining: selected area electron diffraction pattern corresponds to a [110] grain orientation.

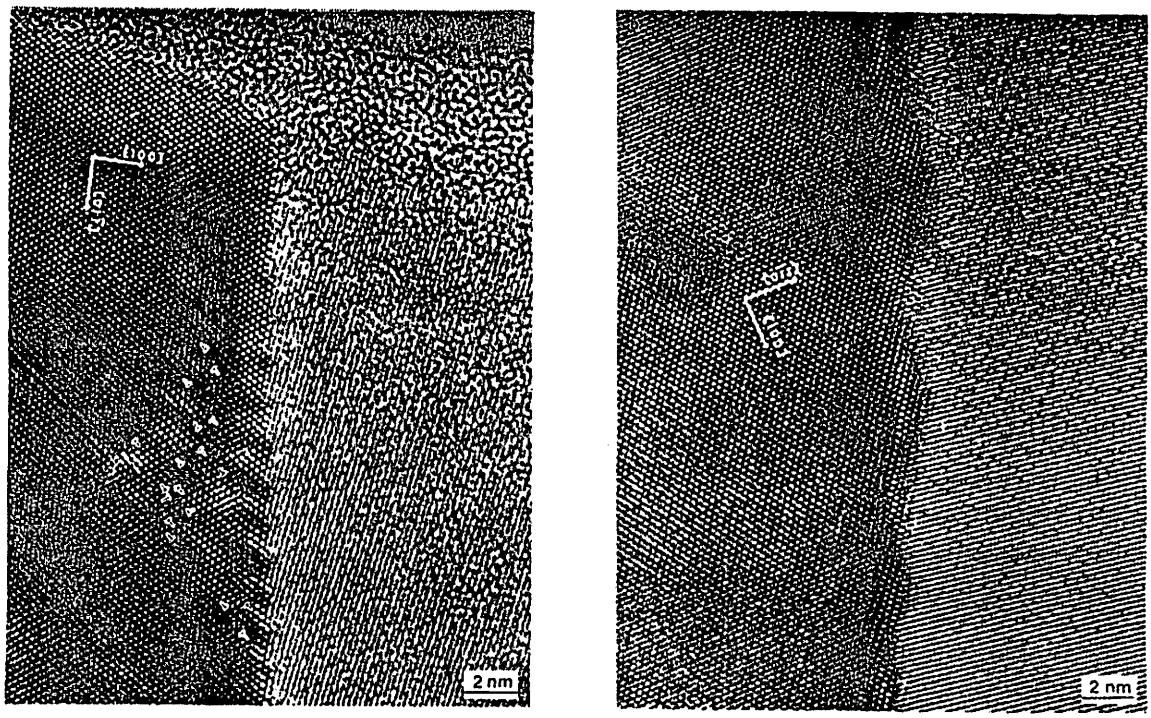

(a) (b)

Fig. 5 Enlargements of grain boundaries at (a) region A and (b) region B in Fig 4, showing wavy and facetted nature of the boundaries.

left of the grain boundary in Fig. 5(a). It is important to note that the presence of some lattice dilatation adjacent to the grain boundaries appears to be a consistent feature of ultrafine-grained materials produced by intense plastic straining techniques [9]. In Fig. 5(b), taken from region B of Fig. 4, it is apparent that the grain boundary has a distinct zigzag configuration. Measurements of the facet densities in the boundary regions at A and B of Fig. 4 gave values of $\sim 10^9$ and $\sim 2 \times 10^8$ m^{-1}, respectively.

From these observations, it is concluded that the grain boundaries of the ultrafine-grained Al-3% Mg alloy produced by intense plastic straining are in a high-energy non-equilibrium configuration when examined in the as-fabricated condition. Furthermore, narrow regions adjacent to the grain boundaries show significant distortions and the presence of many lattice dislocations. It is therefore appropriate to examine the role of static annealing in promoting microstructural evolution and the development of a more equilibrated structure.

THE INFLUENCE OF STATIC ANNEALING

Static annealing experiments were conducted in which samples of the ultrafine-grained Al-3% Mg alloy were held at the selected annealing temperature for 1 hour and then quenched in iced water: further information on the results of these experiments are given elsewhere for samples processed by ECA pressing [5,10] and torsion straining [7].

Figure 6 shows examples of the microstructures visible after static annealing at different temperatures for samples processed by (a) ECA pressing and (b) torsion straining. For both processing procedures, it is apparent that (i) there is significant grain growth at the higher annealing temperatures and (ii) there is an evolution into a more equilibrated microstructure as the annealing temperature is increased. In the samples subjected to ECA pressing, shown in Fig. 6(a), there is a gradual increase in grain size such that, at an annealing temperature of 503 K, there is a duplex structure consisting of areas of unrecrystallized grains and areas where recrystallization appears to be essentially complete. This duplex structure is visible also at 533 K, but at higher annealing temperatures the material was fully recrystallized and the microstructure consisted of a uniform distribution of grains separated by high angle equilibrated grain boundaries. A similar microstructural evolution occurred also in the material subjected to torsion straining, as shown in Fig. 6(b), except that the structure in the as-fabricated condition was more uniform, as shown in Fig. 3, and there was no temperature range where there was evidence of a duplex structure of recrystallized and unrecrystallized grains. For both processing routes, the effect of static annealing is an evolution in microstructure from an array of grains containing large internal stresses delineated by non-equilibrium boundaries to an equilibrated structure of reasonably large and relatively dislocation-free grains surrounded by high angle grain boundaries having an equilibrium configuration. Figure 7 shows the growth of the average grain size as a function of the annealing temperature, demonstrating that growth occurs rapidly at temperatures above ~ 500 K.

The microstructural evolution visible in this work has characteristics, including grain growth and dislocation annihilation, which are similar to the observations of continuous dynamic recrystallization reported during the straining of, for example, a pre-worked superplastic 7075 aluminum alloy [11] and a microduplex stainless steel [12]. However, the present evolution is

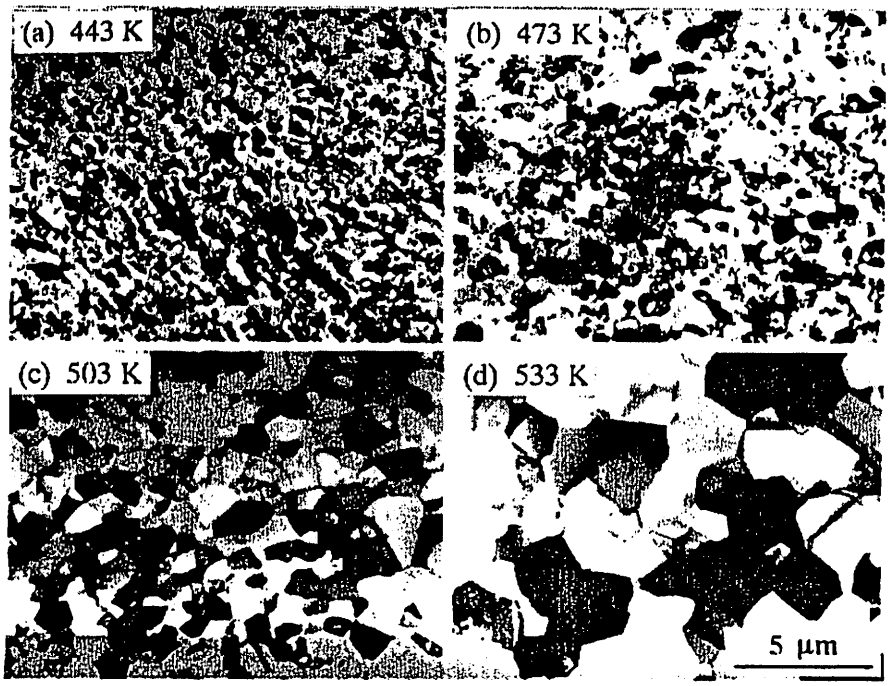

(a)

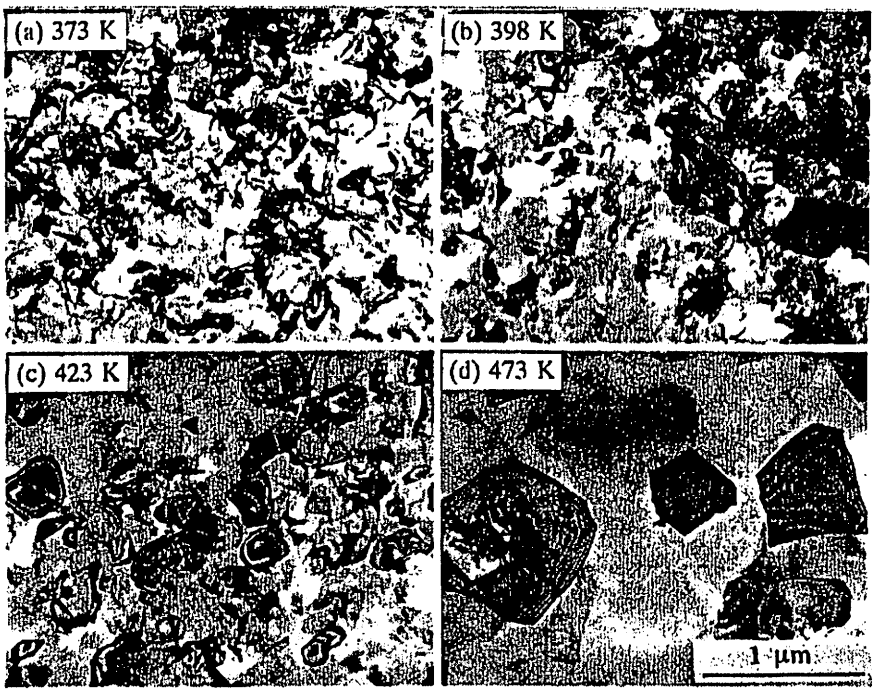

(b)

Fig. 6 Microstructures after static annealing for 1 hour after (a) ECA pressing and (b) torsion straining.

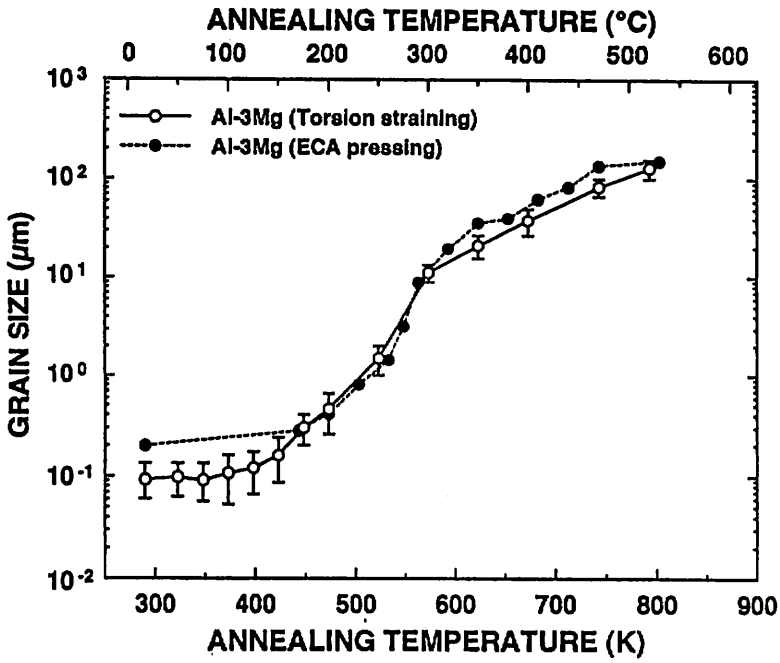

Fig. 7 Variation of grain size with annealing temperature for Al-3% Mg processed by torsion straining or ECA pressing.

different because it occurs under static conditions and it is a direct consequence of thermal activation and the initial non-equilibrium microstructure of the material. Therefore, it is appropriate to designate this process *continuous static recrystallization.*

MICROHARDNESS MEASUREMENTS

The Vickers microhardness, Hv, was measured for each sample after static annealing and Fig. 8 shows the variation of Hv (in kg mm^{-2}) with the annealing temperature for the samples processed using torsion straining or ECA pressing: the error bars denote the total range on seven separate measurements recorded for Hv under each condition. Inspection shows that both materials exhibit a similar trend except only that the individual values of Hv are significantly higher at the lower annealing temperatures for the material subjected to torsion straining because of the smaller grain size in this material (i.e. grain sizes of ~ 0.09 μm after torsion straining and ~ 0.2 μm after ECA pressing). Contrary to earlier reports for an ultrafine-grained Al-1.5% Mg alloy [13] and nanocrystalline Pd [14], there is no evidence for an initial increase in the microhardness at the lower annealing temperatures. Instead, Hv remains reasonably constant up to an annealing temperature of ~ 400 K, and then it decreases to ~ 600 K and remains essentially constant up to the highest annealing temperature of ~ 800 K.

The yield stress of a material is generally related to the grain size, d, through the Hall-Petch equation, and this approach can be extended to the hardness of a material through the expression

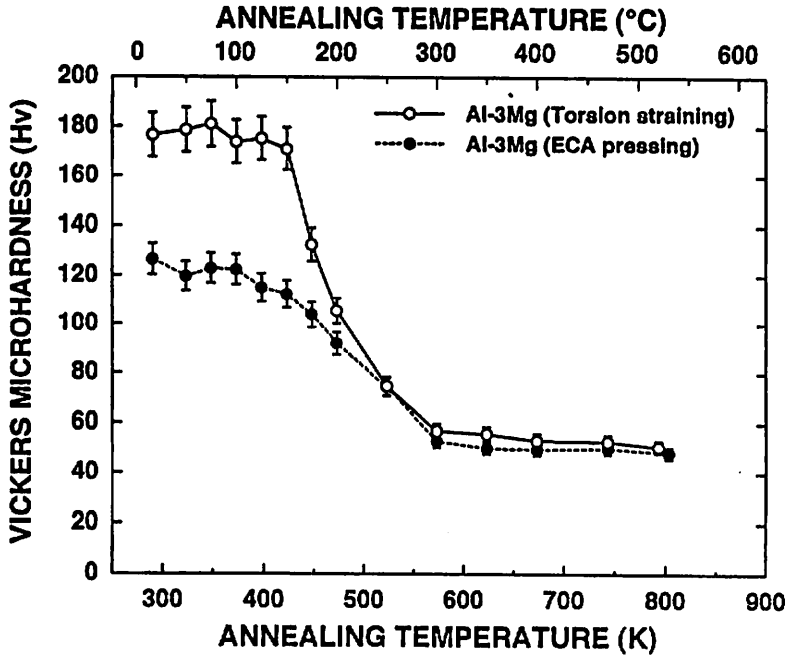

Fig. 8 Variation of Vickers microhardness with annealing temperature for Al-3% Mg processed by torsion straining and ECA pressing.

$$Hv = H_o + k_H d^{-1/2} \qquad (2)$$

where H_o and k_H are constants associated with the hardness measurements.

Figure 9 shows a plot of Hv versus $d^{-1/2}$ for the samples processed by torsion straining or ECA pressing, respectively, with the datum points for the torsion strained material extending to the smallest grain size of ~ 0.09 μm. After ECA pressing, all datum points lie along a single line which is given by equation (2) with H_o = 46 Hv and k_H = 35 Hv $\mu m^{1/2}$. After torsion straining, the datum points also approximate to a straight line with H_o = 47.5 Hv and k_H = 41 Hv $\mu m^{1/2}$ and with the lines of minimum and maximum slope giving values for H_o of 44.5 Hv and 52 Hv and values for k_H of 32.5 Hv $\mu m^{1/2}$ and 52 Hv $\mu m^{1/2}$, respectively.

Closer examination of the experimental datum points for the material processed by torsion straining suggests that, although there is no evidence for the occurrence of a negative slope in the Hall-Petch plot at the smallest grain sizes developed in this investigation, nevertheless the data suggest a possible decrease in slope at grain sizes below ~ 0.15 μm. This possibility is examined in more detail elsewhere and it is proposed that the slope may decrease in the Hall-Petch plot at very small grain sizes because of the movement of extrinsic dislocations in the non-equilibrium grain boundaries during the impingement of the hardness indenter [7]. Thus, it is concluded that there will be a tendency to underestimate the matrix hardness in ultrafine-grained materials if the grain boundaries are in a non-equilibrium configuration.

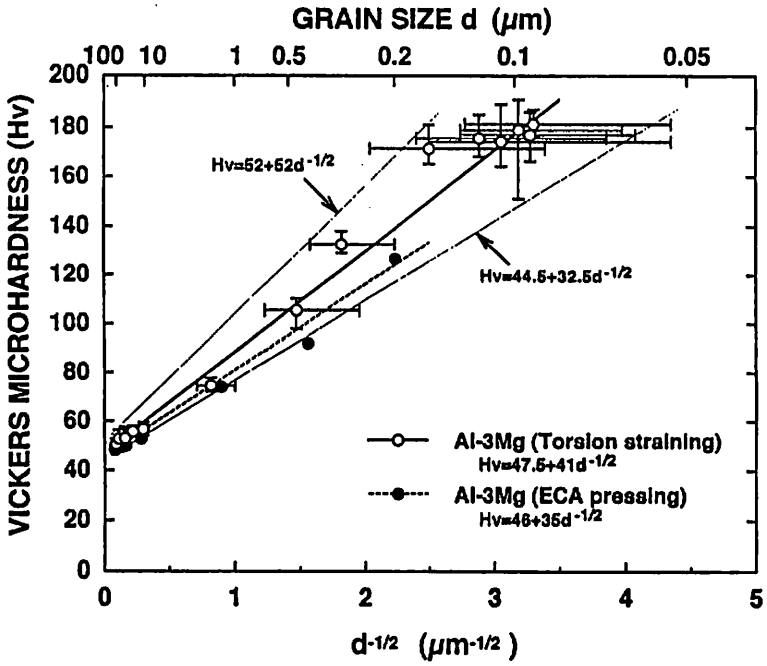

Fig. 9 Vickers microhardness versus the reciprocal of the square root of the grain size for Al-3% Mg processed by torsion straining and ECA pressing.

Grain growth data are usually represented by a relationship of the form

$$d^2 - d_o^2 = k_g t^n \qquad (3)$$

where d and d_o are the instantaneous and initial grain sizes, respectively, t is the time, n is a constant which is usually taken as unity and k_g incorporates the dependence on temperature through an activation energy, Q. Taking the values of d_o as the smallest grain sizes observed experimentally, Fig. 10 shows plots of (d^2 - d_o^2) versus the reciprocal of the absolute temperature for samples processed using either (a) ECA pressing or (b) torsion straining, respectively.

In plotting the data after ECA pressing, a clear distinction is made between the unrecrystallized and recrystallized areas occurring in the duplex structure observed at temperatures of ~500 - 550 K: as noted earlier, no duplex structure was visible in the material processed by torsion straining where the microstructure was more uniform. In both materials, the activation energy is ~85 - 90 kJ mol^{-1} in the recrystallized condition and this is consistent with the value anticipated for grain boundary diffusion in pure Al (~86 kJ mol^{-1} [15]). However, the activation energies in the unrecrystallized condition are ~25 kJ mol^{-1}, and these low values are of the order of ~0.2 Q_ℓ where Q_ℓ is the activation energy for lattice self-diffusion in pure Al [15]. These very low values for the activation energy are attributed to the occurrence of high atomic mobility in the non-equilibrium grain boundaries which make up the microstructure at these smallest grain sizes [16,17].

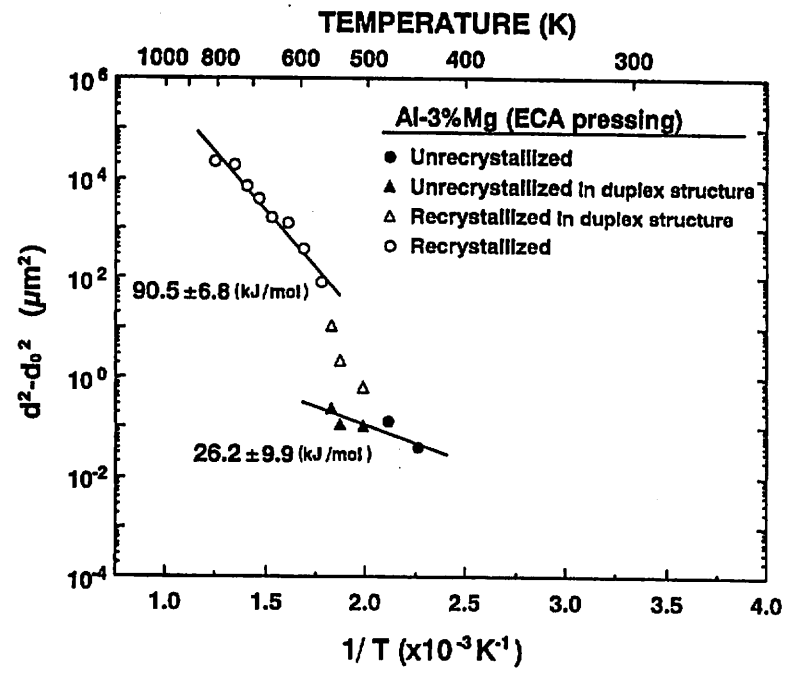

(a)

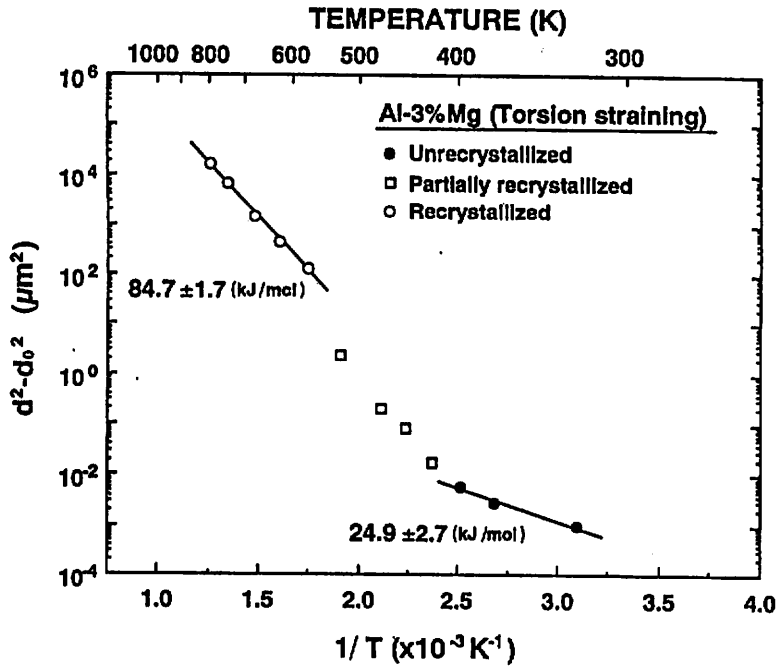

(b)

Fig. 10 Semi-logarithmic plot of (d^2 - d_o^2) versus the reciprocal of absolute temperature for Al-3% Mg processed by (a) ECA pressing and (b) torsion straining.

SUMMARY AND CONCLUSIONS

Ultrafine grain sizes, down to ~90 nm, were produced in an Al-3% Mg alloy using two different intense plastic straining techniques. Inspection showed that the grain boundaries in the as-fabricated materials were in a high energy non-equilibrium configuration. The microstructure evolved into an equilibrated structure during static annealing in a process designated *continuous static recrystallization*. Grain evolution occurred with two different activation energies depending upon whether the material was in an unrecrystallized or recrystallized condition.

ACKNOWLEDGEMENTS

This work was supported by the Light Metals Educational Foundation of Japan, a Grant-in-Aid for Scientific Research from the Ministry of Education, Science, Sports and Culture of Japan, the U.S. Army Research Office under Grant No. DAAH04-96-1-0332 and the National Science Foundation of the United States under Grant No. INT-9404693.

REFERENCES

1. Y. Ma, M. Furukawa, Z. Horita, M. Nemoto, R.Z. Valiev and T.G. Langdon, Mater. Trans. JIM, 37, 1996, p. 336.
2. N.A. Akhmadeev, V.I. Kopylov, R.R. Mulyukov and R.Z. Valiev, Izvest. Akad. Nauk SSSR, Metally, 5, 1992, p. 96.
3. Y. Iwahashi, J. Wang, Z. Horita, M. Nemoto and T.G. Langdon, Scripta Metall., 35, 1996, p. 143.
4. N.A. Smirnova, V.I. Levit, V.I. Pilyugin, R.I. Kuznetsov, L.S. Davydova and V.A. Sazonova, Fiz. Metall. Metalloved., 61, 1986, p. 1170.
5. J. Wang, Y. Iwahashi, Z. Horita, M. Furukawa, M. Nemoto, R.Z. Valiev and T.G. Langdon, Acta Mater., 44, 1996, p. 2973.
6. Z. Horita, D.J. Smith, M. Furukawa, M. Nemoto, R.Z. Valiev and T.G. Langdon, J. Mater. Res., 11, 1996, p. 1880.
7. M. Furukawa, Z. Horita, M. Nemoto, R.Z. Valiev and T.G. Langdon, Acta Mater., 44, 1996, p. 4619.
8. J. Wang, Z. Horita, M. Furukawa, M. Nemoto, N.K. Tsenev, R.Z. Valiev, Y. Ma and T.G. Langdon, J. Mater. Res., 8, 1993, p. 2810.
9. R.Z. Valiev and R.Sh. Musalimov, Phys. Metals Metallogr., 78, 1994, p. 666.
10. J. Wang, M. Furukawa, Z. Horita, M. Nemoto, R.Z. Valiev and T.G. Langdon, Mater. Sci. Eng., A216, 1996, p. 41.
11. X. Yang, H. Miura and T. Sakai, Mater. Trans. JIM, 37, 1996, p. 1379.
12. K. Tsuzaki, X. Huang and T. Maki, Acta Mater., 44, 1996, p. 4491.
13. R.Z. Valiev, F. Chmelik, F. Bordeaux, G. Kapelski and B. Baudelet, Scripta Metall. Mater., 27, 1992, p. 855.
14. J.R. Weertman and P.G. Sanders, Solid State Phenom., 35-36, 1994, p. 249.
15. F.A. Mohamed and T.G. Langdon, Metall. Trans., 5, 1974, p. 2339.
16. R.Z. Valiev, E.V. Kozlov, Yu.F. Ivanov, J. Lian, A.A. Nazarov and B. Baudelet, Acta Metall. Mater., 42, 1994, p. 2467.
17. J. Lian, R.Z. Valiev and B. Baudelet, Acta Metall. Mater., 43, 1995, p. 4165.

Pergamon

PII: S1359-6454(97)00120-1

Acta mater. Vol. 45, No. 11, pp. 4751–4757, 1997
Acta Metallurgica Inc.
Published by Elsevier Science Ltd
Printed in Great Britain
1359-6454/97 $17.00 + 0.00

STRUCTURAL EVOLUTION AND THE HALL–PETCH RELATIONSHIP IN AN Al–Mg–Li–Zr ALLOY WITH ULTRA-FINE GRAIN SIZE

MINORU FURUKAWA[1], YOSHINORI IWAHASHI[2], ZENJI HORITA[2], MINORU NEMOTO[2], NIKOLAI K. TSENEV[3], RUSLAN Z. VALIEV[4] and TERENCE G. LANGDON[5]

[1]Department of Technology, Fukuoka University of Education, Munakata, Fukuoka 811-41, [2]Department of Materials Science and Engineering, Kyushu University, Fukuoka 812-81, Japan, [3]Institute of Chemical Technology, Ufa State Petroleum Technical University, Ufa 450062, [4]Institute of Physics of Advanced Materials, Ufa State Aviation Technical University, Ufa 450000, Russia and [5]Departments of Materials Science and Mechanical Engineering, University of Southern California, Los Angeles, CA 90089-1453, U.S.A.

(Received 20 September 1996; accepted 26 February 1997)

Abstract—Experiments were conducted on an Al–5.5% Mg–2.2% Li–0.12% Zr alloy to investigate the feasibility of introducing an ultra-fine grain size using equal-channel angular (ECA) pressing and of retaining an ultra-fine grain size at elevated temperatures. It is shown that ECA pressing is capable of reducing the grain size from an initial value of $\sim 400\,\mu m$ to a value of $\sim 1.2\,\mu m$. However, the microstructure after ECA pressing is heterogeneous, with many areas of equiaxed grains having high angle grain boundaries and some regions of subgrains with boundaries having low angles of misorientation. Unlike earlier experiments on Al–Mg binary alloys, it is demonstrated that the grain size of the Al–Mg–Li–Zr alloy is reasonably stable up to temperatures as high as ~ 700 K because of the presence in the matrix of a fine dispersion of β'-Al_3Zr precipitates. Microhardness data confirm the Hall–Petch relationship for grain sizes above $\sim 2\,\mu m$ produced by annealing at temperatures above ~ 673 K, but the Hall–Petch relationship breaks down at smaller grain sizes because of variations in the volume fraction of the δ'-Al_3Li precipitates. © *1997 Acta Metallurgica Inc.*

1. INTRODUCTION

Equal-channel angular (ECA) pressing is an established processing technique in which a polycrystalline metal is pressed through a die to achieve a very high plastic strain [1], thereby providing the capability of producing an ultra-fine grain size in the material [2, 3]. This procedure has several advantages over more conventional techniques for the fabrication of materials with ultra-fine grain sizes, such as inert gas condensation [4], high energy ball milling [5] or sliding wear [6], because it is capable of yielding large samples which are free from any residual porosity and readily amenable for mechanical testing and forming operations.

Earlier reports described the fabrication of an ultra-fine-grain size in an Al–3% Mg solid solution alloy using ECA pressing [7], and it was demonstrated that, in an alloy with an initial grain size of $\sim 400\,\mu m$, it was possible to attain an ultra-fine grain size of $\sim 0.2\,\mu m$. Subsequent reports on this alloy described the microstructural stability during static annealing [8], the role of grain growth [9] and the variation of the microhardness with grain size through the Hall–Petch relationship [10].

An important limitation associated with the development of ultra-fine grain sizes in materials such as the Al–3% Mg solid solution alloy is the occurrence of grain growth at elevated temperatures. Specifically, experiments over a wide range of temperatures led to the conclusion that a temperature of the order of 500 K, close to one-half of the absolute melting temperature, represented essentially an upper limit for any utilization of the ultra-fine grained Al–3% Mg alloy in, for example, superplastic forming operations [8]. As a result of these difficulties, the retention of an ultra-fine grain size at superplastic forming temperatures has been identified as the major challenge in any future attempts to commercially utilize the ECA pressing technique [11].

The present investigation was initiated in an attempt to overcome this limitation by using a representative commercial alloy where it may be possible to retain an ultra-fine grain size at elevated temperatures because of the presence of precipitates. Experiments were conducted to investigate the microstructural characteristics associated with the ECA pressing of an Al–Mg–Li–Zr alloy containing a fine dispersion of δ'-Al_3Li and β'-Al_3Zr. This alloy

was selected because of the well-established need to develop a superplastic forming capability in Al–Li alloys at relatively low temperatures, of the order of ~600–700 K, in order to avoid problems associated with Li or Mg depletion [12]. As will be demonstrated, the results from this investigation confirm that it is possible to retain an ultra-fine grain size in this alloy, within the micrometer range, up to temperatures as high as ~ 700 K (equivalent to ~ 0.75 T_m, where T_m is the absolute melting temperature), thereby establishing the utility of this processing technique for the preparation of materials which may be useful for superplastic forming operations.

2. EXPERIMENTAL

The experiments were conducted using a light-weight high strength alloy fabricated in Russia and having a chemical composition of Al–5.5% Mg–2.2% Li–0.12% Zr: this alloy has a designation of 01420 [13].

The alloy was received in the form of a hot-rolled plate and microscopic examination revealed an as-received grain size of ~ 400 μm. A cylindrical sample was cut from the plate for ECA pressing with a diameter of 50 mm and a length of ~ 100 mm. The ECA pressing was performed in air at a temperature of 673 K using a facility similar to that described earlier [8] and with an angle of intersection between the two channels of 90°. The sample was air cooled after ECA pressing and repetitive pressings were conducted up to an equivalent true plastic strain of ~ 3.7.

Following ECA pressing, small samples, having dimensions of 3 × 3 × 4.7 mm^3, were cut from near the center of the pressed material and these samples were annealed in an argon atmosphere for 1 h at various temperatures in the range from 323 to 833 K and then quenched in iced water. After annealing, small discs with a thickness of ~ 200 μm were cut from the annealed samples for examination by transmission electron microscopy (TEM). These discs were ground mechanically to a thickness of ~ 150–180 μm and then thinned to perforation using a twin-jet electropolishing unit and a solution of 10% $HClO_4$, 20% $C_3H_8O_3$ and 70% C_2H_5OH at a temperature of 278 K. Specimens were examined using an Hitachi H-8100 electron microscope operating at 200 kV. Selected area electron diffraction (SAED) patterns were obtained from different regions having diameters of 13 μm. Average grain sizes were measured from TEM photomicrographs by separately identifying and measuring the dimensions of at least 50 different grains. The volume fractions of grains with high and low angle boundaries were estimated by taking SAED patterns along linear traverses in the TEM over total distances of > 100 μm.

The Vickers microhardness, Hv (in kg/mm^{-2}), was measured on each sample after the annealing treatment using an Akashi MVK-E3 microhardness tester with a diamond pyramidal indentor. The values reported for Hv represent the average of seven separate measurements taken at randomly selected points using a load of 50 g for 15 s.

3. RESULTS

3.1. Microstructure initially and after ECA pressing

In the as-received hot rolled condition, the average grain size was very large, of the order of ~ 400 μm, and inspection showed that the grains were elongated along the rolling direction and contained heavily strained subgrains having an average size of ~ 2–4 μm. After annealing samples of the hot rolled material for 1 h at 743 K (corresponding to ~ 0.8 T_m), the grains remained elongated along the rolling direction, there was no clear evidence for any grain growth but the measured average subgrain size increased to ~ 3–7 μm.

By contrast, Fig. 1(a) shows an example of the microstructure of the Al–Mg–Li–Zr alloy after ECA pressing and Fig. 1(b) demonstrates that the selected area electron diffraction patterns taken from regions A and B do not exhibit the net patterns indicative of low angle boundaries but rather the spots are distributed around circles showing the presence of high angle grain boundaries. Examination of Fig. 1(a) therefore reveals an essentially homogeneous microstructure consisting of an array of reasonably equiaxed grains, separated by high angle boundaries, with an average grain size which was measured as ~ 1.2 μm.

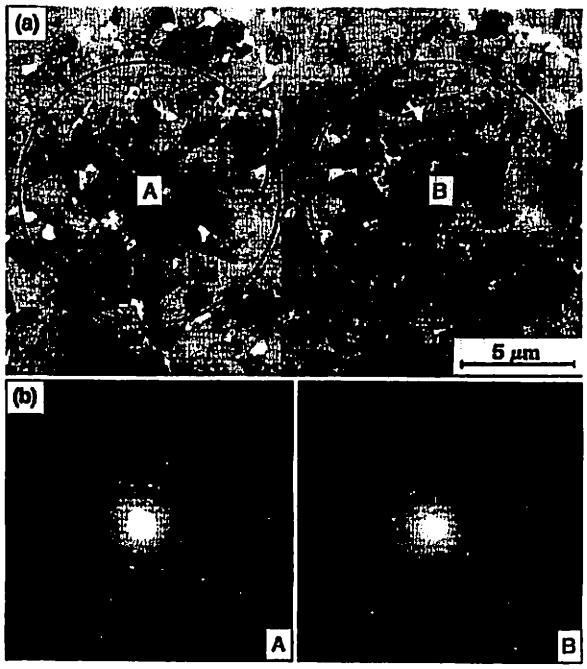

Fig. 1. (a) Microstructure after ECA pressing and (b) selected area electron diffraction patterns from areas A and B.

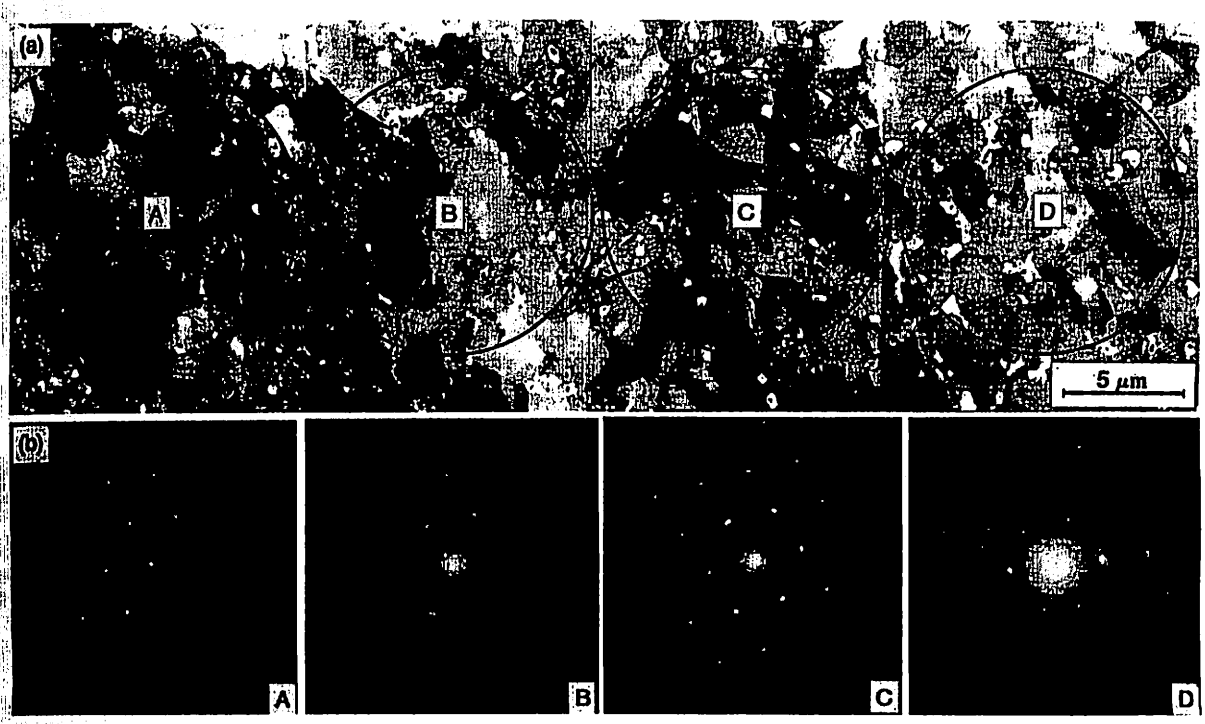

Fig. 2. (a) An example of heterogeneity after ECA pressing with a region of sub-grains and (b) selected area electron diffraction patterns from areas A, B, C and D.

Close inspection revealed two important differences in the present alloy by comparison with the earlier investigation of the Al–3% Mg alloy. First, following ECA pressing the grain size in the Al–Mg–Li–Zr alloy ($\sim 1.2\ \mu m$) is slightly but significantly larger than in the Al–3% Mg alloy ($\sim 0.2\ \mu m$) [7]. Second, the grain boundaries in the Al–Mg–Li–Zr alloy, as evident in Fig. 1(a), are more clearly defined than in the Al–3% Mg alloy where the boundaries were rather diffuse [7]. It was shown earlier that the diffuse boundaries introduced by plastic straining in Al–Mg binary alloys are in a high energy non-equilibrium condition with the presence of many extrinsic dislocations [14], thereby suggesting that the grain boundaries in the Al–Mg–Li–Zr alloy are closer to an equilibrium configuration. Although no detailed experiments were conducted to determine the precise influence of temperature on the microstructures produced in Al-based alloys by ECA pressing, it is reasonable to conclude that this difference in the nature of the grain boundaries arises because the Al–Mg–Li–Zr alloy was pressed at 673 K whereas the Al–3% Mg alloy was pressed at room temperature. It was shown earlier, using a Zn–22% Al alloy, that intense plastic straining at a reasonably high homologous temperature permits a relaxation of the high internal stresses introduced into the ultra-fine grained structure during processing, thereby favoring the development of an array of grain boundaries in a quasi-equilibrium condition [15].

Figure 1 suggests the presence of a homogeneous microstructure throughout the alloy but more extensive observations revealed the presence of some areas of heterogeneity where there were arrays of sub-grain boundaries having low angles of misorientation. An example is shown in Fig. 2 where region D, as revealed by the SAED pattern, is similar to the microstructure in Fig. 1 but regions A, B and C contain arrays of sub-grain boundaries. Careful and extensive microstructural observations after ECA pressing led to estimates of volume fractions of $\sim$ 60–70% for grains with high angle boundaries and $\sim$ 30–40% for grains with low angle boundaries. Generally, these subgrains were contained within regions having diameters of the order of 10–20 μm and the measured average subgrain size ($\sim 1.2\ \mu m$) was identical to the measured grain size.

An additional example of the ECA pressed microstructure is provided by the dark field image in Fig. 3(a) showing a uniform distribution of very fine δ'-Al_3Li precipitates: Fig. 3(b) is the [110] net pattern

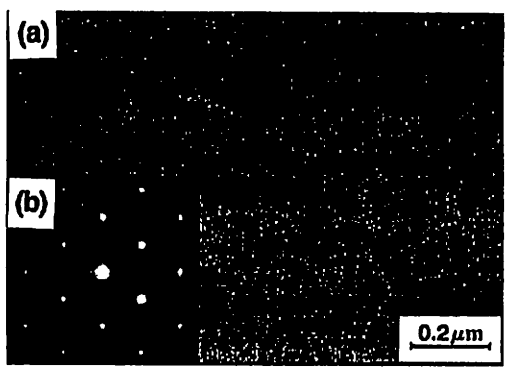

Fig. 3. (a) Dark field image showing uniform distribution of very fine δ'-Al_3Li precipitates and (b) [110] net pattern containing Ll_2 superlattice reflection.

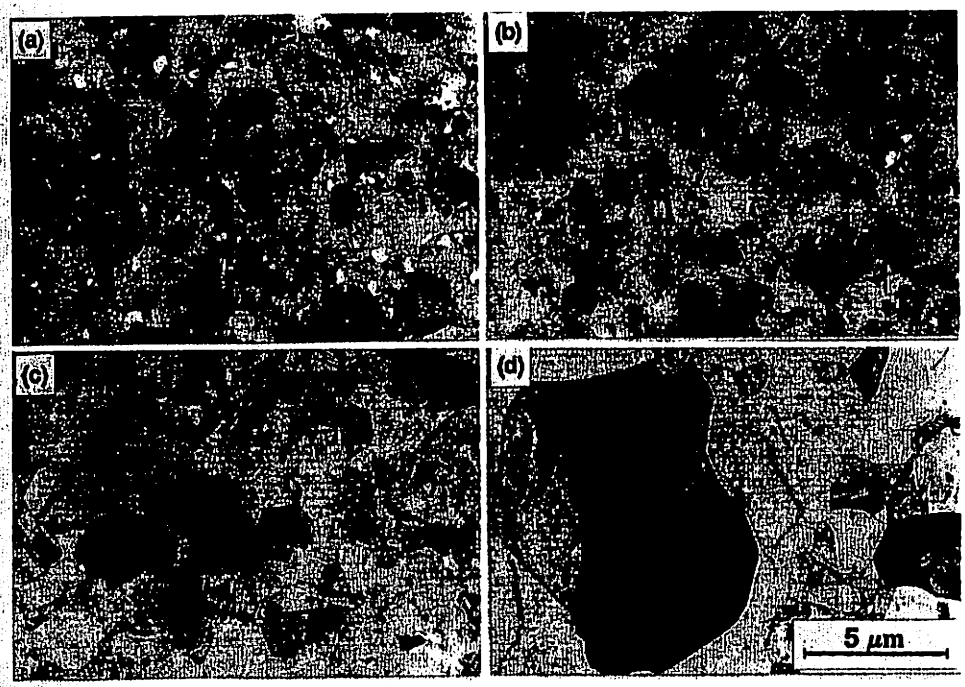

Fig. 4. Microstructures (a) after ECA pressing and (b)–(d) after annealing for 1 h at 573, 673 and 793 K, respectively.

containing the Ll_2 superlattice reflection. It follows from the Al–Li binary alloy phase diagram [16, 17] that ~2.2% Li is in solution in the Al matrix at 673 K and subsequently a small fraction of Li precipitates during cooling as a metastable δ'-Al_3Li phase with the Ll_2 structure [16, 18]. In addition, it has been established that Zr may precipitate as a metastable β'-Al_3Zr phase after rapid cooling from a liquid state and subsequent ageing at ~673 K [19, 20]: the latter phase has the same Ll_2 structure as δ'-Al_3Li and in practice it is difficult to distinguish between the β'-Al_3Zr phase and the δ'-Al_3Li phase in dark field images using a superlattice reflection.†

3.2. *Microstructural evolution during static annealing*

Samples were annealed for 1 h at various temperatures up to 833 K and examples of the microstructures are shown in Fig. 4(a) after ECA pressing but without annealing and (b)–(d) after annealing at 573, 673 and 793 K, respectively. Inspection shows that the grain size after annealing at 573 K is almost identical to the ECA pressed condition [Fig. 4(b)], and this effect continues at 673 K but with a slight additional increase in the average grain size to ~1.6 μm and with some smoothing of many of the grain boundaries [Fig. 4(c)]. However, there is a very obvious change after annealing at 793 K where the microstructre consists of both recrystallized and unrecrystallized grains [Fig. 4(d)].

†This difficulty arises not only because the β' and δ' phases both have the same Ll_2 structure but also because their lattice constants are very similar and the Zr content was only 0.12% for the Al–Mg–Li–Zr alloy used in the present investigation.

The average grain size was measured after each annealing condition and Fig. 5 shows the variation of the grain size with annealing temperature for the Al–Mg–Li–Zr alloy subjected to ECA pressing in this investigation and for the Al–3% Mg solid solution alloy investigated ealier after ECA pressing [8] together with experimental data reported for Al–3% Mg [10] and Al–1.5% Mg [21] alloys where an ultra-fine grain size was introduced by torsion straining. It is clear from this plot that the Al–Mg–Li–Zr alloy behaves very differently from the Al–Mg binary alloys: whereas grain growth occurs fairly rapidly in the binary alloys at temperatures in the vicinity of ~500 K, the grains of the Al–Mg–Li–Zr alloy are stable up to temperatures of the order of

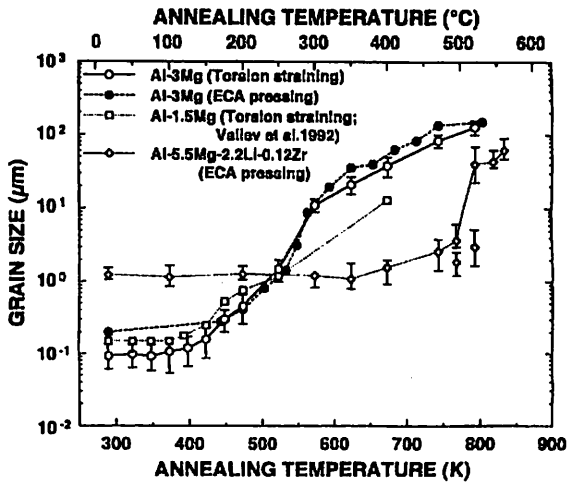

Fig. 5. Variation of average grain size with annealing temperature, including data for an Al–3% Mg alloy after ECA pressing [8] and Al–3% Mg [10] and Al–1.5% Mg [21] alloys after torsion straining.

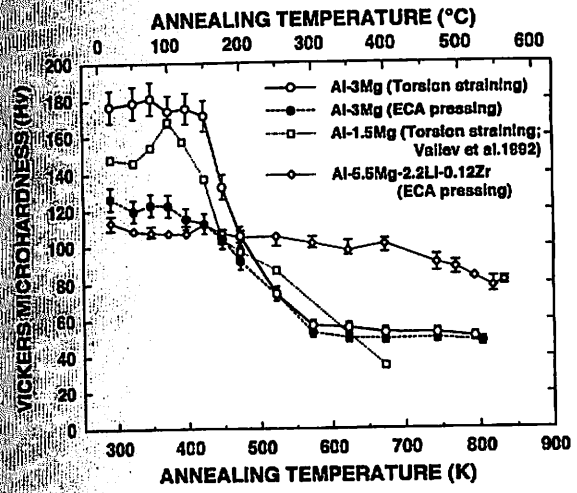

Fig. 6. Vickers microhardness vs annealing temperature for the Al–Mg–Li–Zr alloy and Al–Mg binary alloys [10, 21].

~ 700 K and there is significant grain growth, to sizes outside of the normal superplastic range (> 10 μm), only at temperatures above ~ 750 K.

To evaluate the microstructural characteristics in more detail, a specimen was carefully examined after annealing for 1 h at a temperature of 743 K (~ 0.8 T_m): this temperature was selected because, as shown in Fig. 5, it is close to the apparent upper limiting temperature for a grain size within the superplastic forming range (≤ 10 μm). Inspection showed that the microstructure of this specimen was heterogeneous with a volume fraction of ~ 10% of recrystallized grains having sizes up to ~ 30 μm and with ~ 90% by volume of unrecrystallized grains consisting of approximately one-third by volume of grains with low angle boundaries having average sizes in the range of ~ 3–7 μm and two-thirds by volume of grains with large angle boundaries having an average size of ~ 3 μm. By contrast, detailed inspection of a specimen annealed for 1 h at the highest annealing temperature of 833 K revealed a well-defined and homogeneous microstructure consisting of large equiaxed grains with high angle grain boundaries and with no evidence for the presence of any subgrains: the average grain size in this latter condition was ~ 60 μm.

3.3. *Microhardness measurements*

Figure 6 plots the Vickers microhardness against the annealing temperature for the Al–Mg–Li–Zr alloy and for the other three materials documented ealier in Fig. 5 [10, 21]. Inspection shows that the microhardness of the Al–Mg–Li–Zr alloy is lower than for the Al–Mg binary alloys at temperatures up to ~ 400 K and this difference is due to the higher pressing temperature for the Al–Mg–Li–Zr alloy which leads to a larger initial grain size. Nevertheless, there is only a very small decrease in the hardness of the Al–Mg–Li–Zr alloy up to ~ 700 K but thereafter the decrease is more rapid because of the associated increase in grain size (Fig. 5). The values of Hv for the Al–Mg–Li–Zr alloy are higher than for the Al–Mg alloys at all annealing temperatures above ~ 500 K because of the very rapid increase in grain size in the binary alloys.

3.4. *Validity of the Hall–Petch relationship*

The hardness of a material is generally related to the grain size through a Hall–Petch equation of the form [22, 23]:

$$Hv = H_0 + k_H d^{-1/2}, \quad (1)$$

where d is the grain size and H_0 and k_H are constants associated with the hardness measurements.

In practice, however, care must be exercised in making use of equation (1) for the present data because the alloy was cooled in air after ECA pressing so that δ'-Al_3Li precipitates are present in the ECA pressed material, as revealed in Fig. 3(a). It is anticipated that these precipitates are lost when annealing at high temperatures, above ~ 673 K, and the subsequent quench in iced water will permit only a very minor reprecipitation of the δ' phase. By contrast, there will be a change in the volume fraction of δ' precipitates at annealing temperatures below ~ 673 K because at these lower temperatures the δ' precipitates are only partially dissolved [24]. The effect on Hv of a variation in the volume fraction of δ'-Al_3Li is revealed by the experimental data in Table 1 where, for increasing annealing temperatures up to 623 K, there is clear evidence for a systematic decrease in the values of Hv but with no corresponding increase in the measured grain size.

It is anticipated the the δ' precipitates will be fully dissolved into the Al matrix when annealing at temperatures above ~ 673 K and, in addition, the amount of δ' reprecipitating on quenching will be small and essentially identical for all specimens. Thus, at annealing temperatures above ~ 673 K, corresponding to grain sizes above ~ 2 μm, all of the specimens are in a similar structural state and the Hall–Petch relationship should apply. This conclusion is confirmed in Fig. 7 which shows a plot of Hv vs $d^{-1/2}$ for the Al–Mg–Li–Zr alloy plus the three additional materials documented in Figs 5 and 6 [10, 21]: the error bars on each experimental point denote the range in the measured individual values of Hv and d, respectively. Although the datum points for the Al–Mg–Li–Zr alloy extend over a smaller range of grain sizes than for the binary alloys, the

Table 1. Microhardness, Hv, and measured grain size, d, after annealing for 1 h at temperatures up to 623 K

Annealing temperature (K)	Hv	d (μm)
After ECA pressing with no anneal	113.3	1.24
373	107.0	1.16
473	104.7	1.28
573	101.5	1.22
623	97.6	1.10

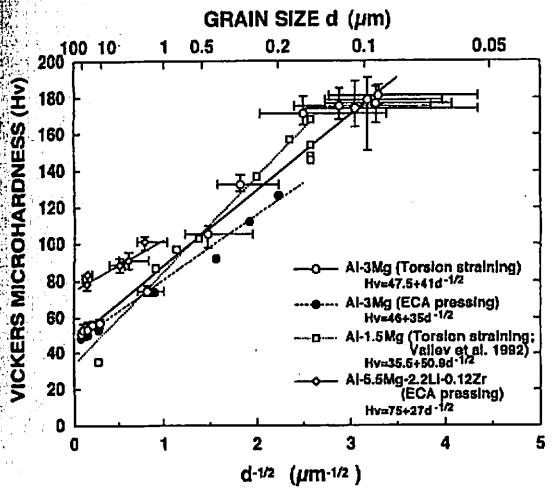

Fig. 7. Vickers microhardness vs $d^{-1/2}$ for the Al–Mg–Li–Zr alloy and Al–Mg binary alloys [10, 21].

limited data are consistent with equation (1) with $H_0 \simeq 75\ Hv$ and $k_H \simeq 27\ Hv\ \mu m^{1/2}$.

4. DISCUSSION

Aluminium–lithium alloys are attractive for structural applications, especially in the aerospace industry, because of their low density and high stiffness [25, 26], but the lack of significant ductility was generally considered a major disadvantage in the early development of the alloys [27]. A considerable effort was therefore initiated in order to improve the deformation characteristics of these alloys and this work has shown that, with appropriate processing treatments, it is possible to achieve high, and even superplastic, ductilities in several Al–Li alloys [28]. As a result of these findings, much attention has been devoted to developing methods of attaining very fine grain sizes in Al–Li alloys which may be amenable for superplastic forming operations.

Fine grain sizes, up to $\sim 10\ \mu m$ in size, are generally obtained in Al–Li alloys either by static recrystallization prior to superplastic deformation [29, 30] or by the occurrence of dynamic recrystallization during deformation under superplastic conditions [31, 32]. More recently, major attempts have been made to develop appropriate thermo-mechanical treatments which will give fine-grained structures capable of producing superplastic ductilities [12, 33, 34]. In practice, a very significant difficulty associated with these studies is the ultimate attainment of an array of high angle grain boundaries rather than an array of low angle sub-boundaries [12, 34]. The presence of boundaries with high angles of misorientation is generally considered an important prerequisite for high tensile ductility because grain boundary sliding, which requires high angle boundaries, is the dominant flow process during superplastic deformation [35].

In the present work, it is shown that the microstructure in the ECA pressed condition is heterogeneous and contains, in addition to arrays of grains with high angle boundaries, a volume fraction of ~ 30–40% of grains with low angle sub-boundaries. Experiments on Al-based alloys have established that the presence of a majority of boundaries with low angles of misorientation (or the order of $\sim 60\%$ of all boundaries) limits the ability to achieve high tensile ductility [36]. Nevertheless, three observations suggest that the microstructure attained by ECA pressing in the present investigation may be capable of providing material which will exhibit reasonably high tensile ductilities. First, there are reports of elongations of up to $> 1000\%$ in an Al–8.0% Mg–1.0% Li–0.15% Zr alloy containing a fine grain size with a mixture of both high and low angle boundaries [37]. Second, there is experimental evidence in an Al–Cu–Li–Mg–Zr alloy for an evolution during superplastic deformation from very fine sub-grains, having sizes of ~ 0.5–$1.0\ \mu m$, into fine grains with high angle grain boundaries and sizes of ~ 6–$7\ \mu m$ [33]. Third, results reported recently for an Al–10% Mg–0.1% Zr alloy show high elongations to failure in a material in which $\sim 22\%$ of all boundaries have low angles of misorientation ($< 15°$) [38].

An important observation in the present work is that it is possible not only to reduce the grain size from $\sim 400\ \mu m$ initially to $\sim 1.2\ \mu m$ through ECA pressing at a temperature of 673 K but also to retain an extremely small grain size even after annealing for 1 h at temperatures as high as ~ 700 K. This grain stability is attributed to the presence of β'-Al_3Zr precipitates which are stable at high temperatues because, by contrast, it is anticipated that the relatively fine δ'-Al_3Li precipitates visible in Fig. 3(a) will dissolve at these temperatures. The retention of a very fine grain size at temperatures up to $\sim$ 700 K is an especially attractive feature of this alloy because of the need to avoid Li [39, 40] or Mg [41] depletion at even higher temperatures.

In practice, the grain size attained in any Al–Li alloy is critically dependent upon the precise alloying elements so that a meaningful appraisal of the significance of the present results requires that these data are compared with other reports using the same commercial alloy. In two independent attempts to obtain a fine and superplastic grain size in this Al–Mg–Li–Zr alloy through appropriate processing, the results were reported to give a distribution of high angle boundaries and measured grain sizes in the range of ~ 15–$45\ \mu m$ [42] and an average grain size of ~ 5–$8\ \mu m$ with boundaries of unspecified misorientations [43]. Thus, the present results demonstrate the exceptional microstructure which may be introduced into this alloy by ECA pressing and they confirm the potential utility of this approach for the fabrication of materials for use in superplastic forming operations.

5. SUMMARY AND CONCLUSIONS

1. An ultra-fine grain size of $\sim 1.2\ \mu m$ was introduced into a commercial Al–5.5% Mg–2.2% Li–0.12% Zr alloy using equal-channel angular (ECA) pressing. The initial microstructure after pressing was heterogeneous, with many areas of equiaxed grains having high angle grain boundaries ($\sim$ 60–70% by volume) and some regions where there were arrays of sub-grains having low angle boundaries ($\sim$ 30–40% by volume).

2. The grain size remained reasonably constant in this alloy after annealing for 1 h at temperatures as high as ~ 700 K (equivalent to $\sim 0.75\ T_m$, where T_m is the absolute melting temperature). This grain stability, which contrasts with an earlier investigation of an Al–3% Mg solid solution alloy, is attributed to the presence of a fine dispersion of β'-Al_3Zr precipitates. At the highest annealing temperature of 833 K, there was a distribution of equiaxed grains with an average size of $\sim 60\ \mu m$.

3. The Vickers microhardness shows only a small decrease up to annealing temperatures of ~ 700 K but thereafter the decrease is more rapid. The microhardness data are consistent with the Hall–Petch relationship for specimens annealed at temperatures above ~ 700 K but at lower annealing temperatures the Hall–Petch relationship breaks down because of the presence of different volume fractions of δ'-Al_3Li precipitates in each specimen.

Acknowledgements—This work was supported in part by the Light Metals Educational Foundation of Japan, in part by a Grant-in-Aid for Scientific Research from the Ministry of Education, Science, Sports and Culture of Japan, and in part by the National Science Foundation of the United states under Grants No. INT-9602919 and DMR-9625969.

REFERENCES

1. Segal, V. M., Reznikov, V. I., Drobyshevskiy, A. E. and Kopylov, V. I., *Metally*, 1981, **1**, 115. [English translation: *Russian Metallurgy*, 1981, **1**, 99].
2. Valiev, R. Z., Krasilnikov, N. A. and Tsenev, N. K., *Mater. Sci. Engng*, 1991, **A137**, 35.
3. Akhmadeev, N. A., Kopylov, V. I., Mulyukov, R. R. and Valiev, R. Z., *Izvest. Akad. Nauk SSSR, Metally*, 1992, **5**, 96.
4. Gleiter, H., *Deformation of Polycrystals: Mechanisms and Microstructures*, ed. N. Hansen, A. Horsewell, T. Leffers and H. Lilholt. Risø National Laboratory, Roskilde, Denmark, 1981, p. 15.
5. Koch, C. C. and Cho, Y. S., *Nanostruct. Mater.*, 1992, **1**, 207.
6. Rigney, D. A., *Ann. Rev. Mater. Sci.*, 1988, **18**, 141.
7. Wang, J., Horita, Z., Furukawa, M., Nemoto, M, Tsenev, N. K., Valiev, R. Z., Ma, Y. and Langdon, T. G., *J. Mater. Res.*, 1993, **8**, 2810.
8. Wang, J., Iwahashi, Y., Horita, Z., Furukawa, M., Nemoto, M., Valiev, R. Z. and Langdon, T. G., *Acta Mater.*, 1996, **44**, 2973.
9. Wang, J., Furukawa, M., Horita, Z., Nemoto, M., Valiev R. Z. and Langdon T. G., *Mater. Sci. Engng*, 1996, **A216**, 41.
10. Furukawa, M., Horita, Z., Nemoto, M., Valiev, R. Z. and Langdon, T. G., *Acta Mater.*, 1996, **44**, 4619.
11. Sherby, O. D., Nieh, T. G. and Wadsworth, J., *Mater. Sci. Forum*, 1997, **243–245**, 11.
12. Pu, H. P., Liu, F. C. and Huang, J. C., *Metall. Mater. Trans. A*, 1995, **26A**, 1153.
13. Fridlyander, I. N., Sandler, V. S. and Nikol'skaya, T. I., *Fiz. Metal. Metalloved.*, 1971, **32**, 767.
14. Horita, Z., Smith, D. J., Furukawa, M., Nemoto, M., Valiev, R. Z. and Langdon, T. G., *J. Mater. Res.*, 1996, **11**, 1880.
15. Furukawa, M., Horita, Z., Nemoto, M., Valiev, R. Z. and Langdon, T. G., *J. Mater. Res.*, 1996, **11**, 2128.
16. Costas, L. P. and Marshall, R. P., *Trans. Met. Soc. AIME*, 1962, **224**, 970.
17. Nozato, R. and Nakai, G., *Trans. Japan Inst. Metals*, 1977, **18**, 679.
18. Noble, B. and Thompson, G. E., *Metal Sci. J.*, 1971, **5**, 114.
19. Furukawa, M., Wang, H. and Nemoto, M., *J. Japan Inst. Light Metals*, 1990, **40**, 20.
20. Wang, H., Furukawa, M. and Nemoto, M., *J. Japan Inst. Light Metals*, 1990, **40**, 27.
21. Valiev, R. Z., Chmelik, F., Bordeaux, F., Kapelski, G. and Baudelet, B., *Scripta Metall. Mater.*, 1992, **27**, 855.
22. Hall, E. O., *Proc. Phys. Soc.*, 1951, **B64**, 747.
23. Petch, N. J., *J. Iron Steel Inst.*, 1953, **174**, 25.
24. Ghosh, G., *Ternary Alloys*, Vol. 6, ed. G. Petzow and G. Effenburg. VCH, Weinheim, Germany, 1993, p. 356.
25. Lavernia, E. J. and Grant, N. J., *J. Mater. Sci.*, 1987, **22**, 1521.
26. Lavernia, E. J., Srivatsan, T. S. and Mohamed, F. A., *J. Mater. Sci.*, 1990, **25**, 1137.
27. Webster, D., *Aluminum–Lithium Alloys*, ed. T. H. Sanders and E. A. Starke. The Metallurgical Society of AIME, Warrendale, PA, 1981, p. 229.
28. Wadsworth, J., Palmer, I. G., Crooks, D. D. and Lewis, R. E., *Aluminum–Lithium Alloys II*, ed. T. H. Sanders and E. A. Starke. The Metallurgical Society of AIME, Warrendale, PA, 1984, p. 111.
29. Wadsworth, J., Pelton, A. R. and Lewis, R. E., *Metall. Trans.*, 1985, **16A**, 2319.
30. Chokshi, A. H. and Mukherjee, A. K., *Mater. Sci. Eng.*, 1989, **A110**, 49.
31. Wadsworth, J., Palmer, I. G. and Crooks, D. D., *Scripta Metall.*, 1983, **17**, 347.
32. Shakesheff, A. J. and Partridge, P. G., *J. Mater. Sci.*, 1986, **21**, 1368.
33. Moon, I. G., Park, J. W. and Yoo, J. E., *Mater. Sci. Forum*, 1994, **170–172**, 255.
34. Pu, H. P. and Huang, J. C., *Scripta Metall. Mater.*, 1995, **33**, 383.
35. Langdon, T. G., *Mater. Sci. Eng.*, 1994, **A174**, 225.
36. Crooks, R., Hales, S. J. and McNelley, T. R., *Superplasticity and Superplastic Forming*, ed. C. H. Hamilton and N. E. Paton. The Minerals, Metals and Materials Society, Warrendale, PA, 1988, p. 389.
37. Hales, S. J., McNelley, T. R. and Munro, I. G., *Scripta Metall.*, 1989, **23**, 967.
38. McNelley, T. R., McMahon, M. E. and Hales, S. J., *Scripta Mater.*, 1997, **36**, 369.
39. Ueda, H., Matsui, A., Furukawa, M., Miura, Y. and Nemoto, M., *J. Japan Inst. Metals*, 1985, **49**, 562.
40. Papazian, J. M., Schulte, R. L. and Adler, P. N., *Metall. Trans.*, 1986, **17A**, 635.
41. Ahmad, M., *Metall. Trans.*, 1987, **18A**, 681.
42. Witters, J. J., Lee, E. W., Lisagor, W. B., Herner, S. B., Kilmer, R. J. and Talia, J. E., *Aluminum–Lithium*, ed. M. Peters and P.-J. Winkler. Informationsgesellschaft, Oberursel, Germany, 1992, p. 351.
43. Kolobnev, N. I., Khokhlatova, L. B., Makarov, V. D., Semenova, E. Y. and Redchits, V. V., *Aluminum–Lithium*, ed. M. Peters and P.-J. Winkler. Informationsgesellschaft, Oberursel, Germany, 1992, p. 1053.

ELSEVIER

Materials Science and Engineering A241 (1998) 122–128

MATERIALS SCIENCE & ENGINEERING A

Microstructural characteristics and superplastic ductility in a Zn-22% Al alloy with submicrometer grain size

Minoru Furukawa [a], Yan Ma [1,b], Zenji Horita [c], Minoru Nemoto [c], Ruslan Z. Valiev [d], Terence G. Langdon [b,*]

[a] *Department of Technology, Fukuoka University of Education, Munakata, Fukuoka, 811-41, Japan*
[b] *Departments of Materials Science and Mechanical Engineering, University of Southern California, Los Angeles, CA 90089-1453, USA*
[c] *Department of Materials Science and Engineering, Faculty of Engineering, Kyushu University, Fukuoka, 812-81, Japan*
[d] *Institute of Physics of Advanced Materials, Ufa State Aviation Technical University, Ufa, 450000, Russia*

Received 7 April 1997

Abstract

Submicrometer grain sizes were introduced into a Zn-22% Al eutectoid alloy using two different procedures: torsion straining and equal-channel angular (ECA) pressing. Microstructural examination showed that torsion straining gives an essentially equiaxed grain configuration with some mixing of the two separate phases. After ECA pressing to a strain of ~ 8 at a temperature of 373 K, there is a submicrometer grain size but with agglomerates of ultrafine Al-rich and Zn-rich grains which are formed by the separate division of the original grains into smaller submicrometer grains with only very limited mixing of the two phases. Tensile testing of the ECA pressed material gave neck-free superplastic flow but, except only at 473 K at the fastest strain rate of $\sim 10^{-1}$ s^{-1} where the elongation was unusually high, the elongations to failure were similar to those reported earlier for a commercial alloy with a grain size of ~ 2.5 μm. The results demonstrate the need to develop an ECA pressing procedure which avoids the formation of agglomerates of the two phases. © 1998 Elsevier Science S.A.

Keywords: Equal-channel angular pressing; Submicrometer grains; Superplasticity; Torsion straining; Zn-22% Al alloy

1. Introduction

High tensile or superplastic ductilities may be observed in metals when the grain size is very small, typically < 10 μm, and when the testing is conducted at a relatively high homologous temperature of the order of at least $0.5T_m$, where T_m is the melting point of the material in degrees Kelvin [1]. Experiments show that superplastic ductilities are achieved over a limited range of strain rates, typically in the vicinity of $\sim 10^{-3}$–10^{-1} s^{-1}, and there is a diminution in the superplastic effect at both faster and slower strain rates [2]. This loss in the superplastic capability at the faster strain rates is especially important when attempts are made to use these materials in superplastic forming operations.

Grain boundary sliding is the dominant flow process in superplasticity [3] and there is experimental evidence showing that a decrease in the grain size leads not only to an increase in the overall ductility of the material under optimum superplastic conditions but also to the occurrence of these higher elongations at faster strain rates: for example, a decrease in grain size from 4.2 to 2.5 μm in the Zn-22% Al eutectoid alloy increased the ductility at 473 K from a maximum of $\sim 2000\%$ to a value of $\sim 2800\%$ [4]. There are also experimental results on an Al–Cu–Zr [5] and a Mg alloy [6] showing that a reduction in grain size reduces the temperature for optimum superplastic flow. Both of these trends would be beneficial for industrial forming processes because there is the potential for fabricating pieces more rapidly and at a lower forming temperature where tool wear is reduced.

The Zn-22% Al eutectoid alloy is a classic superplastic material which has been subjected to extensive mechanical testing in laboratory experiments [7]. The

* Corresponding author. E-mail: langdon@usc.edu
[1] Present address: AEM, Inc., 11525 Sorrento Valley Road, San Diego, CA 92121, USA.

PII S0921-5093(97)00481-4

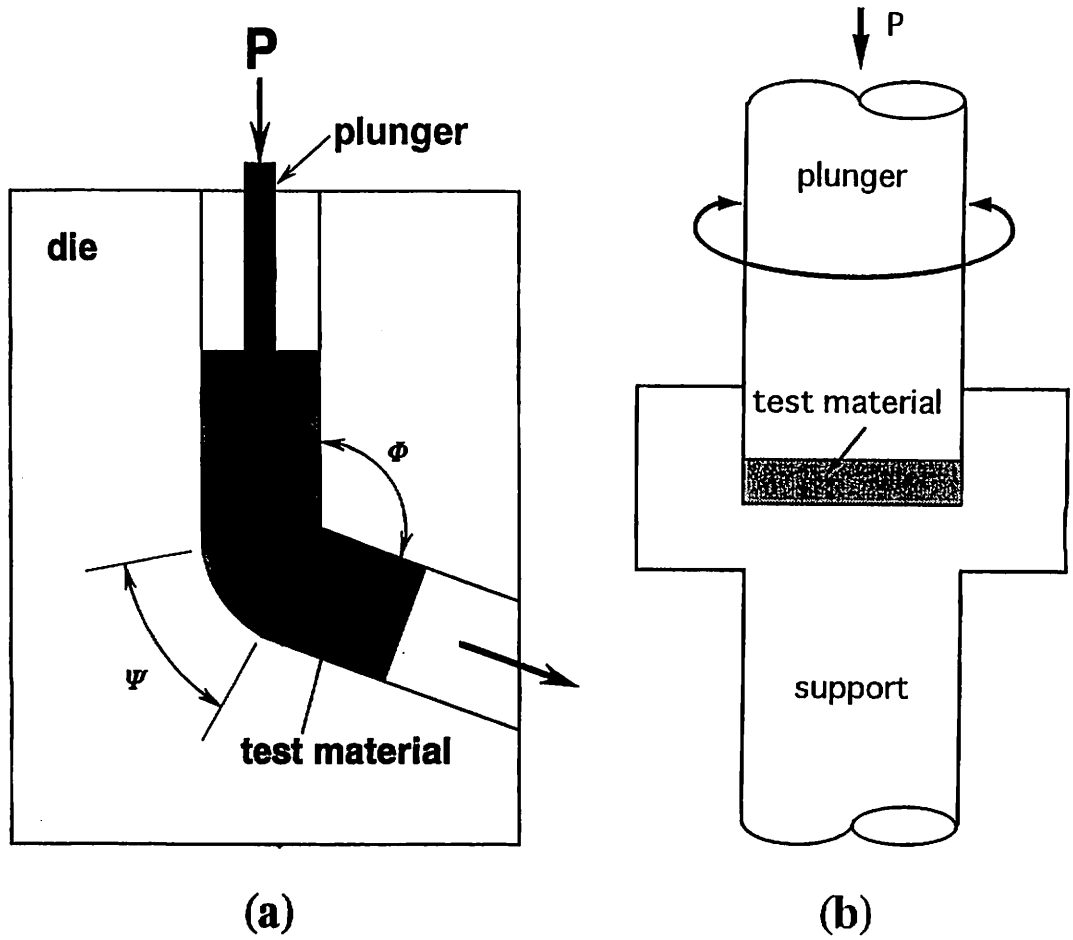

Fig. 1. Principles of (a) ECA pressing and (b) torsion straining.

utility of the Zn-22% Al eutectoid for sheet thermoforming processes was first recognized more than 30 years ago [8] and the alloy is now well-established as a material for use in industrial forming operations [9]. However, normal grain refining of the Zn-22% Al eutectoid alloy generally gives a minimum grain size of the order of $\sim 1-2$ μm.

Recent experiments have shown that it is feasible to introduce a submicrometer grain size into the Zn-22% Al alloy by subjecting the material to a very high plastic strain using a torsion straining procedure [10] but the material processed in this way was in the form of small disks which precluded the possibility of simple tensile testing. It has been established that ultrafine grain sizes may be induced in bulk samples using the process of equal-channel angular (ECA) pressing and this procedure has been used with a wide range of materials [11–14]. Therefore, the purpose of the present investigation was two-fold. First, to investigate the possibility of using ECA pressing to attain a submicrometer grain size in the Zn-22% Al alloy and to compare the resultant microstructure with that obtained using torsion straining. Second, to conduct tensile tests on material prepared by ECA pressing to determine the potential for superplastic flow.

2. Experimental material and procedures

A commercial Zn-22% Al binary alloy was obtained in a superplastic condition with an as-received grain size of ~ 1 μm. Samples were prepared for intense plastic straining using the procedures of either ECA pressing or torsion straining as illustrated schematically in Fig. 1(a) and (b), respectively.

In ECA pressing, illustrated in Fig. 1(a), a sample is pressed through a die with a plunger under an imposed load P. The die consists of two channels of equal cross-section intersecting at an angle Φ and with an angle Ψ defining the outer arc of curvature at the point where the two channels intersect. Samples for ECA pressing were prepared in the form of cylinders with

diameters of 20 mm and total lengths of ~70 mm. Samples were pressed at a temperature of 373 K using a facility having $\Phi = 90°$. When a sample is pressed through the die, it can be shown that a strain, ϵ, is introduced which is given by [15]

$$\epsilon = \left[\frac{2\cot\left(\frac{\Phi}{2}+\frac{\Psi}{2}\right)+\Psi\,\mathrm{cosec}\left(\frac{\Phi}{2}+\frac{\Psi}{2}\right)}{\sqrt{3}}\right] \quad (1)$$

Therefore, if the pressings are repeated on a single sample to give N passes through the die, the total strain is $N\epsilon$. For the present experiments, all samples were pressed for eight passes to give a total strain of ~8.

Torsion straining is illustrated in Fig. 1(b) and the principle was described in earlier reports [11,16,17]. Samples were prepared in the form of disks with a diameter of 15 mm and a thickness of 0.3 mm. These disks were held in place in the straining facility under a pressure, P, of 5.5 GPa and they were strained in torsion at room temperature. In this procedure, the strain, ϵ, is given by

$$\epsilon = \ln\left(\frac{\phi r}{l}\right) \quad (2)$$

where ϕ is the rotation angle in radians and r and l are the radius and thickness of the disk, respectively. Samples were strained in torsion to a maximum strain of ~7 at the perimeters of the disks.

The microstructures of the as-received and processed materials were examined using transmission electron microscopy (TEM) by cutting samples, polishing to a thickness of ~150–180 μm, and then punching out small disks with a diameter of 3 mm. A twin-jet electropolishing unit was used with a solution of 10% $HClO_4$, 20% $C_3H_8O_3$ and 70% C_2H_5OH and samples were thinned to perforation at a temperature of 278 K. Specimens were examined by TEM at 200 kV using either an Hitachi H-8100 electron microscope or a JEM-2000 FX analytical electron microscope. Selected area electron diffraction patterns were obtained from regions with a diameter of 6.2 μm.

For tensile testing following ECA pressing, the samples were rolled into sheets at room temperature and tensile specimens, with gauge lengths of 7 mm and cross-sections of 2×5 mm^2, were machined from these sheets taking care to avoid the extensive cracking which occurred near the sheet edges. The tensile specimens were pulled to failure using an Instron testing machine operating at a constant rate of cross-head displacement and with the specimens immersed in a bath of silicone oil, stirred with bubbling argon, to give selected temperatures from 373 to 473 K.

Microstructures near the fracture tips of selected specimens were examined after testing by preparing samples using a focused ion beam facility (Hitachi FB-2000) in which a very small area of the specimen (typically $\sim 30 \times 40$ μm^2) is thinned with a Ga ion beam oriented parallel to the specimen surface. In the present investigation, areas near to the fracture tips having thicknesses of ~45 μm were thinned to thicknesses of ~500 nm and then these samples were examined using TEM.

3. Experimental results

3.1. Microstructural characteristics

Fig. 2 shows an example of the microstructure in the as-received condition prior to straining. It is apparent that there is essentially a random distribution of equiaxed Al and Zn grains with an average size of ~1 μm. Analytical electron microscopy revealed that the bright and dark grains correspond to the Al-rich and the Zn-rich grains, respectively. In this condition, almost no dislocations are visible in the individual grains. Some white areas in Fig. 2 and the subsequent photomicrographs are holes in the foil where the Zn-rich phase was preferentially dissolved during electropolishing. The use of the focused ion beam method avoids the problem of preferential dissolution and produces a foil of essentially uniform thickness.

The microstructure after ECA pressing to a strain of ~8 at 373 K is shown in Fig. 3. In this condition, the grain size is in the range of 0.4–0.8 μm and the structure is heterogeneous with areas of relatively fine grains (shown on the left in Fig. 3) and areas of coarser grains (shown on the right in Fig. 3). In addition, the grains are elongated and there are agglomerates of Al-rich and Zn-rich grains, suggesting that the ultrafine grain size is achieved not through a true mixing of the two phases but rather by the division of existing grains

Fig. 2. Microstructure in the as-received condition: the bright and dark grains are Al-rich and Zn-rich, respectively.

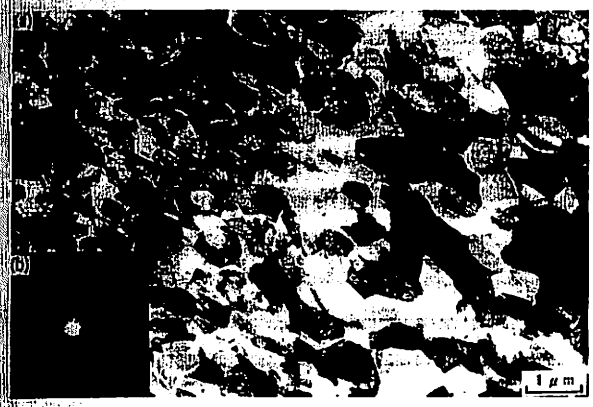

Fig. 3. Microstructure after ECA pressing.

into smaller grains through the formation of additional boundaries. Close inspection showed that the grains contain relatively few dislocations and the grain boundaries are reasonably smooth.

Fig. 4 shows the microstructure after torsion straining, where the grain size is ~0.1–0.5 μm, the grains are in an equiaxed array and there appears to be only limited agglomeration suggesting that the processing method has led to some mixing of the two separate phases. As with the samples strained by ECA pressing, there are few intragranular dislocations and the grain boundaries have a smooth appearance. These observations suggest that torsion straining may be preferable for producing an ultrafine equiaxed and fully mixed microstructure but nevertheless there is again a heterogeneity with areas of coarser grains (~0.5 μm) co-existing with areas of finer grains (~0.1 μm): this co-existence of areas with different grain sizes is apparent in Fig. 4.

As noted earlier for specimens processed by torsion straining [10], there was also evidence that processing, either by torsion straining or by ECA pressing, led to a decrease in the extent of the rod-shaped precipitates of

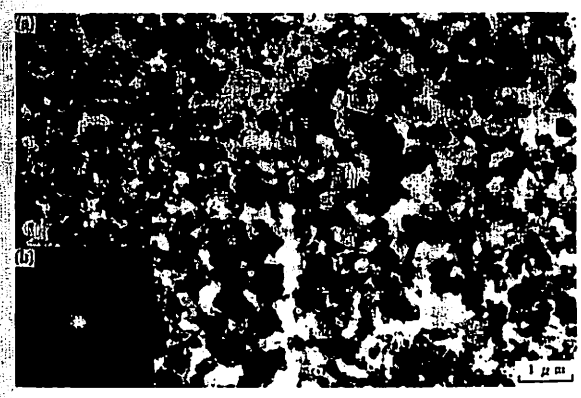

Fig. 4. Microstructure after torsion straining.

the stable hcp Zn which are visible within the Al-rich grains in the as-received material. These observations suggest that the Zn precipitates are absorbed by the Zn-rich grains during the intense straining procedure.

3.2. Mechanical testing after ECA pressing

Because of problems associated with cracking during rolling, it was possible to obtain only a small number of tensile specimens. These specimens were pulled to failure under different conditions and the results, including the flow stresses and elongations to failure, are summarized in Table 1. In addition, Fig. 5 shows the appearance of the two specimens exhibiting the highest elongations to failure after testing at 473 K.

Inspection of Fig. 5 shows that the specimens tested at 473 K pull out in a quasi-uniform manner, without any significant necking, and ultimately they break with a very small cross-sectional area: this flow behavior is characteristic of superplasticity and was described earlier for Zn-22% Al specimens tested without ECA pressing and with a grain size of ~2.5 μm [18]. Nevertheless, the overall elongations to failure, as documented in Table 1, are fairly similar to those reported for the same eutectoid alloy without ECA pressing [4] suggesting that, at least for the present experiments, there has been little significant improvement in the superplastic properties through ECA pressing.

Fig. 6 shows the microstructure in the vicinity of the fracture tip for a sample prepared using the focused ion beam method and taken at a point ~1 mm from the tip of the specimen, shown in Fig. 5, pulled to an elongation of 1970% at 473 K using an initial strain rate of 3.3×10^{-2} s^{-1}. It is apparent that grain growth has occurred during testing, to a grain size of ~1.5–2.0 μm, and the grains are now randomly distributed with no evidence for any agglomeration. The direction of the tensile axis is indicated in Fig. 6 and it is apparent also that the grains are equiaxed with no significant elongation in the direction of tensile straining. As with other materials deformed superplastically [19], the grain boundaries are smooth and very few dislocations are visible within the grains.

4. Discussion

In order to examine the ductility of the ECA pressed specimens in more detail, it is necessary to make a direct comparison with earlier and more extensive data obtained for specimens of a similar commercial alloy which was not subjected to pressing [4]. The earlier results are shown as the open points in Fig. 7 for specimens having a spatial grain size, d, of 2.5 μm tested at different absolute temperatures, T: the upper plot gives the percentage elongation at fracture, $\Delta L/$

Table 1
Experimental data for tensile testing after ECA pressing

Temperature (K)	Strain rate (s^{-1})	Flow stress (MPa)	Elongation to failure
373	3.3×10^{-4}	17.0	450%
423	3.3×10^{-4}	11.0	700%
	3.3×10^{-3}	25.9	940%
473	3.3×10^{-2}	26.8	1970%
	3.3×10^{-1}	66.3	1540%

L_0%, and the lower plot gives the flow stress, σ, as a function of the initial strain rate, $\dot{\epsilon}$, where ΔL is the total increase in length at the point of failure and L_0 is the initial gauge length. These results show the division of the stress–strain rate curve into three distinct regions, with optimum superplasticity occurring at intermediate strain rates in region II: the slopes of the lines indicated in the lower plot of Fig. 7 give the values of the strain rate sensitivity, m, defined as $(\partial \ln \sigma/\partial \ln \dot{\epsilon})$. A comparison shows that the flow stresses documented in Table 1 are similar in magnitude to those plotted in Fig. 7 and reported earlier with a grain size of 2.5 μm.

Superimposed on the upper plot in Fig. 7, and shown as solid symbols, are the data obtained in the present experiments at 423 and 473 K with a submicrometer grain size. It is clear that the ECA pressed material tends to exhibit lower elongations to failure except only at the highest strain rate of $\sim 10^{-1}\ s^{-1}$ at 473 K where there is an increase in the elongation by a factor of almost 1.5×. The advent of a higher ductility at the fastest strain rate is consistent with the anticipated trend for a material with an ultrafine grain size but nevertheless it is important to examine the reason for the relatively poor ductility of the ECA pressed material at the slower strain rates.

In the as-received condition, Fig. 2 shows that the grains are equiaxed and there is a random distribution of the two phases. However, the microstructure after ECA pressing consists of agglomerates of Al-rich and Zn-rich grains with only a very limited mixing of the two phases. It is probable that the presence of these agglomerates after ECA pressing, and the absence of a uniform and random array of Al-rich and Zn-rich grains, accounts for the failure to observe a very substantial improvement in the overall ductility when the grain size is reduced to the submicrometer level.

It has been well established through experiments that the different types of interfaces in superplastic microduplex alloys behave differently in their susceptibility to exhibiting grain boundary sliding [20]. In the Zn-22% Al eutectoid alloy, for example, maximum sliding occurs on the Zn-Zn intercrystalline boundaries, there is less sliding at the Zn-Al interphase boundaries and sliding is a minimum at the Al–Al intercrystalline boundaries [21]. Thus, the development of a microstructure consisting of Al-rich and Zn-rich agglomerates, as after ECA pressing in the present experiments, leads to an excess of intercrystalline boundaries, and the presence of a large number of Al–Al intercrystalline interfaces has little significant benefit in promoting easy sliding. It appears that easy sliding may be achieved under these conditions only when the testing temperature is sufficiently high that these Al–Al boundaries are removed through grain growth, as in the tests conducted in these experiments at 473 K. It is therefore concluded from these observations that it is important to develop an alternative processing route for ECA

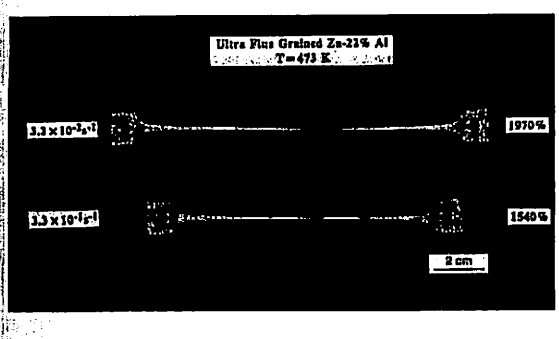

Fig. 5. Specimens subjected to ECA pressing and then tested in tension to failure at 473 K.

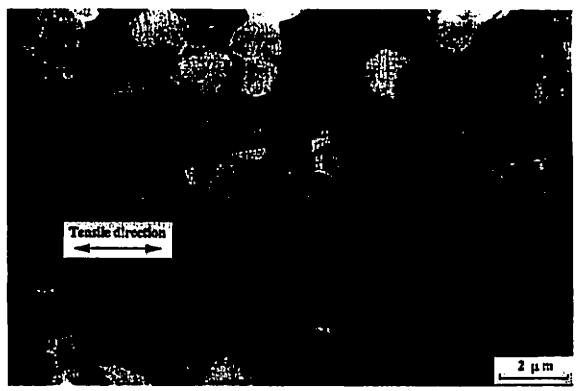

Fig. 6. Microstructure in the vicinity of the fracture tip of a specimen pulled to failure at an elongation of 1970% at 473 K using an initial strain rate of $3.3\times10^{-2}\ s^{-1}$.

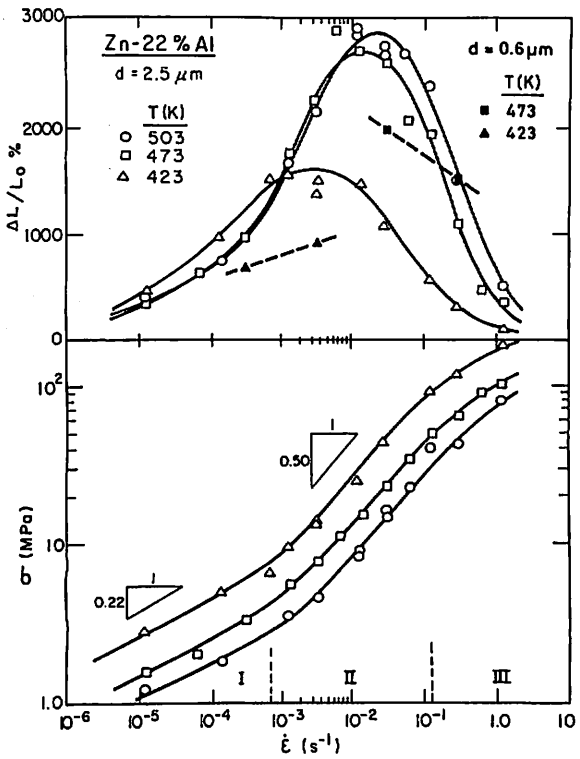

Fig. 7. Elongation to failure (upper) and flow stress (lower) versus initial strain rate for Zn-22% Al specimens with a grain size of 2.5 μm (open points) [4] and for four specimens with an average grain size of ~0.6 μm after ECA pressing (closed points).

pressing to avoid the formation of any agglomerates. For example, it is possible that an improved microstructure may be obtained by performing the ECA pressing at a higher temperature and following the pressing with a rapid quench or by performing the pressing on an alloy following rapid quenching from a high temperature.

An earlier report examined the grain boundaries in Al–Mg solid solution alloys subjected to torsion straining and it was shown that these boundaries were in a high-energy non-equilibrium configuration, they contained a large number of extrinsic dislocations, and there were also many dislocations within the grains [17]. This observation contrasts with the present report where, after both ECA pressing (Fig. 3) and torsion straining (Fig. 4), the grain boundaries are reasonably smooth, they appear to be closer to an essentially equilibrium configuration and, in addition, there are very few intragranular dislocations. This difference is attributed to the low melting temperature of the Zn-22% Al alloy which leads to an easier relaxation of the high internal stresses introduced by intense plastic straining.

5. Summary and conclusions

A submicrometer grain size may be introduced into a Zn-22% Al eutectoid alloy by equal-channel angular (ECA) pressing or by torsion straining.

After ECA pressing to a strain of ~8 at a temperature of 373 K, the grains are elongated and there are agglomerates of Al-rich and Zn-rich grains. After torsion straining at room temperature to a strain of ~7, the grains are equiaxed and there is some mixing of the two phases.

Tensile testing of samples subjected to ECA pressing gave superplastic flow but the elongations were not as high as anticipated for a material containing a submicrometer grain size. It is concluded that the failure to obtain a substantial increase in overall ductility after ECA pressing is due to the presence of agglomerates and the absence of a uniform and random array of Al-rich and Zn-rich grains.

Acknowledgements

This work was supported in part by the Light Metals Educational Foundation of Japan, in part by a Grant-in-Aid for Scientific Research from the Ministry of Education, Science, Sports and Culture of Japan, in part by the National Science Foundation of the United States under Grant No. INT-9602919, and in part by the U.S. Army Research Office under Grants No. DAAH04-96-1-0332 and N68171-96-6-9006.

References

[1] T.G. Langdon, Metall. Trans. 13A (1982) 689.
[2] H. Ishikawa, F.A. Mohamed, T.G. Langdon, Phil. Mag. 32 (1975) 1269.
[3] T.G. Langdon, Mater. Sci. Eng. A174 (1994) 225.
[4] F.A. Mohamed, M.M.I. Ahmed, T.G. Langdon, Metall. Trans. 8A (1977) 933.
[5] R.Z. Valiev, O.A. Kaibyshev, R.I. Kuznetsov, R.Sh. Musalimov, N.K. Tsenev, Dokl. Akad. Nauk SSSR 301 (1988) 864.
[6] M. Mabuchi, H. Iwasaki, K. Yanase, K. Higashi, Scripta Mater. 36 (1997) 681.
[7] P. Yavari, T.G. Langdon, Mater. Sci. Eng. 57 (1983) 55.
[8] D. S Fields, IBM J. 9 (1965) 134.
[9] T.G. Langdon, in: G. Torres-Villaseñor, Y. Zhu, C. Piña-Barba (Eds.), Recent Advances in Science, Technology and Applications of Zn–Al Alloys, Universidad Nacional Autónoma de México, Mexico City, 1994, p. 177.
[10] M. Furukawa, Z. Horita, M. Nemoto, R.Z. Valiev, T.G. Langdon, J. Mater. Res. 11 (1996) 2128.
[11] R.Z. Valiev, N.A. Krasilnikov, N.K. Tsenev, Mater. Sci. Eng. A137 (1991) 35.
[12] N.A. Akhmadeev, V.I. Kopylov, R.R. Mulyukov, R.Z. Valiev, Izvest. Akad. Nauk SSSR, Metally 5 (1992) 96.

[13] N.A. Akhmadeev, N.P. Kobelev, R.R. Mulyukov, Ya.M. Soifer, R.Z. Valiev, Acta Metall. Mater. 41 (1993) 1041.
[14] J. Wang, Y. Iwahashi, Z. Horita, M. Furukawa, M. Nemoto, R.Z. Valiev, T.G. Langdon, Acta Mater. 44 (1996) 2973.
[15] Y. Iwahashi, J. Wang, Z. Horita, M. Nemoto, T.G. Langdon, Scripta Mater. 35 (1996) 143.
[16] R.Z. Valiev, A.V. Korznikov, R.R. Mulyukov, Mater. Sci. Eng. A168 (1993) 141.
[17] Z. Horita, D.J. Smith, M. Furukawa, M. Nemoto, R.Z. Valiev, T.G. Langdon, J. Mater. Res. 11 (1996) 1880.
[18] M.M.I. Ahmed, F.A. Mohamed, T.G. Langdon, J. Mater. Sci. 14 (1979) 2913.
[19] A.H. Chokshi, A.K. Mukherjee, T.G. Langdon, Mater. Sci. Eng. R10 (1993) 237.
[20] R.B. Vastava, T.G. Langdon, Acta Metall. 27 (1979) 253.
[21] P. Shariat, R.B. Vastava, T.G. Langdon, Acta Metall. 30 (1982) 285.

Age Hardening and the Potential for Superplasticity in a Fine-Grained Al-Mg-Li-Zr Alloy

MINORU FURUKAWA, PATRICK B. BERBON, ZENJI HORITA, MINORU NEMOTO, NIKOLAI K. TSENEV, RUSLAN Z. VALIEV, and TERENCE G. LANGDON

Experiments were conducted to determine the age-hardening characteristics and the mechanical properties of an Al-5.5 pct Mg-2.2 pct Li-0.12 pct Zr alloy processed by equal-channel angular (ECA) pressing to give a very fine grain size of ~1.2 μm. The results show that peak aging occurs more rapidly when the grain size is very fine, and this effect is interpreted in terms of the higher volume of precipitate-free zones in the fine-grained material. Mechanical testing demonstrates that the ECA-pressed material exhibits high strength and good ductility at room temperature compared to conventional Al alloys containing Li. Elongations of up to ~550 pct may be achieved at an elevated temperature of 603 K in the ECA-pressed condition, thereby confirming that, in this condition, the alloy may be a suitable candidate material for use in superplastic forming operations.

I. INTRODUCTION

IT is well established that the addition of lithium to aluminum-based alloys simultaneously decreases the density and increases the elastic modulus, thereby providing lightweight alloys for potential use in structural applications.[1,2] This article describes a series of experiments conducted on a commercial Al-5.5 pct Mg-2.2 pct Li-0.12 pct Zr alloy in which hardening is achieved through the presence of δ'-Al_3Li precipitates and Zr is added to improve the overall ductility.[3,4]

An earlier investigation showed that it was possible to attain a very fine grain size in this alloy, on the order of ~1.2 μm, by introducing an intense plastic strain through the process of equal-channel angular (ECA) pressing.[5] By conducting static annealing tests for 1 hour over a range of temperatures on specimens subjected to ECA pressing, it was demonstrated that, because of the presence of metastable β'-Al_3Zr precipitates, a very fine grain size was retained up to temperatures as high as ~700 K, equivalent to ~0.75 T_m where T_m is the absolute melting temperature of the material. These earlier results suggest two significant possibilities. First, it may be feasible to age harden the alloy to obtain a high strength and good ductility at low temperatures. Second, high tensile and superplastic-like ductilities may be achieved at elevated temperatures, making the alloy suitable for consideration as a candidate material for use in superplastic forming operations.

MINORU FURUKAWA, Associate Professor, is with the Department of Technology, Fukuoka University of Education, Fukuoka 811-41, Japan. PATRICK B. BERBON, Research Assistant, Department of Materials Science, and TERENCE G. LANGDON, Professor, Departments of Materials Science and Mechanical Engineering, are with the University of Southern California, Los Angeles, CA 90089-1453. ZENJI HORITA, Associate Professor, and MINORU NEMOTO, Professor, are with the Department of Materials Science and Engineering, Kyushu University, Fukuoka 812-81, Japan. NIKOLAI K. TSENEV, Senior Scientist, is with the Institute of Chemical Technology, Ufa State Petroleum Technical University, Ufa 450062, Russia. RUSLAN Z. VALIEV, Professor, is with the Institute of Physics of Advanced Materials, Ufa State Aviation Technical University, Ufa 450000, Russia.

Manuscript submitted April 18, 1997.

Accordingly, this article describes a series of experiments designed to investigate the age-hardening characteristics and the mechanical properties of the Al-Mg-Li-Zr alloy after ECA pressing. Some tests were also conducted using the same alloy in a hot-rolled condition without ECA pressing. As will be demonstrated, peak aging of the ECA-pressed material leads to excellent strength and good ductility at room temperature. In addition, high tensile elongations may be achieved at elevated temperatures, including elongations of up to >500 pct at a testing temperature of 603 K.

II. EXPERIMENTAL MATERIAL AND PROCEDURES

The experiments were conducted using the same Al-5.5 pct Mg-2.2 pct Li-0.12 pct Zr alloy as in the earlier investigation;[5] this is a commercial Russian alloy with the designation 01420.[6] The alloy was received in the hot-rolled condition with an initial grain size of ~400 μm. The ECA pressing was conducted in air at a temperature of 673 K using a cylindrical sample with a diameter of 50 mm and a length of ~100 mm. The ECA pressing facility is illustrated schematically in Figure 1, and a detailed description of the principles of ECA pressing was given earlier.[7] Briefly, samples are pressed through a die in which there are two channels, equal in cross section, intersecting at an angle of Φ. A second angle, Ψ, defines the arc of curvature at the outer point of the intersection of the two channels. The strain introduced into the sample from a single pressing through the die may be calculated using the procedure described elsewhere.[8] In the present investigation, repetitive pressings of the same sample were conducted to achieve a total strain of ~3.7, with the sample cooled in air after each separate pressing.

To investigate the age-hardening behavior after ECA pressing, samples having dimensions of 3 × 3 × 4.7 mm^3 were cut from near to the center of the ECA-pressed material, and these samples were solution treated in an argon atmosphere for either 3 hours at 673 K or 1 hour at 818 K

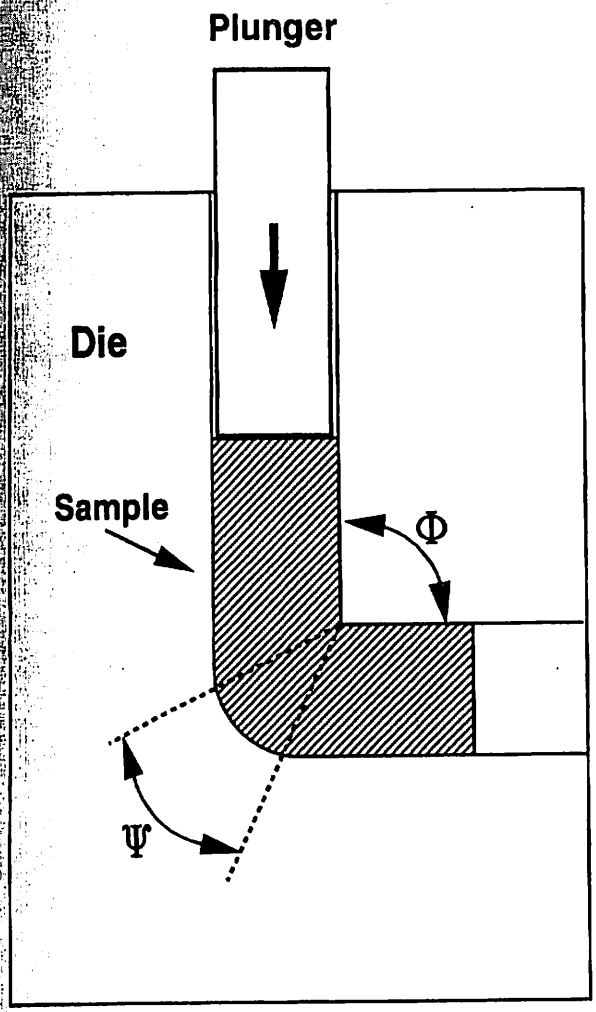

Fig. 1—Schematic illustration of the facility for ECA pressing.

followed by quenching in iced water.* Aging was conducted in an Ar atmosphere for periods of time varying from 0.1 to 300 hours at a temperature of 448 K, with subsequent quenching in iced water; it should be noted that 448 K is the standard temperature for aging in a T6 heat treatment.

The Vickers microhardness, Hv (in kg mm^{-2}), was determined using an Akashi MVK-E3 microhardness tester with a diamond pyramidal indenter. A load of 50 g was applied for 15 seconds and the reported values of Hv are the average of seven separate measurements.

The 0.2 pct proof stress was determined by tensile testing using specimens solution treated for 1 hour at either 673 or 818 K followed by quenching in iced water. For comparison purposes, some additional tests were conducted using the hot-rolled alloy in the as-received condition without any ECA pressing. All of the tests in tension used miniature specimens having gage lengths of 6.4 mm and gage thicknesses of 2.5 mm, and the tests were performed at 298 K in air under an initial strain rate of 3.3×10^{-4} s^{-1}. Each specimen was pulled to failure to determine the total elongation for each testing condition.

The superplastic characteristics of the alloy were investigated by conducting tests in tension at 298 and 603 K and using initial strain rates from 3.3×10^{-4} to 3.3×10^{-2} s^{-1}. Tests were performed on samples in both the ECA-pressed and the hot-rolled conditions, and in order to simplify the processing route for any potential forming application, all samples were tested without any prior solution treatment or aging.

Specimens were prepared for examination by transmission electron microscopy (TEM) using the procedure described earlier.[5] All TEM photomicrographs were obtained with a Hitachi H-8100 electron microscope operating at 200 kV. Selected-area electron diffraction (SAED) patterns were taken from different regions with diameters of 13 μm. Grain sizes were estimated directly from the photomicrographs by identifying and measuring at least 50 different grains.

III. EXPERIMENTAL RESULTS

A. *Microstructures after Solution Annealing*

As described in the earlier report,[5] the microstructure of the alloy after ECA pressing consists both of homogeneous regions of equiaxed grains with high-angle grain boundaries and an average grain size of ~1.2 μm and of areas of heterogeneity where there are arrays of subgrains with an average size of ~1.2 μm and with boundaries having low angles of misorientation. There is also evidence, after ECA pressing, of a uniform distribution of very fine δ'-Al_3Li precipitates which are formed upon cooling in air from the ECA pressing temperature of 673 K.*

Figures 2 and 3 give examples of the microstructures after solution annealing for either 3 hours at 673 K or 1 hour at 818 K, respectively; for each photomicrograph, the SAED patterns were taken from the regions marked A, B, and C. After a solution treatment for 3 hours at the lower temperature of 673 K, inspection of Figure 2 shows that the microstructure consists of an array of fine grains with the presence of some subgrain boundaries. The average grain size in this condition was measured as ~1.5 to 2.0 μm, thereby confirming that there is only very limited grain growth during this solution treatment. At the higher temperature of 818 K, shown in Figure 3, the grains are relatively coarse, with an average size of ~40 to 50 μm, and the grain boundaries have high angles of misorientation. Thus, significant grain growth occurs after annealing at this higher temperature.

B. *Influence of Aging on Hardness*

Several specimens were prepared using the two solution treatments established in Section III–A, and these speci-

*These temperatures were selected because it has been established that 2.2 pct of Li will be in solution in Al matrix alloys at these two temperatures.[9,10] In practice, a temperature of 673 K is essentially the lowest possible temperature for dissolution of all of the Li atoms and therefore, as shown earlier,[5] it is close to the upper limiting temperature for retention of an extremely fine grain size. The higher temperature of 818 K was selected in order to examine the effect of a combination of Li dissolution with some concurrent grain growth.

*In practice, the cooling rate following ECA pressing is not critical, because experiments show that there is a precipitation of δ'-Al_3Li in Al-Li alloys even after extremely rapid quenching.[11,12]

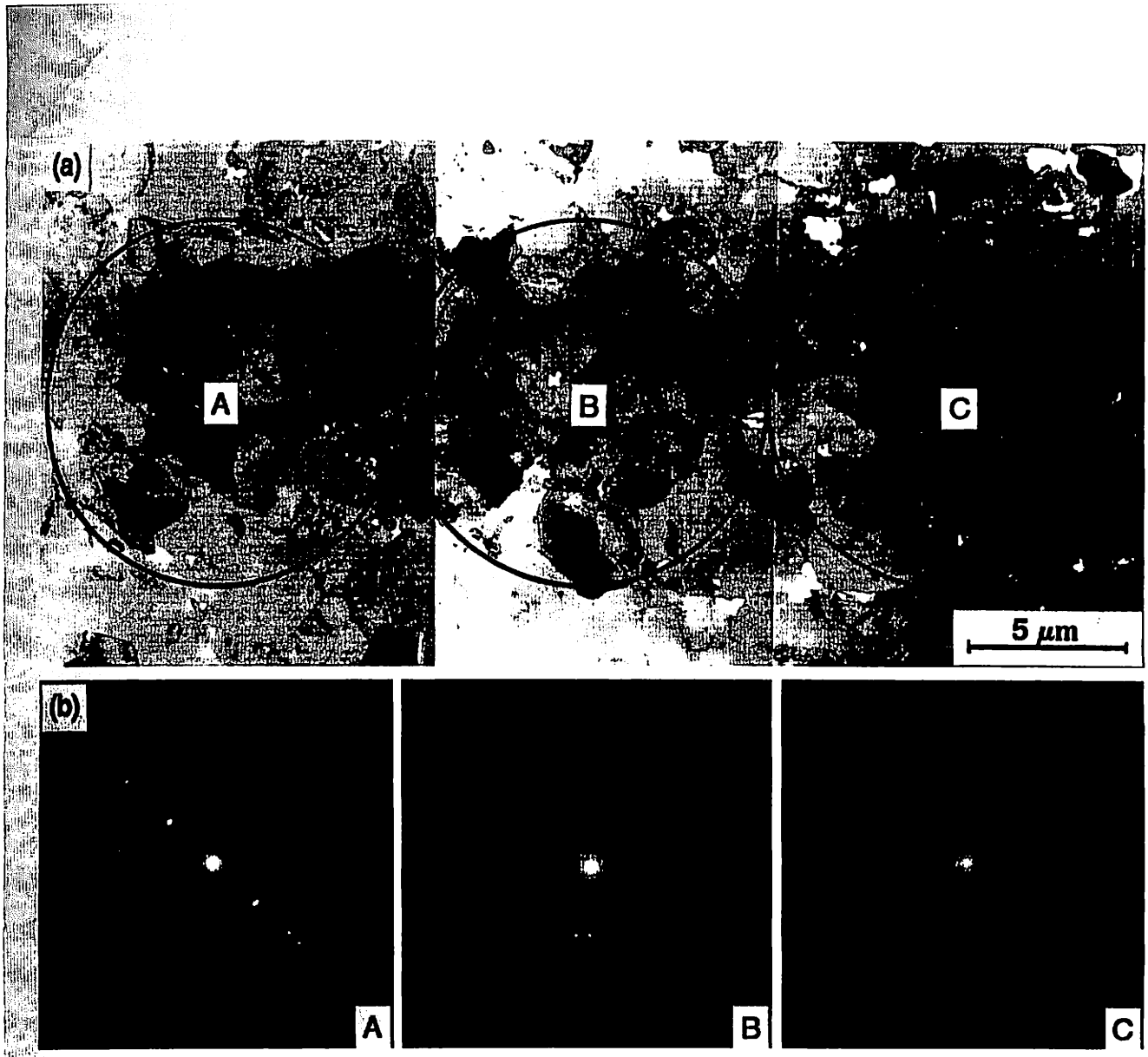

Fig. 2—(*a*) Microstructure in the ECA-pressed material after solution annealing for 3 h at 673 K, and (*b*) SAED patterns taken from the regions marked A, B, and C.

mens were then aged at 448 K for different periods of time up to a maximum of 300 hours. Figure 4 shows a plot of the Vickers microhardness as a function of the aging time for these two sets of experimental conditions.

Examining the two data points for the as-quenched condition prior to aging, it is apparent from Figure 4 that Hv is higher after solution annealing at 673 K. As will be demonstrated, there is no obvious difference in the distribution of δ' particles for these two conditions and, therefore, it is reasonable to conclude that this difference in hardness is a direct consequence of the finer grain size after solution annealing at the lower temperature. In addition, this higher hardness persists in the finer-grained material up to an aging time of ~3 hours, but thereafter, the fine-grained material is weaker than the relatively coarse-grained material aged at 818 K. Both materials exhibit an initial age hardening due to the further precipitation of metastable δ'-Al_3Li particles but, subsequently, there is overaging and a consequent softening due, in part, to the growth of the δ'-Al_3Li particles beyond a critical size for maximum strengthening.[13] Since the two curves in Figure 4 intersect at an aging time of ~3 hours, it is apparent that an overaged condition is reached more rapidly in the fine-grained material.

In order to obtain an understanding of these results, Figure 5 shows a series of (100) dark-field images which summarize the microstructural characteristics under the two different aging conditions: the top four photomicrographs relate to samples solution treated at 673 K for 3 hours and quenched in iced water, with subsequent aging at 448 K for (a) 0 hours, (b) 0.3 hours, (c) 3 hours, and (d) 300 hours, respectively; the lower four photomicrographs are for samples solution treated at 818 K for 1 hour and quenched in iced water, with subsequent ageing at 448 K for (e) 0 hours, (f) 0.3 hours, (g) 30 hours, and (h) 300 hours, respectively. Careful inspection of the samples by TEM revealed an essentially identical and uniform distribution of δ'-Al_3Li particles in the two as-quenched samples (Figures 5(a) and (e)), but in both sets of samples there was an increase with increasing annealing time in the volume fraction of the δ' phase combined with a tendency for greater spheroidization of the δ' particles. It was also apparent that there were no

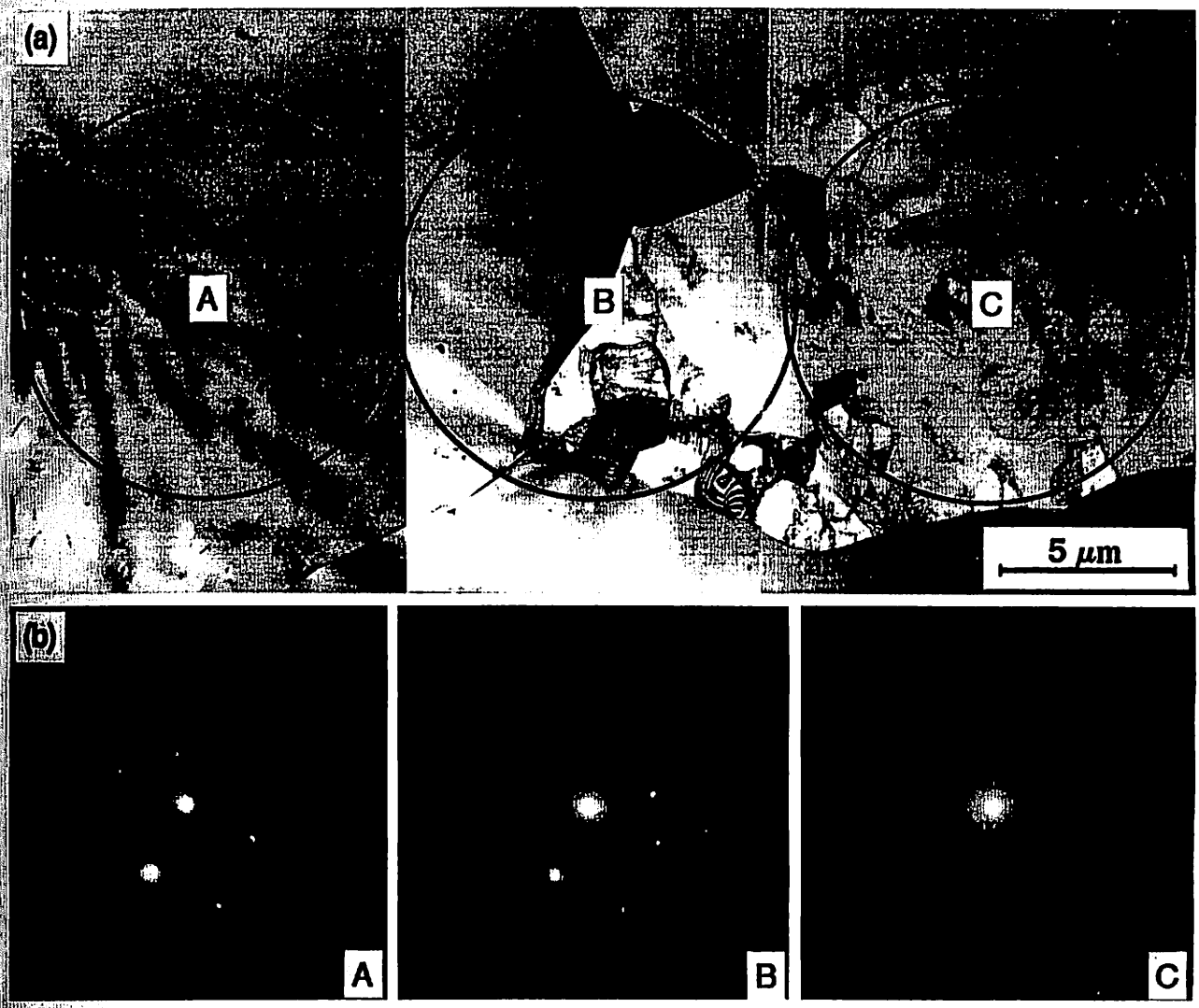

Fig. 3—(*a*) Microstructure in the ECA-pressed material after solution annealing for 1 h at 818 K, and (*b*) SAED patterns taken from the regions marked A, B, and C.

significant differences in the volume fraction, shape, and/or size of the δ' particles for the two sets of samples after any selected time of aging. Thus, the morphology of the δ'-Al_3Li particles is not a sufficient parameter to provide an explanation for the more rapid attainment of an overaged condition in the finer-grained material, as documented in Figure 4.

In practice, it is anticipated that some β'-Al_3Zr particles will form in this material even in the as-quenched condition. However, age hardening due to precipitation of the metastable β' particles is unlikely because the alloy contains only 0.12 pct of Zr, and it has been shown that age hardening from β' particles requires ≥0.2 pct Zr and a rapid cooling from the liquid state.[14,15] Since the β' phase has the same Ll_2 structure as the δ' phase, the β' particles are not easily distinguishable from the δ' particles in dark-field images in the as-quenched condition, but they are visible in the bright field, as shown in Figure 6(a) for a sample solution treated at 818 K for 1 hour and subsequently aged at 448 K for 0.3 hours, corresponding to an underaged con-

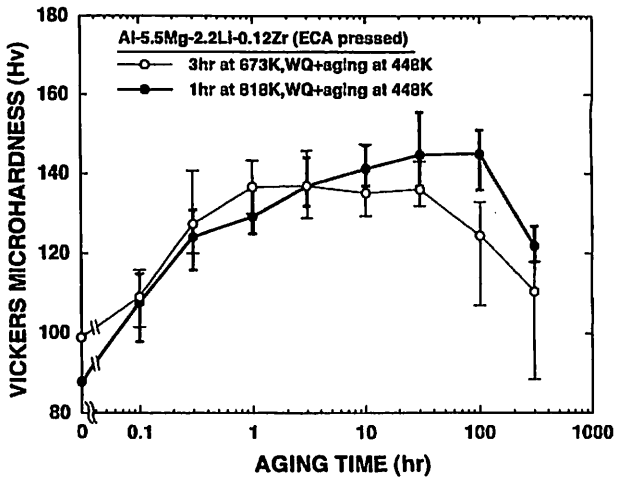

Fig. 4—Vickers microhardness *vs* aging time for the ECA-pressed material after two different solution treatments.

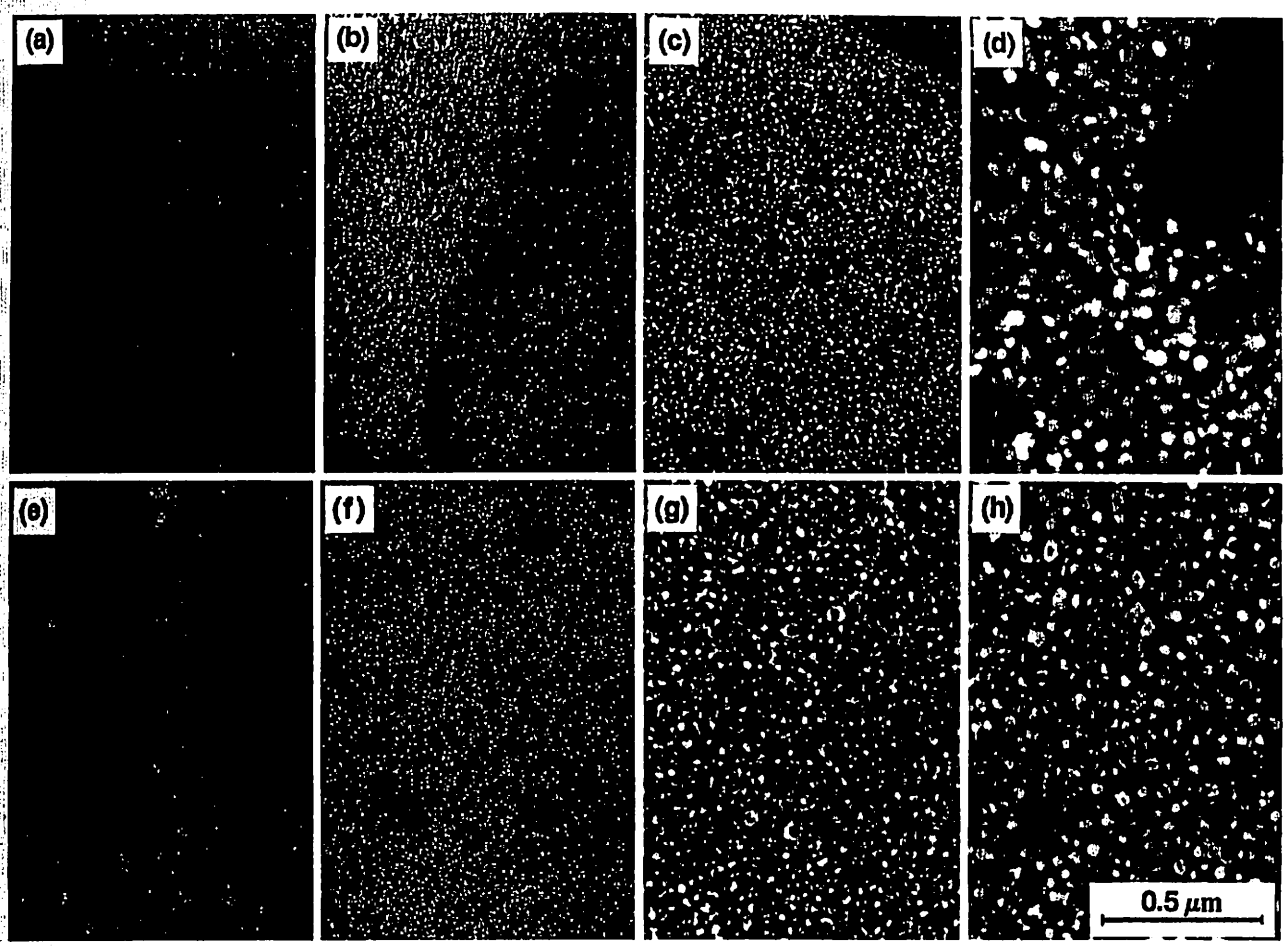

Fig. 5—Dark-field images of ECA-pressed material after solution treatment at 673 K and subsequent aging for (*a*) 0 h, (*b*) 0.3 h, (*c*) 3 h, and (*d*) 300 h, and after solution treatment at 818 K and subsequent aging for (*e*) 0 h, (*f*) 0.3 h, (*g*) 30 h, and (*h*) 300 h.

dition. The same area is shown in Figure 6(b) as a (100) dark-field image, and it is apparent that the β' particles are now visible due, it has been suggested,[14] to the growth during aging of a shell of δ' around each particle.

With progressive aging for longer times, there is a growth of the δ'-Al_3Li particles, but some of these particles are also lost to the stable δ-AlLi phase which precipitates, together with the T-Al_2MgLi phase, along the grain boundaries and within the grains. An example of this effect is shown in Figure 7 for a sample solution treated at 673 K for 3 hours and subsequently aged at 448 K for 300 hours into the overaged condition. Figure 7(a) shows a bright-field image with a grain boundary (marked GB) at the upper right of the photomicrograph and with δ and/or T phase precipitation (marked); the same area is shown in Figure 7(b) in a (100) dark-field image. It is clear from inspection of Figure 7(a) that the δ and T phases are surrounded by precipitate-free zones (PFZ) where there are few or no δ' particles. Thus, it is concluded that a peak is attained more rapidly in the aging curve for the finer-grained material, as shown in Figure 4, because the grain size is very small and there is a larger volume of grain boundaries and, consequently, more precipitation sites for the δ and T phases, leading to a higher volume of PFZ.

It was shown earlier that the hardness of this alloy after ECA pressing varies with the instantaneous grain size, at grain sizes above ~2 μm, through a Hall–Petch relationship of the form

$$H_v = H_0 + k_{II} d^{-1/2} \qquad [1]$$

where d is the grain size and H_0 and k_{II} are constants determined experimentally as ~75 Hv and ~32 Hv $\mu m^{1/2}$, respectively.[5]* This plot and the associated data points are shown in Figure 8 together with lines representing the best fit and the upper and lower limits. Superimposed in the upper portion of the plot are two points representing the peak aged conditions from Figure 4; these points are for samples either solution treated for 3 hours at 673 K and aged for 3 hours at 448 K or solution treated for 1 hour at 818 K and aged for 30 hours at 448 K. Both of these experimental points, when plotted for their appropriate grain sizes, exhibit a considerable deviation from the single Hall–Petch relationship reported earlier from static annealing experiments.[5] Thus, the hardness or strength of the alloy is a strong function not only of the instantaneous grain size but also, because of changes in the precipitate morphology with temperature and time, of the precise aging condition.

*The Hall–Petch relationship breaks down at smaller grain sizes because of variations in the volume fractions of δ-Al_3Li precipitates.[5]

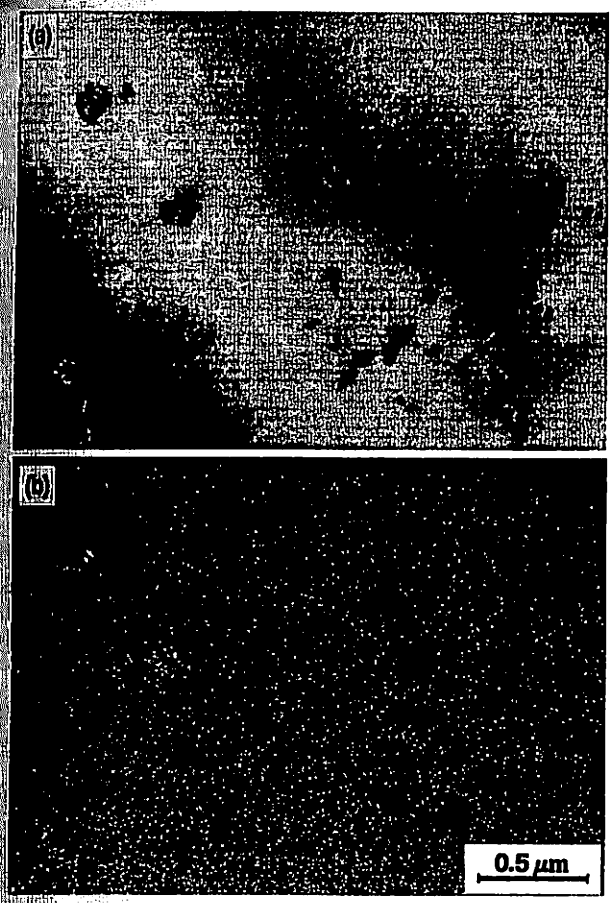

Fig. 6—(*a*) Bright-field and (*b*) dark-field images of the same area of the ECA-pressed material after solution treatment at 818 K and underaging at 448 K.

C. *Mechanical Properties at Low and Elevated Temperatures*

In order to obtain information on the strength and plasticity of this alloy after ECA pressing, tests were conducted on three different sets of samples: (1) the as-received hot-rolled alloy without ECA pressing but with a solution treatment of 1 hour at 673 K and quenching in iced water, (2) an ECA-pressed alloy with a solution treatment for 1 hour at 673 K and quenching in ice water and (3) an ECA-pressed alloy with a solution treatment for 1 hour at 818 K with subsequent iced water quenching. The microstructure for the latter condition corresponds to Figure 3. The microstructure after 1 hour of treatment at 673 K was similar to Figure 2, except the average grain size was slightly finer ($\sim$1.2 to 1.5 μm) because of the shorter time at temperature. Figure 9 shows the microstructure of the as-received hot-rolled alloy, where there were very large grains containing a slightly elongated array of subgrains. Full details of the microstructural characteristics for these three conditions are summarized in Table I.

Using these three sets of samples, Figure 10 shows a plot of the 0.2 pct proof stress against the elongation to failure for specimens tested at room temperature (298 K) at a strain rate ($\dot{\varepsilon}$) of 3.3×10^{-4} s^{-1} and following different aging conditions. Three conclusions may be reached from inspection of Figure 10. First, aging of the material after quench-

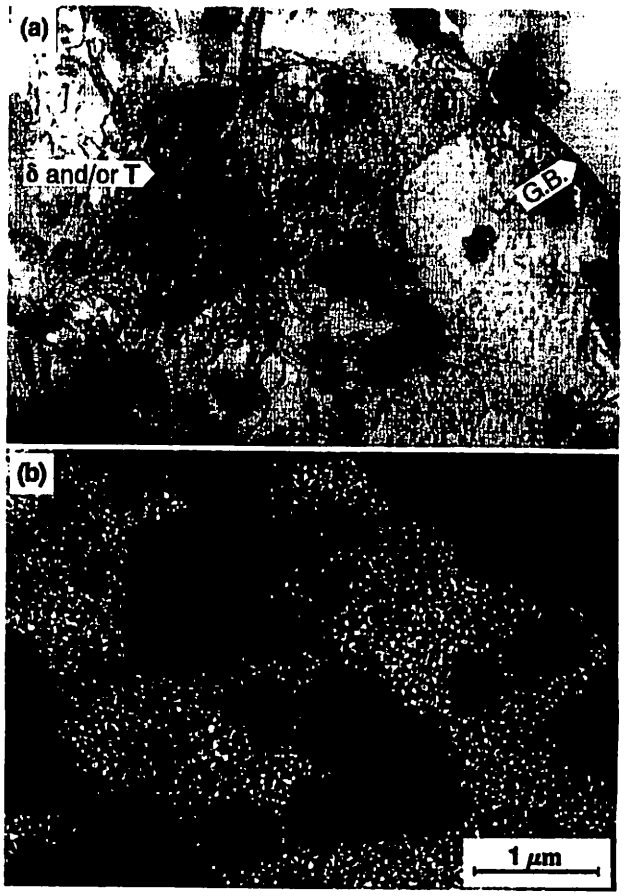

Fig. 7—(*a*) Bright-field and (*b*) dark-field images of the same area of the ECA-pressed material after solution treatment at 673 K and overaging at 448 K.

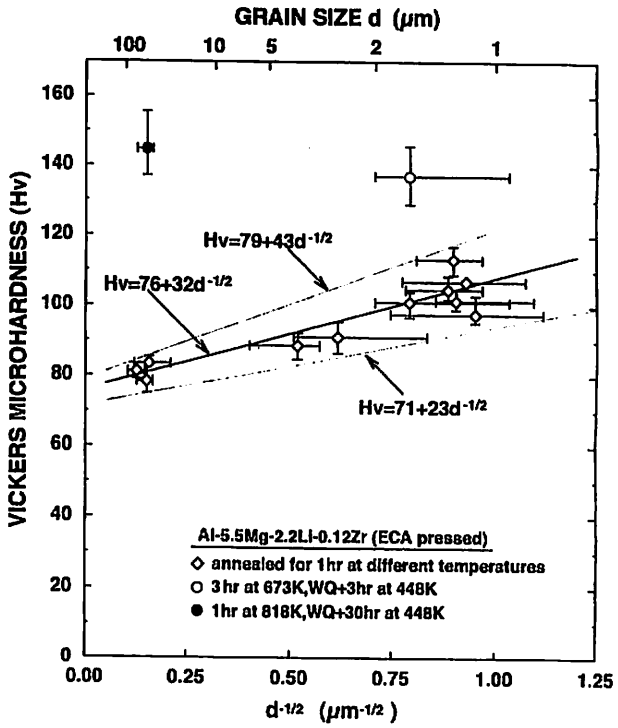

Fig. 8—Variation of Vickers microhardness with $d^{-1/2}$ for the ECA-pressed material after static annealing (lower points) and after the peak aged condition following solution treatments at 673 or 818 K (two upper points).

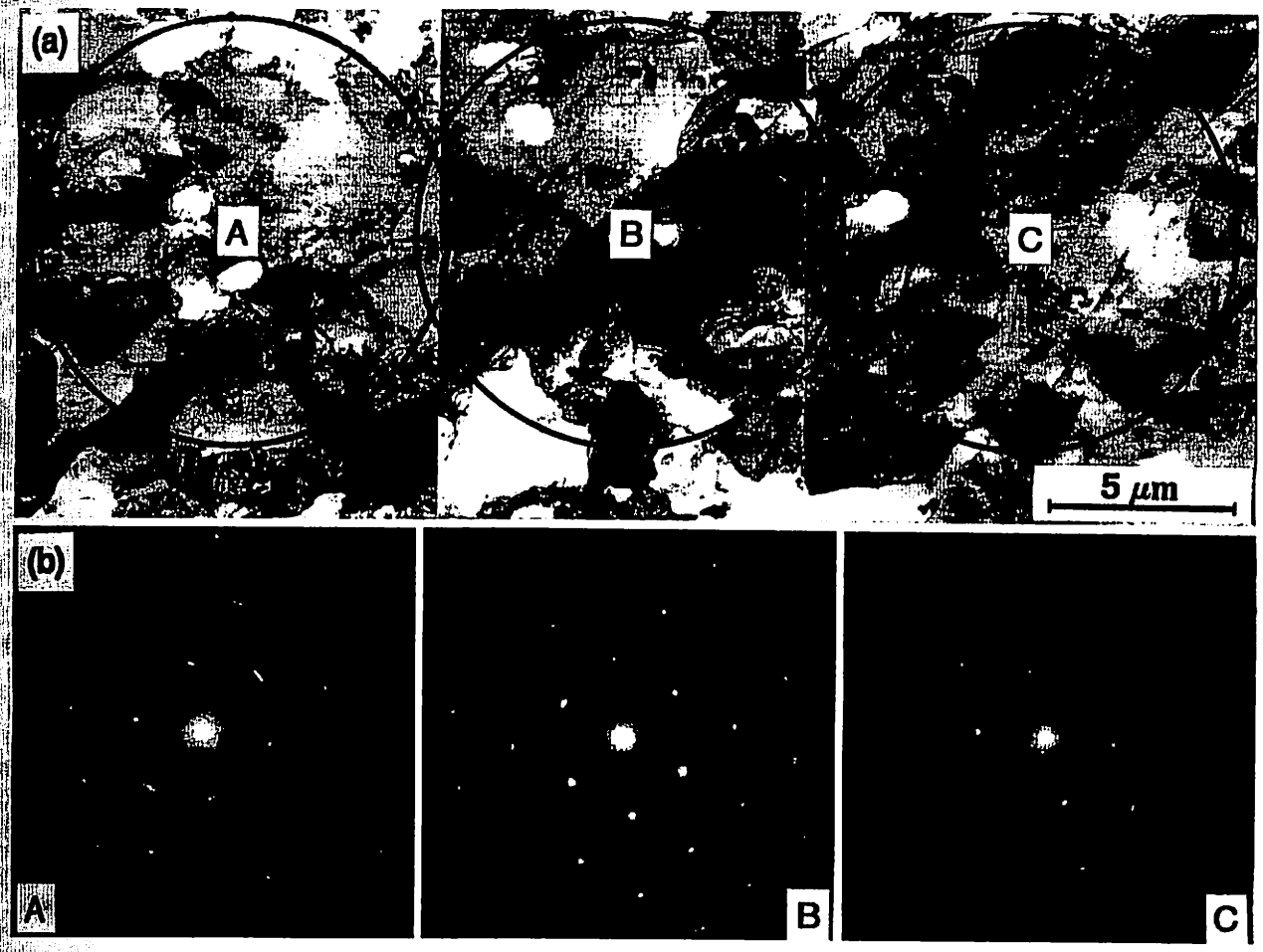

Fig. 9—(*a*) Microstructure of the hot-rolled Al-Mg-Li-Zr alloy without ECA pressing, and (*b*) SAED patterns taken from the regions marked A, B, and C.

ing from a solution treatment at 673 K leads both to an increase in the 0.2-pct proof stress because of the hardening introduced by precipitation of δ'-Al_3Li particles and to an associated decrease in the measured elongation to failure. Second, there is a consistent increase in the values of the 0.2-pct proof stresses and the elongations to failure with decreasing grain or subgrain size. Third, the ECA-pressed material with the very fine grain size exhibits the highest

Table I. Microstructures of the Samples Used for Proof Stress and Elongation Measurements in Figure 10

Experimental Condition	Microstructure
Hot-rolled (without ECA pressing) + 1 h at 673 K + WQ*	very large grains (~400 μm) containing elongated subgrains (length ~4 μm and width ~2 μm)
ECA pressed + 1 h at 673 K + WQ*	fine grains (~1.2 to 1.5 μm) surrounded by boundaries having both high and low angles of misorientation
ECA pressed + 1 h at 818 K + WQ*	coarse grains (~40 to 50 μm) with boundaries having high angles of misorientation

*WQ = iced water quench.

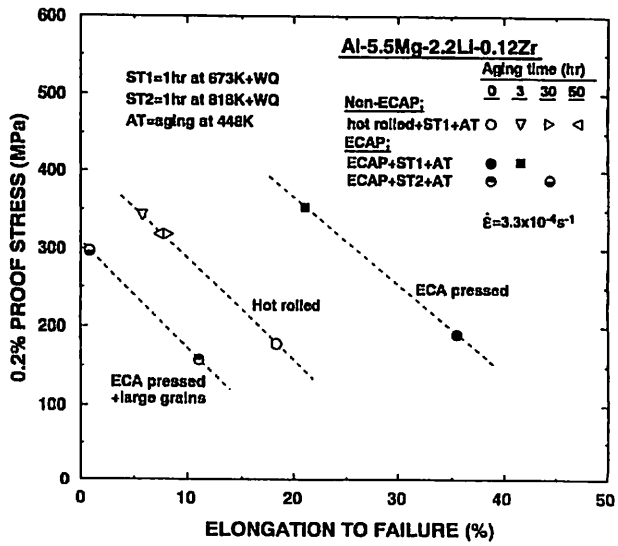

Fig. 10—Values of the 0.2 pct proof stress *vs* elongation to failure for specimens tested at room temperature with and without ECA pressing and following different aging conditions.

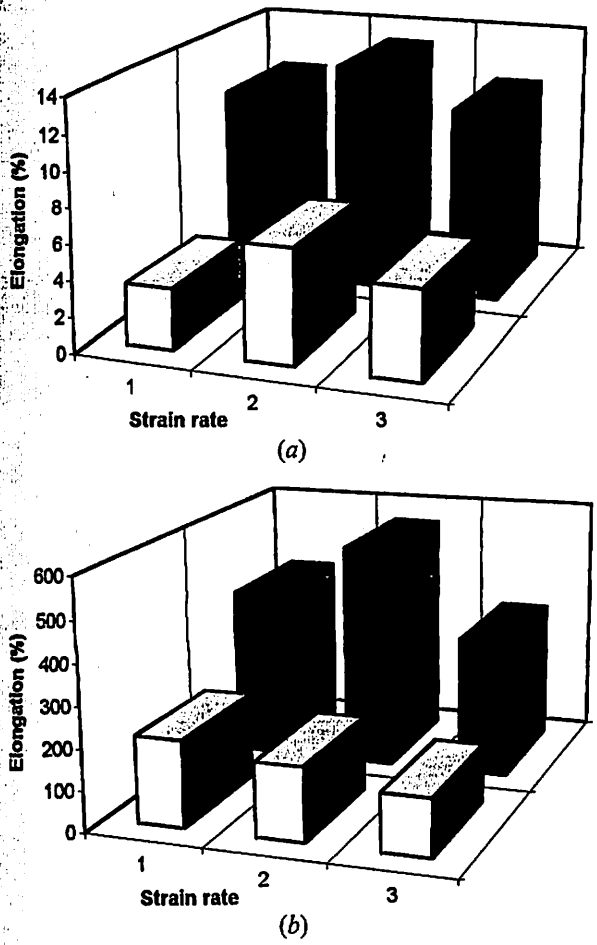

Fig. 11—Schematic illustration of the elongation to failure as a percentage *vs* the initial strain rate for tests conducted on the alloy without ECA pressing (front) and with ECA pressing (rear) at temperatures of (*a*) 298 K and (*b*) 603 K; the initial strain rates are designated as (1) 3.3×10^{-4} s^{-1}, (2) 3.3×10^{-3} s^{-1}, and (3) 3.3×10^{-2} s^{-1}.

strength and, by comparison with other similar alloys,[3,16,17] exceptionally good ductility at room temperature.

To check on the potential for utilization of the ECA-pressed alloy in superplastic forming applications, tests were conducted at 298 and 603 K using specimens either in the ECA-pressed or in the hot-rolled condition without any solution treatment; a detailed description of the microstructural condition after ECA pressing was given earlier, and a testing temperature of 603 K was selected because the earlier results demonstrated that the grain size remained at ~1.2 μm up to this temperature.[5] The results are illustrated schematically in Figure 11, where the elongation to failure as a percentage is plotted for three different initial strain rates designated as (1) 3.3×10^{-4}, (2) 3.3×10^{-3}, and (3) 3.3×10^{-2} s^{-1} for tests conducted at (a) 298 K (top) and (b) 603 K (bottom); data are shown for the material without ECA pressing (front) and with ECA pressing (rear). Inspection shows that the ECA-pressed material gives substantially higher elongations to failure for each testing condition: at 298 K, the maximum elongations are ~13 and ~6 pct for the ECA-pressed and hot-rolled conditions, respectively, whereas at 603 K, the maximum elongations are ~550 pct at 3.3×10^{-3} s^{-1} and ~210 pct at 3.3×10^{-4} s^{-1} for these two conditions, respectively. Thus, the total elongation to failure is not only substantially increased for the fine-grained material but, as anticipated from experimental data on typical superplastic alloys,[18] a reduction in grain size also leads to the occurrence of the maximum elongation at a faster strain rate. This increase in strain rate is especially attractive because it brings the superplastic capability of the alloy closer to the strain rate range utilized in commercial hot-working processes (~10^{-1} to 10^{2} s^{-1}).[19]

IV. DISCUSSION

Earlier experiments demonstrated that it was possible to use ECA pressing to reduce the grain size of a commercial Al-Mg-Li-Zr alloy from an initial size of ~400 μm to a size of ~1.2 μm and, in addition, to retain a grain size of <2 μm up to temperatures as high as ~700 K because of the presence of β'-Al_3Zr precipitates.[5] The present experiments extend these results by showing that the ECA-pressed material exhibits good strength and ductility at room temperature as compared to conventional Al-based alloys containing Li. Furthermore, as illustrated in Figure 10, the strength and elongation to failure may be manipulated through appropriate heat treatments.

An important objective of these experiments was to determine whether the ECA-pressed material was capable of exhibiting high tensile and superplastic-like ductility at elevated temperatures. Insufficient material was available in the ECA-pressed condition for extensive testing; but, nevertheless, the present limited results provide very clear evidence for the occurrence of superplastic flow at 603 K in the fine-grained material processed by ECA pressing. It should be noted that the maximum tensile ductility of ~550 pct obtained at a strain rate of ~10^{-3} s^{-1} exceeds the true effective strain of ~150 pct which has been recommended for the design of candidate parts in superplastic forming operations,[20] and it also exceeds the strains of up to ~200 to 300 pct which have been cited as the maximum strains incurred in the superplastic forming of sheet metal structures in aerospace and other applications.[21,22]

It is instructive to make a direct comparison between the tensile capability reported for the present alloy in the ECA-pressed condition and the superplastic Al-5083 alloy which has become well established as one of the two major alloys currently in use in the superplastic forming industry.[21]*

*The Al-5083 alloy contains, typically, 4.5 pct Mg, 0.7 pct Mn, and 0.1 pct Cr.

Experiments on high-purity samples of the Al-5083 alloy, with low Fe and Si contents, gave maximum elongations of ~450 pct at a temperature of 783 K using a strain rate of ~2×10^{-4} s^{-1}[23] and ~700 pct at 798 K with a strain rate of 2×10^{-4} s^{-1},[24] respectively. However, subsequent experiments on a commercial Al-5083 alloy suggested a maximum elongation only slightly in excess of 300 pct when testing at 783 K at a strain rate of ~4×10^{-4} s^{-1}.[25] This is consistent with, although a little lower than, the results documented in a detailed discussion of the properties and applications of the commercial superplastic Al-5083 alloy, where a potential maximum elongation of up to ~460 pct was reported at 783 K under a strain rate of ~2

$\times 10^{-4}$ s^{-1}.[26]* By comparison with the present very limited results for the ECA-pressed Al-Mg-Li-Zr alloy, it is apparent that the commercial Al-5083 alloy yields lower values for the maximum elongations to failure and, also, that these maximum values occur in the Al-5083 alloy both at higher testing temperatures and at lower strain rates. For industrial applications, lower forming temperatures are favored because they lead to a minimization of tool wear, and faster strain rates are beneficial because they increase the potential uses for the formed parts by facilitating an extension of the production runs to larger numbers of units.[28] It is therefore concluded that the present data on an ECA-pressed commercial Al-Mg-Li-Zr alloy serve to establish this Li-bearing alloy as a potential and attractive candidate material for use in superplastic forming applications.

*Elongations of up to 700 pct have also been reported in a modified Al-5083 alloy where 0.6 pct Cu was added as a grain refiner.[27]

V. SUMMARY AND CONCLUSIONS

1. Experiments were conducted on an Al-5.5 pct Mg-2.2 pct Li-0.12 pct Zr alloy subjected to ECA pressing to give a grain size of ~1.2 μm.
2. Following solution treatments at 673 or 818 K, aging was conducted for various times at a temperature of 448 K. Microhardness measurements after aging show that the peak aging is reached more rapidly when the grain size is very fine. This is attributed to the higher volume of PFZs around the δ-AlLi and/or T-Al_2MgLi phases in this condition.
3. Mechanical testing shows that the ECA-pressed material exhibits good ductility at room temperature, especially as compared to conventional Al-based alloys containing Li.
4. Elongations to fracture of up to ~550 pct may be achieved in the ECA-pressed material at 603 K when testing at an initial strain rate of $\sim 10^{-3}$ s^{-1}. These results, therefore, confirm the potential for use of the ECA-pressed alloy in superplastic forming operations.

ACKNOWLEDGMENTS

This work was supported in part by the Light Metals Educational Foundation of Japan; in part by a Grant-in-Aid for Scientific Research from the Ministry of Education, Science, Sports and Culture of Japan; in part by the National Science Foundation of the United States under Grant No. INT-9602919; and in part by the United States Army Research Office under Grant Nos. DAAH04-96-1-0332 and N68171-96-6-9006.

REFERENCES

1. E.J. Lavernia and N.J. Grant: *J. Mater. Sci.*, 1987, vol. 22, pp. 1521-29.
2. E.J. Lavernia, T.S. Srivatsan, and F.A. Mohamed: *J. Mater. Sci.*, 1990, vol. 25, pp. 1137-58.
3. I.G. Palmer, R.E. Lewis, and D.D. Crooks: in *Aluminum-Lithium Alloys*, T.H. Sanders and E.A. Starke, eds., TMS-AIME, Warrendale, PA, 1981, pp. 241-62.
4. M. Pridham, B. Noble, and S.J. Harris: in *Aluminium-Lithium Alloys III*, C. Baker, P.J. Gregson, S.J. Harris, and C.J. Peel, eds., The Institute of Metals, London, 1986, pp. 547-54.
5. M. Furukawa, Y. Iwahashi, Z. Horita, M. Nemoto, N.K. Tsenev, R.Z. Valiev, and T.G. Langdon: *Acta Mater.*, 1997, vol. 45, pp. 4751-57.
6. I.N. Fridlyander, V.S. Sandler, and T.I. Nikol'skaya: *Fiz. Metal. Metalloved.*, 1971, vol. 32, pp. 767-74.
7. J. Wang, Y. Iwahashi, Z. Horita, M. Furukawa, M. Nemoto, R.Z. Valiev, and T.G. Langdon: *Acta Mater.*, 1996, vol. 44, pp. 2973-82.
8. Y. Iwahashi, J. Wang, Z. Horita, M. Nemoto, and T.G. Langdon: *Scripta Mater.*, 1996, vol. 35, pp. 143-46.
9. L.P. Costas and R.P. Marshall: *Trans. TMS-AIME*, 1962, vol. 224, pp. 970-74.
10. R. Nozato and G. Nakai: *Trans. Jpn. Inst. Met.*, 1977, vol. 18, pp. 679-89.
11. D.B. Williams and J.W. Edington: *Phil. Mag.*, 1974, vol. 30, pp. 1147-53.
12. D.B. Williams and J.W. Edington: *Met. Sci.*, 1975, vol. 9, pp. 529-32.
13. M. Furukawa, Y. Miura, and M. Nemoto: *Trans. Jpn. Inst. Met., 1985*, vol. 26, pp. 225-29.
14. M. Furukawa, Y. Miura, and M. Nemoto: *J. Phys., Coll. C3*, 1987, vol. 48, pp. C3-557-C3-563.
15. M. Furukawa, H. Wang, and M. Nemoto: *J. Jpn. Inst. Light Met.*, 1990, vol. 40, pp. 20-26.
16. E.S. Balmuth and R. Schmit: in *Aluminum-Lithium Alloys*, T.H. Sanders and E.A. Starke, eds., TMS-AIME, Warrendale, PA, 1981, pp. 69-88.
17. B. Noble, S.J. Harris, and K. Marlow: in *Aluminum-Lithium Alloys II*, T.H. Sanders and E.A. Starke, eds., TMS-AIME, Warrendale, PA, 1984, pp. 65-77.
18. F.A. Mohamed, M.M.I. Ahmed and T.G. Langdon: *Metall. Trans.*, 1977, vol. 8A, pp. 933-38.
19. K. Higashi, M. Mabuchi, and T.G. Langdon: *Iron Steel Inst. Jpn. Int.*, 1996, vol. 36, pp. 1423-38.
20. J.M. Story: in *Superplasticity in Aerospace II*, T.R. McNelley and H.C. Heikkenen, eds., TMS, Warrendale, PA, 1990, pp. 151-66.
21. A.J. Barnes: *Mater. Sci. Forum*, 1994, vols. 170-172, pp. 701-14.
22. C.F. Dressel: in *Superplasticity: 60 Years After Pearson*, N. Ridley, ed., The Institute of Materials, London, 1995, pp. 359-76.
23. H. Iwasaki, K. Higashi, S. Tanimura, T. Komatubara, and S. Hayami: in *Superplasticity in Advanced Materials*, S. Hori, M. Tokizane, and N. Furushiro, eds., The Japan Society for Research on Superplasticity, Osaka, 1991, pp. 447-52.
24. H. Imamura and N. Ridley: in *Superplasticity in Advanced Materials*, S. Hori, M. Tokizane, and N. Furushiro, eds., The Japan Society for Research on Superplasticity, Osaka, 1991, pp. 453-58.
25. J.S. Vetrano, C.A. Lavender, C.H. Hamilton, M.T. Smith, and S.M. Bruemmer: *Scripta Metall. Mater.*, 1994, vol. 30, pp. 565-70.
26. M. Matsuo: in *Superplasticity: 60 Years After Pearson*, N. Ridley, ed., The Institute of Materials, London, 1995, pp. 277-83.
27. H. Watanabe, K. Ohori, and Y. Takeuchi: *Trans. Iron Steel Inst. Jpn.*, 1987, vol. 27, pp. 730-33.
28. Y. Ma, M. Furukawa, Z. Horita, M. Nemoto, R.Z. Valiev, and T.G. Langdon: *Mater. Trans. JIM*, 1996, vol. 28, pp. 336-39.

FABRICATION AND PROPERTIES OF A SUBMICROMETER-GRAINED Zn-22% Al ALLOY

Minoru Furukawa,[1] Yan Ma,[2] Zenji Horita,[3] Minoru Nemoto,[3]
Ruslan Z. Valiev[4] and Terence G. Langdon[2]

[1]Department of Technology, Fukuoka University of Education
Munakata, Fukuoka 811-41, Japan
[2]Departments of Materials Science and Mechanical Engineering
University of Southern California, Los Angeles, CA 90089-1453, U.S.A.
[3]Department of Materials Science and Engineering, Faculty of Engineering 36
Kyushu University, Fukuoka 812-81, Japan
[4]Institute of Physics of Advanced Materials
Ufa State Aviation Technical University, Ufa 450000, Russia

Abstract

Numerous investigations have demonstrated the superplastic properties of the Zn-22% Al eutectoid alloy. It is possible to retain a very small grain size in this two-phase material, of the order of ~1 - 2 μm, and tensile testing gives superplastic elongations up to >2000% at elevated temperatures.

Experiments were conducted to investigate the feasibility of introducing an ultra-fine submicrometer grain size into the Zn-22% Al alloy. A reduction in grain size is potentially beneficial both for increasing the elongations to failure and for increasing the strain rates associated with superplastic flow. Two different procedures were used to obtain a submicrometer grain size. First, samples were prepared in the form of disks and they were subjected to torsion straining under a high pressure at room temperature up to a maximum strain of ~7. Examination showed these samples had an equiaxed grain size in the range of 0.1 - 0.5 μm. Second, bulk samples were deformed to a strain of ~8 using the procedure of equal-channel angular (ECA) pressing. Inspection showed that these samples contained elongated grains with sizes of the order of 0.4 - 0.8 μm and tensile testing gave a maximum elongation of ~1970% at a testing temperature of 473 K using an initial strain rate of 3.3×10^{-2} s^{-1}. The significance of the microstructure in optimizing the superplastic characteristics is discussed.

THERMEC'97
International Conference on Thermomechanical
Processing of Steels & Other Materials
Edited by T. Chandra and T. Sakai
The Minerals, Metals & Materials Society, 1997

Introduction

Superplasticity has been defined as "the ability of a polycrystalline material to exhibit, in a generally isotropic manner, very high tensile elongations prior to failure" [1]. It is now well established that there are two major requirements in order to achieve superplasticity in metals [2]. First, the grain size must be very small and typically <10 μm. Second, the testing temperature must be reasonably high and typically at least $0.5T_m$, where T_m is the absolute melting temperature of the material.

The Zn-22% Al eutectoid alloy is a classic superplastic material in which a very fine and stable grain size may be attained because of the presence of two separate phases. Typically, superplasticity is achieved in the Zn-22% Al alloy when the grain size is in the range of ~ 1 - 5 μm: for example, there are reports of tensile elongations in this alloy in excess of 2000% over almost two orders of magnitude of strain rate [3] although the precise elongations to failure are dependent upon the testing temperature and the specimen grain size [4]. Experimental evidence with the Zn-22% Al alloy suggests that a decrease in grain size will lead to an increase in the elongations to failure and, in addition, the maximum elongations will occur at faster strain rates [4]. There is also evidence from experiments on an Al-Cu-Zr alloy that a reduction in grain size will reduce the temperature associated with optimum superplasticity [5]. In practice, both of these trends would be beneficial for superplastic forming processes. However, normal grain refining of the Zn-22% Al eutectoid alloy leads generally to a minimum grain size of ~ 1 - 2 μm.

It was shown recently that a submicrometer grain size may be introduced into the alloy by imposing intense plastic straining using a torsion technique [6] but the samples thus fabricated were too small for normal tensile testing. Therefore, the purpose of the present paper is to extend these earlier results by examining the microstructural development and the tensile properties of a submicrometer-grained Zn-22% Al alloy produced using an alternative processing method.

Experimental material and procedures

The material used in this investigation was a commercial Zn-22% Al binary alloy received in the superplastic condition in the form of as-rolled sheet with a grain size of the order of ~ 1 μm. The microstructure in the as-received condition is shown in Fig. 1, and it consists of an essentially random distribution of equiaxed Al and Zn grains; these two phases are revealed as bright and dark grains in Fig. 1, respectively. Chemical analysis of the as-received material revealed the following impurities in ppm: Cr $<$ 10, Cu 45, Fe 390, Mg 2, Mn $<$ 10 and Si 75. Two different procedures were used to introduce a submicrometer grain size into this alloy and these procedures are illustrated schematically in Fig. 2.

Equal-channel angular (ECA) pressing is a procedure, described elsewhere [7], in which a sample is pressed with a plunger through a die consisting of two channels of equal cross-section which intersect at an angle Φ. In the present work, the samples used for ECA pressing were cut from the as-rolled sheet in the form of cylinders with diameters of 20 mm and a total length of $\sim$70 mm. The experimental facility is illustrated on the left in Fig. 2 where P is the imposed load and the angle Ψ defines the outer arc of curvature at the point where the two channels intersect. In practice, the same sample can be pressed repetitively through the die in order to accumulate a large total strain. It can be shown that a single passage through a die of this form leads to a strain, ε, which is given by [8]

Figure 1 - Microstructure of Zn-22% Al in the as-received condition.

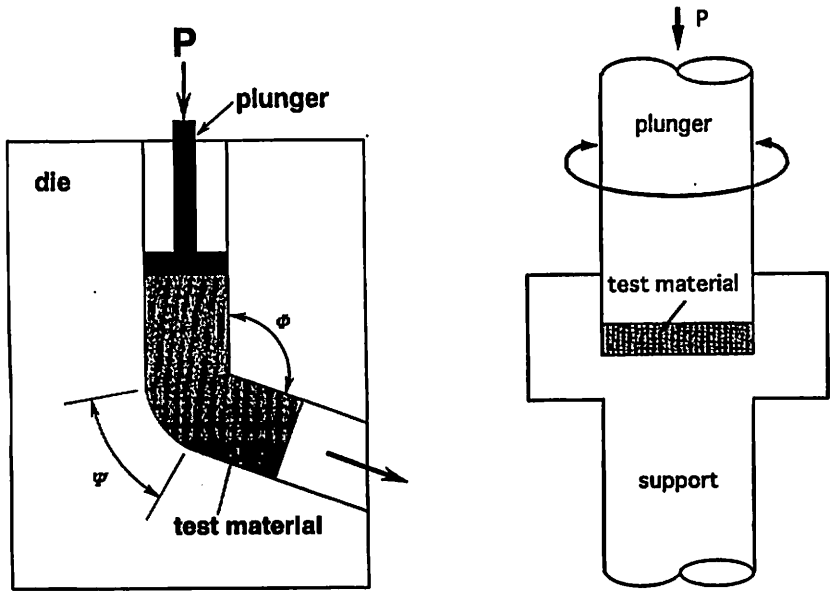

Figure 2 - Schematic illustration of ECA pressing (on left) and torsion straining (on right).

$$\varepsilon = \left[\frac{2\cot\left(\frac{\Phi}{2}+\frac{\Psi}{2}\right)+\Psi\,\mathrm{cosec}\left(\frac{\Phi}{2}+\frac{\Psi}{2}\right)}{\sqrt{3}} \right] \qquad (1)$$

so that, for N repetitive pressings, the total strain is $N\varepsilon$. In the present experiments, the ECA pressing was conducted at 373 K using a facility with $\Phi = 90°$ and each sample was pressed through the die for 8 passes to give a total strain of ~ 8.

The principle of torsion straining was described earlier [9] and it is illustrated schematically on the right in Fig. 2. The samples, in the form of disks of diameter 15 mm and thickness 0.3 mm, were held in place in a torsion straining facility under a pressure, P, of 5.5 GPa and then they were strained in torsion at room temperature. In this procedure, the strain is given by

$$\varepsilon = \ln\left(\frac{\phi r}{\ell}\right) \qquad (2)$$

where ϕ is the rotation angle in radians and r and ℓ are the diameter and thickness of the disk, respectively. Samples were strained in these experiments to give a maximum strain of ~ 7 at the perimeters of the disks.

Microstructures were examined after straining using transmission electron microscopy (TEM) and selected area electron diffraction patterns were obtained from regions having diameters of 6.2 μm. Samples prepared using ECA pressing were rolled into sheets at room temperature and tensile specimens were machined with a gauge length of 7 mm and gauge cross-section of 2×5 mm^2. Tensile tests were conducted at temperatures from 373 to 473 K by immersing the specimens in an oil bath and using an Instron testing machine operating at constant rates of cross-head displacement from 3.3×10^{-4} to 3.3×10^{-1} s^{-1}.

Experimental results and discussion

The typical microstructure after ECA pressing is shown in Fig. 3. The grain size measured from TEM photomicrographs was in the range of 0.4 - 0.8 μm and inspection showed the grains were elongated and there was a co-existence of areas with relatively fine grains (on the left in Fig. 3) and areas with coarser grains (on the right in Fig. 3). The grains after ECA pressing showed only minor evidence for a mixing of the two phases but rather there were agglomerates of Al-rich and Zn-rich grains which were divided into smaller grains through the formation of additional grain boundaries within each grain. There appeared to be less agglomeration after torsion straining, as shown in Fig. 4 where the grains are essentially equiaxed and they have average sizes varying from ~ 0.1 μm (on the left in Fig. 4) to ~ 0.5 μm (on the right in Fig. 4). The higher magnification photomicrographs shown in Fig. 5 demonstrate that the Al-rich grains contain (a) rod-shaped precipitates of stable hcp Zn in the as-received material and (b) very little evidence for these Zn precipitates after torsion straining. These observations suggest that the Zn precipitates are absorbed by Zn-rich grains during the intense plastic straining.

Table 1 summarizes the data obtained from the tensile testing of samples of the ECA pressed

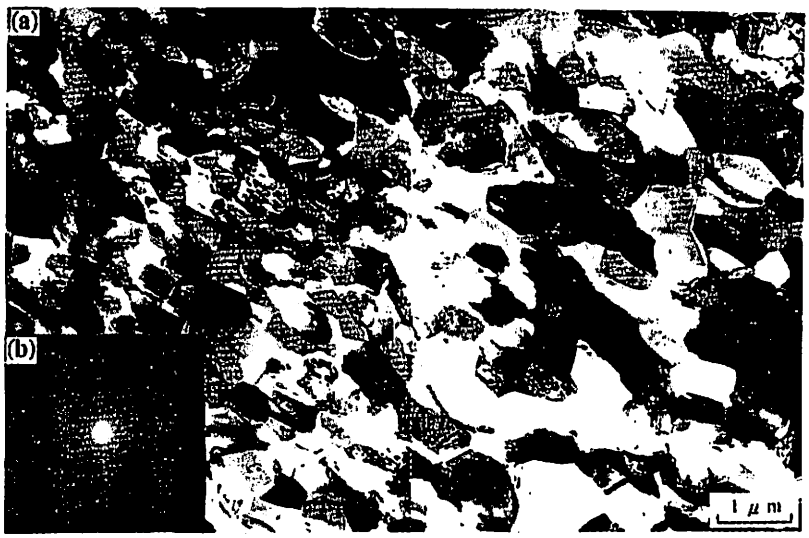

Figure 3 - Microstructure after ECA pressing.

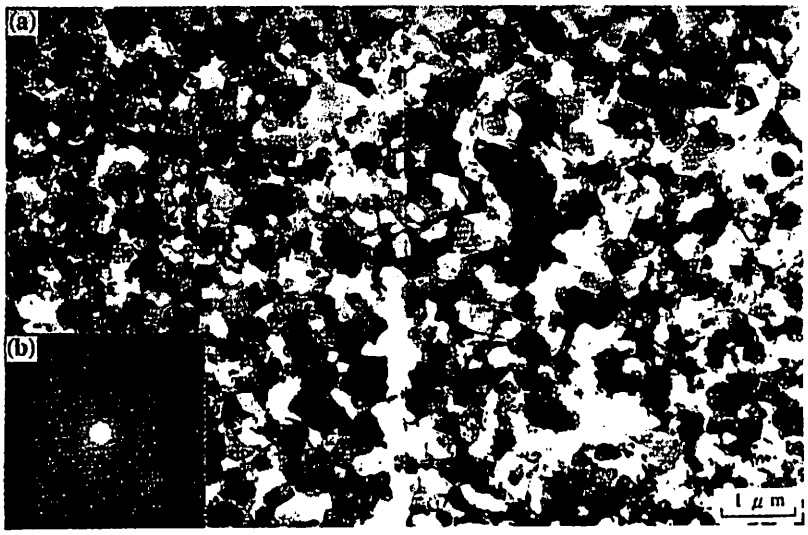

Figure 4 - Microstructure after torsion straining.

Figure 5 - Aluminum-rich grains (a) in as-received condition and (b) after torsion straining.

Table 1 - Elongations and flow stresses for ECA pressed samples.

Temperature (K)	Strain rate (s^{-1})	Flow stress (MPa)	Elongation to failure
373	3.3×10^{-4}	17.0	450%
423	3.3×10^{-4}	11.0	700%
	3.3×10^{-3}	25.9	940%
473	3.3×10^{-2}	26.8	1970%
	3.3×10^{-1}	66.3	1540%

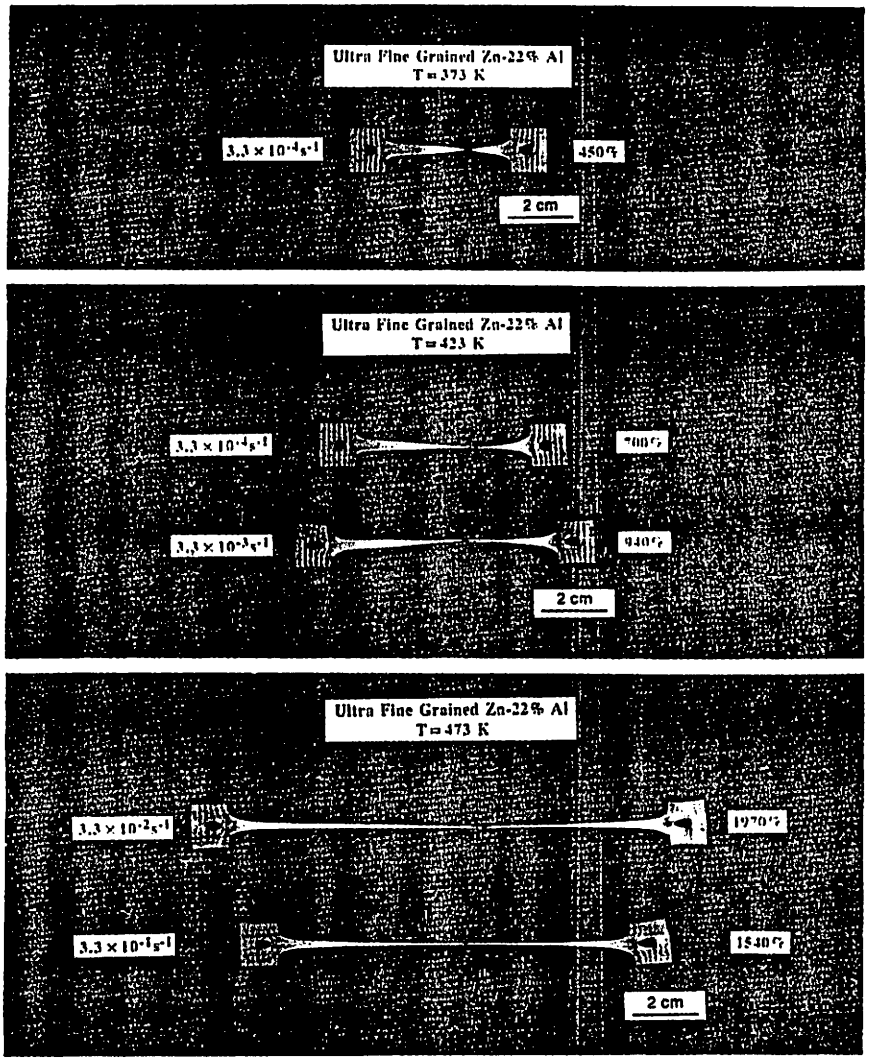

Figure 6 - Tensile testing after ECA pressing at 373 K (upper), 423 K (center) and 473 K (lower).

material where specimens were pulled to failure in the temperature range from 373 to 473 K and Fig. 6 shows the appearance of the specimens after testing at temperatures of 373 K (upper), 423 K (center) and 473 K (lower). It is apparent from Fig. 6 that all specimens pull out in a manner which is typical of superplastic materials tested in or close to the optimum conditions for maximum ductility, and in particular the two specimens tested at 473 K exhibit the quasi-uniform and neck-free deformation reported in the Zn-22% Al alloy without ECA pressing [10]. Figure 7 shows the appearance of the microstructure at a distance of ~ 1 mm from the fracture tip of the specimen pulled to a strain of 1970% at 473 K using an initial strain rate of 3.3×10^{-2} s^{-1}: there is evidence for the growth of grains to ~ 1.5 - 2.0 μm and there is no longer any agglomeration.

The elongations to failure observed in these experiments are fairly similar to those reported earlier in the same eutectoid alloy without ECA pressing and with a grain size of 2.5 μm [3,4]. However, it is significant to note that the elongation of 1540% observed at 473 K at the fastest strain rate of $\sim 10^{-1}$ s^{-1} is higher than the value of $\sim 1100\%$ achieved earlier and suggests a potential for attaining high elongations at reasonably rapid strain rates. The failure to observe

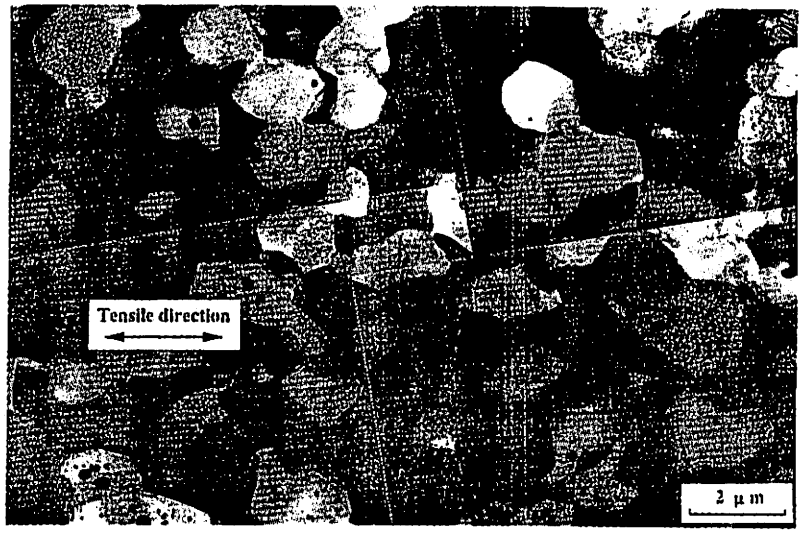

Figure 7 - Appearance of grains near the fracture tip of a specimen pulled to failure at 1970% at 473 K with an initial strain rate of 3.3×10^{-2} s^{-1}.

even higher elongations after ECA pressing in these experiments is probably due to the formation of agglomerates of submicrometer-sized Al-rich and Zn-rich phases rather than the creation of a true mixture of the two phases. Thus, it appears important to produce a uniform and random array of Al-rich and Zn-rich grains without significant agglomeration.

Acknowledgements

This work was supported in part by the Light Metals Educational Foundation of Japan, in part by a Grant-in-Aid for Scientific Research from the Ministry of Education, Science, Sports and Culture of Japan, in part by the National Science Foundation of the United States under Grant No. INT-9602919, and in part by the U.S. Army Research Office under Grants No. DAAH04-96-1-0332 and N68171-96-6-9006.

References

1. T.G. Langdon and J. Wadsworth, Superplasticity in Advanced Materials, S. Hori, M. Tokizane and N. Furushiro, eds (Osaka, Japan: The Japan Society for Research on Superplasticity, 1991), 847.
2. T.G. Langdon, Metall. Trans. A 13A (1982) 689.
3. H. Ishikawa, F.A. Mohamed and T.G. Langdon, Phil. Mag. 32 (1975) 1269.
4. F.A. Mohamed, M.M.I. Ahmed and T.G. Langdon, Metall. Trans. A 8A (1977) 933.
5. R.Z. Valiev, O.A. Kaibyshev, R.I. Kuznetsov, R.Sh. Musalimov and N.K. Tsenev, Dokl. Akad. Nauk SSSR 301 (1988) 864.
6. M. Furukawa, Z. Horita, M. Nemoto, R.Z. Valiev and T.G. Langdon, J. Mater. Res. 11 (1996) 2128.
7. J. Wang, Y. Iwahashi, Z. Horita, M. Furukawa, M. Nemoto, R.Z. Valiev and T.G. Langdon, Acta Mater. 44 (1996) 2973.
8. Y. Iwahashi, J. Wang, Z. Horita, M. Nemoto and T.G. Langdon, Scripta Mater. 35 (1996) 143.
9. Z. Horita, D.J. Smith, M. Furukawa, M. Nemoto, R.Z. Valiev and T.G. Langdon, J. Mater. Res. 11 (1996) 1880.
10. M.M.I. Ahmed, F.A. Mohamed and T.G. Langdon, J. Mater. Sci. 14 (1979) 2913.

CHARACTERIZATION OF ULTRA-FINE GRAINED MATERIALS PRODUCED BY TORSION STRAINING

Zenji Horita,[1] David J.Smith,[2] Minoru Furukawa,[3] Minoru Nemoto[1]
Ruslan Z.Valiev[4] and Terence G.Langdon[5]

[1]Department of Materials Science and Engineering, Faculty of Engineering
Kyushu University, Fukuoka 812-81, Japan
[2]Department of Physics and Astronomy and Center for Solid State Science
Arizona State University, Tempe, AZ 85287-1504, U.S.A.
[3]Department of Technology, Fukuoka University of Education
Munakata, Fukuoka 811-41, Japan
[4]Institute of Physics of Advanced Materials, Ufa State Aviation Technical University
Ufa 450000, Russia
[5]Departments of Materials Science and Mechanical Engineering,
University of Southern California,
Los Angeles, CA 90089-1453, U.S.A.

Abstract

It is well established that superplasticity occurs by the process of grain boundary sliding and it requires a very small grain size, typically in the range of ~1-10 μm. It is anticipated that further reduction of grain size, especially below 1μm, will lead to superplasticity at high strain rates or low temperatures, which is clearly beneficial for superplastic forming processes.

Several methods are available for reducing the grain size of polycrystalline samples based on subjecting the materials to intense plastic straining. Of these procedures, torsion straining under high pressure leads to small disks, with diameter of ~15 mm, which can be easily prepared for examination by transmission electron microscopy.

This paper describes the synthesis and characterizations of three different materials (Al-3%Mg, Cu and Ni) prepared in a submicrometer condition using the torsion straining technique. Specimens were examined using high-resolution electron microscopy and it is demonstrated that the grain boundaries of these materials are in a high-energy and non-equilibrium configuration and contain regular and irregular arrangements of facets and steps. This paper describes the nature of the boundaries in these three materials and the significance of processing at different fractions of the melting temperatures.

THERMEC'97
International Conference on Thermomechanical
Processing of Steels & Other Materials
Edited by T. Chandra and T. Sakai
The Minerals, Metals & Materials Society, 1997

Introduction

High-strain-rate superplasticity or low-temperature superplasticity may be achieved by reducing the grain size to the submicrometer range [1]. However, the grain boundary structure significantly affects the overall ductility as grain boundary sliding is a dominant process in the superplasticity regime [2]. The cavitation accompanying grain boundary sliding may be detrimental to the ductility [3]. The control of grain boundary structure as well as the reduction of grain size is therefore important in order to attain superplasticity at high strain rates or low temperatures.

It was shown that metallic materials with submicrometer grains can be produced by imposing intense plastic strain under quasi-hydrostatic pressure [4-6]. With this technique, the grain size can be reduced to the submicron level or, occasionally, to the nanometer level. The technique is now gaining popularity because it is capable of producing a large quantity of the submicrometer-grained (SMG) materials without introducing any porosity.

Microstructural observations using transmission electron microscopy showed that many grain boundaries, after being subjected to intense plastic straining, are curved, wavy or poorly defined [7,8]. Such observations suggest that the grain boundaries are in a high-energy non-equilibrium configuration. This conclusion has been confirmed by recent studies using high-resolution electron microscopy (HREM) where atomic structures of the grain boundaries and their vicinities were examined [9]. In this paper, the results of the HREM observations are reviewed with three different materials, Al-3%Mg, Cu and Ni. The fabrication of SMG structures usually creates an array of non-equilibrium grain boundaries which may be partially relaxed into a more equilibrated structure [10]. Therefore, the present review with three different materials having different melting points should be significant in order to deduce the grain boundary structures of the SMG samples produced by the intense plastic straining technique.

Experimental materials and procedures

The SMG structure was produced in samples of Al-3%Mg, high purity (99.98%) Cu and high purity (99.99%) Ni using a torsion straining technique. The details of the technique were described elsewhere [4,5,9]. The initial grain size of Al-3%Mg was ~500 μm and those of Cu and Ni were both ~50 μm. Each sample was cut to disks with dimensions of ~15 mm diameter and ~0.3 mm thickness and subjected to torsion straining up to a strain of ~7. The straining was conducted at room temperature which corresponds to ~0.32 T_m for Al-3%Mg, ~0.22 T_m for Cu and ~0.17 T_m for Ni. The disks after straining were cut and ground to small disks having diameters of 3 mm and thicknesses of ~0.15 mm. The small disks were then thinned for transmission electron microscopy using a twin-jet electropolishing technique in solutions of 10%$HClO_4$, 20%$C_3H_8O_3$ plus 70%C_2H_5OH for Al-3%Mg, 30%HNO_3 plus 70%$C_3H_8O_3$ for Cu and 10%H_2SO_4, 10%CH_3OH plus 80%C_2H_5OH for Ni at a temperature of 278 K. The thinned specimens were examined using an H-8100 electron microscope and a JEM-2000FX electron microscope, both operating at 200 kV and a JEM-4000EX high-resolution electron microscope operating at 400 kV. The former microscopes were used for observations of grains and grain boundary configurations at lower magnification, and the latter microscope was used for higher magnification and lattice image observations at and near the grain boundaries. Lattice images were taken at close to the optimum defocus condition, typically at magnifications of 500,000 times. Since the grain sizes were much less than 1 μm, individual grains could not

always be tilted during observation. However, a sufficient number of grains oriented close to <110> was found for lattice imaging.

Experimental results and discussion

Typical microstructures after torsion straining are shown in Figs. 1, 2 and 3 for Al-3%Mg, Cu and Ni, respectively. The selected-area electron diffraction (SAED) patterns are also included, taken from regions of 1.9 μm for Al-3%Mg and of 1.3 μm for Cu and Ni. Each SAED pattern consists of rings with many diffracted beams and thus demonstrates that there are many grains with multiple orientation within the selected field of view. The average grain sizes measured from the electron micrographs were ~0.09 μm for Al-3%Mg, ~0.17 μm for Cu and ~0.13 μm for Ni. The image contrast within the grains is not uniform but changes in a complex way. There are many grain boundaries which are wavy, curved or not well defined. All of these observations suggest that the grains and grain boundaries after the torsion straining are in a high-energy and non-equilibrium state.

Figures 4, 5 and 6 are higher magnification images of grains in the as-strained structures for Al-3%Mg, Cu and Ni, respectively. Common features to all three images are that the grain boundaries are wavy, curved or corrugated along their length and some portions of the boundaries are inclined to the surface normal. Dislocations are also visible within the grains.

A lattice image of the region marked A in Fig.4 of the SMG Al-3%Mg is shown in Fig.7. The boundary exhibits a periodic, stepwise arrangement of facets parallel to {111} planes and each facet consists of about 10 layers of {111} planes. The facet density is estimated to be ~$5x10^8$ m^{-1}. Regular arrangements of facets and steps were also observed on other boundaries in the SMG Al-3%Mg. Figure 8 shows a lattice image of the boundary region indicated by A in Fig.5 of the SMG Cu. The boundary exhibits an irregular nature consisting of facets and steps without any defined periodicity. There is a region marked B, with a width of ~4 nm, where one dimensional {111} lattice fringes from the lower grain are bent at ~9°. The region B appears to be fragmented from the lower grain. Some lattice fringes terminated at points marked T, suggesting the presence of dislocations. The region indicated by A in Fig 6 of the SMG Ni is enlarged in Fig. 9 to provide a close examination of the grain boundary structure. The boundary exhibits a zigzag configuration but there is no periodicity in the zigzag nature.

The HREM observations reveal that the grain boundaries in the three different SMG samples are not smooth but they have a zigzag nature, which then demonstrates that they are in high-energy and non-equilibrium configuration. Furthermore, the boundaries have high angles of misorientation and narrow width. In earlier reports, it was shown that the grain boundary structures of an SMG Al-3%Mg alloy evolved into more stable configuration as a result of irradiation by high-energy electrons during HREM observations [9,11,12]. It is then concluded that the non-equilibrium nature of the grain boundaries observed by HREM is representative of the structures inherent in or very close to the as-strained condition.

The structural features of the grain boundary are essentially similar in all three samples. However, the steps and facets observed in the boundaries of the SMG Al-3%Mg alloy are more ordered and uniformly distributed by comparison with the SMG Cu and Ni. This suggests that some relaxation of the grain boundary structure has occurred in the SMG Al-3%Mg during intense straining. It is reasonable that a partial relaxation of the grain boundary structure may be

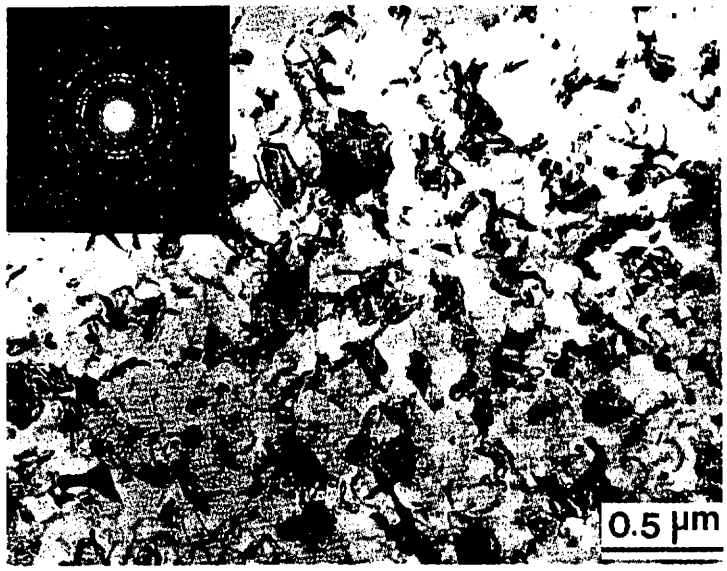

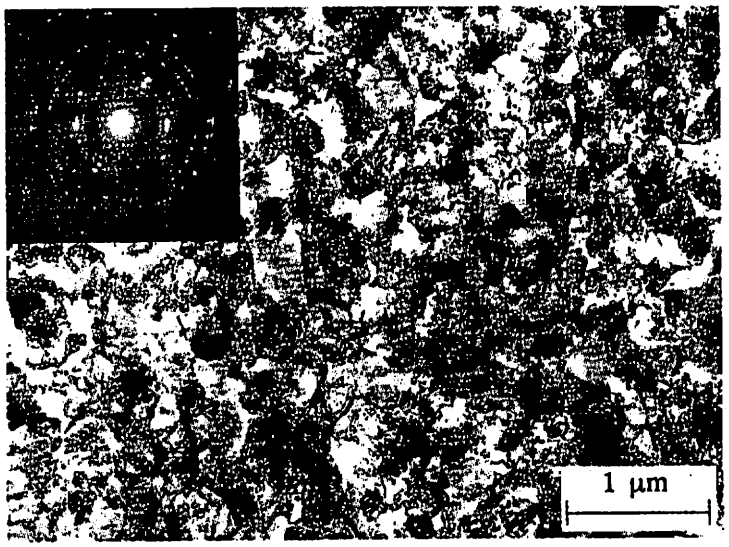

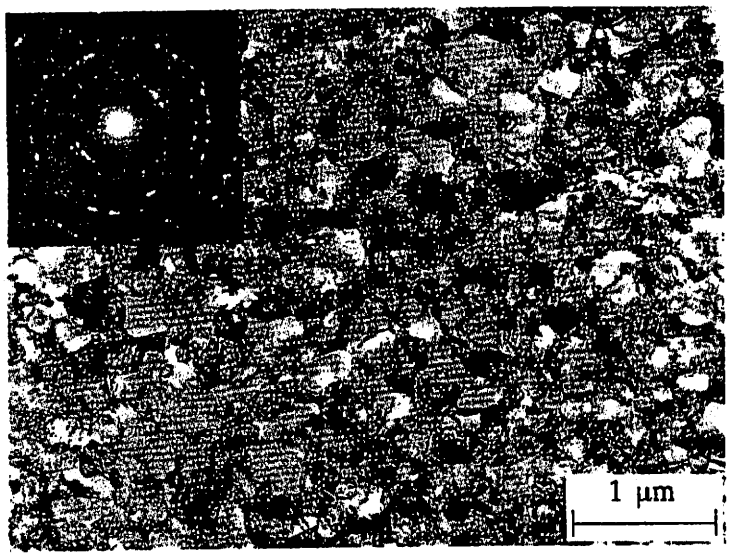

Figure 1 (top) - Low magnification image of Al-3%Mg with SAED pattern inset.
Figure 2 (center) - Low magnification image of Cu with SAED pattern inset.
Figure 3 (bottom) - Low magnification image of Ni with SAED pattern inset.

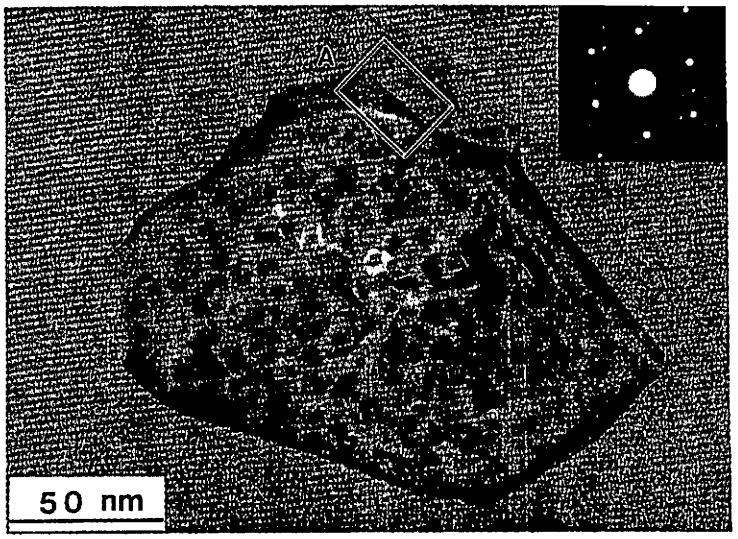

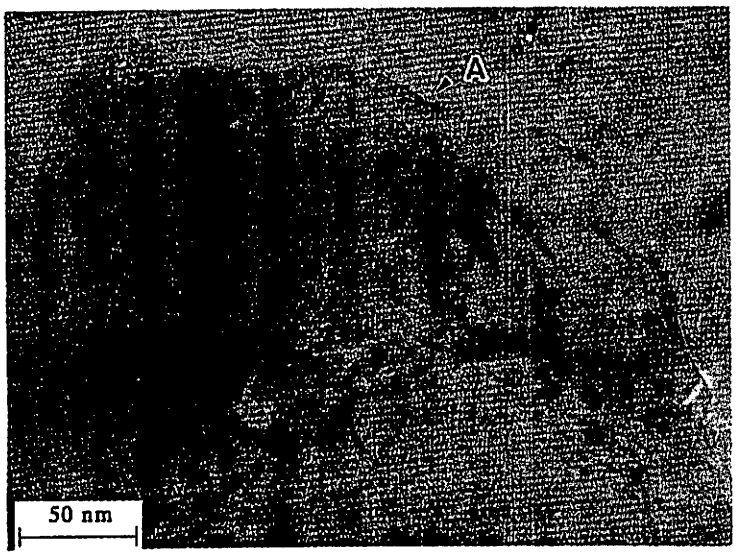

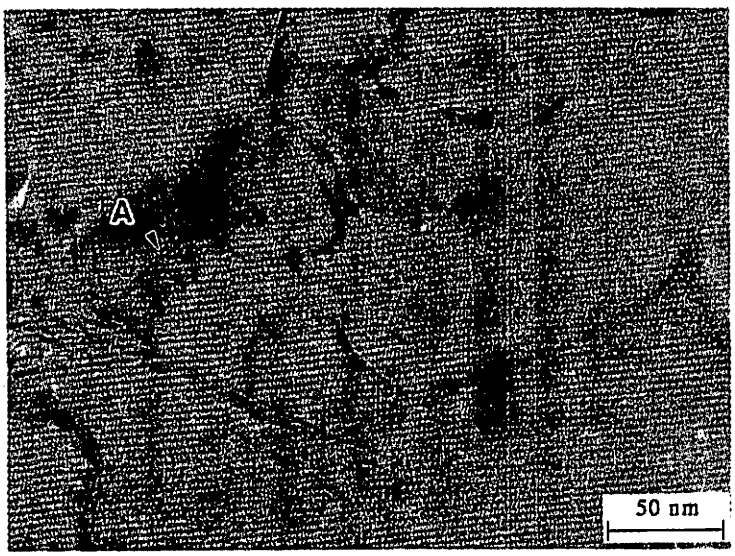

Figure 4 (top) - Electron micrograph and SAED pattern (inset) from grain in Al-3%Mg. Region A shown enlarged in Fig.7.

Figure 5 (center) - Electron micrograph from grain in Cu. Region A shown enlarged in Fig.8.

Figure 6 (bottom) - Electron micrograph from grains in Ni. Region A shown enlarged in Fig.9.

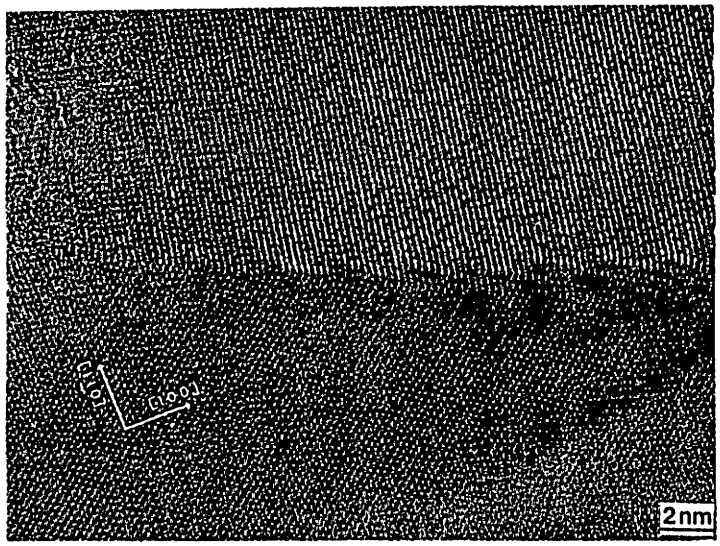

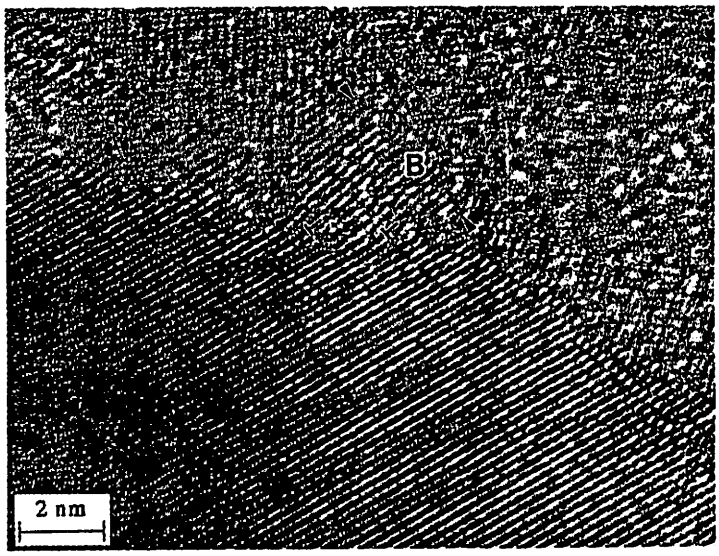

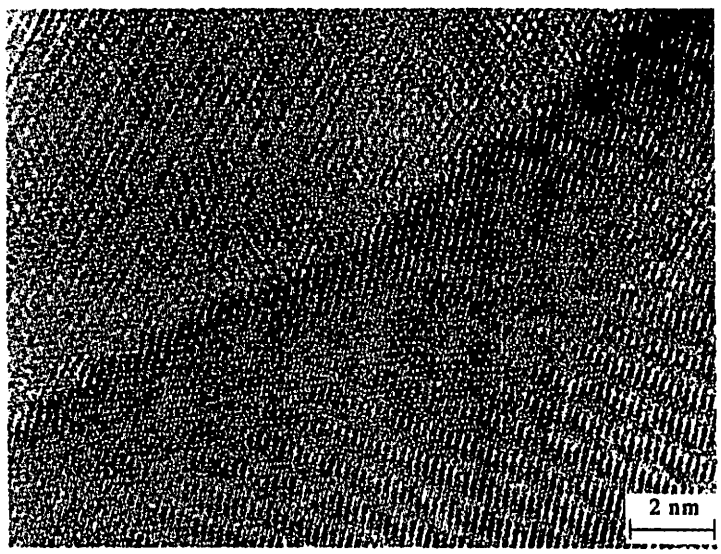

Figure 7 (top) - Enlargement of region A shown in Fig.4: note periodic faceting of boundary.
Figure 8 (center) - Enlargement of region A shown in Fig.5: note lattice fringes terminating at points labeled T and fragmentation of region B appearing from lower grain.
Figure 9 (bottom) - Enlargement of region A shown in Fig.6: note zigzag configuration of grain boundary.

introduced in the Al-3%Mg because the room temperature where intense straining has been performed corresponds to ~0.32 T_m for Al-3%Mg and this homologous temperature is significantly higher than those of ~0.22 T_m for Cu and ~0.17 T_m for Ni.

Summary and conclusions

1. Submicrometer grain (SMG) sizes were introduced into samples of polycrystalline Al-3%Mg, Cu and Ni using intense plastic plastic straining in torsion at room temperature.

2. High-resolution electron microscopy (HREM) showed that the grain boundaries in all three SMG samples exhibit zigzag configurations, indicating that they were in high-energy and non-equilibrium state. The boundaries also have high angles of misorientation with a narrow width.

3. Close observations by HREM suggested that a partial relaxation of the grain boundary structure occurs during straining process in the SMG Al-3%Mg but there is less in the SMG Cu and Ni.

Acknowledgements

This work was supported in part by the Light Metals Educational Foundation of Japan, in part by a Grant-in-Aid for Scientific Research from the Ministry of Education, Science, Sports and Culture of Japan, and in part by the National Science Foundation of the United States under Grants No.INT-9602919 and DMR-9625969. The center for High Resolution Electron Microscopy at Arizona State University is supported by the National Science Foundation under Grant No. DMR-9314326.

References

1. R.Z. Valiev, O.A. Kaibyshev, R.I. Kuznetsov, R.Sh. Musalimov and N.K. Tsenev, Dokl. Akad. Nauk SSSR **301** (1988) 864.
2. T.G. Langdon, Mater. Sci. Eng. **A174** (1994) 225.
3. A.H. Chokshi, A.K. Mukherjee and T.G. Langdon, Mater. Sci. Eng. **R10** (1993) 237.
4. N.A.Smirnova, V.I.Levit, V.I.Pilyugin, R.I.Kuznetsov, L.S.Davydova and V.A.Sazonova, Fiz. Met. Metalloved. **61** (1986) 1170.
5. R.Z.Valiev, N.A. Krasilnikov and N.K. Tsenev, Mater. Sci. Eng. **A137** (1991) 35.
6. N.A.Akhmadeev, V.I.Kopylov, R.R.Mulyukov and R.Z.Valiev, Izvest. Akad. Nauk SSSR, Metally **5** (1992) 96.
7. J. Wang, Z. Horita, M. Furukawa, M. Nemoto, N.K. Tsenev, R.Z. Valiev, Y. Ma and T.G. Langdon, J. Mater. Res. **8** (1993) 2810.
8. J. Wang, Y. Iwahashi, Z. Horita, M. Furukawa, M. Nemoto, R.Z. Valiev, and T.G. Langdon, Acta Mater. **44** (1996) 2973.
9. Z. Horita, D.J. Smith, M. Furukawa, M. Nemoto, R.Z. Valiev and T.G. Langdon, J. Mater. Res. **11** (1996) 1880.
10. R.Z. Valiev, A.V. Korznikov and R.R. Mulyukov, Mater. Sci. Eng. **A168** (1993) 141.
11. Z. Horita, D.J. Smith, M. Furukawa, M. Nemoto, R.Z. Valiev and T.G. Langdon, Annales de Chimie, **21** (1996) 417.
12. Z. Horita, D.J. Smith, M. Furukawa, M. Nemoto, R.Z. Valiev and T.G. Langdon, Materials Characterization, **37** (1997) in press.

SUPERPLASTICITY IN ALLOYS

PROCESSED BY EQUAL-CHANNEL ANGULAR PRESSING

Patrick B. Berbon,[1] Nikolai K. Tsenev,[2] Ruslan Z. Valiev,[3] Minoru Furukawa,[4]
Zenji Horita,[5] Minoru Nemoto[5] and Terence G. Langdon[1]

[1]Departments of Materials Science and Mechanical Engineering
University of Southern California, Los Angeles, CA 90089-1453, U.S.A.
[2]Institute of Chemical Technology
Ufa State Petroleum Technical University, Ufa 450062, Russia
[3]Institute of Physics of Advanced Materials
Ufa State Aviation Technical University, Ufa 450000, Russia
[4]Department of Technology, Fukuoka University of Education
Munakata, Fukuoka 811-41, Japan
[5]Department of Materials Science and Engineering, Faculty of Engineering
Kyushu University, Fukuoka 812-81, Japan

Abstract

Equal-channel angular (ECA) pressing was used to produce ultra-fine grain sizes in two commercial Al alloys: an Al-Mg-Li-Zr alloy and an Al-Cu-Zr alloy. The results demonstrate the potential for using this procedure in order to achieve high strain rate superplasticity (HSR SP). In the present experiments, elongations up to and above 1000% were obtained at strain rates $\geq 10^{-2}$ s^{-1}.

Superplasticity and Superplastic Forming 1998
Edited by A.K. Ghosh and T.R. Bieler
The Minerals, Metals & Materials Society, 1998

Introduction

Superplastic materials have the capability of exhibiting very high elongations when pulled in tension under optimum conditions [1]. In general, there are two important requirements in order to achieve superplasticity in metals [2]. First, superplasticity occurs through the relative displacements of adjacent grains and it requires a very small grain size, typically of the order of ~ 1 - 10 μm. Second, the superplastic process is diffusion-controlled and therefore it is necessary that the temperature is sufficiently high that deformation occurs within the diffusion regime. In practice, this means a temperature of at least $\sim 0.5\ T_m$, where T_m is the absolute melting temperature of the material. These two requirements are generally incompatible because of the ease of grain growth at elevated temperatures. Therefore, metals exhibiting high tensile ductility usually either incorporate a fine dispersion of a second phase or they are two-phase eutectic or eutectoid alloys.

Superplastic forming has become an established production technique for the fabrication of parts within the aerospace, transportation and architectural industries under conditions where the number of parts is limited to $< 10{,}000$ units [3]. This limitation arises because of the slow strain rates generally associated with the optimization of the superplastic forming process. Thus, forming is usually conducted at strain rates of the order of $\sim 10^{-3}$ - $10^{-2}\ s^{-1}$ where the superplastic ductility is maximized but in practice these strain rates require forming times of, typically, ~ 20 - 30 minutes. The current technology is therefore not readily amenable for the mass production of very large numbers of identical components.

There is experimental evidence suggesting that a decrease in grain size will lead both to an increase in the maximum elongations to failure and to the occurrence of these higher elongations at faster testing strain rates: for example, this effect is apparent from tests conducted on the Zn-22% Al eutectoid alloy with grain sizes of 2.5 and 4.2 μm [4]. However, conventional superplastic metal alloys have grain sizes larger than ~ 1 μm and it is difficult to reduce the grain size to the submicrometer level. There is considerable current interest in fabricating ultrafine-grained materials, with grain sizes in the nanometer range, using an inert gas condensation technique [5] but this procedure has the disadvantage that there remains some residual porosity, of the order of $\sim 2\%$, even when using improved compaction techniques [6]. As a result of these problems, the possibility has been suggested of using an intense plastic straining technique in order to achieve an ultrafine grain size for subsequent superplastic forming operations [7]. This suggestion was put forward because of the well-established ability to produce submicrometer grain sizes using intense plastic straining in procedures such as torsion straining under pressure [8] and pressing through a special die in the procedure known as equal-channel angular (ECA) pressing [9,10]. The present investigation was therefore initiated to investigate the ECA pressing of Al-based alloys with two specific objectives. First, to determine the feasibility of introducing an ultrafine grain size into selected alloys and of retaining these small grain sizes at reasonably high temperatures. Second, to examine the potential for attaining high strain rate superplasticity (HSR SP) after pressing.

Experimental materials and procedures

The experiments were conducted using two different conventional commercial alloys produced by casting. First, the Russian alloy 01420 is a light-weight high strength material described by Fridlyander *et al.* [11] and having a chemical composition of Al-5.5% Mg-2.2% Li-0.12% Zr. Second, the British Supral 100 alloy is an Al-2004 alloy which is very widely used in the superplastic forming industry [3] and with a chemical composition close to Al-6% Cu-0.4% Zr. This latter alloy contains a dispersion of coarse $CuAl_2$ and fine Al_3Zr particles which serve to

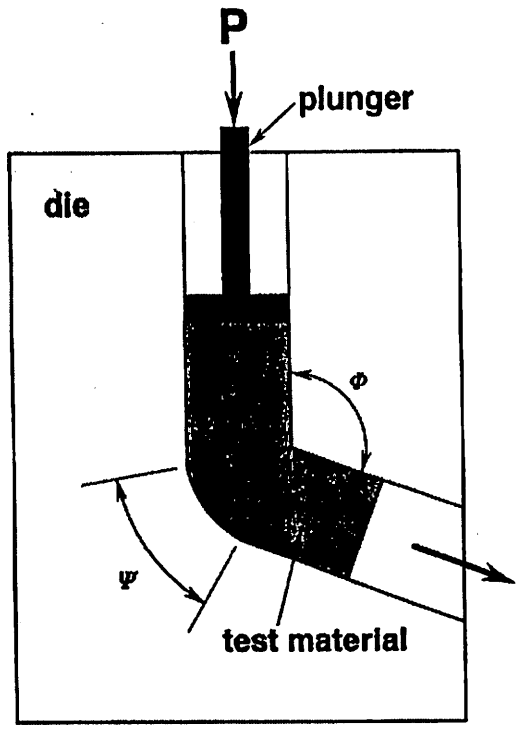

Figure 1 - Principle of ECA pressing through a die: P is the imposed load.

retain the very small grain size introduced by dynamic recrystallization in the early stages of deformation [12].

Samples of both alloys were prepared for ECA pressing in the form of cylinders with diameters of ~20 mm and total lengths of ~70 mm. These samples were subjected to ECA pressing using a die shown schematically in Fig. 1. The die contained two channels, equal in cross-section, which intersected at an angle of Φ and with an angle Ψ defining the outer arc of curvature at the point of intersection. In the present experiments, the pressing was performed in air using a facility with $\Phi = 90°$ and $\Psi = 0°$. As indicated in Fig. 1, the test material was pressed through the die with a plunger operating under a load P. It has been shown that the total strain, ε, accumulated on each passage through the die is given by [13]

$$\varepsilon = \frac{N}{\sqrt{3}}\left[2\cot\left(\frac{\Phi}{2}+\frac{\Psi}{2}\right)+\Psi\,\mathrm{cosec}\left(\frac{\Phi}{2}+\frac{\Psi}{2}\right)\right] \qquad (1)$$

where N is the number of passes through the die. For a die with $\Phi = 90°$, eqn. (1) leads to a strain which is close to ~1 on each passage through the die regardless of the value of Ψ, and in the present investigation consecutive pressings of the same sample were performed in order to achieve high total strains. Model experiments have confirmed the validity of eqn. (1) except when there are friction effects at the channel walls [14].

Following ECA pressing, tensile specimens having gauge lengths of 4 mm were machined from the pressed samples and tested in air using a machine operating at a constant rate of cross-head displacement. Testing temperatures were maintained constant to within $\pm 2°C$. Transmission electron microscopy was conducted on some samples and selected area electron diffraction (SAED) patterns were taken from areas having diameters of 13 μm.

Experimental results

Al-Mg-Li-Zr alloy (01420)

Initial experiments were conducted in which the sample was subjected to ECA pressing for a total of 4 passes at a temperature of 673 K: further details concerning the microstructural characteristics of this material after ECA pressing are given elsewhere [15]. Figure 2 shows (a) an example of the microstructure in the pressed condition together with (b) two SAED patterns taken from the regions A and B. It is apparent from Fig. 2(a) that the grain size is very small and measurements gave an average grain size of $\sim 1.2\ \mu m$. The SAED patterns in Fig. 2(b) demonstrate that the boundaries have high angles of misorientation. Nevertheless, more extensive inspections showed that there were also areas where there were arrays of low angle sub-boundaries, with the sub-grains occupying an estimated total volume fraction of ~30 - 40% [15]. Testing showed that this material was fairly ductile with elongations to failure up to >500% [16]. Furthermore, the grain size of this alloy is reasonably stable up to high temperatures of ~700 K, as shown in Fig. 3 where the average grain size was measured in samples annealed for 1 hour at different selected temperatures. Figure 3 also includes data reported earlier for ultra-fine grained Al-3% Mg solid solution alloys prepared by torsion straining [17] or ECA pressing [18] where the grain size increases rapidly at temperatures above ~550 K. The stability of the grains in the Al-Mg-Li-Zr alloy is due to the presence of β'-Al_3Zr precipitates which are stable at these high temperatures [15].

In an attempt to improve on the superplastic properties after ECA pressing, samples were pressed through 8 passes at 673 K and 4 passes at 473 K, giving a total strain of ~12. Inspection showed that the grain size of this material was again close to $\sim 1.2\ \mu m$ and all of the boundaries were now in a high angle configuration. Tensile testing revealed high superplastic ductilities in this material: Fig. 4 shows an example of the variation of true stress with strain for tests conducted at a temperature of 623 K and Fig. 5 compares the tensile elongations at 623 K with those obtained on the unpressed alloy at a similar testing temperature of 603 K. Thus, a reduction in the grain size from an initial value of ~400 to $\sim 1.2\ \mu m$ has a very significant effect on the overall ductility, leading to elongations of close to 400% even at a testing strain rate as high as $1\ s^{-1}$. Figure 6 shows the appearance of the two specimens tested at 10^{-2} and $10^{-1}\ s^{-1}$: it should be noted that the test at $10^{-2}\ s^{-1}$ was discontinued without failure at a total elongation of 1180%. It is apparent from the appearance of the tested specimens in Fig. 6 that, as in true superplasticity at lower strain rates, these samples gradually pull out without the development of necking within the gauge length. Thus, this is a clear example of the achievement of HSR SP after ECA pressing.

Al-Cu-Zr alloy (Supral 100)

The Supral alloy was also subjected to 8 passes at 673 K and 4 additional passes at 473 K, giving a total strain of ~12. After ECA pressing, the measured grain size was $\sim 0.5\ \mu m$. An example of the true stress-strain curves is shown in Fig. 7 for two tests conducted at 573 K and a single test at 623 K. It is apparent that these specimens also exhibit very high tensile ductility, with elongations up to a maximum of 970% at 573 K when testing with a strain rate of $1 \times 10^{-2}\ s^{-1}$. The appearance of these three specimens after testing is shown in Fig. 8. These results are significant because they demonstrate not only the potential for HSR SP but also that very high ductilities may be achieved at relatively low testing temperatures. For example, a detailed investigation of the Supral 100 alloy revealed elongations of up to >1000% but these occurred at the much higher testing temperatures of ~700 - 750 K and at the low strain rates of $\sim 10^{-4}$ to $10^{-3}\ s^{-1}$ [19].

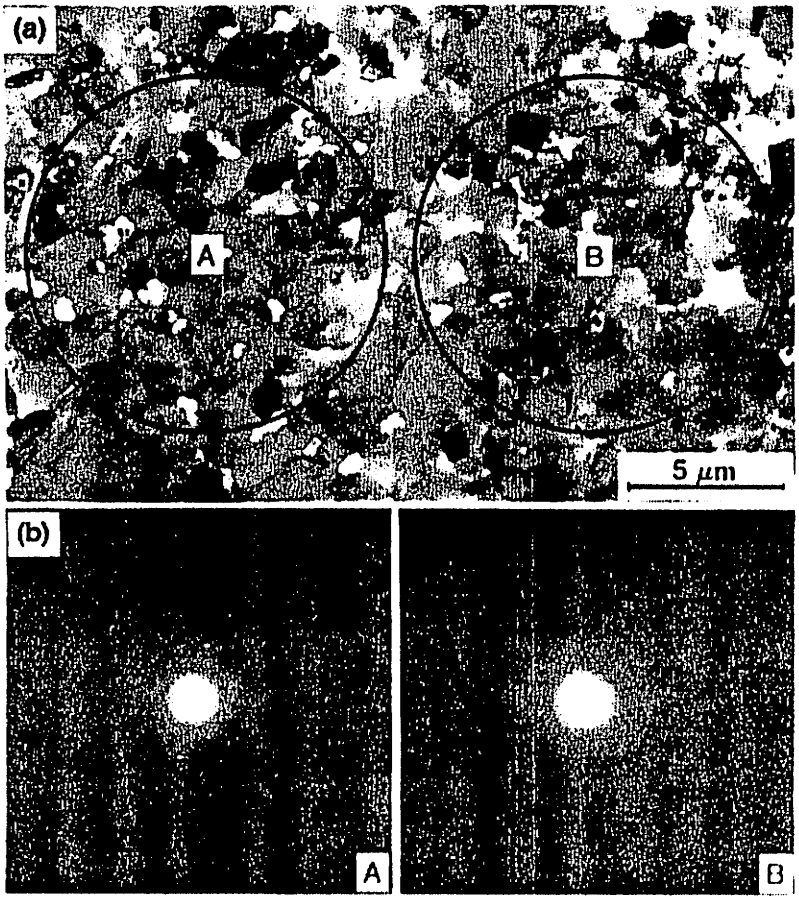

Figure 2 - (a) Microstructure after ECA pressing and (b) SAED patterns from regions A and B.

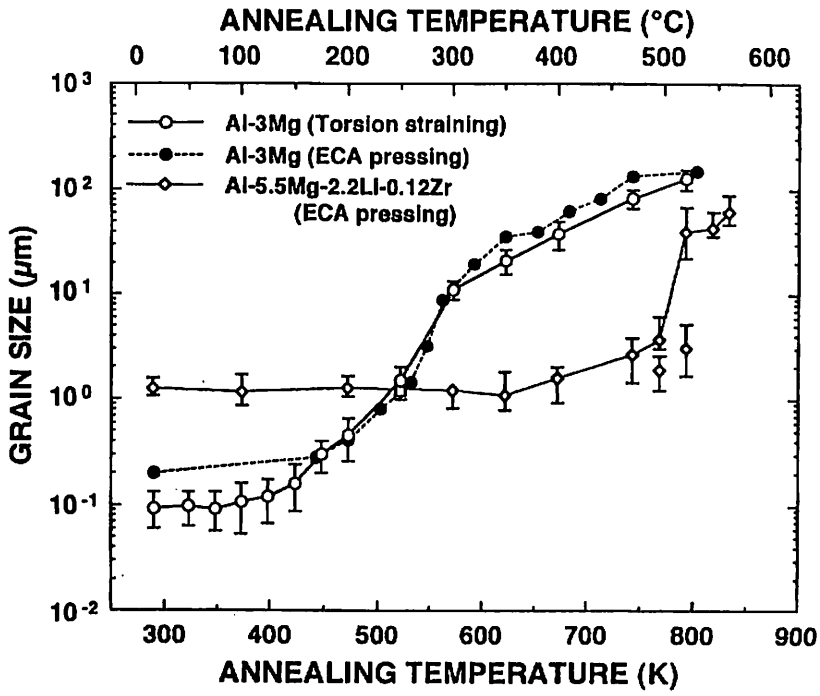

Figure 3 - Variation of grain size with annealing temperature, including data for Al-3% Mg after torsion straining [17] and ECA pressing [18].

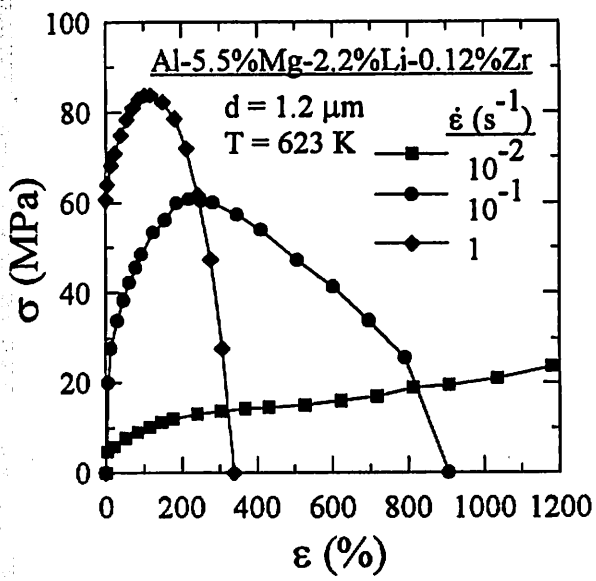

Figure 4 - True stress versus strain for tensile tests conducted at 623 K.

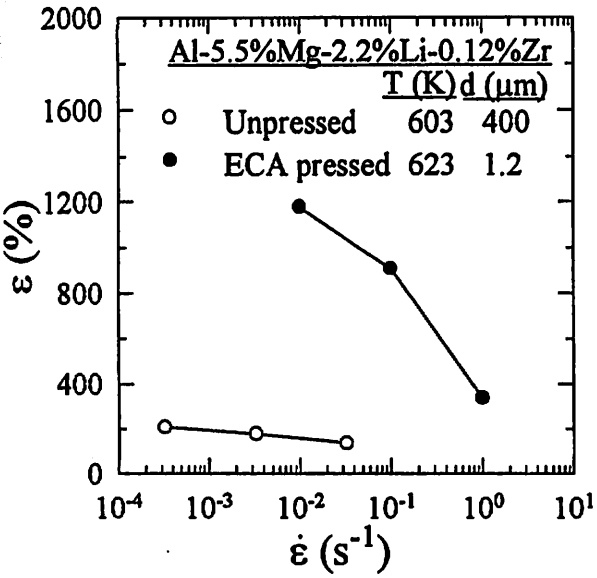

Figure 5 - Elongation versus strain rate for ECA pressed and unpressed samples.

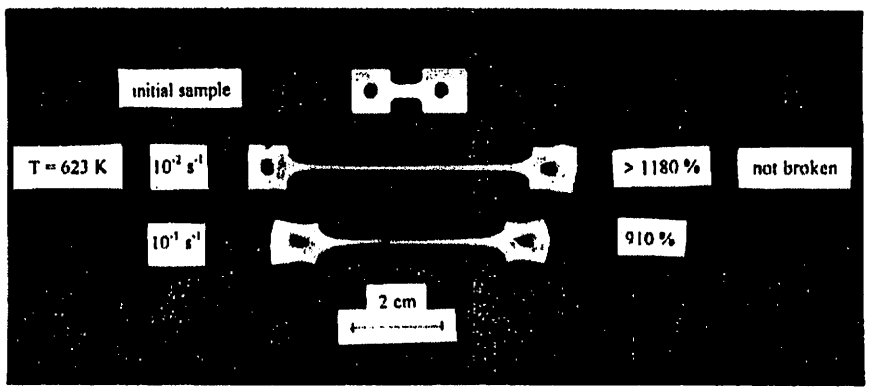

Figure 6 - Samples of the Al-Mg-Li-Zr alloy after tensile testing: the upper specimen is untested.

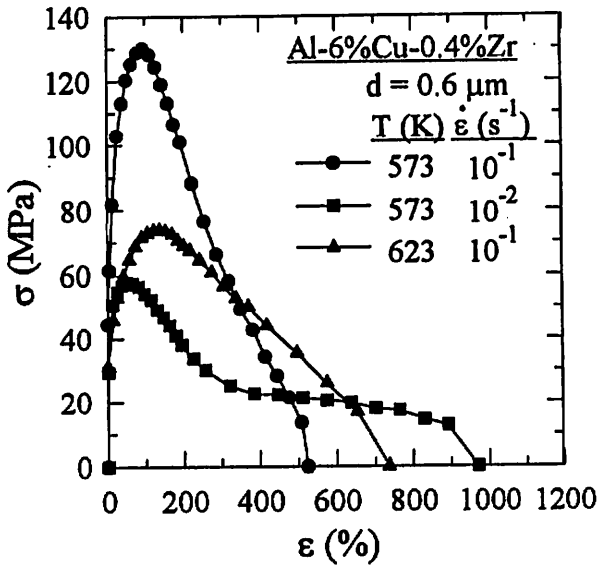

Figure 7 - True stress versus strain for tensile tests on the Al-Cu-Zr alloy.

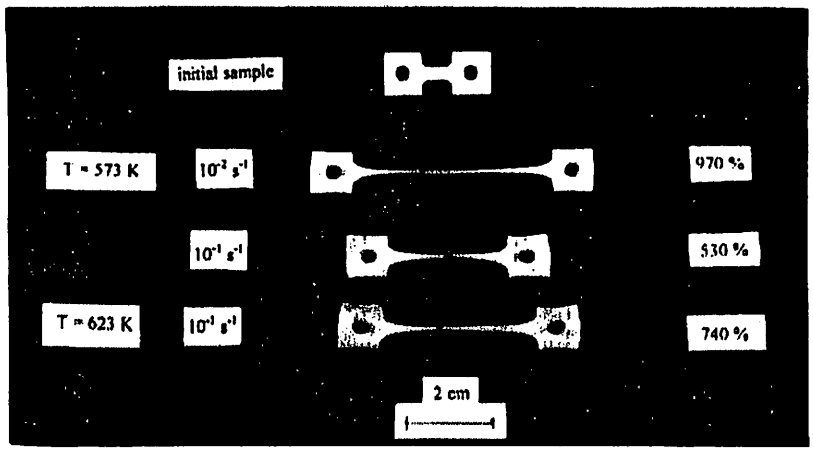

Figure 8 - Samples of the Al-Cu-Zr alloy after tensile testing: the upper specimen is untested.

Conclusions

Equal-channel angular (ECA) pressing is an effective tool for producing an ultra-fine grain size in metals. These small grain sizes may be retained to high temperatures when precipitates are available to retard grain growth. The results from this investigation demonstrate that high strain rate superplasticity (HSR SP) may be achieved in two commercial cast aluminum alloys (the 01420 alloy and Supral 100). Very high elongations to failure were recorded at strain rates up to 1 s^{-1}.

Acknowledgements

This work was supported in part by the Light Metals Educational Foundation of Japan, in part by a Grant-in-Aid for Scientific Research from the Ministry of Education, Science, Sports and Culture of Japan, in part by the National Science Foundation of the United States under Grants No. DMR-9625969 and INT-9602919 and in part by the U.S. Army Research Office under Grants No. DAAH04-96-1-0332 and N68171-96-6-9006.

References

1. A.H. Chokshi, A.K. Mukherjee and T.G. Langdon, "Superplasticity in *Advanced* Materials," Mater. Sci. Eng., R10 (1993) 237-274.
2. T.G. Langdon, "The Mechanical Properties of Superplastic Materials," Metall. Trans., 13A (1982) 689-701.
3. A.J. Barnes, "Superplastic Forming of Aluminum Alloys," Mater. Sci. Forum, 170-172 (1994) 701-714.
4. F.A. Mohamed, M.M.I. Ahmed and T.G. Langdon, "Factors Influencing Ductility in the Superplastic Zn-22 Pct Al Eutectoid," Metall. Trans., 8A (1977) 933-938.
5. H. Gleiter, "Materials with Ultra-fine Grain Sizes," in Deformation of Polycrystals: Mechanisms and Microstructures, ed. N. Hansen, A. Horsewell, T. Leffers and H. Lilholt (Roskilde, Denmark: Risø National Laboratory, 1981), 15-21.
6. P.G. Sanders, G.E. Fougere, L.J. Thompson, J.A. Eastman and J.R. Weertman, "Improvements in the Synthesis and Compaction of Nanocrystalline Materials," Nanostruct. Mater., 8 (1997) 243-252.
7. Y. Ma, M. Furukawa, Z. Horita, M. Nemoto, R.Z. Valiev and T.G. Langdon, "Significance of Microstructural Control for Superplastic Deformation and Forming," Mater. Trans. JIM, 37 (1996) 336-339.
8. M. Furukawa, Z. Horita, M. Nemoto, R.Z. Valiev and T.G. Langdon, "Structural Evolution and Validity of Hall-Petch Relationship in an Al-3% Mg Alloy with Submicron Grain Size," Mater. Sci. Forum, 204-206 (1996) 431-436.
9. R.Z. Valiev and N.K. Tsenev, "Structure and Superplasticity of Al-based Submicron Grained Alloys," in Hot Deformation of Aluminum Alloys, ed. T.G. Langdon, H.D. Merchant, J.G. Morris and M.A. Zaidi (Warrendale, PA: The Minerals, Metals and Materials Society, 1991), 319-329.
10. R.Z. Valiev, N.A. Krasilnikov and N.K. Tsenev, "Plastic Deformation of Alloys with Submicron-grained Structure," Mater. Sci. Engng, A137 (1991) 35-40.
11. I.N. Fridlyander, V.S. Sandler and T.I. Nikol'skaya, "Investigation of the Ageing of Aluminium-Magnesium-Lithium Alloys," Fiz. Metal. Metalloved, 32 (1971) 767-774.
12. R. Grimes, C. Baker, M.J. Stowell and B.M. Watts, "Development of Superplastic Aluminium Alloys," Aluminium, 51 (1975) 720-723.
13. Y. Iwahashi, J. Wang, Z. Horita, M. Nemoto and T.G. Langdon, "Principle of Equal-Channel Angular Pressing for the Processing of Ultra-fine Grained Materials," Scripta Mater., 35 (1996) 143-146.
14. Y. Wu and I. Baker, "An Experimental Study of Equal Channel Angular Extrusion," Scripta Mater., 37 (1997) 437-441.
15. M. Furukawa, Y. Iwahashi, Z. Horita, M. Nemoto, N.K. Tsenev, R.Z. Valiev and T.G. Langdon, "Structural Evolution and the Hall-Petch Relationship in an Al-Mg-Li-Zr Alloy with Ultra-fine Grain Size," Acta Mater., in press.
16. M. Furukawa, P.B. Berbon, Z. Horita, M. Nemoto, N.K. Tsenev, R.Z. Valiev and T.G. Langdon, "Age Hardening and the Potential for Superplasticity in a Fine-grained Al-Mg-Li-Zr Alloy," Metall. Trans., in press.
17. M. Furukawa, Z. Horita, M. Nemoto, R.Z. Valiev and T.G. Langdon, "Microhardness Measurements and the Hall-Petch Relationship in an Al-Mg Alloy with Submicrometer Grain Size," Acta Mater., 44 (1996) 4619-4629.
18. J. Wang, Y. Iwahashi, Z. Horita, M. Furukawa, M. Nemoto, R.Z. Valiev and T.G. Langdon, "An Investigation of Microstructural Stability in an Al-Mg Alloy with Submicrometer Grain Size," Acta Mater., 44 (1996) 2973-2982.
19. R. Grimes, M.J. Stowell and B.M. Watts, "Superplastic Aluminium-based Alloys," Metals Tech., 3 (1976) 154-160.

MICROSTRUCTURAL EVOLUTION IN PURE ALUMINUM DURING EQUAL-CHANNEL ANGULAR PRESSING

Minoru Furukawa,[1] Zenji Horita,[2] Minoru Nemoto[2]
and Terence G. Langdon[3]

[1]Department of Technology, Fukuoka University of Education
Munakata, Fukuoka 811-41, Japan
[2]Department of Materials Science and Engineering, Faculty of Engineering
Kyushu University, Fukuoka 812-81, Japan
[3]Departments of Materials Science and Mechanical Engineering
University of Southern California, Los Angeles, CA 90089-1453, U.S.A.

Abstract

Samples of high purity aluminum were deformed to different levels of strain using the procedure of equal-channel angular (ECA) pressing in which an intense plastic strain is introduced by pressing a sample through a special die. The results demonstrate the potential for using the ECA pressing technique to reduce the grain size from ~ 1 mm initially to a final equiaxed array of grains having a size close to ~ 1 μm.

Modeling the Mechanical Response of
Structural Materials
Edited by E.M. Taleff and R.K. Mahidhara
The Minerals, Metals & Materials Society, 1997

Introduction

Equal-channel angular (ECA) pressing is a processing procedure developed several years ago by Segal and co-workers [1]. The principle of this procedure is based on the observation that metal working by simple shear provides close to an ideal method for structure and texture formation [2]. An important advantage of the process is that the intense plastic straining introduced using ECA pressing is capable of producing an ultra-fine grain size at the submicrometer or even nanometer level [3-5].

Although there have been several reports to date of the properties developed in materials after ECA pressing, there are relatively few reports dealing with the microstructural development during the pressing process [6-8]. Therefore, this report describes some of the results obtained in a detailed investigation designed to examine the nature of the formation and development of arrays of ultra-fine grains during the ECA pressing of samples of high purity aluminum.

Experimental material and procedures

The experiments were conducted using aluminum of 99.99% purity. The material was received in the form of an ingot which was subjected to cold rolling and subsequent annealing for 1 hour at 773 K. Metallographic inspection revealed a large initial grain size of ~ 1.0 mm.

The ECA pressing was performed using a die of the type described earlier [9]. Briefly, two blocks of tool steel were bolted together such that an internal channel, of square cross-section, was continuous through the block and formed an L-shape configuration subtending an angle of 90° between the two channels. There was also an angle of 20° defining the outer arc of curvature at the point where the two channels intersected. A relationship was derived earlier [10] giving the magnitude of the strain introduced into a sample when it is pressed through the die: the validity of this relationship has been confirmed in a series of model experiments using plasticine layers contained within a plexiglass pressing facility [11]. In the present investigation, a single pressing through the die gave a strain of the order of ~ 1.

The ECA pressing was conducted using Al samples having dimensions of 10×10 mm^2 and lengths of the order of ~ 75 mm. Specimens were polished on the longitudinal faces prior to pressing at room temperature using an MoS_2 lubricant and specimens were pressed up to several times through the die to give a high cumulative strain. In practice, it is possible to define three distinct processing routes, as illustrated in Fig. 1: route A refers to the situation where the repetitive pressings are conducted without any rotation of the sample, route B denotes pressings where there is a rotation of the sample by 90° in the same direction between each separate pressing and route C denotes repetitive pressings with a rotation between pressings of 180°. Samples were pressed using routes A, B or C for up to 4 passes through the die.

After pressing to a selected total strain, samples were thinned for inspection by transmission electron microscopy (TEM). Observations were made by TEM using samples oriented in three mutually perpendicular planes as defined in Fig. 2, where x, y and z are the planes perpendicular to the longitudinal axis of the sample, parallel to the side face at the point of exit from the die or parallel to the top face at the point of exit, respectively. The procedure for preparation of the TEM samples was described earlier [8]. Representative microstructures were recorded by TEM and selected area electron diffraction (SAED) patterns were taken from regions having diameters of 12.3 μm. Subgrain and grain sizes were measured directly from the TEM photomicrographs using the standard linear intercept method.

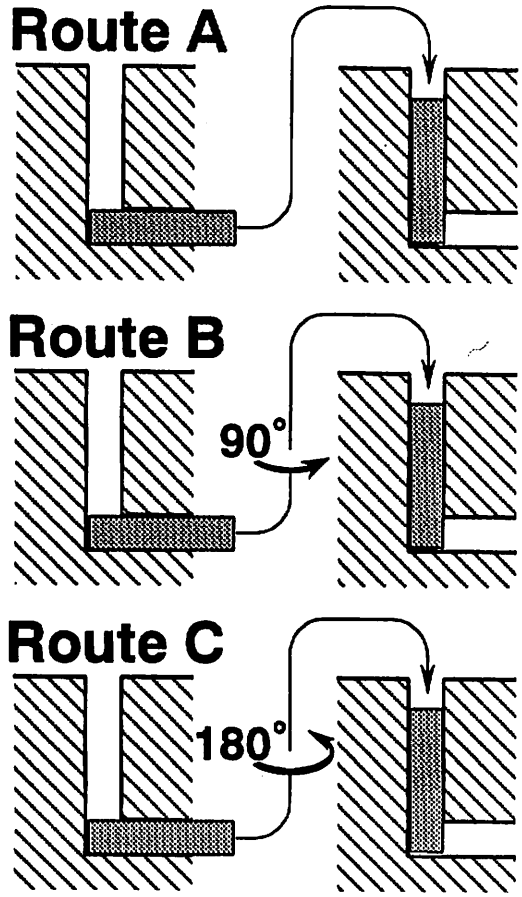

Figure 1 - Processing routes A, B and C in ECA pressing.

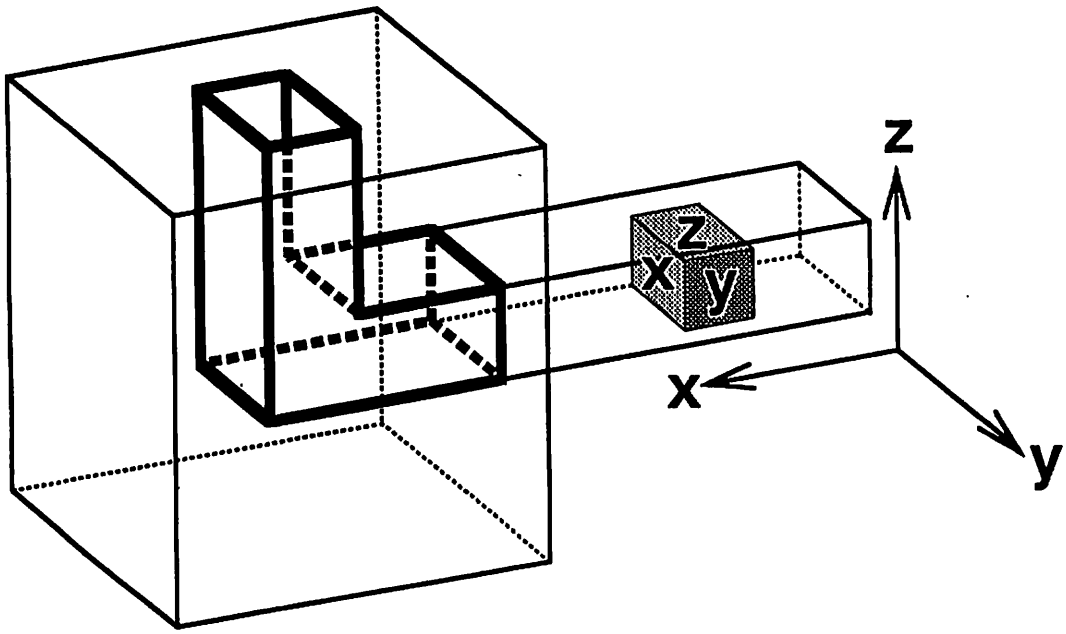

Figure 2 - Definitions of planes x, y and z.

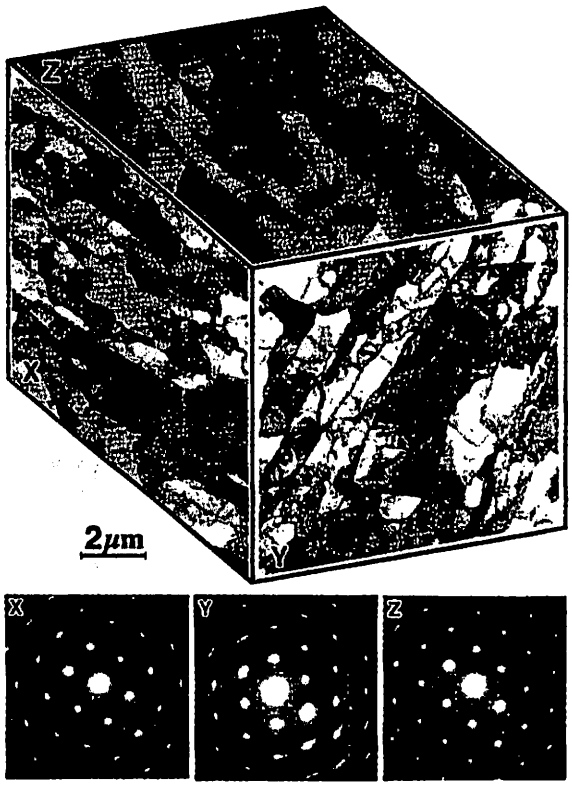

Figure 3 - Microstructure and SAED patterns after a single passage through the die.

Experimental results and discussion

Figure 3 shows the microstructures in the x, y and z planes after a single pressing, together with the corresponding SAED patterns for each plane. Inspection shows that a single passage through the die, giving a total strain of ~ 1, leads to the formation of bands of subgrains where, based on the SAED patterns, the boundaries have low angles of misorientation. These subgrain bands lie essentially at 45° to the top and bottom edges of the y plane and therefore the bands are oriented in the direction of shearing as the sample proceeds through the die. These bands are also parallel to the top and bottom edges of the x plane and perpendicular to the pressing direction in the z plane. The marker for 2 μm serves to illustrate the very small subgrain size which is achieved on a single passage through the die. Thus, one pass and a strain of ~ 1 gives an array of subgrains having an average size of < 1 μm. Detailed microstructural measurements are given elsewhere [8] for routes A and C up to 10 pressings.

Figures 4 - 6 illustrate the effect of 4 pressings through the die to a total strain of ~ 4 for samples processed using routes A, B and C, respectively. A comparison of these three sets of photomicrographs shows that microstructural evolution is most rapid when using route B whereby the sample is rotated in the same direction by 90° between each separate pressing. In Fig. 5, illustrating route B, the subgrain bands are no longer visible after 4 pressings and instead there are arrays of grains in the x, y and z planes which appear to be reasonably equiaxed. The SAED patterns for each plane in Fig. 5 show diffracted beams scattered around rings, thereby demonstrating that the boundaries are now in high angle misorientations. By contrast, there is very clear evidence for the continued presence of subgrain bands after 4 pressings when using route A, as illustrated in Fig. 4, and some subgrain bands are also visible when using route C, as illustrated in Fig. 6.

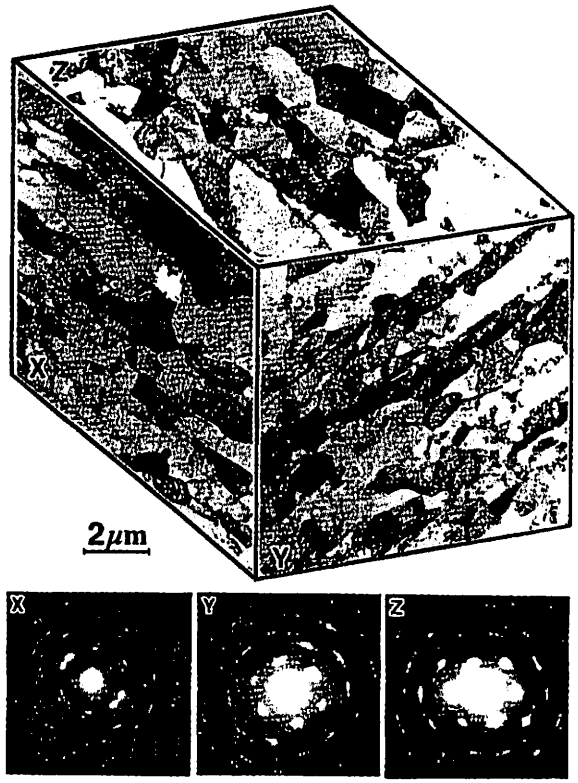

Figure 4 - Microstructure and SAED patterns after 4 pressings through the die using route A.

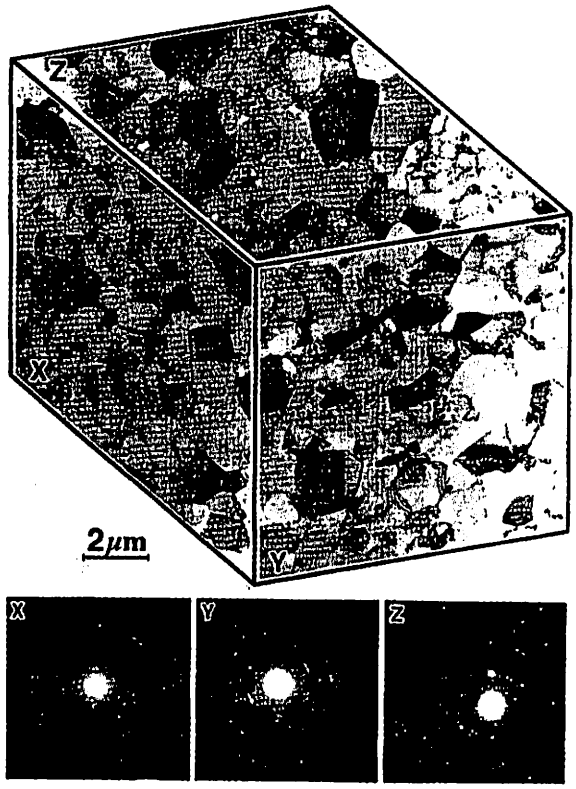

Figure 5 - Microstructure and SAED patterns after 4 pressings through the die using route B.

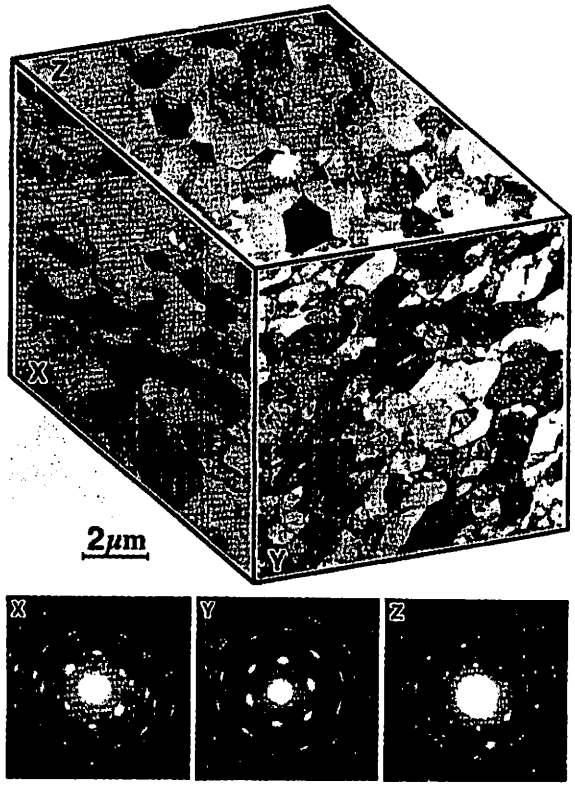

Figure 6 - Microstructure and SAED patterns after 4 pressings through the die using route C.

It is apparent from these observations that ECA pressing of high purity aluminum leads rapidly to the formation of arrays of subgrain bands within each grain and these subgrain boundaries evolve with further pressings into high angle grain boundaries. Measurements were taken of the subgrain sizes and grain sizes after 1, 2, 3 and 4 pressings and the results are shown in Fig. 7 for ECA pressing conducted using (a) route A, (b) route B and (c) route C, respectively. Separate points are shown in Fig. 7 for the x, y and z planes, and the open, half-closed and closed symbols are used to differentiate between microstructures consisting only of subgrains, of a mixture of subgrains and grains and of fully developed grains separated by high angle grain boundaries, respectively: where the subgrains were elongated, as in the early stages of ECA pressing, the sizes reported in Fig. 7 are the average lengths of the short axis, equivalent to the widths of the subgrain bands visible in Fig. 4.

Inspection of Fig. 7 confirms that an array of grains with high angle boundaries is achieved most rapidly when using processing route B and least rapidly with route A. With route B, there is an evolution after 4 pressings to a reasonably equiaxed structure with a grain size of ~ 1.3 μm in each plane of sectioning. Therefore, the grain size has been reduced from ~ 1.0 mm to ~ 1.3 μm in only 4 pressings through the die but with a rotation of 90° between each pressing. The results suggest that an evolution to a similar final grain size will occur also when using routes A and C but more pressings are then required to attain an array of high angle grain boundaries. These results are therefore consistent with those described earlier when using routes A and C [8]. Close inspection of Fig. 7 suggests also a difference between the three different planes of observation. In general, the smallest subgrains tend to be observed in the y plane where the subgrain bands are most clearly delineated, and these subgrains remain essentially unchanged in size at ~ 0.6 μm when using routes A and C but they increase in size with route B to the final equiaxed grain size of ~ 1.3 μm.

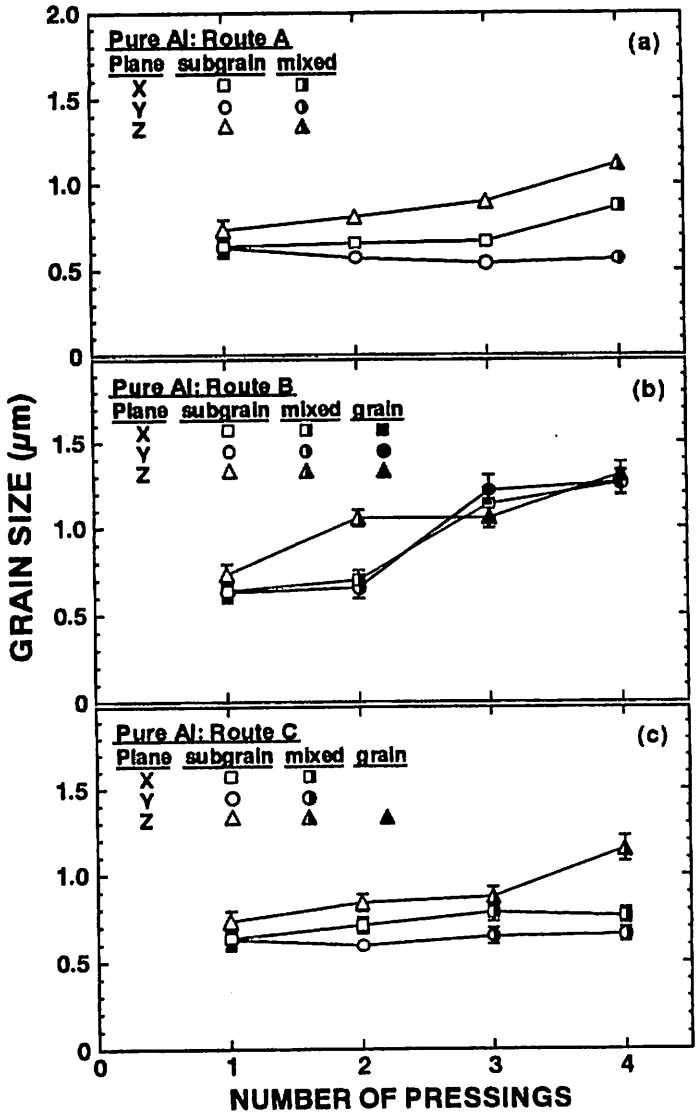

Figure 7 - Grain size measurements for routes A, B and C.

The results obtained in this investigation after small strains have similarities with earlier reports of microstructural evolution in pure Al after cold rolling, where it has been shown that reductions of ~15% - 30% lead to the formation of bands of elongated subgrains with sizes of, typically, ~1 - 2 μm [12-14]. However, a more detailed analysis of ECA pressing is required, including inspection by optical microscopy, in order to develop a complete understanding of the nature of grain refinement in the ECA pressing procedure.

Conclusions

Samples of high purity aluminum were subjected to equal-channel angular (ECA) pressing up to total strains of ~4 and using three different processing procedures: route A without rotation of the sample between consecutive pressings and routes B and C with rotations of 90° and 180° between each pressing. Microstructural observations show that subgrain bands are formed after a single pressing through the die, and these bands evolve after 4 pressings into an array of equiaxed grains with an average size of ~1.3 μm when using processing route B.

Acknowledgements

This work was supported in part by the Light Metals Educational Foundation of Japan, in part by a Grant-in-Aid for Scientific Research from the Ministry of Education, Science, Sports and Culture of Japan, in part by the Japan Society for the Promotion of Science and in part by the National Science Foundation under Grants No. DMR-9625969 and INT-9602919.

References

1. V.M. Segal, V.I. Reznikov, A.E. Drobyshevskiy and V.I. Kopylov, "Plastic Working of Metals by Simple Shear," Russian Metallurgy (Metally), 1 (1981) 99-105.
2. V.M. Segal, "Materials Processing by Simple Shear," Mater. Sci. Engng, A197 (1995) 157-164.
3. R.Z. Valiev and N.K. Tsenev, "Structure and Superplasticity of Al-based Submicron Grained Alloys," in Hot Deformation of Aluminum Alloys, ed. T.G. Langdon, H.D. Merchant, J.G. Morris and M.A. Zaidi (Warrendale, PA: The Minerals, Metals and Materials Society, 1991), 319-329.
4. R.Z. Valiev, N.A. Krasilnikov and N.K. Tsenev, "Plastic Deformation of Alloys with Submicron-grained Structure," Mater. Sci. Engng, A137 (1991) 35-40.
5. V.M. Segal, R.E. Goforth and K.T. Hartwig, "The Application of Equal Channel Angular Extrusion to Produce Extraordinary Properties in Advanced Metallic Materials," in First International Conference on Processing Materials for Properties, ed. H. Henein and T. Oki (Warrendale, PA: The Minerals, Metals and Materials Society, 1993), 971-974.
6. S. Ferrasse, V.M. Segal, K.T. Hartwig and R.E. Goforth, "Microstructure and Properties of Copper and Aluminum Alloy 3003 Heavily Worked by Equal Channel Angular Extrusion," Metall. Mater. Trans., 28A (1997) 1047-1057.
7. S. Ferrasse, V.M. Segal, K.T. Hartwig and R.E. Goforth, "Development of a Submicrometer-grained Microstructure in Aluminum 6061 Using Equal Channel Angular Extrusion," J. Mater. Res., 12 (1997) 1253-1261.
8. Y. Iwahashi, Z. Horita, M. Nemoto and T.G. Langdon, "An Investigation of Microstructural Evolution During Equal-Channel Angular Pressing," Acta Mater., in press.
9. J. Wang, Y. Iwahashi, Z. Horita, M. Furukawa, M. Nemoto, R.Z. Valiev and T.G. Langdon, "An Investigation of Microstructural Stability in an Al-Mg Alloy with Submicrometer Grain Size," Acta Mater., 44 (1996) 2973-2982.
10. Y. Iwahashi, J. Wang, Z. Horita, M. Nemoto and T.G. Langdon, "Principle of Equal-Channel Angular Pressing for the Processing of Ultra-fine Grained Materials," Scripta Mater., 35 (1996) 143-146.
11. Y. Wu and I. Baker, "An Experimental Study of Equal Channel Angular Extrusion," Scripta Mater., 37 (1997) 437-441.
12. B. Bay and N. Hansen, "Microstructures in Cold-Rolled Polycrystalline Aluminium," in Deformation of Polycrystals: Mechanisms and Microstructures, ed. N. Hansen, A. Horsewell, T. Leffers and H. Lilholt (Roskilde, Denmark: Risø National Laboratory, 1981), 137-144.
13. B. Bay and N. Hansen, "Deformed and Recovered Microstructures in Pure Aluminium," in Annealing Processes - Recovery, Recrystallization and Growth, ed. N. Hansen, D. Juul Jensen, T. Leffers and B. Ralph (Roskilde, Denmark: Risø National Laboratory, 1986), 215-220.
14. B. Bay, N. Hansen, D.A. Hughes and D. Kuhlmann-Wilsdorf, "Evolution of f.c.c. Deformation Structures in Polyslip," Acta Metall. Mater., 40 (1992) 205-219.

Introduction

High ductilities have been observed in some coarse-grained materials [1] but by far the most common phenomenon for very high ductilities is superplasticity. Among the most stringent requirement for superplasticity is the necessity to have a very small grain size [2]. In industry, this translates into additional preparation steps and additional cost and it has given rise to an extensive search for ways to reduce the grain size of a material. Several powder metallugy techniques have emerged but their optimization is a long task and the shortcomings of residual porosity, very small sample size and the introduction of oxide particles remain [3]. Other techniques are based on the mechanical alloying method but again the shortcomings are numerous [4]. Thus, the most promising path may be the introduction of severe plastic deformation inside the material [5]. The strain introduced often gives rise to the appearance of small subgrains or grains. The two leading techniques for introducing a high strain are torsion straining (TS) and equal-channel angular (ECA) pressing [6]. TS uses a combination of compression and rotation whereas ECA pressing introduces strain through simple shear by forcing the material through an angled die [7]. In this study, several Al alloys were processed following different procedures in order to observe the effect of the various ECA parameters. The first goal was the production of a fine grained structure and the second goal was the introduction of superplastic behavior.

Experimental materials and procedures

Experiments were conducted using two different Al-based alloys: an Al-5%Zn solid solution alloy and a commercial Russian aluminum alloy known as Al-1420 and containing 5.5%Mg, 2.2%Li and 0.12%Zr [8]. All ECA pressing was performed using dies in which the two channels intersected at an angle of 90°. In this condition, each pass introduced a strain of ~ 1 inside the deformed piece [9] and therefore the total strain is equal to the number of passes.

The various ECA pressing procedures used for the Al-5%Zn are summarized in Table I. The number of passes through the die was varied from 4 to 8 and the specimen was rotated by 90° in the same direction between each pass in a procedure designated route B. The material was prepared for observation by transmission electron microscopy (TEM) by polishing to 300 μm thickness, trimming to 3 mm diameter, polishing to 150 μm, and electropolishing at -15 °C in a mixture of 20% nitric acid and 80% methyl alcohol. All TEM specimens were prepared from within the grip sections. The observations were performed using a Hitachi H8100 operating at 200 kV.

The various ECA pressing procedures used for the Al-5.5%Mg-2.2%Li-0.12%Zr alloy are summarized in Table II. For this material, the number of passes through the die and the pressing temperature were varied and there was no rotation of the piece between passes in the procedure designated route A. The initial grain size of this material was ~ 400 μm. The material was prepared for TEM observations following the same technique as for the Al-5%Zn alloy with an electrolyte of 10% perchloric acid, 20% glycerin and 70% ethyl alcohol at ~ 5 °C. Rectangular tensile specimens with a gauge length of 4 mm, a gauge section of 2 × 3 mm^2, and a total length of 24 mm were machined from the pressed samples and tested in an Instron machine operating at a constant cross-head displacement. The testing temperatures were from 298 to 673 K controlled to within ± 2 K and the testing strain rates were from 10^{-4} to 1 s^{-1}.

Table I: The three procedures used for Al-5%Zn

Procedure	Route	Processing procedure (strain and temperature)
A1	B	4 @ 298 K
A2	B	6 @ 298 K
A3	B	8 @ 298 K

Table II: The three procedures used for the Al-1420 alloy

Procedure	Route	Processing procedure (strain and temperature)
B1	A	4 @ 673 K
B2	A	8 @ 673 K + 4 @ 473 K
B3	A	8 @ 573 K

Results and discussion

Al-5%Zn

The evolution of the microstructure with the number of passes (*i.e.* with the amount of strain introduced) is apparent from the photomicrographs in Fig. 1 after 4, 6 and 8 passes through the die. The photomicrographs are very similar in these three cases, with the grain size decreasing slightly from Fig. 1(a) to (c). However, important differences can be observed in the selected area electron diffraction (SAED) patterns. In fig. 1(a), the SAED pattern consists of a slightly elongated net pattern, showing the importance of subgrains. Misorientation angles lower than 10° dominate the structure. In Fig. 1(b), a mixture of grains and subgrains is observed. The pattern is not close to a net pattern but it is also not random. In Fig. 1(c), the structure consists of large angle grain boundaries as is evident from the random pattern.

This result gives an interesting insight into the mechanism leading to grain refinement via ECA pressing of Al alloys, and it is in agreement with the conclusions of Ferrasse et al. [10]. It appears that subgrains form first, followed by evolution into large-angled grain boundaries. It is likely that this sequence of events can be generalized to all cell-forming materials [11,12]. Therefore, ECA pressing represents a serious candidate procedure for the processing of all cell-forming alloys and for the introduction of small grains separated by large angle boundaries.

On the other hand, if the processed alloy contains appropriate particulates to hinder grain growth at high temperature it will be expected to exhibit a superplastic behavior [13]. No attempt has been made in this investigation to examine the precise structure of the grain boundaries in the Al-5%Zn alloy after ECA pressing. This is important to determine if they have a non-equilibrium character of the type described by Nazarov et al. [14].

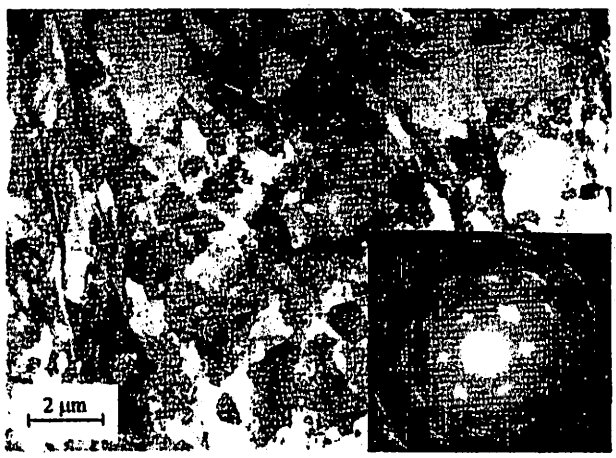

(a)

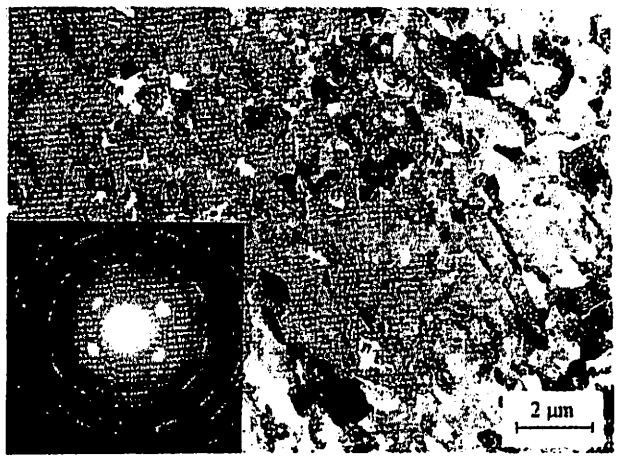

(b)

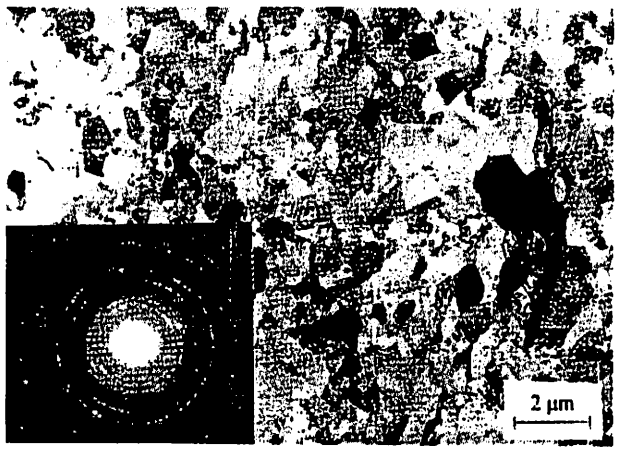

(c)

Figure 1: TEM photomicrographs and SAED patterns for Al-5%Zn after (a) 4, (b) 6 and (c) 8 passes, respectively

Al-1420

The Russian Al-1420 alloy appears as a good candidate for further study since it contains finely dispersed Al_3Li and Al_3Zr particulates. It has been observed that the ordered Al_3Zr particulates are particularly effective in pinning grain boundaries at high temperatures [15].

The microstructure in the as-pressed condition via procedure B1 showed a grain size of ~ 1.2 μm and a mixture of grains and subgrains [16]. Figure 2 shows the material processed via procedure B2 which has a similar grain size but all areas consisted of large-angled grain boundaries. This is in agreement with the preceding result on Al-5%Zn. It should be noted that the numerous white spots apparent in Fig. 2 are due to the preferential electropolishing of the stable AlLi particulates. Very little grain growth was detected in the material on testing up to 623 K, where the grain size was ~ 2 μm as shown in Fig. 3. However, a temperature of 673 K was sufficient to introduce abnormal grain growth as shown in Fig. 4.

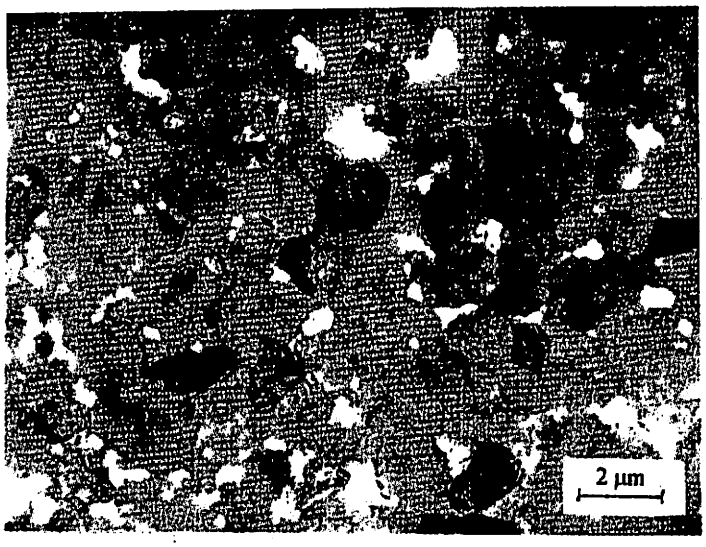

Figure 2: Al-1420 processed via procedure B2, as-pressed

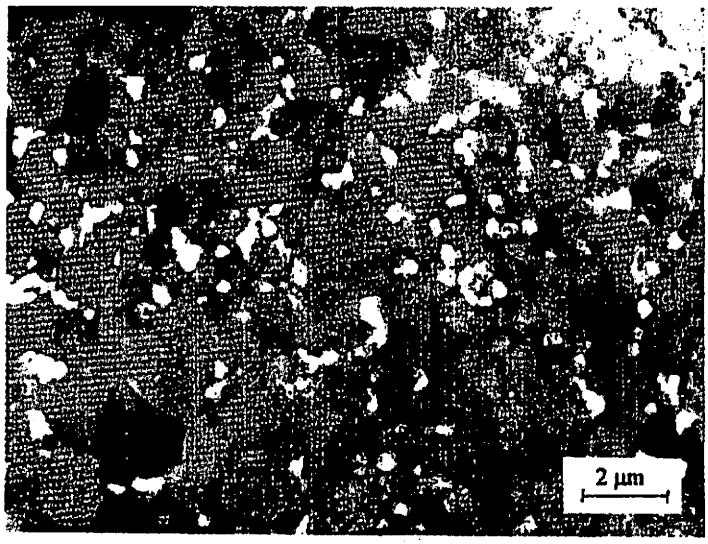

Figure 3: Al-1420 processed via procedure B2, after testing at 623 K

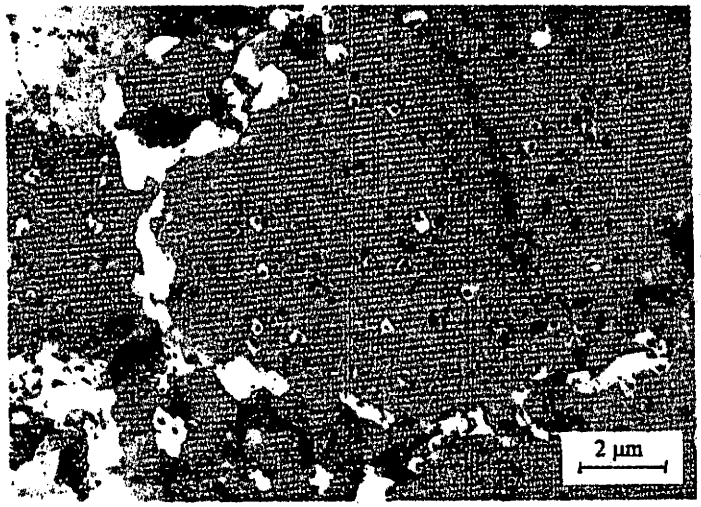

Figure 4: Al-1420 processed via procedure B2, after testing at 673 K

The mechanical tests performed on the Al-1420 alloy are summarized in Table III where they are compared to the results for the initial unpressed material. It can be seen that the ductility of the material processed via procedure B1 is already greatly enhanced, and the elongation before fracture of 550% at 603 K demonstrates the possibility of limited superplasticity.

The properties of the material processed via procedure B2 show excellent elongations, reaching more than 1180% at 623K with a strain rate of 10^{-2} s^{-1}. The values at the strain rates of 10^{-1} and 1 s^{-1} demonstrate that this material can deform in the range of high strain rate superplasticity (HSR SP) [17]. These strain rates are more than two orders of magnitude higher than the conventional superplastic forming strain rates. It is of interest to note that, due to the low testing temperatures, the presence of a liquid phase is impossible in this material, therefore constituing evidence for the occurrence of HSR SP without an interboundary or triple junction liquid phase. Previous results on metal matrix composites and mechanically alloyed alloys showed that the presence of a thin liquid layer at triple junctions may enhance the superplastic characteristics through the phenomenon of stress relief inside the liquid [18, 19]. The present result is more likely to be evidence of normal superplasticity which takes place at a high strain rate. This is in agreement with the expected shift in optimum strain rate for superplasticity with decreasing grain size [20]. Tests at higher temperatures led to a decrease in superplastic behavior, in agreement with the advent of grain growth observed in the TEM analysis. This suggests a possible shortcoming of this result because higher temperatures are necessary in order to reduce the yield stresses. Table III shows that the yield stresses may be too high to use the material in conventional superplastic forming presses, where stresses lower than 10 MPa are preferable.

The preliminary results on the material processed via procedure B3 show that the superplastic state is also achieved after introducing a strain of 8. This is of interest for further development of the ECA procedure. It is a reasonable result since the TEM analysis of the material processed via route B1 (4 passes) already contained 60 to 70 % of regions with large angle boundaries. More tests need to be performed on this material to verify the evolution of the percentage high angle boundaries with strain.

Table III: Mechanical results on Al-1420

ECA preparation	T (K)	strain rate (s^{-1})	EF (%)	YS (MPa)
initial material	603	$3.3x10^{-4}$	210	21
		$3.3x10^{-3}$	180	62
		$3.3x10^{-2}$	140	95
procedure B1	603	$3.3x10^{-4}$	416	9
		$3.3x10^{-3}$	550	39
		$3.3x10^{-2}$	341	75
procedure B2	573	$1x10^{-2}$	1041	19
		$1x10^{-1}$	383	43
		1	197	113
	623	$1x10^{-2}$	> 1180	5
		$1x10^{-1}$	907	20
		1	339	61
	673	$1x10^{-1}$	209	69
		1	199	77
procedure B3	623	$1x10^{-2}$	1160	10

Conclusions

1. An investigation of equal-channel angular (ECA) pressing of Al-5%Zn gives insight into the mechanism responsible for grain refinement through the introduction of strain in the material: the formation of subgrains followed by the evolution of low angle sub-boundaries into large angle grain boundaries.
2. An investigation of Al-5.5%Mg-2.2%Li-0.12%Zr shows that the ECA pressing technique emerges as a viable method to produce superplastic Al alloys.
3. The introduction of a true strain of 8 in the Al-1420 alloy appears to be sufficient to produce a structure consisting entirely of high angle boundaries.
4. Superplastic behavior was achieved at a high strain rate, more than one order of magnitude higher than the usual strain rates for commercial Al alloys.
5. Superplasticity was achieved at a temperature of ~ 0.7 T_M, where T_M is the absolute melting temperature, therefore incipient melting cannot occur at triple junctions or grain boundaries. This is evidence for normal superplasticity occurring at a high strain rate.

Acknowledgements

This work was supported in part by the Light Metals Educational Foundation of Japan, in part by a Grant-in-Aid for Scientific Research from the Ministry of Education, Science, Sports and Culture of Japan, in part by the National Science Foundation of the United States under Grants No. DMR-9625969 and INT-9602919, and in part by the U.S. Army Research Office under Grants No. DAAH04-96-1-0332 and N68171-96-6-9006

References

1. E. M. Taleff, G. A. Henshall, D. R. Lesuer, T. G. Nieh and J. Wadsworth, "Enhanced tensile ductility of coarse-grain Al-Mg alloys", in Superplasticity and Superplastic

Forming, eds. A. K. Ghosh and T. R. Bieler, TMS, Warrendale, PA (1995), 3-10
2. T. G. Langdon, "The mechanical properties of superplastic materials", Metall. Trans. A13 (1982), 689-701
3. P.G. Sanders, G.E. Fougere, L.J. Thompson, J.A. Eastman and J.R. Weertman, "Improvements in the synthesis and compaction of nanocrystalline materials," Nanostruct. Mater. 8 (1997), 243-252
4. S. K. Pabi and B. S. Murty, "Mechanism of mechanical alloying in Ni-Al and Cu-Zn systems", Mater. Sci. Eng. A214 (1996), 146-152
5. R. Z. Valiev special editor, Ultra-fine grained materials produced by severe plastic deformation, Annales de Chimie, 21 (1996)
6. M. Furukawa, P. B. Berbon, Z. Horita, M. Nemoto, N. K. Tsenev, R. Z. Valiev and T. G. Langdon, "Production of Ultrafine-Grained Metallic Materials Using an Intense Plastic Straining Technique", Mater. Sci. Forum, 233 (1997), 177-184
7. V. M. Segal, "Materials processing by simple shear", Mater. Sci. Eng. A197 (1995), 157-164
8. I. N. Fridlyander, V. S. Sandler and T. I. Nikol'skaya, "Investigation of the ageing of aluminum-magnesium-lithium alloys", Fiz. Metal. Metalloved, 32 (1971), 767-774
9. Y. Iwahashi, J. Wang, Z. Horita, M. Nemoto and T. G. Langdon, "Principle of equal-channel angular pressing for the processing of ultra-fine grained materials", Scripta Mater. 35 (1996), 143-146
10. S. Ferrasse, V. M. Segal, K. T. Hartwig and R. E. Goforth, "Development of a submicrometer-grained microstructure in aluminum 6061 using equal channel angular extrusion", J. Mater. Res. 12 (1997), 1253-1261
11. B. Bay, N. Hansen, D. A. Hughes and D. Kuhlmann-Wilsdorf, "Evolution of f.c.c. deformation structures in polyslip", Acta Metall. Mater. 40 (1992), 205-219
12. F. R. N. Nabarro and D. Kuhlmann-Wilsdorf, "Nucleation of small-angle boundaries", Scripta Mater. 35 (1996), 1331-1333
13. H. S. Yang, M. Shaarbaf and K. R. Brown, "On the fabrication aspect of commercial superplastic 5083 aluminum alloy sheets", in Superplasticity and Superplastic Forming, eds. A. K. Ghosh and T. R. Bieler, TMS, Warrendale, PA (1995), 17-24
14. A. A. Nazarov, A. E. Romanov and R. Z. Valiev, "On the nature of high internal stresses in ultrafine grained materials", Nanostruct. Mater. 4 (1994), 93-101
15. M. Furukawa, H. Wang and M. Nemoto, "Precipitation hardening of Al-0.5%Zr alloy", J. Japan Inst. Light Metals, 40 (1990), 20-26
16. P. B. Berbon, M. Furukawa, Z. Horita, M. Nemoto, N. K. Tsenev, R. Z. Valiev and T. G. Langdon, "An investigation of the properties of an Al-Mg-Li-Zr alloy after equal-channel angular pressing", Mater. Sci. Forum, 217-222 (1996), 1013-1018
17. K. Higashi, "Positive exponent superplasticity in advanced aluminum alloys with nano or near-nano scale grained structures", Mater. Sci. Eng. A166 (1993), 109-118
18. T. G. Nieh and J. Wadsworth, "High-strain-rate superplasticity in aluminum matrix composites", Mater. Sci. Eng. A147 (1991), 129-142
19. K. Higashi, T. Okada, T. Mukai, S. Tanimura, T. G. Nieh and J. Wadsworth, "Superplastic behavior in a mechanically alloyed aluminum composite reinforced with SiC particulates", Scripta Metall. Mater. 26 (1992), 185-190
20. K. Higashi, T. Okada, T. Mukai and S. Tanimura, "Positive exponent strain-rate superplasticity in mechanically alloyed aluminum IN 9021", Scripta Metall. Mater. 25 (1991), 2053-2057

拘束強ひずみ加工で作製した超微細粒組織

九州大学工学部　小村章吾*　宇都宮　淳*　堀田善治*　根本　實*
福岡教育大学　古川　稔**
University of Southern California　Patrick B. Berbon***, Terence G. Langdon***

Fig. 1　室温 ECAP で相当ひずみ 8 を課した Al-3%Mg-0.2%Sc の(a) 微細粒組織と(b) 制限視野回折パターン.

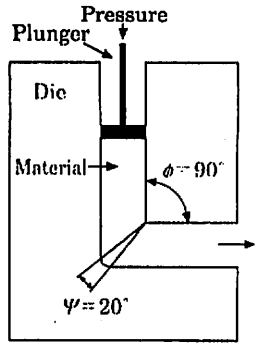

Fig. 2　ECAP 法の模式図.

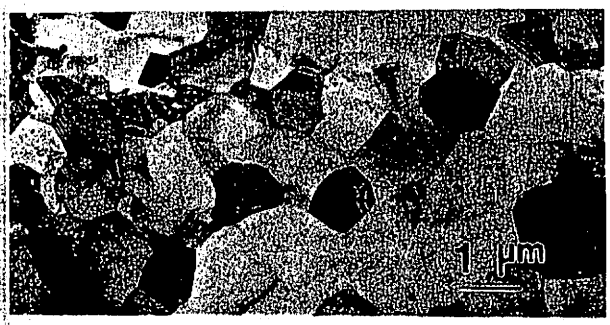

Fig. 3　ECAP 材(Fig. 1)の 673 K, 3.6 ks(1 h)における焼鈍組織.

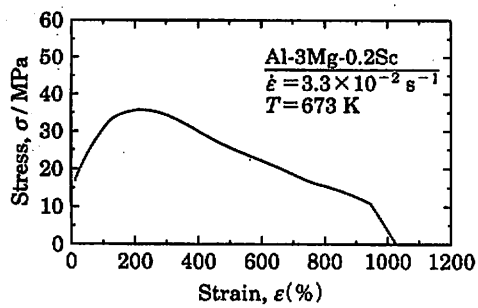

Fig. 4　ECAP 材(Fig. 1)の 673 K, $3.3 \times 10^{-2}\ s^{-1}$ における応力-ひずみ曲線.

Fig. 1(a)は，Al-3%Mg-0.2%Sc 合金の透過電子顕微鏡写真である．図中のスケールや Fig. 1(b)の直径約 2.5 μm の制限視野回折パターンからサブミクロンレベルの微細結晶粒が形成されていることがわかる．平均結晶粒径は約 0.2 μm と測定される．**Fig. 2** はこの結晶粒微細化に用いた方法を模式的に示したもので，ECAP(equal-channel angular pressing)法と呼ばれている[(1)-(3)]．図のような拘束条件下で強せん断ひずみを導入することで結晶粒微細化が図られる．Fig. 1 は特に室温での ECAP で得られた微細粒組織である．

この室温 ECAP 材を 673 K で 3.6 ks 焼鈍したのが **Fig. 3** である．焼鈍温度が高温($0.7T_m$, T_m：融点)にもかかわらず，結晶粒度は約 1 μm と小さい．すなわち超塑性の出現が十分期待できる．実際，この室温 ECAP 材を 673 K で引張試験すると $3.3 \times 10^{-2}\ s^{-1}$ の高ひずみ速度で，**Fig. 4** に示すように，1000%を超す超塑性伸びが得られた．

ECAP 法は，これまでの粉末冶金法と異なり残留空隙のないバルク状試料が大量に製造できる[(4)]．また，再結晶による結晶粒微細化法と異なり必ずしも熱処理過程を必要としない．しかも，高ひずみ速度あるいは低温度超塑性の実現可能性を秘めている．ECAP 法による結晶粒微細化プロセスは省エネルギーや地球温暖化抑制という観点から有望視される．

文　献

(1) V. M. Segal, V. I. Reznikov, A. E. Drobyshevsky and V. I. Kopylov: Russian Metallurgy (Metally), 1(1981), 99.
(2) R. Z. Valiev, N. A. Krasilnikov and N. K. Tsenev: Mater. Sci. Eng., A137(1991), 35.
(3) 堀田善治，王 経 涛，古川 稔，根本 実，R. Z. Valiev, Y. Ma, T. G. Langdon：日本金属学会会報，32(1993), 898.
(4) Y. Iwahashi, Z. Horita, M. Nemoto and T. G. Langdon: Acta Mater., 45(1997), 4733.

(1998年1月26日受理)

Ultrafine-Grained Structure Produced by Equal-Channel Angular Pressing; Shogo Komura*, Atsushi Ustunomiya*, Zenji Horita*, Minoru Nemoto*, Minoru Furukawa**, Patirck B. Berbon***, Terence G. Langdon***(*Faculty of Engineering Kyushu University, Fukuoka. **Fukuoka University of Education, Munakata, Fukuoka. ***University of Southern California, Los Angeles, CA, USA)
Keywords: *aluminum-magnesium-scandium, ultrafine-grained structure, superplasticity*
TEM specimen preparation: jet electropolishing　TEM utilized: H-8100(200 kV)

Using Intense Plastic Straining for High-Strain-Rate Superplasticity

Terence G. Langdon, Minoru Furukawa, Zenji Horita, and Minoru Nemoto

Ultrafine grain sizes may be introduced into bulk samples by using the intense plastic straining technique equal-channel angular pressing. This article describes the principles of equal-channel angular pressing and demonstrates the application of this procedure to attain ultrafine grain sizes in an Al-3Mg solid-solution alloy and a commercial cast Al-Mg-Li-Zr alloy. Provided there is stability of these ultrafine grains at elevated temperatures, as in the Al-Mg-Li-Zr alloy, equal-channel angular pressing may be used as a processing tool to achieve high-strain-rate superplasticity in materials that are not potentially superplastic. These results have important implications for reducing the long production times that are associated with the fabrication of complex parts using superplastic forming.

INTRODUCTION

Superplasticity refers to the ability of a material to pull out uniformly to a very high elongation when tested in tension.[1] This process is important because it provides the potential for the fabrication of complex shapes from sheet metals using superplastic forming (SPF).[2] However, an important limiting characteristic of SPF is that the optimum superplastic conditions, and therefore the maximum ductilities, are generally attained at relatively low strain rates,[3] typically of the order of ~10^{-3}–10^{-2} s^{-1}, so that the forming times are consequently very long. These long production times, which may extend up to ~30 minutes, severely restrict the utilization of SPF to the fabrication of high-value components associated with limited applications in industries such as aerospace and construction.

Detailed experiments by Nieh et al.,[4] conducted just over a decade ago, demonstrated the potential for achieving high-strain-rate superplasticity (HSR SP) in at least some metallic systems. Specifically, their experiments revealed that a maximum elongation of up to ~300 percent may be achieved at the very high strain rate of 3.3×10^{-1} s^{-1} using a metal-matrix composite consisting of an Al-2124 matrix alloy with a reinforcement of SiC whiskers. Furthermore, it was shown also that the elongations to failure decreased by only a minor extent at even faster strain rates.

These early results generated much interest and led to the initiation of numerous investigations that were designed primarily to quantify the properties and characteristics associated with the HSR SP process. Much of this work was summarized in a recent review,[5] and HSR SP has now become established as an important and reproducible feature of a number of metal-matrix composites, mechanically alloyed materials, and alloys produced using powder-metallurgy techniques.[6] Very recently, the Japanese Standards Association produced a standard, which was designated JIS H7007, formally defining HSR SP as the occurrence of high superplastic-like elongations at strain rates at or above 10^{-2} s^{-1}.

The introduction of HSR SP provides the potential for increasing the utility of the SPF procedure by substantially increasing the rates associated with the forming process. It is instructive, therefore, to examine the possible methods that may be employed in order to increase the strain rates associated with optimum superplastic flow. Early laboratory experiments showed that a reduction in specimen grain size in conventional superplastic alloys may lead both to an increase in the optimum elongations to failure and a displacement of these higher elongations to faster strain rates.[7] Results of this type led to the suggestion that HSR SP may be achieved in conventional alloys through a significant reduction in the grain size.[8] For example, superplastic metals generally have grain sizes of ~2–5 μm so that it appears advisable to reduce these sizes to within the submicrometer level.

There is considerable interest in developing methods for the processing of materials with ultrafine grain sizes; methods under current investigation include inert gas condensation,[9,10] high-energy ball milling,[11–13] and sliding wear.[14] However, these various procedures are not yet capable of producing large fully dense bulk materials, and, therefore, they appear inappropriate for the development of metals for subsequent use in SPF. Because of these limitations, attention has been directed instead toward the possibility of refining the microstructure in bulk samples using intense plastic straining techniques.

Two major methods are available for refining the microstructure using intense plastic straining: torsion straining under high pressure[15–18] and equal-channel angular (ECA) pressing.[16,17,19–22] Of these two procedures, ECA pressing is especially attractive because it has the ability to provide large bulk samples in a fully dense condition.

The preceding article by Mabuchi and Higashi[23] on page 34 of this issue gives a broad overview of the general characteristics of HSR SP; this article summarizes the recent developments associated with attaining HSR SP using intense plastic straining. Specifically, experiments are described that led to a refinement of the microstructures of an Al-Mg solid-solution alloy and a commercial Al-Mg-Li-Zr alloy. ECA pressing is capable of producing an ultrafine grain size in these materials, but in practice grain stability at elevated temperatures is an important additional requirement in order to achieve HSR SP in these materials.

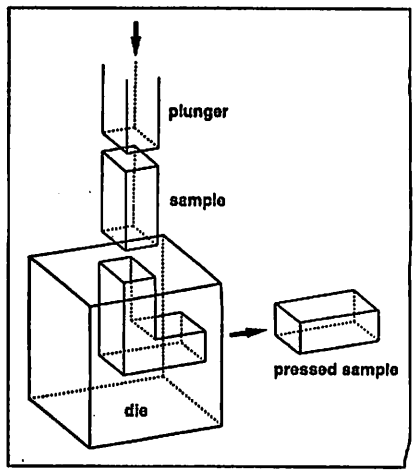

Figure 1. A schematic of ECA pressing.

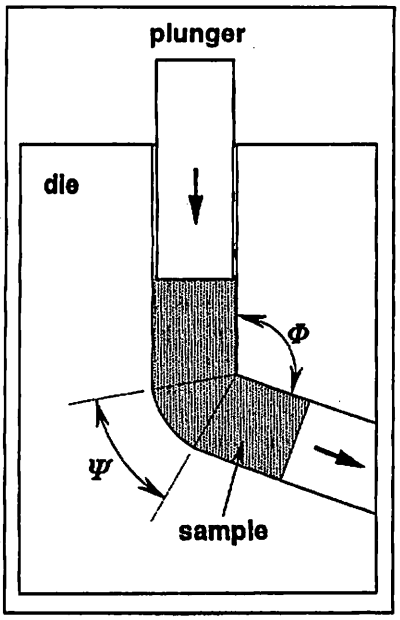

Figure 2. A section through the ECA pressing die showing the internal angles ϕ and ψ.

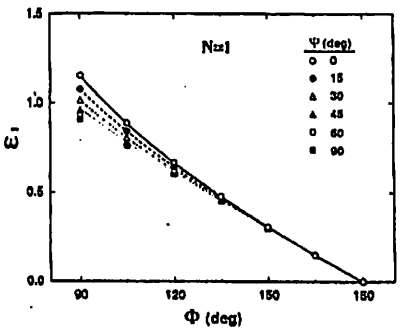

Figure 3. The variation of strain with angles ϕ and ψ in a single passage through an ECA pressing die.

Table I. Rotations Associated with ECA Pressing through Routes

	Number of Pressings						
Route	Two	Three	Four	Five	Six	Seven	Eight
A	0°	0°	0°	0°	0°	0°	0°
B_A	90° CCW	90° CW	90° CCW	90° CW	90° CCW	90° CCW	90° CCW
B_C	90° CCW	90° CCW	90° CCW	90° CCW	90° CCW	90° CCW	90° CCW
C	180°	180°	180°	180°	180°	180°	180°

CW—clockwise; CCW—counterclockwise.

ECA PRESSING

Intense plastic straining is introduced into a sample by pressing it through a die within a channel, which is bent at a selected angle in order to impose the requisite strain by shear. Figure 1 is a schematic of the principle of ECA pressing. A test sample is machined to fit within the die and is pressed through the die using a plunger. Since the two sections of the channel within the die are equal in cross section, it follows that, neglecting any end effects, the pressed sample has the same dimensions as the original sample. Thus, repetitive pressings may be easily undertaken in order to achieve a very high total strain.

Two angles may be used to specify the strain imposed on each passage through the die. These angles, illustrated in Figure 2, represent the angle of intersection of the two channels, ϕ, and the angle subtended by the outer arc of curvature at the point of intersection of the two channels, ψ. The strain imposed on a single passage through the die is determined exclusively by the values of ϕ and ψ, and in practice it has been shown that the total strain, ε_N, accrued from N passages through the die is given by the relationship[24]

$$\varepsilon_N = \frac{N}{\sqrt{3}}\left[2\cot\left(\frac{\Phi}{2}+\frac{\Psi}{2}\right)+\Psi\,\mathrm{cosec}\left(\frac{\Phi}{2}+\frac{\Psi}{2}\right)\right]$$

Model experiments have confirmed the validity of this relationship with the exception only of the sample edges where the strain may be affected by frictional effects.[25]

The implications of this relationship can be illustrated by plotting the strain accrued on a single passage through the die, ε_1, against the intersection angle, ϕ, for a range of values of ψ from 0° to 90° (Figure 3). The value of ψ has a relatively minor influence on the total strain. In practice, a strain of ~1 is achieved on a single pass when ϕ = 90°, so that a total of ten passes will give a strain close to ~10. It has been shown experimentally that an ultrafine grain size is attained most readily when the strain imposed is very intense;[26] therefore, the present experiments were conducted using dies having ϕ = 90°.

When repetitive pressings are made on the same sample, different processing routes may be followed for the second and subsequent pressings. Three separate possibilities are illustrated schematically in Figure 4. In route A, the sample is pressed each time with no rotation; in route B the sample is rotated by 90° between each pressing, and in route C the sample is rotated by 180° between each pressing. In practice, route B may be further differentiated into route B_A, where the sample is rotated alternately by 90° in forward and backward directions between each pressing, and route B_C, where the sample is rotated by 90° in the same direction between each pressing. These designations are given because of the similarities in the shearing patterns between routes A and B_A and routes C and B_C, respectively. The principles of these four routes are illustrated in Table I for a total of eight pressings. Experiments have shown that an ultrafine grain size with high-angle boundaries is achieved most rapidly when using route B_C.[22,27] The experiments reported here were conducted using route A with no rotation between consecutive pressings.

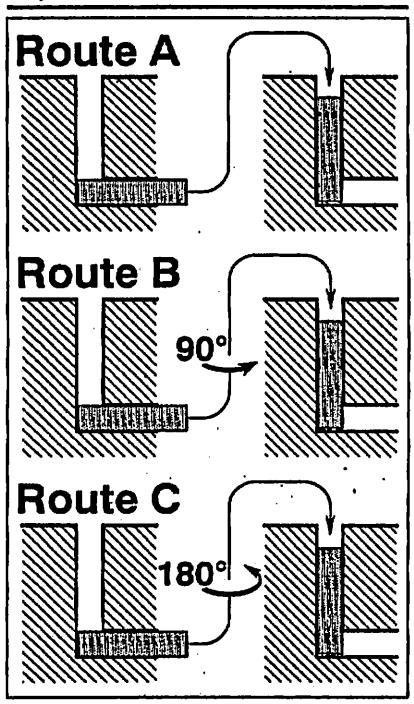

Figure 4. Three processing routes for ECA pressing.

EXPERIMENTAL RESULTS

The ability to substantially refine the microstructure by intense plastic straining may be illustrated by the photomi-

crograph in Figure 5 for a specimen of the Al-3Mg alloy following ECA pressing to a strain of ~4; the selected-area electron diffraction (SAED) pattern was obtained from a region having a diameter of 1.9 μm. Following ECA pressing, the microstructure was essentially homogeneous, and it is apparent from the SAED pattern that the grain boundaries have high angles of misorientation. Measurements showed that the mean linear intercept grain size in this condition was ~0.23 μm, thereby demonstrating a very substantial reduction from the initial grain size of ~500 μm. Careful inspection of the microstructure in this condition showed that, as observed also in Al-Mg alloys[18] and in copper and nickel samples[36] after intense straining in torsion, the grain boundaries were generally poorly delineated and are characteristic of a high-energy non-equilibrium configuration.[37,38]

The effect of static annealing of the as-pressed Al-3Mg alloy at selected temperatures for one hour is illustrated in Figure 6 for annealing temperatures of 443 K, 503 K, 533 K, and 563 K, respectively. The average grain size increases with increasing temperature; at intermediate temperatures (e.g., 533 K), there is a duplex structure consisting of areas of recrystallized and unrecrystallized grains. In addition, it is apparent that the grain boundary structures also evolve into more equilibrated configurations with increasing temperature. This recrystallization has been designated continuous static recrystallization[39] and is a consequence both of the advent of thermal activation and of the initial non-equilibrium nature of the microstructure following the ECA pressing.

Substantial grain growth is evident in Figure 6 at the highest annealing temperature. This growth may be illustrated directly by plotting the equilibrium grain size after static annealing as a function of the annealing temperature, as given by the solid points in Figure 7; the open points are for the Al-Mg-Li-Zr alloy that is discussed later. It is apparent that the ultrafine grain size introduced into the Al-3Mg alloy is not stable at elevated temperatures, and in practice there is rapid grain growth at temperatures above ~500 K. Since superplasticity is a diffusion-controlled process[3] requiring a temperature of the order of ~0.5 T_m or higher, where T_m is the absolute melting temperature, these results show that the Al-3Mg alloy is not a suitable candidate material for the development of HSR SP at high temperatures.

The commercial Al-Mg-Li-Zr alloy was subjected to two different ECA processing conditions. Figures 8 and 9 show typical microstructures in the as-pressed material and the associated SAED patterns after pressing through routes one and two, respectively.

Careful inspection of a large area of the sample processed via route one revealed a heterogeneous microstructure consisting of areas of ultrafine grains with grain boundaries having high angles of misorientation (Figure 8) and areas of subgrains where the boundaries were in low angles of misorientation. Measurements showed that the volume fraction of material having high-angle boundaries in this as-pressed condition was of the order of ~60–70 percent, and the remaining volume of ~30–40 percent contained subgrains with low-angle boundaries. The average grain size and subgrain size were essentially identical at ~1.2 μm. This equilibrium size is higher than in the Al-3Mg alloy, but it again demonstrates substantial grain refinement through ECA pressing from the initial grain size of ~400 μm.

Although these observations confirm the occurrence of grain refinement, the dominant deformation process in superplasticity is nevertheless grain boundary sliding.[40,41] This necessitates the presence of an array of high-angle grain boundaries that can slide easily. For example, it is well established that tensile ductility is substantially inhibited in materials having large numbers of boundaries with low angles of misorientation.[42] Since it has been estab-

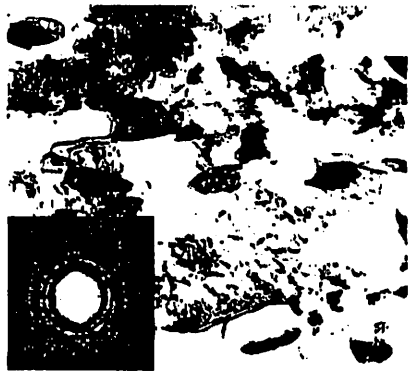

Figure 5. The microstructure of the Al-3Mg alloy after ECA pressing and the SAED pattern (inset).

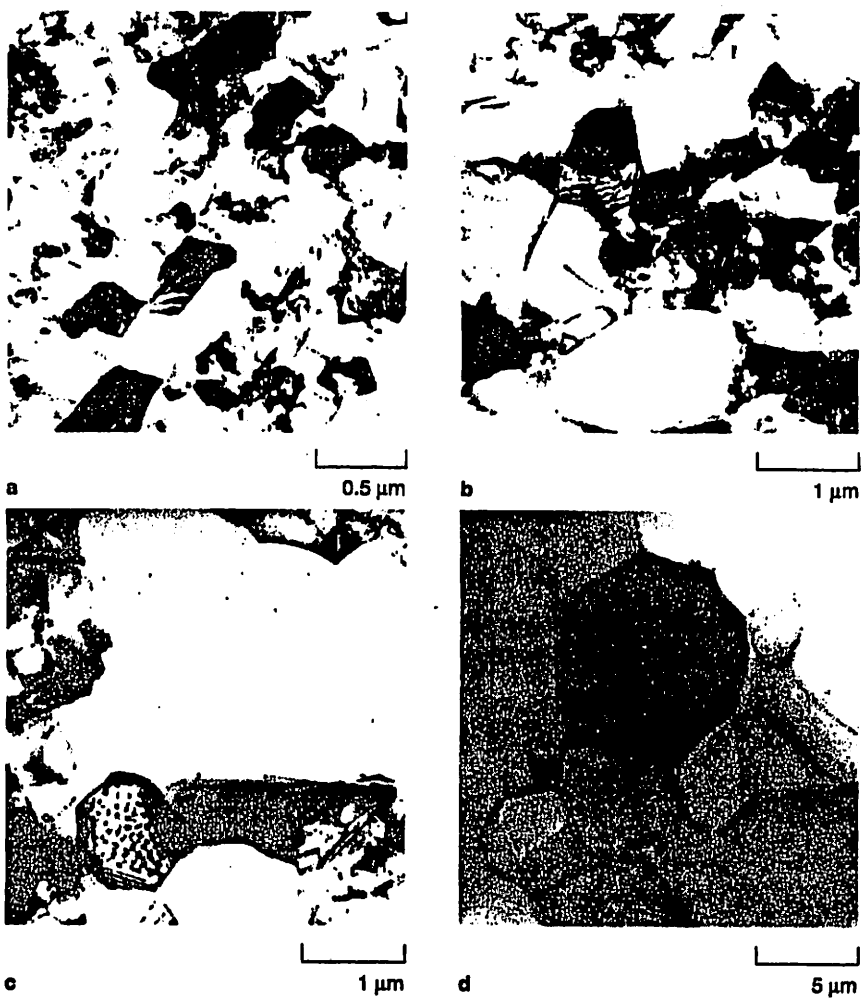

Figure 6. Microstructures in the Al-3Mg alloy after annealing for one hour at (a) 443 K, (b) 503 K, (c) 533 K, and (d) 563 K.

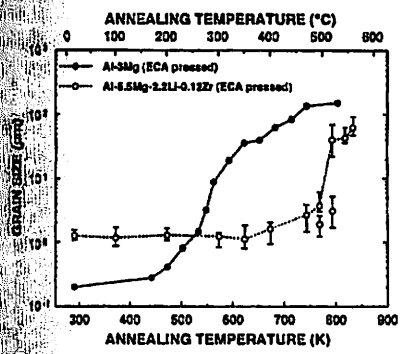

Figure 7. Grain size versus annealing temperature for the Al-3Mg and Al-Mg-Li-Zr alloys.

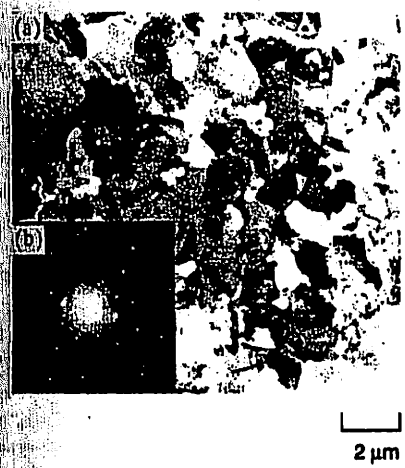

Figure 8. (a) The microstructure of the Al-Mg-Li-Zr alloy after ECA pressing through route one and (b) the SAED pattern.

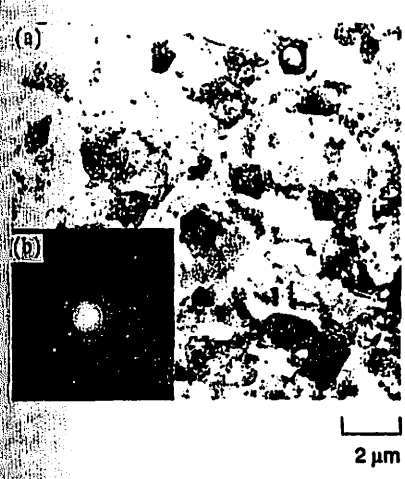

Figure 9. (a) The microstructure of the Al-Mg-Li-Zr alloy after ECA pressing through route two and (b) the SAED pattern.

EXPERIMENTAL METHODS

Intense plastic straining procedures have been used with a number of different materials but, for simplicity, this article deals exclusively with experiments conducted on an Al-Mg solid-solution alloy and a commercial Al-Mg-Li-Zr alloy. As noted by Mabuchi and Higashi,[23] most reports of HSR SP to date have concentrated on aluminum-based materials.

An Al-3Mg solid-solution alloy was obtained in a hot-rolled condition with a grain size of ~500 μm. It was subjected to ECA pressing in air at room temperature for a total of four passes through the die to give a total strain of ~4. More detailed information concerning the material and the experimental observations are given elsewhere.[29-32]

A commercial cast lightweight Al-5.5Mg-2.2Li-0.12Zr alloy, with the Russian designation of 01420,[33] was obtained in a hot-rolled condition with a grain size of ~400 μm and was subjected to ECA pressing in air under two different conditions defined as routes one and two, respectively. Route one denotes a total of four passes at a temperature of 673 K to give a strain of ~4; route two denotes a total of eight passes at 673 K and an additional four passes at 473 K to give a total strain of ~12, where the lower temperature of 473 K was employed for the final pressings in an attempt to minimize grain growth. For each processing route, the samples were cooled in air between consecutive pressings. Further details regarding this material and the experimental results are also provided elsewhere.[32,34,35]

Static annealing experiments were conducted on both materials after ECA pressing by cutting small samples and annealing for one hour over a selected range of temperatures up to ~800 K, with the temperature held constant during annealing to within ±1 K. Selected samples were examined after pressing by transmission electron microscopy using the preparation procedure described earlier.[29] To check on the ductility introduced by the ECA pressing, tensile specimens were prepared with gauge lengths cut parallel to the longitudinal axes after pressing. These samples were pulled in air at selected elevated temperatures using an Instron testing machine operating at a constant rate of cross-head displacement with the temperatures controlled to within ±2 K during each test. In addition, some samples of the Al-Mg-Li-Zr alloy were also tested in tension in the as-received condition without any subsequent ECA pressing.

lished also in ECA pressing that the boundaries developed in the ultrafine grain structure evolve with increasing strain,[21,22] it is reasonable to anticipate that the microstructure may be less heterogeneous after pressing through route two to a total strain of ~12.

Figure 9 shows the as-pressed microstructure after ECA pressing via route two. In this condition, the microstructure is homogeneous, and essentially all of the boundaries have high angles of misorientation. In addition, the measured average grain size was ~1.2 μm, which is identical to the grain size recorded after processing via route one to a total strain of ~4. Thus, it is apparent that additional pressings of the same sample through the ECA die and, hence, the introduction of higher strains have no significant effect on the measured grain size, but rather serve primarily to increase the average misorientations at the boundaries.

The effect of static annealing of the Al-Mg-Li-Zr alloy is shown in Figure 10 for annealing temperatures of 473 K, 573 K, 673 K, and 793 K, respectively. Inspection shows that grain growth is very much inhibited in this alloy, and the grains remain small even at a temperature of 673 K. Thus, it may be concluded that the equilibrium grain size in the Al-Mg-Li-Zr alloy pressed at 673 K is larger than in the Al-3Mg alloy pressed at room temperature, but the grains of the Al-Mg-Li-Zr alloy show remarkable stability at elevated temperatures, suggesting that this commercial alloy may be an appropriate candidate material for HSR SP. Detailed microstructural analysis has established that the grain stability of this commercial alloy is due to the stability within the matrix of a very fine dispersion of β'-Al_3Zr precipitates.[34]

Figure 7 includes grain growth data for the Al-Mg-Li-Zr alloy (shown by the open points). Thus, the grain size of this alloy remains at ~1.2 μm up to temperatures close to 700 K, and it is within the superplastic range of <10 μm up to temperatures above 750 K. However, the grains grow very rapidly at the very highest temperatures such that the grain size is ~60 μm at a temperature only slightly above 800 K.

The effect of this small grain size on the tensile ductility is documented in Figure 11, where the elongation to failure is plotted against the initial testing strain rate for experiments conducted at similar temperatures of 603 K and 623 K. The lower open points show the very low ductility of this alloy in the unpressed condition, and the two sets of solid points show the effect of ECA pressing through route one to a strain of ~4 and route two to a strain of ~12, respectively. Thus, the unpressed samples exhibit elongations to failure of up to a maximum of ~200 percent over the strain rate range from ~10^{-4}–10^{-1} s^{-1}, whereas the samples pressed through route one and having the heterogeneous microstructure give evidence of the advent of superplastic-like flow. The samples pressed through route two show exceptionally high elongations even at the highest testing strain rate of 1 s^{-1}. Further details of the results obtained on the Al-Mg-Li-Zr alloy are given elsewhere[43] together with similar data obtained on the traditional superplastic Supral 100 alloy of Al-6Cu-0.4Zr. It is important to note that very high ductility was achieved in the Al-Mg-Li-Zr alloy only after processing via route two, and in this condition there was uniform deformation within the gauge lengths of the superplastic samples. The highest ductility attained in these tests was an elongation of 1,180% without failure at a testing temperature of 623 K and an initial strain rate of 10^{-2} s^{-1}. Work currently in progress has revealed the possibility of attaining similar high ductilities in an Al-3Mg alloy with the addition of 0.2% scandium.[44]

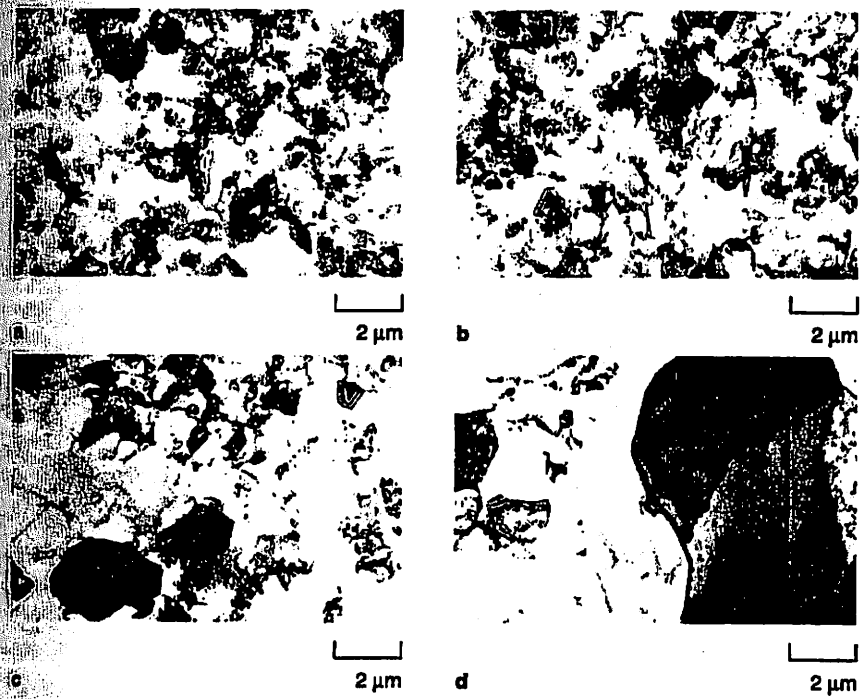

Figure 10. Microstructures in the Al-Mg-Li-Zr alloy after annealing for one hour at (a) 473 K, (b) 673 K, (c) 673 K, and (d) 793 K.

CONCLUSION

These results serve to demonstrate that ECA pressing is a very effective tool for refining the grain size of bulk samples; provided there is grain stability at elevated temperatures, this gives the potential for achieving HSR SP in a number of materials. Also, HSR SP is not confined exclusively to a limited range of metal-matrix composites, mechanically alloyed materials, and alloys produced by powder-metallurgy techniques but may also be achieved in cast alloys by using and optimizing ECA pressing.

References

1. A.H. Chokshi, A.K. Mukherjee, and T.G. Langdon, *Mater. Sci. Eng.*, R10 (1993), pp. 237–274.
2. A.J. Barnes, *Mater. Sci. Forum*, 170–172 (1984), pp. 701–714.
3. T.G. Langdon, *Metall. Trans.*, 13A (1982), pp. 689–701.
4. T.G. Nieh, C.A. Henshall, and J. Wadsworth, *Scripta Metall.*, 18 (1984), pp. 1405–1408.
5. K. Higashi, M. Mabuchi, and T.G. Langdon, *ISIJ Intl.*, 36 (1996), pp. 1423–1438.
6. T.G. Nieh, J. Wadsworth, and O.D. Sherby, *Superplasticity in Metals and Ceramics* (Cambridge, U.K.: Cambridge University Press, 1997), pp. 154–188.
7. F.A. Mohamed, M.M.I. Ahmed, and T.G. Langdon, *Metall. Trans.*, 8A (1977), pp. 933–938.
8. Y. Ma et al., *Mater. Trans. JIM*, 37 (1996), pp. 336–339.
9. H. Gleiter, *Deformation of Polycrystals: Mechanisms and Microstructures*, eds. N. Hansen et al. (Roskilde, Denmark: Riso National Laboratory, 1981), pp. 15–21.
10. P.G. Sanders et al., *Nanostruct. Mater.*, 8 (1997), pp. 243–252.
11. C.C. Koch and Y.S. Cho, *Nanostruct. Mater.*, 1 (1992), pp. 207–212.
12. J. Eckert et al., *J. Mater. Res.*, 7 (1992), pp. 1751–1761.
13. C.C. Koch, *Nanostruct. Mater.*, 9 (1997), pp. 13–22.
14. D.A. Rigney, *Ann. Rev. Mater. Sci.*, 18 (1988), pp. 141–163.
15. N.A. Smirnova et al., *Fiz. Metal. Metalloved.*, 61 (1986), pp. 1170–1177.
16. R.Z. Valiev, N.A. Krasilnikov, and N.K. Tsenev, *Mater. Sci. Eng.*, 137A (1991), pp. 35–40.
17. R.Z. Valiev, A.V. Korznikov, and R.R. Mulyukov, *Mater. Sci. Eng.*, 168A (1993), pp. 141–148.
18. Z. Horita et al., *J. Mater. Res.*, 11 (1996), pp. 1880–1890.
19. V.M. Segal et al., *Russian Metallurgy (Metally)*, 1 (1981), pp. 99–105.
20. R.Z. Valiev and N.K. Tsenev, *Hot Deformation of Aluminum Alloys*, eds. T.G. Langdon et al. (Warrendale, PA: TMS, 1991), pp. 319–329.
21. Y. Iwahashi et al., *Acta Mater.*, 45 (1997), pp. 4733–4741.
22. Y. Iwahashi et al., *Acta Mater.* 49 (1998), pp. 3317–3331.
23. M. Mabuchi and K. Higashi, *JOM*, 50 (6) 1998), pp. 34–39.
24. Y. Iwahashi et al., *Scripta Mater.*, 35 (1996), pp. 143–146.
25. Y. Wu and I. Baker, *Scripta Mater.*, 37 (1997), pp. 437–441.
26. K. Nakashima et al., *Acta Mater.*, 46 (1998), pp. 1589–1599.
27. K. Oh-ishi et al., *Metall. Mater. Trans.* (in press).
28. J. Wang et al., *J. Mater. Res.*, 8 (1993), pp. 2810–2818.
29. J. Wang et al., *Acta Mater.*, 44 (1996), pp. 2973–2982.
30. M. Furukawa et al., *Acta Mater.*, 44 (1996), pp. 4619–4629.
31. J. Wang et al., *Mater. Sci. Eng.*, A216 (1996), pp. 41–46.
32. M. Furukawa et al., *Phil. Mag. A* (in press).
33. I.N. Fridlyander, V.S. Sandler, and T.I. Nikolskaya, *Fiz. Metal. Metalloved*, 32 (1971), pp. 767–774.
34. M. Furukawa et al., *Acta Mater.*, 45 (1997), pp. 4751–4757.
35. M. Furukawa et al., *Metall. Mater. Trans. A*, 29A (1998), pp. 169–177.
36. Z. Horita et al., *J. Mater. Res.*, 13 (1998), pp. 446–450.
37. R.Z. Valiev, R.Sh. Musalimov, and N.K. Tsenev, *Phys. Stat. Sol. (a)*, 115 (1989), pp. 451–457.
38. A.A. Nazarov, A.E. Romanov, and R.Z. Valiev, *Acta Metall. Mater.*, 41 (1993), pp. 1033–1040.
39. M. Furukawa et al., *Proceedings of ReX'96: The Third International Conference on Recrystallization and Related Phenomena*, ed. T.R. McNelley (Monterey, CA: Monterey Institute of Advanced Studies, 1997), pp. 149–160.
40. T.G. Langdon, *Acta Metall. Mater.*, 42 (1994), pp. 2487–2492.
41. T.G. Langdon, *Mater. Sci. Eng.*, A174 (1994), pp. 225–230.
42. R. Crooks, S.J. Hales, and T.R. McNelley, *Superplasticity and Superplastic Forming*, ed. C.H. Hamilton and N.E. Paton (Warrendale, PA: TMS, 1988), pp. 389–393.
43. R.Z. Valiev et al., *Scripta Mater.*, 37 (1997), pp. 1945–1950.
44. S. Komura et al., *Scripta Mater.* 38 (1998), pp. 1851–1856.

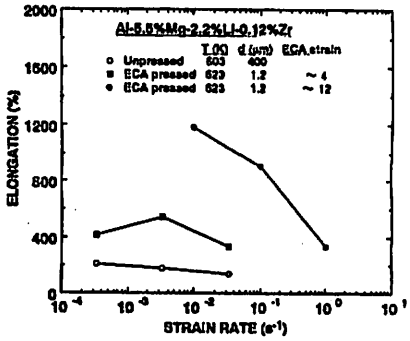

Figure 11. Elongation versus strain rate for samples of the Al-Mg-Li-Zr alloy tested at similar temperatures in the unpressed condition and after ECA pressing through route one to a strain of ~4 and route two to a strain of ~12, respectively.

ACKNOWLEDGEMENTS

This report was prepared during the appointment of T.G. Langdon as visiting professor in the Department of Physics at the Danish Technical University. The work was supported in part by the Light Metals Educational Foundation of Japan; a Grant-in-Aid for Scientific Research from the Ministry of Education, Science, Sports and Culture of Japan; the Japan Society for the Promotion of Science; the U.S. National Science Foundation under grants no. DMR-9625969 and INT-9602919; and the U.S. Army Research Office under grant no. DAAH04-96-1-0332.

ABOUT THE AUTHORS

Terence G. Langdon earned his Ph.D. in physical metallurgy at Imperial College, University of London, in 1965. He is currently professor of materials science and mechanical engineering at the University of Southern California, Los Angeles. Dr. Langdon is a member of TMS.

Minoru Furukawa earned his D.Eng. in metallurgy at Kyushu University in 1988. He is currently an associate professor at Fukuoka University of Education, Munakata, Japan. Dr. Furukawa is also a member of TMS.

Zenji Horita earned his Ph.D. in materials science at the University of Southern California in 1983. He is currently an associate professor of materials science and engineering at Kyushu University, Fukuoka, Japan. Dr. Horita is also a member of TMS.

Minoru Nemoto earned his D.Eng. in materials science and engineering at Tohoku University in 1966. He is currently a professor of materials science and engineering at Kyushu University, Fukuoka, Japan. Dr. Nemoto is also a member of TMS.

For more information, contact T.G. Langdon, University of Southern California, Los Angeles, California 90089; (213) 740-0491; fax (213) 740-7797; e-mail langdon@usc.edu.

PHILOSOPHICAL MAGAZINE A, 1998, VOL. 78, NO. 1, 203–215

Factors influencing the flow and hardness of materials with ultrafine grain sizes

By MINORU FURUKAWA†, ZENJI HORITA‡, MINORU NEMOTO‡, RUSLAN Z. VALIEV§ and TERENCE G. LANGDON¶

† Department of Technology, Fukuoka University of Education, Munakata, Fukuoka 811-41, Japan
‡ Department of Materials Science and Engineering, Kyushu University, Fukuoka 812-81, Japan
§ Institute of Physics of Advanced Materials, Ufa State Aviation Technical University, Ufa 450000, Russia
¶ Departments of Materials Science and Mechanical Engineering, University of Southern California, Los Angeles, CA 90089-1453, USA

[*Received 9 October 1997 and accepted 25 November 1997*]

ABSTRACT

Ultrafine grain sizes were introduced into an Al–3wt%Mg solid solution alloy and a commercial Al–Mg–Li–Zr alloy through intense plastic straining by equal-channel angular (ECA) pressing at room temperature and at 673 K respectively. Tensile testing of pressed samples at room temperature revealed markedly different stress–strain curves for these two alloys, with the Al–3wt%Mg alloy exhibiting a high yield stress with little subsequent strain hardening and the Al–Mg–Li–Zr alloy exhibiting a lower yield stress and extensive strain hardening after yielding. These and other experimental results are interpreted in terms of the nature of the microstructure introduced by the ECA pressing procedure. It is concluded that significant variations may occur in the mechanical properties of nominally similar ultrafine-grained materials depending upon the pressing conditions and the extent of any relaxation which may occur during the straining process.

§1. INTRODUCTION

Although there is considerable current interest in fabricating metals with ultrafine grain sizes, very limited information is available concerning the mechanical properties of these materials. This deficiency arises because it is difficult to use standard fabrication methods, such as inert gas condensation, to produce large fully dense structures (Sanders *et al.* 1997) and samples are invariably either tested using procedures such as the miniature disc-bend test (Gertsman *et al.* 1994, Ma *et al.* 1995) or attempts are made to interpret the properties solely from microhardness measurements despite the apparent difficulties associated with this procedure (Yost 1983).

Equal-channel angular (ECA) pressing is a processing method based on simple shear (Segal *et al.* 1981, Segal 1995), in which an ultrafine grain size may be introduced into a material by pressing the sample through a special die to introduce an intense plastic strain (Valiev and Tsenev 1991, Valiev *et al.* 1991); further details of the principles of ECA pressing are given in the literature (Iwahashi *et al.* 1996, Wang *et al.* 1996b, Prangnell *et al.* 1997, Wu and Baker 1997). The ECA pressing procedure has the advantage that it provides large fully dense samples which can be used for standard mechanical testing.

Recently, a series of tensile and compressive tests were conducted on samples of pure Cu subjected to ECA pressing at room temperature to produce a grain size of $\sim 0.2\,\mu m$ (Gertsman *et al.* 1996). The results of these experiments led to three important conclusions. First, the yield stress of Cu after ECA pressing is much higher than in a conventional Cu sample with a large grain size and the ductility of the ultrafine-grained material is also exceptionally high. Second, the stress–strain curve of the ECA pressed material at room temperature exhibits a very short initial region of strain hardening but this is followed by a very extensive flow region where there is no strain hardening and then a subsequent region where the rate of strain hardening is low. This latter result is similar to an earlier report, also on pure Cu subjected to ECA pressing and testing in compression at room temperature, where the initial strain hardening occurred within a strain of $\sim 5\%$ and the region with no significant strain hardening extended up to a strain of $\sim 50\%$ (Valiev *et al.* 1994). Third, the ratio $H_V/\sigma_{0.1}$ is consistently greater than three and increases in the ECA pressed material with increasing annealing temperature and therefore with increasing grain size (H_V is the measured microhardness and $\sigma_{0.1}$ is the 0.1% proof stress). This latter conclusion has important implications in any attempts to interpret the mechanical properties of these ultrafine-grained materials from microhardness data especially since, for comparison purposes, the hardness and yield stress data are generally related by taking a ratio of three (Nieman *et al.* 1991, Suryanarayana *et al.* 1992, Lian and Baudelet 1993).

The results of Gertsman *et al.* (1996) demonstrate that pure Cu with an ultrafine grain size is capable of exhibiting an unusual combination of high strength and high ductility at room temperature and with extensive flow having little or no significant strain hardening. However, no similar data have been reported for other metals and it is difficult to judge whether the results on Cu have a general applicability. The present investigation was therefore undertaken to provide information on the flow and hardness of two Al-based alloys subjected to ECA pressing. The results demonstrate that the mechanical properties of these materials, and in particular the shapes of the stress–strain curves, are dictated not only by the size of the grains but also by the characteristics of the grain boundaries introduced by the ECA pressing procedure.

§2. Experimental materials and procedures

The experiments were conducted using two different materials: an Al–3wt%Mg solid solution alloy and a Russian commercial alloy, designated 01420, with a chemical composition of Al–5.5wt% Mg–2.2wt% Li–0.12wt% Zr (Fridlyander *et al.* 1971).

The as-received grain size for the Al–3%Mg alloy was $\sim 500\,\mu m$ and it was subjected to ECA pressing in air at room temperature to a true plastic strain of ~ 4. Following ECA pressing, it was rolled at room temperature to give a sheet with a thickness of ~ 1 mm. Inspection after ECA pressing revealed a heterogeneous microstructure with an average grain size of $\sim 0.2\,\mu m$. Further details concerning this alloy after ECA pressing are given elsewhere (Wang *et al.* 1993, Furukawa *et al.* 1996b, Wang *et al.* 1996a).

The Al–Mg–Li–Zr alloy had an as-received grain size of $\sim 400\,\mu m$ and it was subjected to ECA pressing in air at a temperature of 673 K. Individual samples were cooled in air between repetitive pressings to a total true plastic strain of ~ 4. The microstructure after ECA pressing contained a mixture of high angle and subgrain

boundaries with an average grain size of $\sim 1.2\,\mu m$. Further details of the characteristics of this alloy after ECA pressing are also given elsewhere (Furukawa *et al.* 1997).

Specimens were cut from the ECA pressed samples with dimensions of $2.5 \times 2.5 \times 3.9$ mm^3 for the Al–Mg alloy and $3.0 \times 3.0 \times 4.7$ mm^3 for the Al–Mg–Li–Zr alloy and they were tested in compression in air at room temperature using an initial strain rate of $\sim 4 \times 10^{-4}$ s^{-1} in a testing machine operating at a constant rate of cross-head displacement. The 0.2% proof stress was measured for each sample as the 0.2% offset from the elastic portion of the stress–strain curve. Prior to testing, some samples of each alloy were annealed in an argon atmosphere for 1 h at various temperatures, quenched in iced water, and the Vickers microhardness, H_V (in kg mm^{-2}), was measured using a microhardness tester with a diamond pyramidal indenter under a load of 50 g applied for 15 s: the hardness datum points documented in this report represent the average of seven separate measurements at randomly selected points. Average grain sizes were measured after annealing treatments using either transmission electron microscopy (TEM) or optical microscopy; samples were prepared for inspection by TEM using a standard procedure for Al-based alloys (Furukawa *et al.* 1996b)

§3. Experimental results

The variation of grain size with annealing temperature is shown for each alloy in figure 1. It is apparent that both alloys exhibit an ultrafine grain size immediately after ECA pressing, with values of $\sim 0.2\,\mu m$ and $\sim 1\,\mu m$ for Al–3%Mg and the Al–Mg–Li–Zr alloy respectively. However, the Al–3%Mg solid solution alloy exhibits rapid grain growth at temperatures above ~ 500 K but the commercial Al–Mg–Li–Zr alloy has a relatively stable grain size up to temperatures of ~ 750 K because of the presence of Al_3Zr precipitates (Furukawa *et al.* 1997).

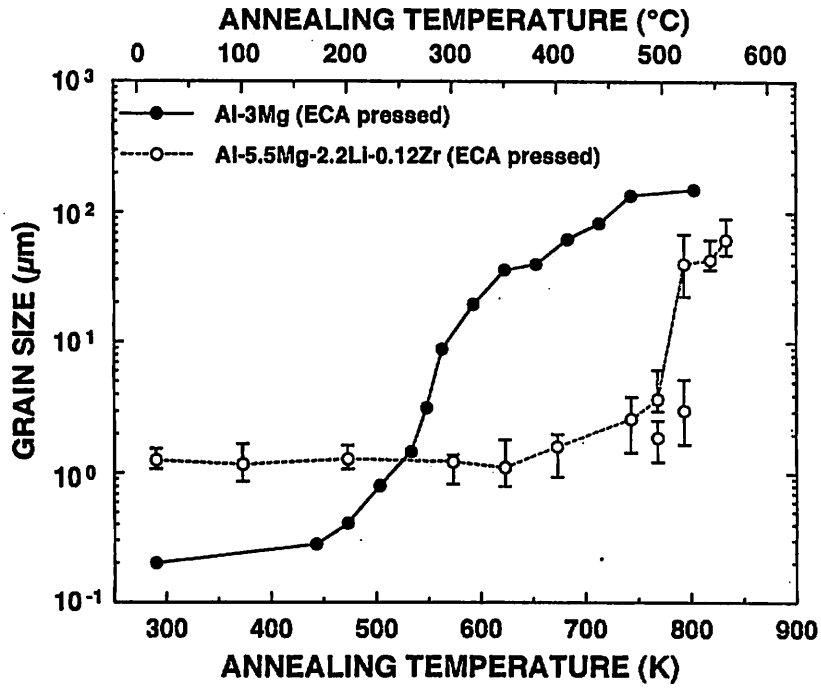

Figure 1. Grain size versus annealing temperature for Al–3%Mg and the Al–Mg–Li–Zr alloy prepared by ECA pressing.

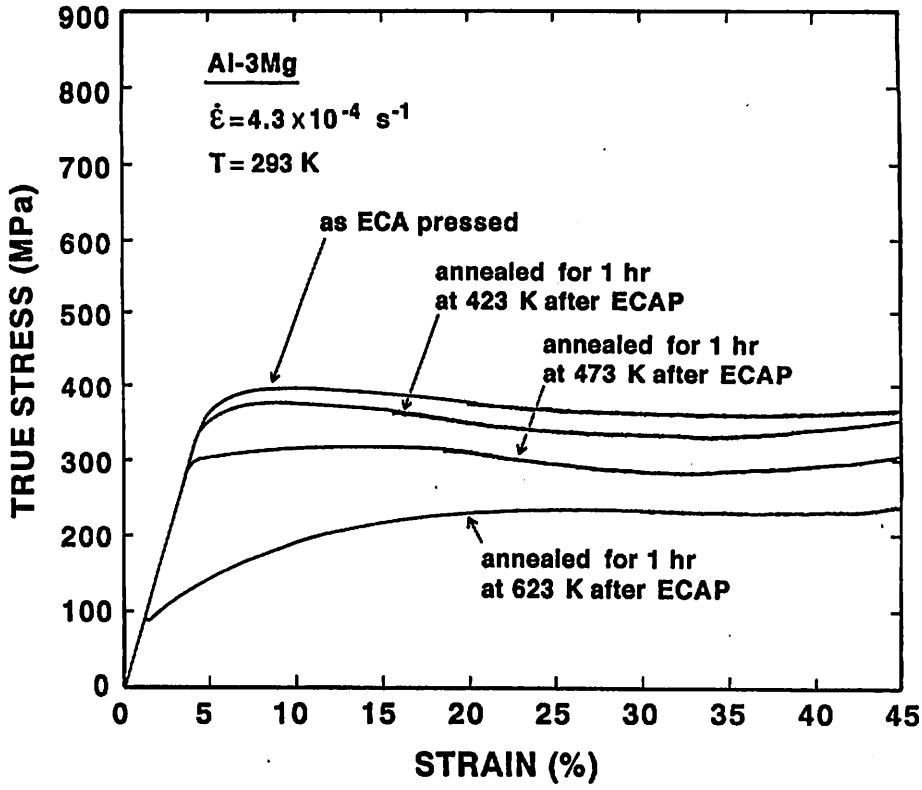

(*a*)

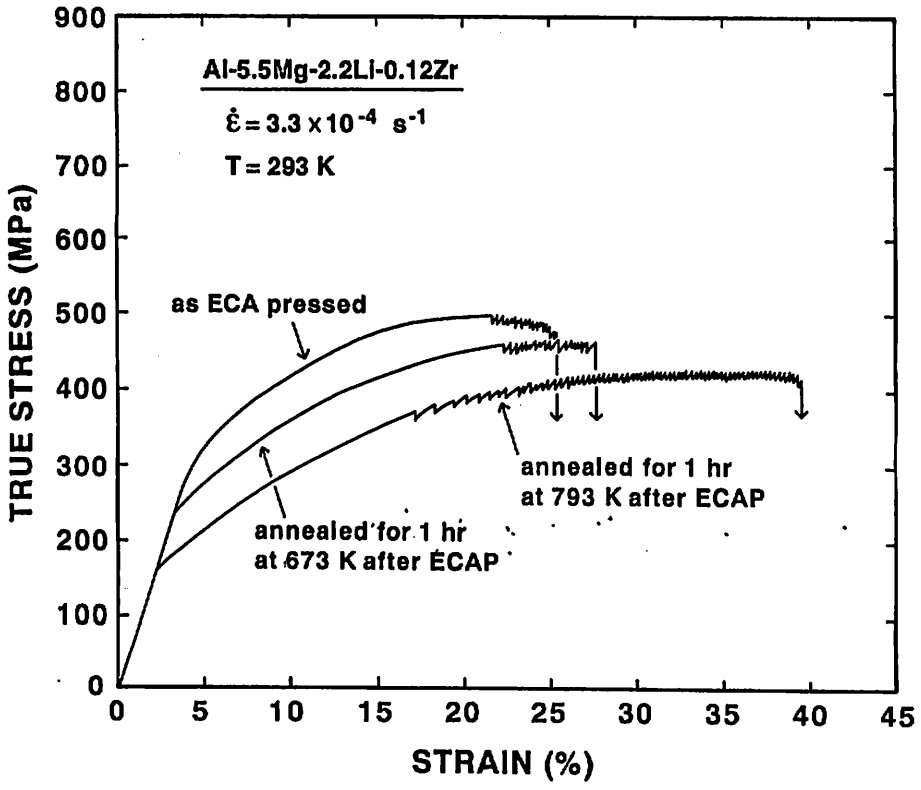

(*b*)

Figure 2. True stress versus strain for (*a*) Al–3%Mg and (*b*) the Al–Mg–Li–Zr alloy tested in compression at room temperature.

Figure 2 shows representative plots of true stress versus strain for samples of (*a*) Al–3%Mg and (*b*) the Al–Mg–Li–Zr alloy. Inspection shows that, although all tests were conducted at room temperature using similar initial strain rates in the vicinity of $\sim 4 \times 10^{-4}$ s^{-1}, the shapes of the two curves in the ECA pressed condition are very different: the Al–3%Mg alloy exhibits a stress–strain curve with little strain hardening which is similar in appearance to the earlier reports on pure Cu by Gertsman *et al.* (1996) and Valiev *et al.* (1994) but the Al–Mg–Li–Zr alloy exhibits very extensive strain hardening after yielding.

Three additional curves are also recorded in figure 2(*a*) for specimens subjected to ECA pressing and then annealing for 1 h at temperatures of 423, 473 and 623 K corresponding to grain sizes, from figure 1, of ~ 0.2, ~ 0.4 and $\sim 36\,\mu$m respectively. Annealing at 423 K gives no measurable change in the grain size and the stress–strain curve again exhibits no significant strain hardening although the yield stress is slightly reduced, and annealing at 473 K increases the grain size by a factor of about two and this leads both to a decrease in the yield stress and to the introduction of some very limited strain hardening. By contrast, annealing at 623 K to give a grain size of $\sim 36\,\mu$m leads to a very low yield stress and extensive strain hardening after yielding. It is important to note that all samples of the Al–3%Mg alloy were taken to a total strain of $\sim 55\%$ without failure and all curves exhibited small but fairly regular serrations at strains above $\sim 15\%$. For the Al–Mg–Li–Zr alloy in figure 2(*b*), two additional stress–strain curves are shown for specimens annealed for 1 h at 673 and 793 K giving grain sizes of ~ 1.6 and $\sim 40\,\mu$m respectively. Both of these additional curves exhibit extensive strain hardening and, as indicated in figure 2(*b*), there were prominent serrations at strains above $\sim 20\%$. In addition, the total ductilities recorded for these samples were limited and in the range of ~ 25–40%.

The variations with annealing temperature of (*a*) the Vickers microhardness and (*b*) the 0.2% proof stress are shown in figure 3 for the Al–3%Mg and the Al–Mg–Li–Zr alloys. It is apparent from figure 3(*a*) that the microhardness of the Al–Mg–Li–Zr alloy is lower than that of the Al–3%Mg alloy for annealing temperatures up to ~ 430 K but thereafter the Al–3%Mg alloy has a lower hardness. This result is a direct consequence of the grain growth data shown in figure 1 and thus to the failure to maintain a very small grain size in the Al–3%Mg alloy in the absence of any precipitates. Inspection of figure 3(*b*) shows that the variation of the 0.2% proof stress with annealing temperature exhibits a similar trend.

The Hall–Petch equation relates the yield stress of a polycrystalline material, σ_y, to the grain size, d, through an expression of the form (Hall 1951, Petch 1953)

$$\sigma_y = \sigma_0 + k_y d^{-1/2} \tag{1}$$

where σ_0 is termed the friction stress and k_y is a constant of yielding having a value which can be derived explicitly for models involving the propagation of slip across a grain and the pile up of intragranular dislocations at the opposing grain boundary (Pande *et al.* 1993, Furukawa *et al.* 1996a, Nazarov 1996) but which may also incorporate an effect due to solid solution strengthening (Winterhoff and Nembach 1996). Equation (1) is well established for materials with large grain sizes and it may be extended to incorporate measurements of the hardness of a material, H_V, by noting that, in the absence of appreciable strain hardening, the

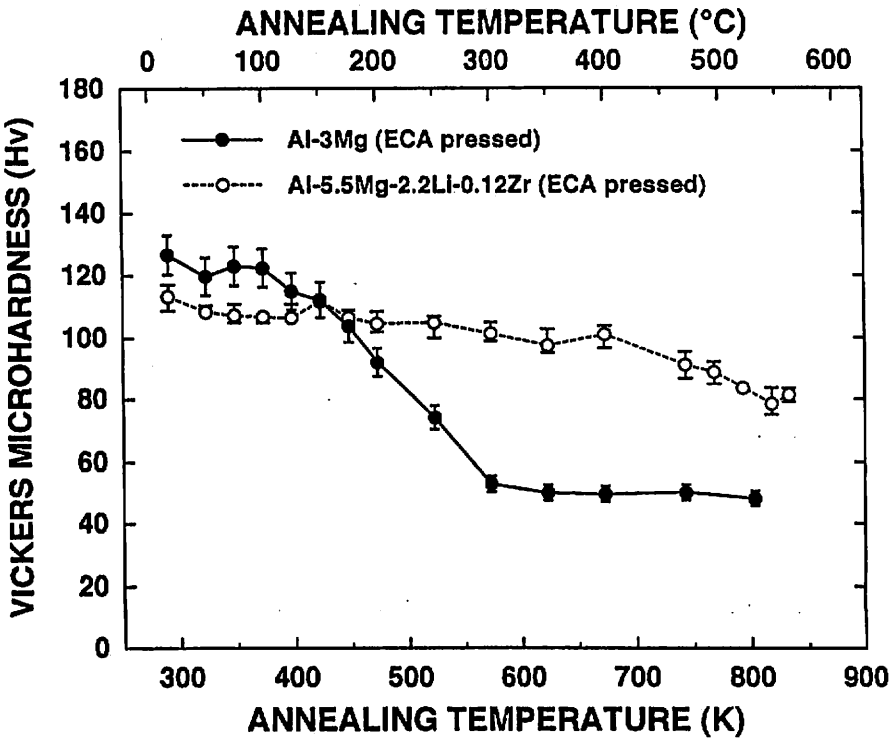

(*a*)

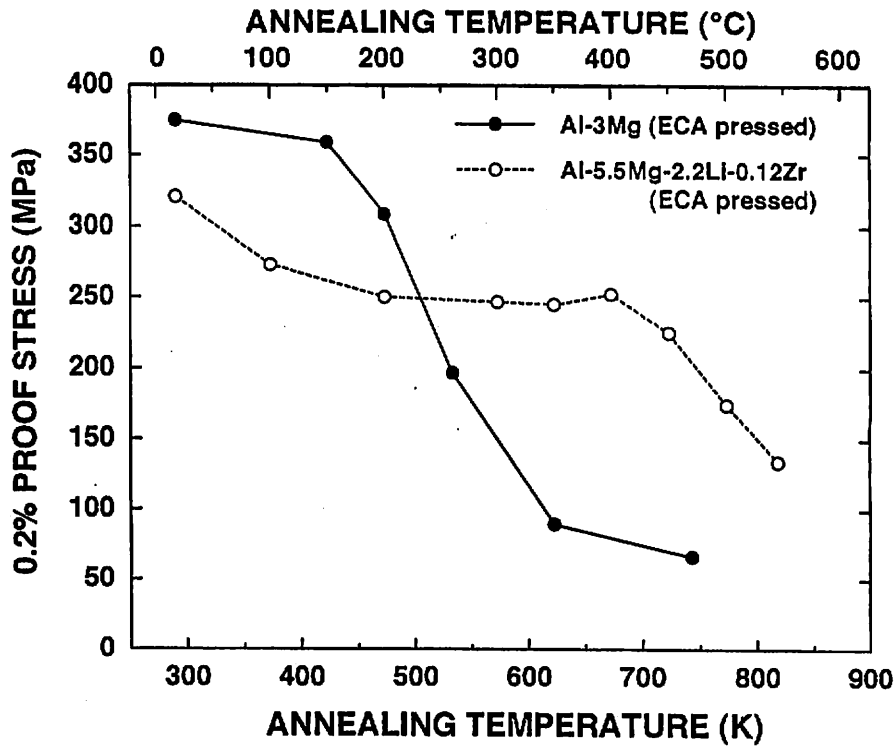

(*b*)

Figure 3. Variation of (*a*) the Vickers microhardness and (*b*) the 0.2% proof stress with annealing temperature for Al–3%Mg and the Al–Mg–Li–Zr alloy.

hardness measured with a pyramidal indenter is related to the yield stress through the expression (Ashby and Jones 1980)

$$H_V = k'\sigma_y \tag{2}$$

where k' is a constant having a value of approximately three.

Equation (1) is therefore reformulated in terms of hardness through the relationship

$$H_V = H_0 + k_H d^{-1/2} \tag{3}$$

where H_0 and k_H are the appropriate constants associated with the hardness measurements.

The validity of equations (1) and (3) may be examined by plotting the microhardness and the 0.2% proof stress as a function of $d^{-1/2}$ and these plots are given in figures 4 (*a*) and (*b*). Inspection shows that there is generally good agreement between the experimental data and the predictions of equations (1) and (3) for these two materials. However, it should be noted that the experimental data in figures 4(*a*) and (*b*) exclude points for the Al–Mg–Li–Zr alloy at the very smallest grain sizes where the Hall–Petch relationship breaks down because of variations in the volume fractions of the Al_3Li precipitates between different specimens (Furukawa *et al.* 1997).

§4. Discussion

There is a clear dichotomy in the results obtained in these experiments. On the one hand, the stress–strain curve for the Al–3%Mg alloy after ECA pressing is generally similar to the curve reported earlier for pure Cu (Valiev *et al.* 1994, Gertsman *et al.* 1996) including a long region with no strain hardening in the as-pressed condition (figure 2(*a*)); on the other hand, the stress–strain curve for the Al–Mg–Li–Zr alloy after pressing exhibits extensive strain hardening (figure 2 (*b*)). Furthermore, the yield stress of the Al–3%Mg alloy is very high after pressing, similar to the results reported for pure Cu (Gertsman *et al.* 1996), but ECA pressing fails to produce a correspondingly high yield stress in the Al–Mg–Li–Zr alloy. In order to understand the differences in behaviour between these two alloys, it is necessary to consider the characteristics of the microstructures introduced by ECA pressing.

Two factors may serve to influence the stress–strain behaviour observed in ultrafine-grained materials: (i) the grain size of the material and (ii) the precise structural features associated with the grain boundaries. In the earlier experiments on Cu by Gertsman *et al.* (1996), it was shown that a very rapid anneal for 3 min at 473 K after completion of the ECA pressing gave a significant decrease in the yield stress and subsequent strain hardening after yielding although the annealing time was so short that it served only to reduce the internal stresses in the sample with no corresponding change in the measurable grain size. From this observation, it may be concluded that the microstructural features of the ultrafine-grained materials are of primary importance in determining the shapes of the subsequent stress–strain curves.

High-resolution electron microscopy (HREM) was used earlier to examine samples of Al–Mg alloys where a grain size of ~ 0.1 μm was produced by intense plastic straining at room temperature using a torsion straining technique (Horita *et al.* 1996). These observations showed that the microstructure consisted of an array of high-energy grain boundaries which were in a non-equilibrium configuration with a

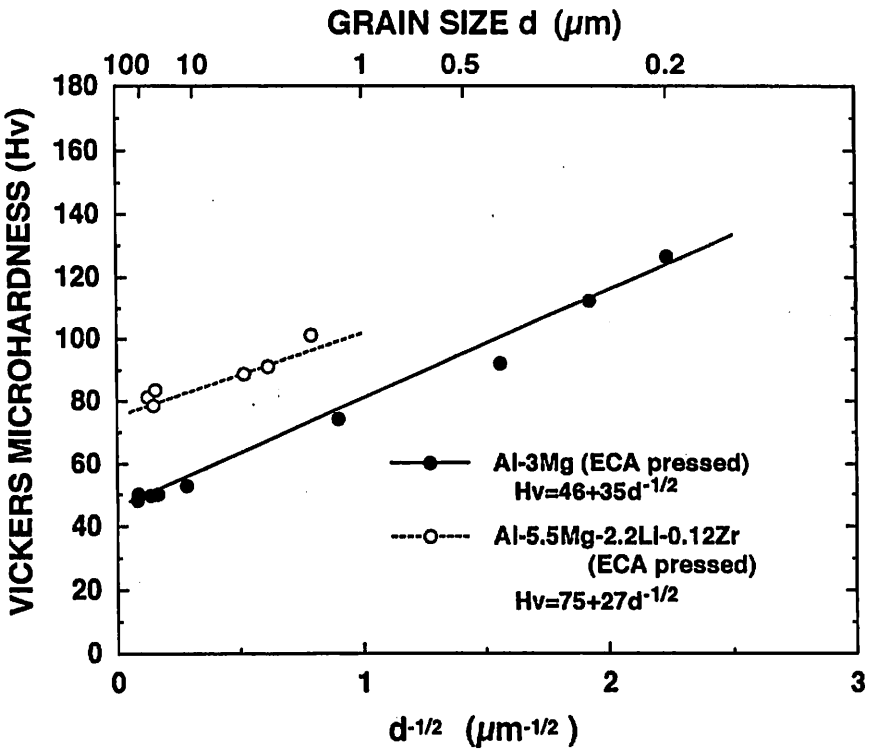

(*a*)

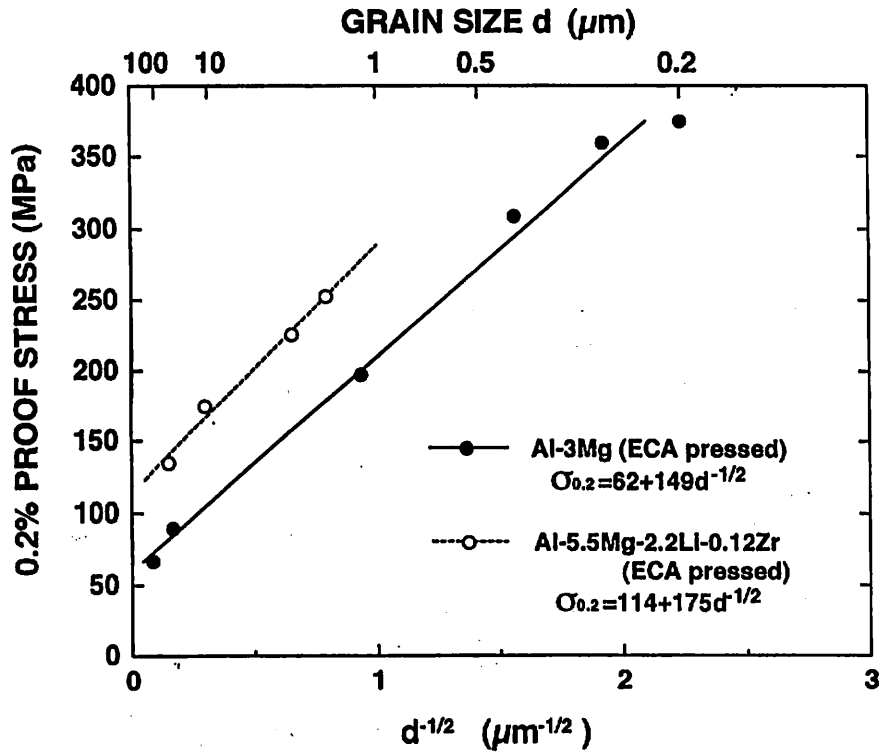

(*b*)

Figure 4. Variation of (*a*) the Vickers microhardness and (*b*) the 0.2% proof stress with $d^{-1/2}$ for Al–3%Mg and the Al–Mg–Li–Zr alloy.

high density of extrinsic dislocations. Similar boundary configurations were observed also in samples of pure Cu subjected to torsion straining at room temperature to give a grain size of $\sim 0.2\,\mu m$ (Horita *et al.* 1998). It is reasonable to assume that the grain boundary structures observed in these materials are similar to those present in the Al–3%Mg alloy in this investigation and in the samples of pure Cu investigated earlier by Gertsman *et al.* (1996) and Valiev *et al.* (1994). Thus, all of these materials exhibit stress–strain curves with little or no strain hardening after an initial rapid straining within a strain increment of $\sim 5\%$.

Valiev *et al.* (1994) interpreted the results on pure Cu in terms of a model in which yielding occurred through a dislocation bow-out mechanism (Lian *et al.* 1993) and the subsequent extensive region without strain hardening was attributed to the occurrence of an approximate balance between the processes of strain hardening and recovery, where the recovery processes include dislocation absorption within the boundaries, boundary sliding due to the movement of extrinsic dislocations along the boundaries† and boundary migration. The same interpretation can be used to explain the stress–strain curves observed in the present experiments for the Al–3%Mg alloy with an ultrafine grain size.

An additional significant observation, obtained from the investigation using HREM, was that the facets observed in the non-equilibrium grain boundaries of the Al–Mg alloys were more ordered and uniformly distributed than in ultrafine-grained samples of Cu or Ni, where all materials were prepared by torsion straining at room temperature (Horita *et al.* 1998). The important factor distinguishing these three materials was that the fabrication was conducted at equivalent homologous temperatures of $\sim 0.32\ T_m$, $\sim 0.22\ T_m$ and $\sim 0.17\ T_m$ for the Al–Mg alloys, Cu and Ni respectively. It was therefore concluded that some relaxation of the grain boundary structure may occur when intense plastic straining is conducted at a sufficiently high homologous temperature, and this conclusion is further supported by observations on an ultrafine-grained Zn–22%Al alloy where the high internal stresses were able to relax because of the low melting temperature of the material (Furukawa *et al.* 1996c).

In the present experiments, ECA pressing was performed at room temperature for the Al–3%Mg alloy and at 673 K for the Al–Mg–Li–Zr alloy and this corresponds to homologous temperatures of $\sim 0.32\ T_m$ and $\sim 0.72\ T_m$ respectively. Since the ultrafine-grained Al–Mg–Li–Zr alloy was prepared at a high homologous temperature, it is anticipated there will be a consequent relaxation of the internal stresses leading to a microstructure where the grain boundaries are closer to an equilibrium configuration. Under these conditions, structural recovery through a process such as dislocation absorption becomes less important so that strain hardening is able to

† When grain boundary sliding occurs in polycrystalline materials under creep conditions at elevated temperatures, the sliding requires an associated accommodation process such that the activation energy for sliding depends upon the nature of the accommodation and it is equal to the activation energies for either lattice or grain boundary diffusion (Langdon 1994, 1996). As a result, normal grain boundary sliding is a diffusion-controlled high-temperature creep process which cannot occur at temperatures very much below $\sim 0.45\ T_m$, where T_m is the absolute melting temperature of the material (Gifkins and Langdon 1964–65). It appears that these well established trends may not be followed in ultrafine-grained materials because there is evidence for exceptionally low experimental values for the activation energy for grain boundary diffusion (Dickenscheid *et al.* 1991, Valiev *et al.* 1994) due, it is reasonable to assume, to the presence of a very high density of extrinsic grain boundary dislocations which serve to enhance the grain boundary diffusivity.

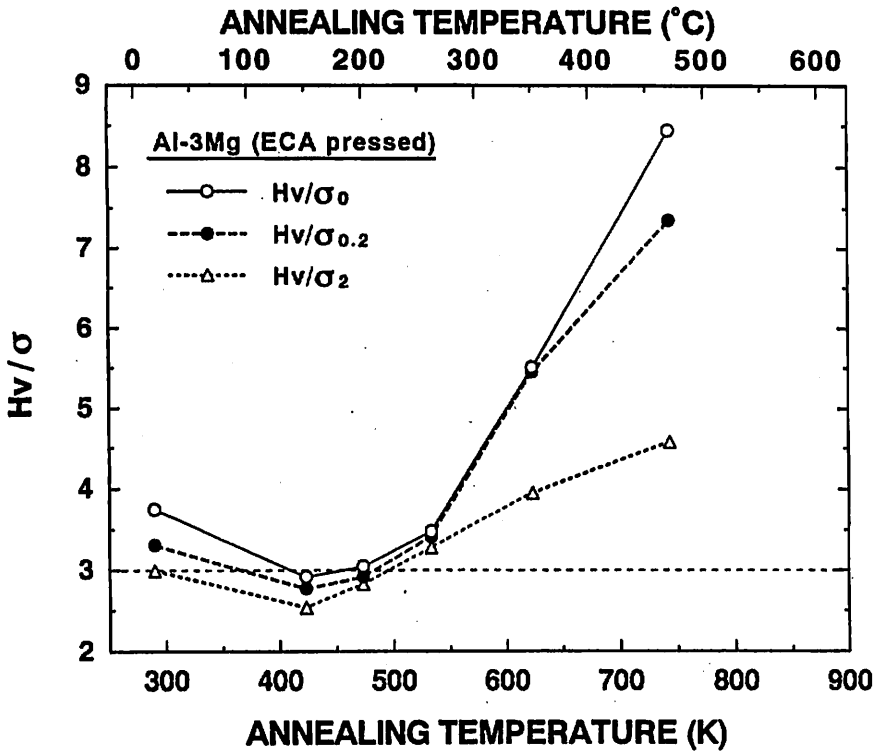

(*a*)

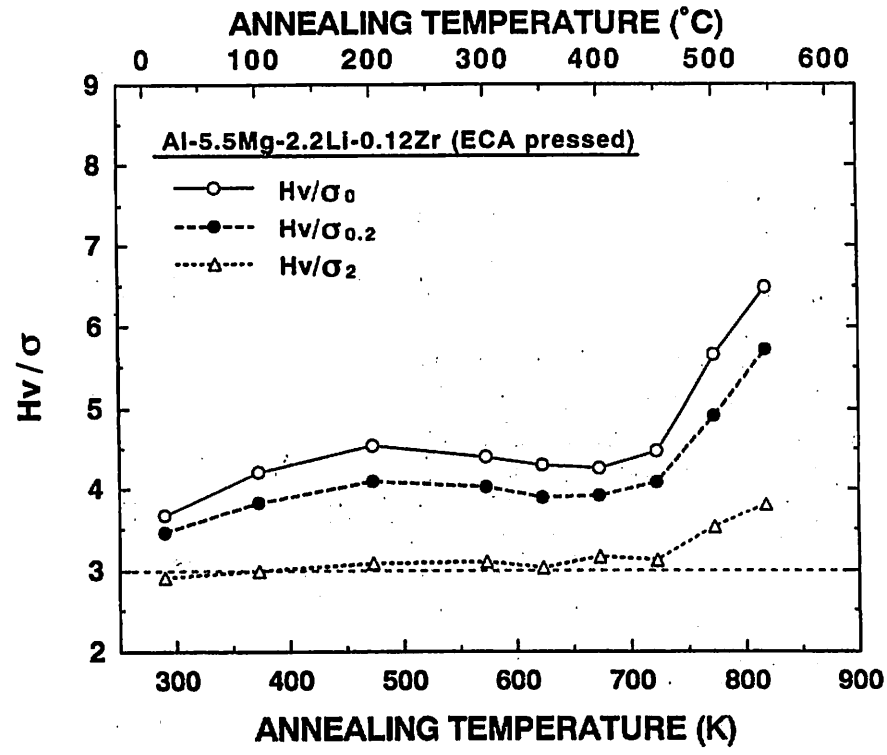

(*b*)

Figure 5. The ratios H_V/σ_0, $H_V/\sigma_{0.2}$ and H_V/σ_2 versus annealing temperature for Al–3%Mg and the Al–Mg–Li–Zr alloy, where σ_0, $\sigma_{0.2}$ and σ_2 are the yield stress, the 0.2% proof stress and the 2% proof stress respectively.

occur as in materials with larger grain sizes (figure 2 (*b*)). It may be concluded from these observations there will be an absence of strain hardening in the stress–strain curves of ultrafine-grained materials produced by ECA pressing provided the pressing is conducted at an homologous temperature which is sufficiently low that there is very little relaxation of the internal stresses during pressing. This conclusion is further confirmed by noting the close similarity in the shapes of the stress–strain curves in figure 2 (*b*) for the Al–Mg–Li–Zr alloy having grain sizes in the range ~ 1.2 to $\sim 42\,\mu m$.

These observations suggest that the mechanical properties of ultrafine-grained materials produced by ECA pressing, including the yield stress and the strain hardening rate, may show significant variations between specimens of the same material even when the measured grain size is identical. These differences will be a direct consequence of variations in the magnitudes of the internal stresses in the samples arising from changes in the characteristics of the grain boundaries reflecting different processing or annealing procedures.

Numerous experiments have attempted to determine the mechanical properties of materials with ultrafine grain sizes from measurements of the microhardness. In the present experiments, it is first necessary to note that, as shown in figures 4 (*a*) and (*b*), both the Vickers microhardness, H_V, and the 0.2% proof stress, $\sigma_{0.2}$, scale with the reciprocal of the square root of the grain size, $d^{-1/2}$, through equations (1) and (3). Gertsman *et al.* (1996) reported a value for the ratio $H_V/\sigma_{0.1} > 3$ in experiments on ultrafine-grained Cu, with the ratio increasing to ~ 5 at the higher annealing temperatures. To check the validity of equation (2) in the present experiments, figure 5 shows plots of H_V/σ_0, $H_V/\sigma_{0.2}$ and H_V/σ_2 versus the annealing temperature for (*a*) Al–3%Mg and (*b*) the Al–Mg–Li–Zr alloy, where σ_0 is the yield stress and σ_2 is the 2% proof stress.

Inspection of figure 5 (*a*) shows that the ratio H_V/σ in the Al–3%Mg alloy is reasonably close to three up to temperatures of $\sim 550\,K$, corresponding to a grain size of $\sim 5\,\mu m$, but at higher temperatures, where strain hardening becomes significant, the ratio at yielding increases to ~ 8.5. In the Al–Mg–Li–Zr alloy curve shown in figure 5 (*b*), the ratio at yielding is greater than three and in the range of about four to five up to an annealing temperature of $\sim 750\,K$. At higher temperatures, in the presence of grain growth and strain hardening, the ratio increases to ~ 6.5. These trends are consistent with the conclusion of Gertsman *et al.* (1996) that measurements of H_V may significantly overestimate the magnitude of the yield stress and they also support the analytical treatment by Yost (1983). In addition, they follow on from the analysis of Tabor (1951) showing that full plasticity is needed, and a strain typically of the order of $\sim 8\%$ is required, in order to achieve a value of $k' = 3$ in equation (2).

§5. Summary and conclusions

(1) Ultrafine grain sizes of ~ 0.2 and $\sim 1.2\,\mu m$ were introduced into an Al–3%Mg solid solution alloy and a commercial Al–Mg–Li–Zr alloy through the process of ECA pressing conducted at room temperature and at 673 K respectively. Annealing of the samples at elevated temperatures promoted grain growth, thereby permitting an investigation of the influence of grain size on the mechanical properties.

(2) When tested in compression at room temperature, the Al–3%Mg alloy exhibited a high yield stress and little subsequent strain hardening whereas

the Al–Mg–Li–Zr alloy exhibited a lower yield stress and extensive strain hardening. The Vickers microhardness, H_V, and the 0.2% proof stress, $\sigma_{0.2}$, were consistent with the Hall–Petch relationship in both alloys, but the ratio $H_V/\sigma_{0.2}$ was greater than three except only for the Al–3%Mg alloy up to annealing temperatures of ~ 550 K, corresponding to a grain size of $\sim 5\,\mu$m.

(3) The experimental results demonstrate that the flow and hardness of ultra-fine-grained materials depend not only upon the grain size but also upon the characteristics of the grain boundaries introduced during processing. ECA pressing of the Al–3%Mg alloy at room temperature leads to arrays of non-equilibrium grain boundaries with high densities of extrinsic dislocations whereas pressing of the Al–Mg–Li–Zr alloy at a temperature of 673 K permits some relaxation of the internal stresses and the consequent development of a more equilibrated microstructure.

Acknowledgements

We are grateful to Dr Nikolai K. Tsenev for experimental assistance in fabricating the materials by ECA pressing. This work was supported by the Light Metals Educational Foundation of Japan, by a Grant-in-Aid for Scientific Research from the Ministry of Education, Science, Sports and Culture of Japan, and by the National Science Foundation of the United States under Grants No. DMR-9625969 and INT-9602919.

References

Ashby, M. F., and Jones, D. R. H., 1980, *Engineering Materials* Volume 1 (Oxford: Pergamon), p. 105.

Dickenscheid, W., Birringer, R., Gleiter, H., Kanert, O., Michel, B., and Günther, B., 1991, *Solid State Comm.*, **79**, 683.

Fridlyander, I. N., Sandler, V. S., and Nikol'skaya, T. I., 1971, *Fiz. Metal. Metalloved.*, **32**, 767.

Furukawa, M., Horita, Z., Nemoto, M., and Langdon, T. G., 1996a, *Ann. Chim.*, **21**, 493.

Furukawa, M., Horita, Z., Nemoto, M., Valiev, R. Z., and Langdon, T. G., 1996b, *Acta Mater.*, **44**, 4619; 1996c, *J. Mater. Res.* **11**, 2128.

Furukawa, M., Iwahashi, Y., Horita, Z., Nemoto, M., Tsenev, N. K., Valiev, R. Z., and Langdon, T. G., 1997, *Acta Mater.* **45**, 4751.

Gertsman, V. Y., Hoffmann, M., Gleiter, H., and Birringer, R., 1994, *Acta Metall. Mater.* **42**, 3539.

Gertsman, V. Y., Valiev, R. Z., Akhmadeev, N. A., and Mishin, O. V., 1996, *Mater. Sci. Forum*, **225–227**, 739.

Gifkins, R. C., and Langdon, T. G., 1964–65, *J. Inst. Metals*, **93**, 347.

Hall, E. O., 1951, *Proc. Roy. Soc.* B, **64**, 747.

Horita, Z., Smith, D. J., Furukawa, M., Nemoto, M., Valiev, R. Z., and Langdon, T. G., 1996, *J. Mater. Res.* **11**, 1880.

Horita, Z., Smith, D. J., Nemoto, M., Valiev, R .Z., and Langdon, T. G., 1998, *J. Mater. Res.* **13**, 446.

Iwahashi, Y., Wang, J., Horita, Z., Nemoto, M., and Langdon, T. G., 1996, *Scripta Mater.*, **35**, 143.

Langdon, T. G., 1994, *Acta Metall. Mater.*, **42**, 2437; 1996, *Structural Materials: Engineering Applications through Scientific Insight*, edited by E. D. Hondros, and M. McLean (London: Institute of Metals), p. 135.

Lian, J., and Baudelet, B., 1993, *Nanostruct. Mater.*, **2**, 415.

Lian, J., Baudelet, B., and Nazarov, A. A., 1993, *Mater. Sci. Engng.* A, **172**, 23.

Ma, Y., Horita, Z., Furukawa, M., Nemoto, M., Valiev R. Z., and Langdon, T. G., 1995, *Mater. Lett.*, **23**, 283.

Nazarov, A. A., 1996, *Scripta Mater.*, **34**, 697.

NIEMAN, G. W., WEERTMAN, J. R., and SIEGEL, R. W., 1991, *J. Mater. Res.*, **6**, 1012.
PANDE, C. S., MASUMURA, R. A., and ARMSTRONG, R. W., 1993, *Nanostruct. Mater.*, **2**, 323.
PETCH, N. J., 1953, *J. Iron Steel Inst.*, **174**, 25.
PRANGNELL, P. B., HARRIS, C., and ROBERTS, S. M., 1997, *Scripta Mater.*, **37**, 983.
SANDERS, P. G., FOUGERE, G. E., THOMPSON, L. J., EASTMAN, J. A., and WEERTMAN, J. R., 1997, *Nanostruct. Mater.*, **8**, 243.
SEGAL, V. M., 1995, *Mater. Sci. Engng.* A, **197**, 157.
SEGAL, V. M., REZNIKOV, V. I., DROBYSHEVSKIY, A. E., and KOPYLOV, V. I., 1981, *Russian Metallurgy (Metally)*, **1**, 99.
SURYANARAYANA, C., MUKHOPADHYAY, D., PATANKAR, S. N., and FROES, F. H., 1992, *J. Mater. Res.*, **7**, 2114.
TABOR, D., 1951, *The Hardness of Metals* (Oxford: Clarendon Press), p. 69.
VALIEV, R. Z., KOZLOV, E. V., IVANOV, YU. F., LIAN, J., NAZAROV, A. A., and BAUDELET, B., 1994, *Acta Metall. Mater.*, **42**, 2467.
VALIEV, R. Z., KRASILNIKOV, N. A., and TSENEV, N. K., 1991, *Mater. Sci. Engng.* A, **137**, 35.
VALIEV, R. Z., and TSENEV, N. K., 1991, *Hot Deformation of Aluminum Alloys*, edited by T. G. Langdon, H. D. Merchant, J. G. Morris, and M. A. Zaidi (Warrendale, PA: The Minerals, Metals and Materials Society), p. 319.
WANG, J., FURUKAWA, M., HORITA, Z., NEMOTO, M., VALIEV, R. Z., and LANGDON, T. G., 1996a, *Mater. Sci. Engng.* A, **216**, 41.
WANG, J., HORITA, Z., FURUKAWA, M., NEMOTO, M., TSENEV, N. K., VALIEV, R. Z., MA, Y., and LANGDON, T. G., 1993, *J. Mater. Res.*, **8**, 2810.
WANG, J., IWAHASHI, Y., HORITA, Z., FURUKAWA, M., NEMOTO, M., VALIEV R. Z., and LANGDON, T. G., 1996b, *Acta Mater.*, **44**, 2973.
WINTERHOFF, J., and NEMBACH, E., 1996, *Scripta Mater.*, **35**, 999.
WU, Y., and BAKER, I., 1997, *Scripta Mater.*, **37**, 437.
YOST, F. G., 1983, *Metall. Trans.* A, **14**, 947.

Pergamon

Scripta Materialia, Vol. 38, No. 12, pp. 1851–1856, 1998
Elsevier Science Ltd

1359-6462/98 $19.00 + .00

PII S1359-6462(98)00099-2

HIGH STRAIN RATE SUPERPLASTICITY IN AN Al-Mg ALLOY CONTAINING SCANDIUM

Shogo Komura,[†] Patrick B. Berbon,[§] Minoru Furukawa[‡], Zenji Horita,[†] Minoru Nemoto[†] and Terence G. Langdon[§]

[†]Department of Materials Science and Engineering, Faculty of Engineering, Kyushu University, Fukuoka 812-81, Japan [§]Departments of Materials Science and Mechanical Engineering, University of Southern California, Los Angeles, CA 90089-1453, USA [‡]Department of Technology, Fukuoka University of Education, Munakata, Fukuoka 811-41, Japan

(Received February 5, 1998)
(Accepted February 22, 1998)

Introduction

Superplastic forming is a well-established industrial process for the fabrication of complex shapes in sheet metals [1]. In practice, however, the use of superplastic forming is generally limited to low volumes of components because the forming rates are typically $\sim 10^{-3}$–10^{-2} s^{-1}, corresponding to the strain rates associated with optimum superplastic ductility, and the total forming time for each component is consequently very long (up to ~30 minutes).

It has been suggested that it may be possible to achieve superplasticity at high strain rates in conventional materials by making a substantial reduction in the grain size [2]. This may be achieved by using a process such as equal-channel angular (ECA) pressing, where the sample is subjected to intense plastic straining in simple shear [3, 4], because it is well established that ECA pressing leads to significant grain refinement in large-grained polycrystalline materials down to the submicrometer or even the nanometer level [5, 6]. High strain rate superplasticity (HSR SP) has been widely documented in a range of metal matrix composites, mechanically alloyed materials and in alloys fabricated using powder metallurgy procedures [7, 8] and very recently there was a report of HSR SP in commercial cast Al-based alloys after ECA pressing [9].

Experiments were described earlier in which the effect of ECA pressing was evaluated using an Al-3% Mg alloy with an initial grain size of ~500 μm [10]. These experiments confirmed that it was possible to attain a grain size of ~0.2 μm in this alloy but the submicrometer grain size was not stable at elevated temperatures and subsequent annealing after ECA pressing gave rise to rapid grain growth at temperatures above ~500 K. As a result of this lack of thermal stability, the as-pressed material was not suitable for demonstrating the advent of HSR SP when testing at high temperatures.

The present investigation was initiated in order to evaluate the potential for achieving HSR SP in an Al-3% Mg alloy containing a scandium addition. Scandium was selected for use in this investigation because it is well established that dilute amounts of scandium in the Al-Mg system lead to a considerable enhancement in both the strength and the thermal stability of the material. For example,

it has been demonstrated that the presence of only 0.2% Sc in an Al-6.5% Mg alloy is sufficient to raise the recrystallization temperature by 150°C [11]. There are also reports of ductilities of up to >700% in an Al-6% Mg-0.3% Sc alloy [12] and >1000% in Al-4% Mg-0.5% Sc and Al-6% Mg-0.5% Sc alloys [13]. A comprehensive report of the effects of scandium in aluminum alloys was provided recently by Kramer *et al.* [14].

Experimental Material and Procedures

The experiments were performed using Al of 99.99% purity and Sc of 99.999% purity. Aluminum and scandium were arc melted in an argon atmosphere to form an Al-3% Sc alloy and this material was remelted with additional Al and 3% Mg to give an alloy having a composition, in weight per cent, of Al-3% Mg-0.2% Sc. The molten alloy was cast into a steel mold to form an ingot having dimensions of 17 × 55 × 120 mm^3 and the ingot was homogenized in air at 743 K for a period of one day. Following homogenization, each surface was ground to remove ~1 mm and the ingot was then cut into bars having dimensions of 15 × 15 × 120 mm^3. Each bar was swaged into a rod with a diameter of 10 mm and these rods were cut into lengths of ~60 mm. Each rod was annealed in air for 1 hour at 853 K to give an initial grain size of ~200 μm.

Details of the ECA pressing procedure have been given in earlier reports [10, 15]. In the present experiments, the ECA pressing die consisted of a solid block of high strength tool steel containing a single channel, circular in cross-section, which formed an L-shaped configuration. Two angles are generally used to define the characteristics of the ECA pressing [16] and in these experiments the angle subtended by the two channels, ϕ, was 90° and the angle defining the outer arc of curvature at the intersection of the two channels, ψ, was also 90°. These angles lead to a calculated strain of ~1 for a single passage through the die [16] and in practice, since the cross-section of the sample remains unchanged by pressing, repetitive pressings were used to reach high strains. Each rod was subjected to ECA pressing in air at room temperature using a molybdenum disulfide lubricant and a pressing speed of ~19 mm s^{-1}. The rods were pressed through the die for a total of 8 passes to give a total strain of ~8. It has been shown that a rotation of the sample between consecutive pressings changes the shear planes and shear directions and this affects the nature of the as-pressed microstructure [15, 17–19]. In the present experiments, each sample was rotated by 90° in the same direction between repetitive pressings: earlier experiments on pure Al showed that this was the optimum procedure for most rapidly achieving a homogeneous equiaxed microstructure consisting of grains separated by high angle grain boundaries [19].

Following ECA pressing, some rods were sliced perpendicular to the longitudinal axis to give small discs with thicknesses of ~0.4 mm. These discs were used to evaluate the thermal stability of the microstructure at elevated temperatures by annealing for 1 hour in an argon atmosphere within a pyrex glass tube at selected temperatures up to a maximum of 773 K. Some rods were machined into tensile samples with the gauge lengths lying parallel to the longitudinal axes of the rods and with cross-sectional areas and gauge lengths of 1 × 3 mm^2 and 4 mm, respectively. These specimens were pulled to failure in air using an Instron testing machine operating at a constant rate of cross-head displacement with initial strain rates from 3.3 × 10^{-4} to 3.3 × 10^{-2} s^{-1} and at temperatures up to 723 K with the temperature controlled to ±2 K during each test.

Specimens were prepared for examination by transmission electron microscopy using the procedure described earlier [10] and they were examined in an Hitachi H-8100 transmission electron microscope operating at 200 kV.

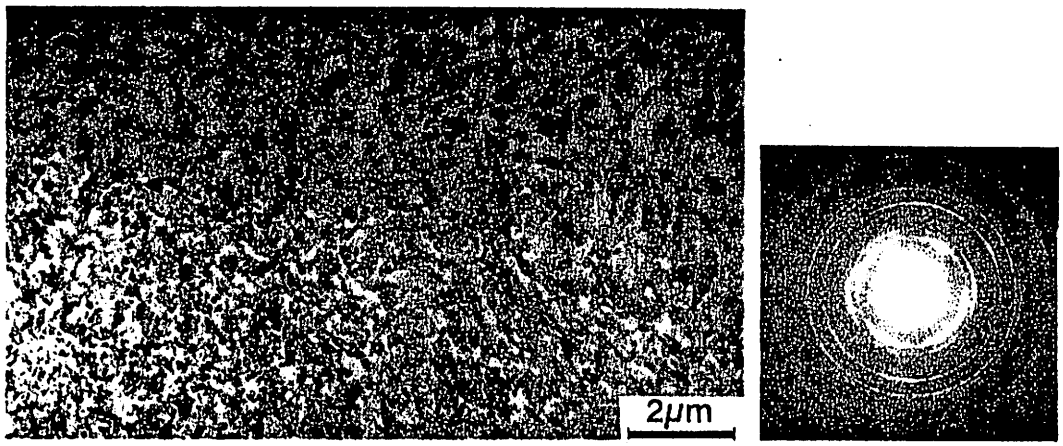

Figure 1. Representative microstructure in the Al-Mg-Sc alloy after ECA pressing.

Experimental Results and Discussion

Figure 1 shows an example of the microstructure in the Al-Mg-Sc alloy after ECA pressing through a total of 8 passes together with a selected area electron diffraction pattern taken from a region with a diameter of 12.3 μm. The microstructure in this condition consisted of an array of grains with an average size of ~0.2 μm and it is apparent from the SAED pattern shown in Fig. 1 that the grain boundaries have high angles of misorientation. In practice, very careful examination of a large number of areas in different specimens revealed that the microstructure was heterogeneous and consisted both of regions of high angle grain boundaries, as in Fig. 1, and some regions of subgrains separated by low angle boundaries. This lack of structural homogeneity contrasts with earlier reports on the Al-3% Mg solid solution alloy where the microstructure was homogeneous after 8 pressings through the die but it is similar to observations on a commercial Al-Mg-Li-Zr alloy where there was a microstructural heterogeneity after pressing at a temperature of 673 K to a strain of ~3.7 [20]. Detailed observations after ECA pressing suggested that the volume fractions of the material containing grains having primarily high angle boundaries and primarily low angle boundaries were of the order of ~90% and ~10%, respectively, and therefore the array of high angle boundaries shown in Fig. 1 is representative of the dominant structure. It should be noted also that the average grain size of ~0.2 μm observed in the Al-Mg-Sc alloy in these experiments is identical to the as-pressed grain size reported earlier for the Al-3% Mg alloy without the scandium addition [10].

It was found by static annealing that the ultrafine microstructure in the Al-Mg-Sc alloy was remarkably stable. Figures 2 (a) and (b) show the microstructures after annealing at temperatures of 573 and 673 K, respectively. For both of these temperatures, there is only minor grain growth and the average grain size remains at <1 μm. This result contrasts with the Al-3% Mg alloy without a scandium addition where the measured grain size in the ECA-pressed material was >20 μm after an anneal for 1 hour at 673 K [10]. Careful inspection of the boundary configurations in a number of samples indicated that the grain boundaries became better defined with increasing annealing temperature, thereby suggesting that the boundaries are in a non-equilibrium configuration after ECA pressing [21, 22] and they evolve gradually with increasing temperature into a more equilibrated structure.

The stability of the ultrafine grains at high temperatures is attributed to the presence of a dispersion of very fine coherent Al_3Sc precipitates which are known to be stable up to temperatures close to the melting point of the material [11, 23]. This grain stability therefore provides an opportunity to test whether the Al-Mg-Sc alloy is capable of exhibiting HSR SP.

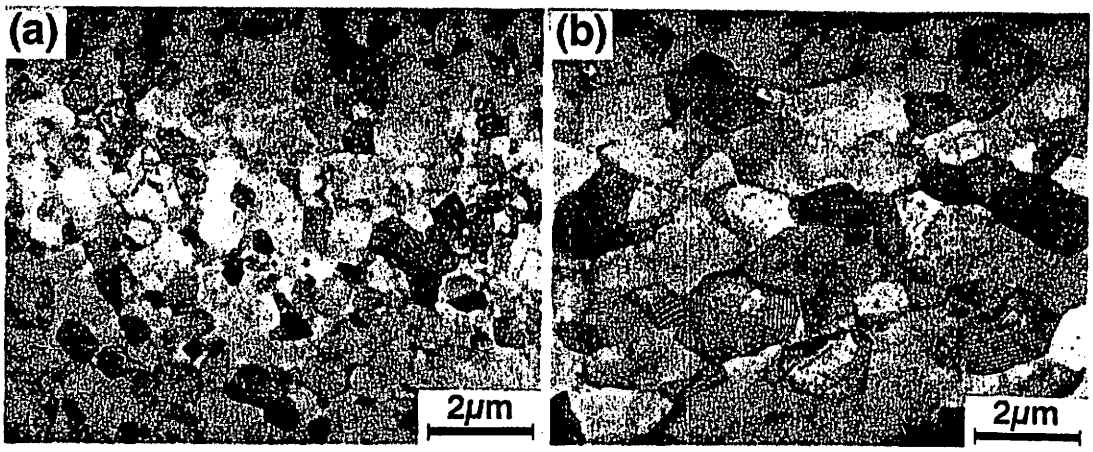

Figure 2. Microstructures after statically annealing for 1 hour at (a) 573 K and (b) 673 K.

Figure 3 plots the elongation to failure versus strain rate for samples of the Al-3% Mg-0.2% Sc alloy tested at temperatures of 573 and 673 K. Also included in Fig. 3 are experimental points reported earlier by Sawtell and Jensen [13] for an Al-4% Mg-0.5% Sc alloy tested at temperatures of 589, 672 and 811 K, respectively, where the tests denoted with the vertical arrows were discontinued without failure at elongations of 1020%. Inspection of Fig. 3 leads to two important conclusions. First, HSR SP was achieved in the present experiments with a measured elongation to failure of 1030% when testing at 673 K with an initial strain rate of 3.3×10^{-2} s^{-1}. Second, the overall ductilities achieved in the present experiments are slightly higher, for similar strain rates and comparable testing temperatures, than in the report by Sawtell and Jensen [13]. Nevertheless, it is apparent that HSR SP was achieved in this earlier work also with an elongation of 1020% without failure at 672 K using an initial strain rate of 1×10^{-2} s^{-1} [13].

It is important to emphasize that the present results demonstrate not only the possibility of achieving HSR SP in an Al-3% Mg alloy by introducing a dilute scandium addition but they show also that a large ductility may be achieved, with an elongation to failure of >1000% at a strain rate faster than 10^{-2} s^{-1},

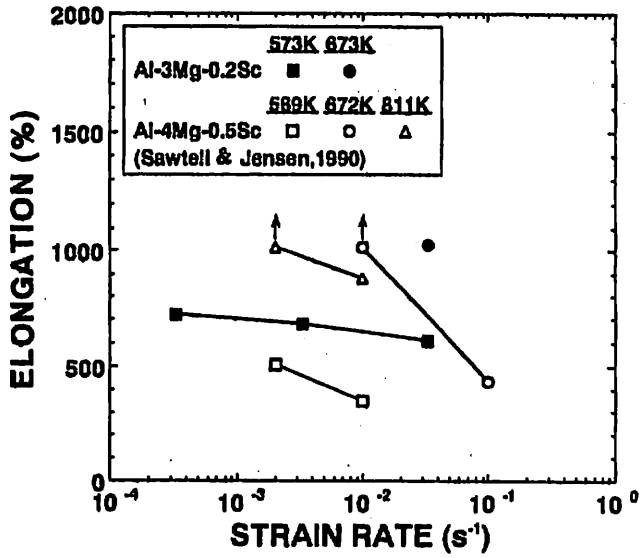

Figure 3. Elongation versus strain rate for the Al-3% Mg-0.2% Sc alloy and for an Al-4% Mg-0.5% Sc alloy reported by Sawtell and Jensen [13].

solely by processing the material at room temperature. Thus, the ECA pressing for grain refinement was performed at ambient temperature and there was no external heating of the sample either during the ECA pressing or between the consecutive pressings needed to achieve a high total strain. These results contrast markedly with conventional grain refinement procedures where thermo-mechanical treatments are generally employed to attain the requisite microstructures. For example, in the experiments of Sawtell and Jensen [13], where the maximum reported elongation was >1000%, the Al-Mg-Sc samples were subjected to a complex sequence of ageing and annealing treatments. Similarly, in the experiments of Nieh *et al.* [12] on an Al-6% Mg-0.3% Sc alloy, where the elongations were up to >700%, the alloy was prepared through a procedure of cold rolling and intermediate annealings. Furthermore, the HSR SP reported recently in cast Al-Mg-Li-Zr and Al-Cu-Zr alloys was achieved after subjecting the materials to ECA pressing at temperatures up to 673 K [9]. By contrast, the present investigation demonstrates conclusively that it is possible to achieve HSR SP in cast aluminum alloys by ECA pressing without the use of any concurrent or intermediate heating.

Summary and Conclusions

1. A cast alloy of Al-3% Mg-0.2% Sc was subjected to equal-channel angular pressing at room temperature to a total strain of ~8. Following ECA pressing, the microstructure was heterogeneous with small areas of subgrains interspersed within larger areas of grains having boundaries with high angles of misorientation. The average grain size was ~0.2 μm.
2. Static annealing revealed that the microstructure was thermally stable because of the presence of the dilute scandium addition. The grain size remained at <1 μm after annealing for 1 hour at temperatures up to 673 K.
3. The alloy exhibited high strain rate superplasticity with an elongation of 1030% when tested in tension at 673 K using an initial strain rate of 3.3×10^{-2} s^{-1}.

Acknowledgments

We thank Atsushi Utsunomiya for experimental assistance. This work was supported in part by the Light Metals Educational Foundation of Japan, in part by a Grant-in-Aid for Scientific Research from the Ministry of Education, Science, Sports and Culture of Japan, in part by the Japan Society for the Promotion of Science and in part by the National Science Foundation of the United States under Grants No. DMR-9625969 and INT-9602919.

References

1. A. J. Barnes, Mater. Sci. Forum. 170–172, 701 (1994).
2. Y. Ma, M. Furukawa, Z. Horita, M. Nemoto, R. Z. Valiev, and T. G. Langdon, Mater. Trans. JIM. 37, 336 (1996).
3. V. M. Segal, V. L. Reznikov, A. E. Drobyshevskiy, and V. I. Kopylov, Russian Metallurgy (Metally). 1, 99 (1981).
4. V. M. Segal, V. I. Reznikov, V. I. Kopylov, D. A. Pavlik, and V. F. Malyshev, Process of Structure Formation During Plastic Straining, Scientific and Technical Publishing, Minsk, Belarus (1994).
5. R. Z. Valiev and N. K. Tsenev, in Hot Deformation of Aluminum Alloys, ed. T. G. Langdon, H. D. Merchant, J. G. Morris, and M. A. Zaidi, p. 319. The Minerals, Metals and Materials Society, Warrendale, PA (1991).
6. R. Z. Valiev, N. A. Krasilnikov, and N. K. Tsenev, Mater. Sci. Eng. A137, 35 (1991).
7. K. Higashi, M. Mabuchi, and T. G. Langdon, ISIJ Int. 36, 1423 (1996).
8. T. G. Nieh, J. Wadsworth, and O. D. Sherby, Superplasticity in Metals and Ceramics, p. 154, Cambridge University Press, Cambridge, England (1997).
9. R. Z. Valiev, D. A. Salimonenko, N. K. Tsenev, P. B. Berbon, and T. G. Langdon, Scripta Mater. 37, 1945 (1997).

10. J. Wang, Y. Iwahashi, Z. Horita, M. Furukawa, M. Nemoto, R. Z. Valiev, and T. G. Langdon, Acta Mater. 44, 2973 (1996).
11. M. E. Drits, S. G. Pavlenko, L. S. Toropova, Yu. G. Bykov, and L. B. Ber, Soviet Phys. Doklady. 26, 344 (1981).
12. T. G. Nieh, R. Kaibyshev, L. M. Hsiung, N. Nguyen, and J. Wadsworth, Scripta Mater. 36, 1011 (1997).
13. R. R. Sawtell and C. L. Jensen, Metall. Trans. 21A, 421 (1990).
14. L. S. Kramer, W. T. Tack, and M. T. Fernandes, Adv. Mater. Proc. 152(10), 23 (1997).
15. Y. Iwahashi, Z. Horita, M. Nemoto, and T. G. Langdon, Acta Mater. 45, 4733 (1997).
16. Y. Iwahashi, J. Wang, Z. Horita, M. Nemoto, and T. G. Langdon, Scripta Mater. 35, 143 (1996).
17. V. M. Segal, Mater. Sci. Eng. A197, 157 (1995).
18. S. Ferrasse, V. M. Segal, K. T. Hartwig, and R. E. Goforth, Metall. Mater. Trans. 28A, 1047 (1997).
19. Y. Iwahashi, Z. Horita, M. Nemoto, and T. G. Langdon, Acta Mater. in press.
20. M. Furukawa, Y. Iwahashi, Z. Horita, M. Nemoto, N. K. Tsenev, R. Z. Valiev, and T. G. Langdon, Acta Mater. 45, 4751 (1997).
21. R. Z. Valiev, R. Sh. Musalimov, and N. K. Tsenev, Phys. Stat. Sol. a. 115, 451 (1989).
22. A. A. Nazarov, A. E. Romanov, and R. Z. Valiev, Acta Metall. Mater. 41, 1033 (1993).
23. N. Blake and M. A. Hopkins, J. Mater. Sci. 20, 2861 (1985).

GRAIN REFINEMENT AND POTENTIAL FOR SUPERPLASTICITY IN Al ALLOYS CONTAINING SMALL PARTICLES

H.Hasegawa[1], S.Komura[1], Z.Horita[1], M.Furukawa[2], M.Nemoto[1] and T.G.Langdon[3]

(1) Department of Materials Science and Engineering, Faculty of Engineering, Kyushu University, Fukuoka 812-81, Japan
(2) Department of Technology, Fukuoka University of Education, Munakata, Fukuoka 811-41, Japan
(3) Departments of Materials Science and Mechanical Engineering, University of Southern California, Los Angeles CA 90089-1453, U.S.A.

Abstract

The possibility of grain refinement was investigated in Al containing 0.12%Zr using the equal-channel angular (ECA) pressing technique whereby an intense plastic strain is introduced into the material. Structural observations using transmission electron microscopy (TEM) revealed that after 4 pressings through the die some regions remain with subgrain structures but after 8 pressings most regions exhibit a grain structure separated by large angle grain boundaries and with a grain size of ~0.7 μm. The ECA-pressed samples were subjected to static annealing at selected temperatures in the range from 373 K to 773 K. It was found that extensive grain growth occurs at a temperature of ~573 K which is higher by 100 degrees than the corresponding temperatures reported earlier for pure Al and Al-Mg alloys. The present study suggests that the addition of Zr is important for achieving superplasticity in fine-grained Al and Al alloys produced by the ECA pressing technique.

The Third Pacific Rim International Conference on Advanced Materials and Processing (PRICM 3)
Edited by M.A. Imam, R. DeNale, S. Hanada, Z. Zhong and D.N. Lee
The Minerals, Metals & Materials Society, 1998

Introduction

Superplastic flow of metallic materials normally appears as the grain size is refined to less than ~10 μm [1]. Further refinement of grain size, especially below 1 μm, may lead to superplasticity at higher strain rates and/or at lower temperatures [2]. Grain refinement is then an important task for the application of superplasticity to industrial forming operations.

It has been shown that equal-channel angular (ECA) pressing is a promising procedure for such grain refinement [3]. With this technique, it is possible to reduce the grain size down to the submicrometer level. The major advantage of the ECA pressing technique over other grain refining techniques is that a large quantity of bulk material is produced without introducing any residual porosity.

Grain refinement using the ECA pressing technique consists of pressing a sample through a single channel with an equal cross-section but bent at an angle of Φ in a solid die. For $\Phi=90^{\circ}$, one pressing creates an equivalent strain of ~1 in the sample. The pressing is repeatable as the entrance and exit dimensions of the channel are the same and thus it is possible to accumulate a large total strain in the sample by repetitive pressings through the channel in the die. Structural homogeneity and the misorientation angles between neighboring grains are controlled by the numbers of pressing and the types of pressing routes as described earlier [4,5].

A study on pure Al [4] showed that subgrain structures prevail after one and two pressings through the die but, with a further increase in the number of pressing, they evolve into grain structures containing large angle grain boundaries. It was also shown that additions of Mg to pure Al give rise to a significant decrease in grain size but static annealing experiments showed that an extensive grain growth occurs in both pure Al and Mg-added Al at a similar temperature corresponding to ~$0.5T_m$ where T_m is the melting point in Kelvin [6,7]. Since superplasticity occurs through a diffusion-controlled process, fine grained structures should be stable especially at the temperature higher than ~$0.5T_m$. It is then important to maintain the submicrometer grain structure above ~$0.5T_m$.

It is known [8,9] that a small addition of Zr is effective to keep grain size stable at higher temperature because Al_3Zr particles formed in the sample inhibit the movement of grain boundaries and thus suppress extensive grain growth at higher temperature above ~$0.5T_m$. In this study, Zr is added to pure Al and the thermal stability of the fine grained structure produced by ECA pressing is examined with respect to the annealing temperature. The results are compared with those obtained using pure Al.

Experimental Procedures

An ingot with dimensions of 17x55x120 mm^3 was made from high purity Al (99.99%) containing 0.12%Zr. The ingot was homogenized at 903 K for 24 hours in air. Thereafter, it was rolled to a thickness of 11.5 mm. Rods with dimensions of 10 mm in diameter and 60 mm in length were machined from the rolled ingot. The rods were annealed at 903 K for 1 hour prior to ECA pressing. Rods having the same dimensions as Al-0.12%Zr were also prepared from pure Al (99.99%) for comparison purposes. The detailed procedure for the preparation was described elsewhere [7]. The average grain size of pure Al before ECA pressing was ~1 mm.

ECA pressing was conducted using a die having a single L-shaped channel with a

channel angle of $\Phi=90^{\circ}$ in a solid block of high strength tool steel (SKD 11). The pressing was made at room temperature without annealing between pressings. Molybdenum disulfide was used for a lubricant during pressing. All specimens were pressed in route B_C where the specimens are rotated by 90° in a forward direction after each pressing [9]. Recent studies showed that the use of route B_C creates a homogeneous equiaxed grain structure following a minimum number of pressings.

After 4 pressings through the die, the ECA-pressed samples for both pure Al and Al-0.12%Zr were cut into pieces with dimensions of 3x3x5 mm^3 and they were encapsulated in a Pyrex glass tube under an argon atmosphere. Each piece was subjected to annealing at selected temperatures in the range from 373 to 773 K for 1 hr.

Discs with dimensions of 3 mm in diameter and ~0.15 mm in thickness were prepared from the ECA-pressed samples and also the annealed samples. These discs were thinned for transmission electron microscopy (TEM) using a twin-jet electro-polishing apparatus in a mixture of 10%$HClO_4$, 20%$C_3H_8O_3$ and 75%C_2H_5OH. Microstructural observations and selected area electron diffraction (SAED) analyses were conducted using an Hitachi H-8100 transmission electron microscope operating at 200 kV. The SAED patterns were taken from regions with diameters of either 6.3 μm or 12.3 μm. TEM observations and analyses were made exclusively in the plane perpendicular to the longitudinal axis of the ECA pressed specimens.

Compression specimens with dimensions of 3x3x5 mm^3 were prepared from the ECA-pressed and annealed samples, where the compression axis was parallel to the longitudinal axis of the ECA-pressed specimens. The compression tests were conducted at room temperature at a strain rate of $3.3x10^{-4}$ s^{-1}. The load variation was recorded with respect to time using a strip chart recorder and the 0.2% proof stresses were measured.

Results and discussion

Figure 1 shows the microstructures of (a) Al and (b) Al-0.12%Zr after 4 and 8 pressings through the die, respectively. The corresponding SAED patterns taken from regions of 6.3 μm in diameter are also included in Fig.1. The SAED patterns exhibit diffracted beams scattered around rings and thus they indicate that the microstructure of each material consists of grains separated

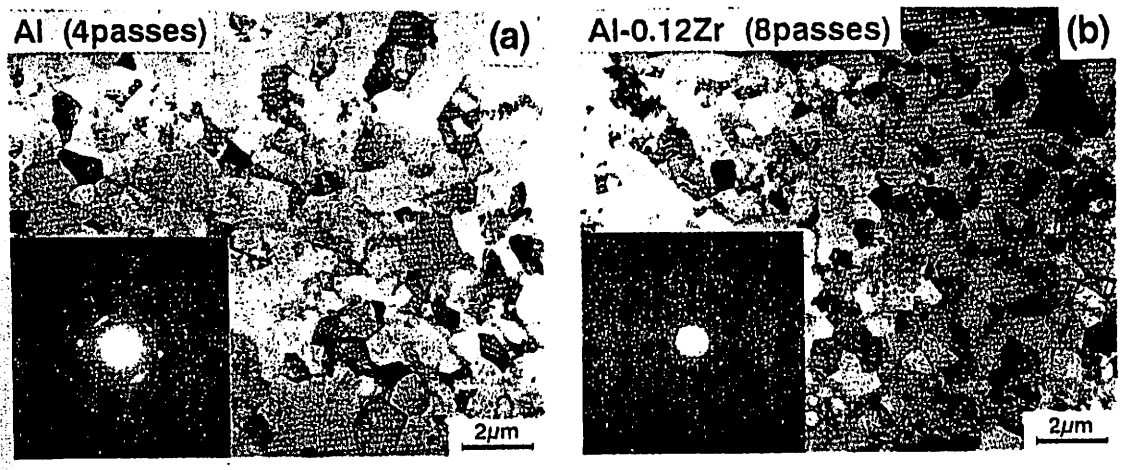

Figure 1: TEM micrographs of (a) Al and (b) Al-0.12%Zr after 4 and 8 pressings, respectively, and corresponding SAED patterns taken from regions of 6.3 μm in diameter.

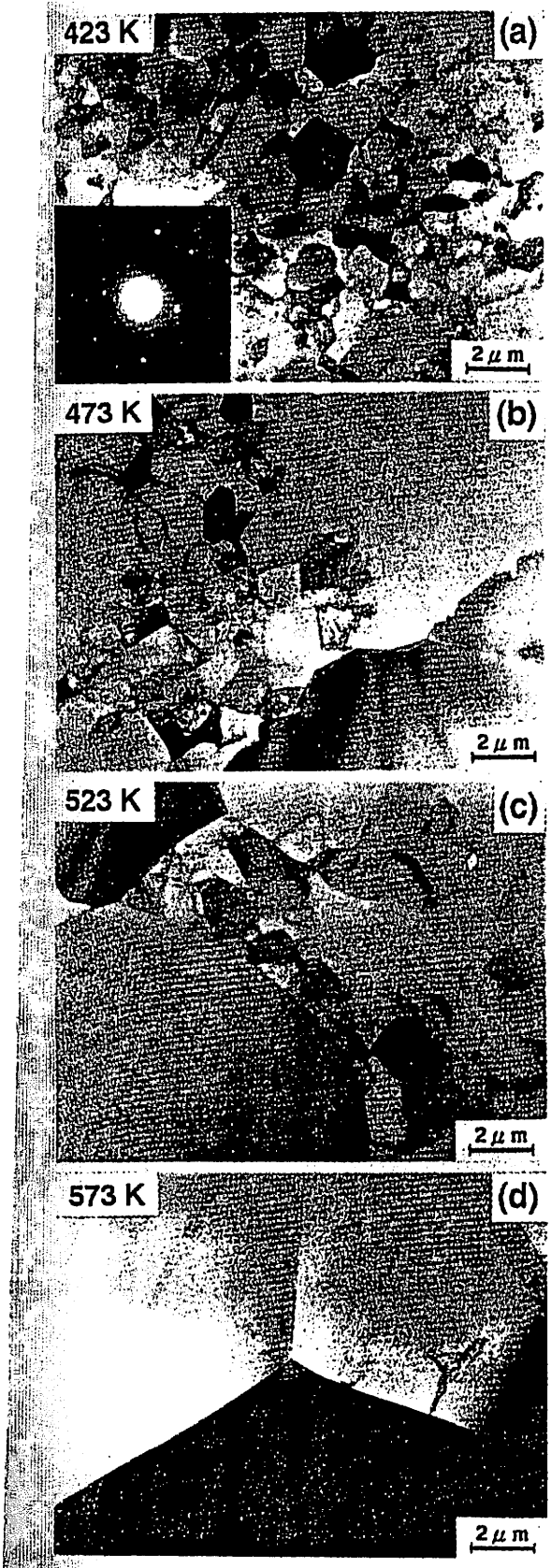

Figure 2: TEM micrographs after annealing at temperatures of (a) 423 K, (b) 473 K, (c) 523 K and (d) 573 K for 1 hour for ECA-pressed Al.

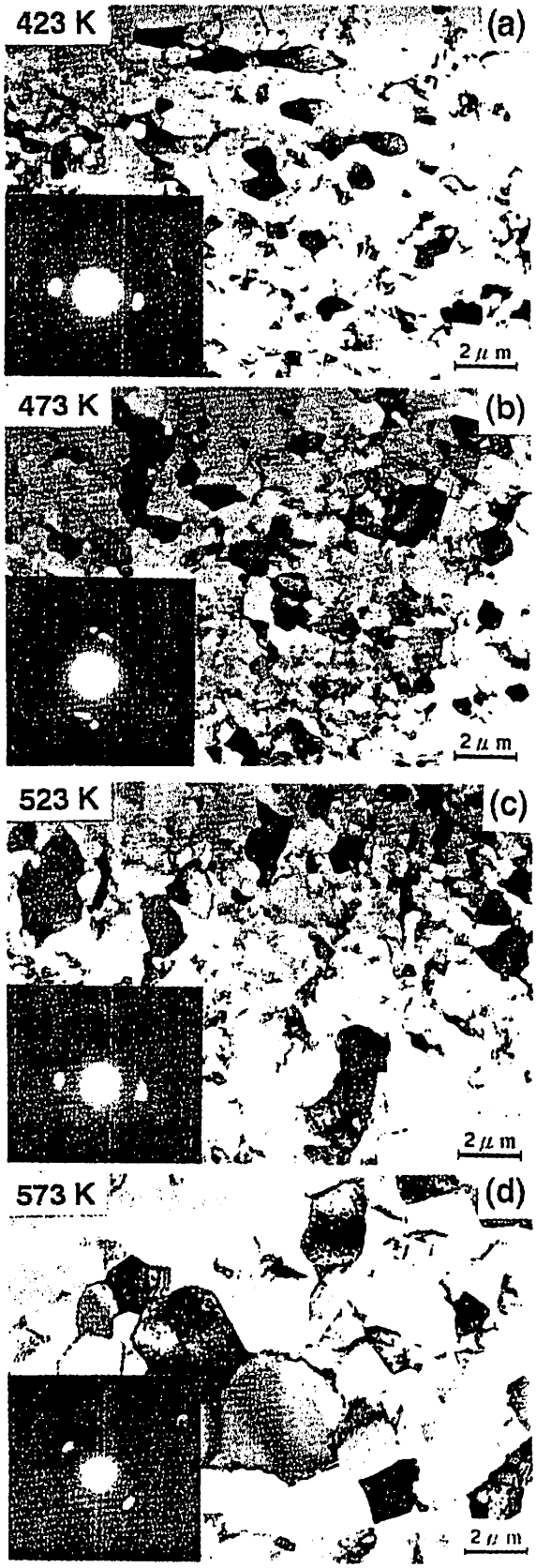

Figure 3: TEM micrographs after annealing at temperatures of (a) 423 K, (b) 473 K, (c) 523 K and (d) 573 K for 1 hour for ECA-pressed Al-0.12%Zr

by large angle grain boundaries. The TEM observations reveal that an equiaxed grain structure was achieved in each material. The grain sizes measured from the micrographs are ~1 μm and ~0.7 μm for Al and Al-0.12%Zr, respectively. It should be noted that the pressing numbers of 4 and 8 for Al and Al-0.12%Zr, respectively, correspond to the minimum numbers to attain equiaxed grain structures with large angle grain boundaries.

The microstructures after annealing at temperatures of 423, 473, 523 and 573 K for 1 hour are shown in Fig.2 (a)-(d) and Fig.3 (a)-(d) for pure Al and Al-0.12%Zr, respectively. For both materials, there appears to be no appreciable change in microstructure after annealing at 423 K when compared with the ECA-pressed structures shown in Fig.1. After annealing above 423 K, the difference between the microstructures of Al and Al-0.12%Zr becomes more apparent. For Al, large grains are visible in some limited regions after annealing at 473 K as shown in Fig.2 (b). A mixture of large and small grains remained present up to the annealing temperature of 523 K but the fraction of large grains increased with an increase of annealing temperature. Regions containing small grains disappeared at and above an annealing temperature of 573 K. For Al-0.12%Zr, by contrast, the fine grained structure remained stable and no region containing large grains was detected even after annealing at 573 K, although a slight increase in grain size was observed as shown in Fig.3 (a)-(d). Regions containing large grains were observed after annealing above 573 K.

Figure 4 plots the grain size measured against the annealing temperature for both Al and Al-0.12%Zr. In Fig.4, the points with arrows indicate that the structure consists of small and large grains but the plotted values represent the average sizes of the grains present with a major fraction in the specimens. Extensive grain growth occurs at an annealing temperature of ~473 K for Al but at ~573 K for Al-0.2%Zr: the latter is higher by ~100 degrees than the former.

Figure 5 plots the 0.2% proof stress against the annealing temperature. For pure Al, the proof stress remains constant up to 473 K, then exhibits an abrupt decrease with an increase of annealing temperature from 473 K to 573 K and again remains constant above 573 K. The

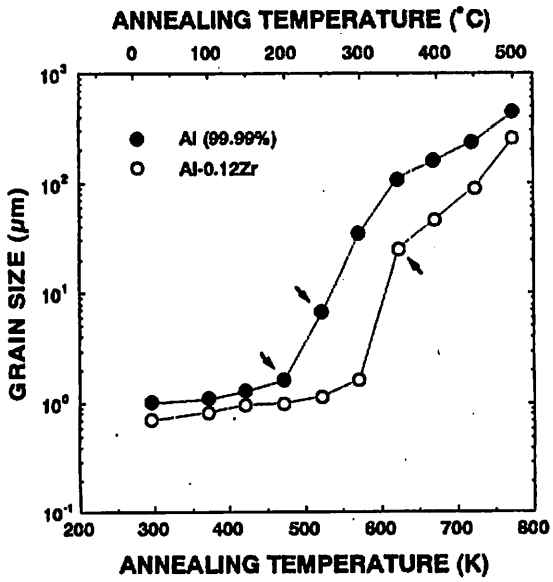

Figure 4: Plots of grain size against annealing temperature for Al and Al-0.12%Zr.

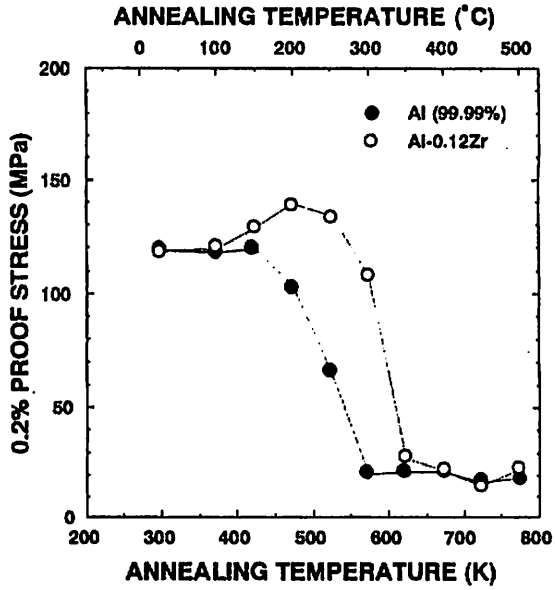

Figure 5: Plots of 0.2% proof stress against annealing temperature for Al and Al-0.12%Zr.

abrupt decrease in proof stress is attributed to the occurrence of extensive grain growth because both variations of proof stress and grain size occur in the same temperature range. The dependence of the proof stress on annealing temperature in Al-0.12%Zr is different in two respects from that in Al. First, the proof stress increases with an increase in annealing temperature up to 473 K. It is considered that this increase is due to the formation of Al_3Zr particles during annealing. Second, an abrupt decrease in proof stress occurs at 523 K, and this is terminated at 623K with almost the same stress level as in Al. This decrease corresponds to the occurrence of extensive grain growth as observed in Al.

Summary and conclusions

1. The addition of 0.12%Zr to pure Al is effective in decreasing the ECA pressed grain size: ~1 μm for Al and ~0.7 μm for Al-0.12%Zr. However, the addition of Zr requires a larger number of ECA pressings to attain a homogeneous equiaxed grain structure containing large angle grain boundaries: 4 pressings for Al and 8 pressings for Al-0.12%Zr, both using route B_C which gives a more effective evolution to a homogeneous equiaxed grain structure than other routes.
2. The addition of Zr is also effective to increase the temperature where extensive grain growth occurs: ~473 K for Al and ~573 K for Al-0.12%Zr. It is considered that this increase is due to the formation of Al_3Zr particles during annealing.
3. The small addition of Zr to pure Al is promising for achieving superplasticity because it stabilizes the ECA pressed fine-grain structure above ~$0.5T_m$.

Acknowledgements

We are grateful to Mr. T. Fujinami of Kyushu University for his cooperation. This work was supported in part by the Light Metals Educational Foundation of Japan, in part by a Grant-in-Aid for Scientific Research from the Ministry of Education, Science, Sports and Culture of Japan, in part by the Japan Society for the Promotion of the Science and in part by the National Science Foundation of the United States under Grants No. INT-9602919 and DMR-9625969.

References

1. T.G. Langdon, Metall. Trans., 13A (1982), 689-702.
2. Y.Ma, M.Furukawa, Z.Horita, M.Nemoto, R.Z. Valiev and T.G. Langdon, Mater.Trans.JIM, 37 (1996), 336-339.
3. R.Z.Valiev, N.A. Krasilnikov and N.K. Tsenev, Mater. Sci. Eng., A137 (1991), 35-40.
4. Y. Iwahashi, Z. Horita, M. Nemoto and T. G. Langdon, Acta Mater., 45 (1997), 4733-4741.
5. Y. Iwahashi, Z. Horita, M. Nemoto and T. G. Langdon, Acta Mater. (in press).
6. M. Furukawa, Z. Horita, M. Nemoto, R. Z. Valiev and T. G. Langdon, Acta Mater., 44 (1996), 4619-4629.
7. Y. Iwahashi, Z. Horita, M. Nemoto and T. G. Langdon, Metall. Mater. Trans. (submitted for publication).
8. N.Ryum, Acta Metall., 17 (1969), 269-278.
9. R.H.Brickenell and J.W.Edington, Metall. Trans. A, 10A (1979), 1257-1263.

Communications

Optimizing the Rotation Conditions for Grain Refinement in Equal-Channel Angular Pressing

KEIICHIRO OH-ISHI, ZENJI HORITA, MINORU FURUKAWA, MINORU NEMOTO, AND TERENCE G. LANGDON

Equal-channel angular (ECA) pressing is rapidly becoming an established procedure for inducing microstructural refinement in polycrystalline materials through the process of intense plastic straining. To date, there have been numerous reports of the use of the ECA pressing procedure to produce grain refinement down to the submicrometer, or occasionally the nanometer, level in a range of metallic materials[1-10] and in some intermetallic compounds.[11,12]

In ECA pressing, a sample is pressed through a die having two channels, equal in cross section, which intersect at an angle of Φ, with simple shear occurring as the sample moves through the angle subtended at the intersection of the two channels.[13,14] Since the cross section of the sample remains unchanged on passage through the die, the procedure is readily amenable to repetitive pressings of the same sample in order to introduce high total strains. Pressings are generally conducted using dies having $\Phi \simeq 90$ deg, and under these conditions the equivalent strain introduced on each passage through the die is approximately equal to 1.[15] In practice, experiments have demonstrated that the microstructural characteristics introduced by ECA pressing, including the structural homogeneity, the average shapes of the individual grains, and the misorientation angles of the boundaries between adjacent grains, are all dependent upon experimental conditions such as the number of passages through the die,[5,9,10,16] the shearing directions in each separate passage as manifested by any rotation of the sample between separate pressings,[5,9,16] and the temperature at which the straining is conducted.[10]

When repetitive pressings are undertaken, it is a standard procedure to identify three different routes, designated A, B, and C, in which the pressings are conducted without any rotation of the sample, with rotation about the longitudinal axis by 90 deg between each pressing and with rotation by 180 deg between each pressing, respectively. Two recent reports have compared directly the efficiency of these different processing routes for establishing a homogeneous structure consisting of an array of equiaxed grains. In experiments by Ferrasse *et al.*[9] on Cu and Al alloys, it was concluded that processing by route C produces a more homogeneous and equiaxed structure than routes A and B. Iwahashi *et al.*[5] used samples of pure Al and confirmed the efficiency of route C over route A, but later showed, in more detailed experiments,[16] that microstructural evolution occurs most rapidly when processing through route B. The apparent inconsistency in these two sets of results appears to arise because Ferrasse *et al.*[9] defined route B as an alternate rotation by 90 deg in a positive and negative direction, whereas Iwahashi *et al.*[16] defined route B as a repetitive rotation by 90 deg in the same direction between each pressing. These two processing routes are illustrated schematically in Figure 1, where the designation route B_A represents the rotation employed by Ferrasse *et al.*, equivalent to 0 deg-90 deg-0 deg-90 deg, and the designation route B_C represents the rotation employed by Iwahashi *et al.*, equivalent to 0 deg-90 deg-180 deg-270 deg. The present investigation was therefore initiated in order both to examine the microstructures produced in three orthogonal planes of sectioning in pure Al when using route B_A and to compare these microstructures with those reported earlier for the same material when using route B_C.[16]

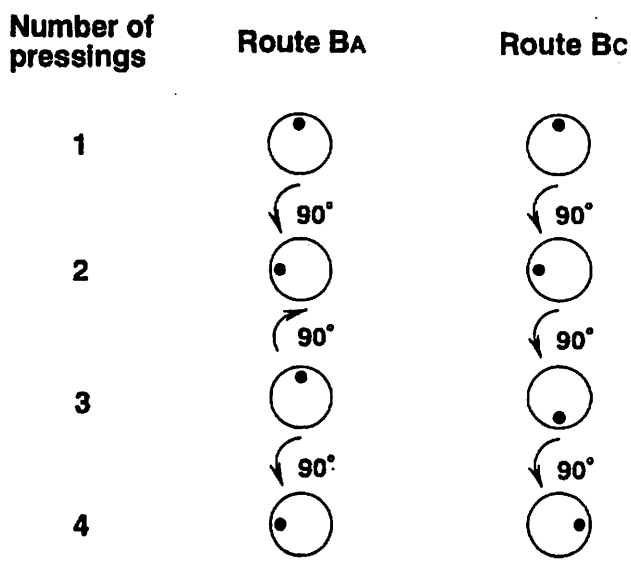

Fig. 1—Schematic illustration of processing routes B_A and B_C, where each sample is rotated by 90 deg between each consecutive pressing.

The experiments were conducted using the same high purity (99.99 pct) aluminum as in earlier experiments.[5,16] An Al block with a diameter of ~30 mm and a length of ~150 mm was swaged into a 10-mm-diameter rod at room temperature, and two samples were cut having lengths of ~60 mm. Each sample was annealed in air for 1 hour at 773 K to give a measured grain size of ~1 mm. The ECA pressing was performed using a solid die of high strength tool steel in which a single channel, with diameters of 10.3 and 10.0 mm at the entrance and exit, respectively, passed through the die with an angle of intersection of $\Phi = 90$ deg. Samples were pressed at room temperature using MoS_2 as a lubricant and with a pressing speed of ~19 mm s^{-1}. Each sample was pressed using route B_A to a total of either three or four passes equivalent to strains of ~3 and ~4, respectively. These strains were selected for comparison with route B_C because the earlier results showed that four

KEIICHIRO OH-ISHI, Research Associate, ZENJI HORITA, Associate Professor, and MINORU NEMOTO, Professor, are with the Department of Materials Science and Engineering, Kyushu University, Fukuoka 812-8581, Japan. MINORU FURUKAWA, Associate Professor, is with the Department of Technology, Fukuoka University of Education, Munakata, Fukuoka 811-4192, Japan. TERENCE G. LANGDON, Professor, is with the Departments of Materials Science and Mechanical Engineering, University of Southern California, Los Angeles, CA 90089-1453.

Manuscript submitted December 23, 1997.

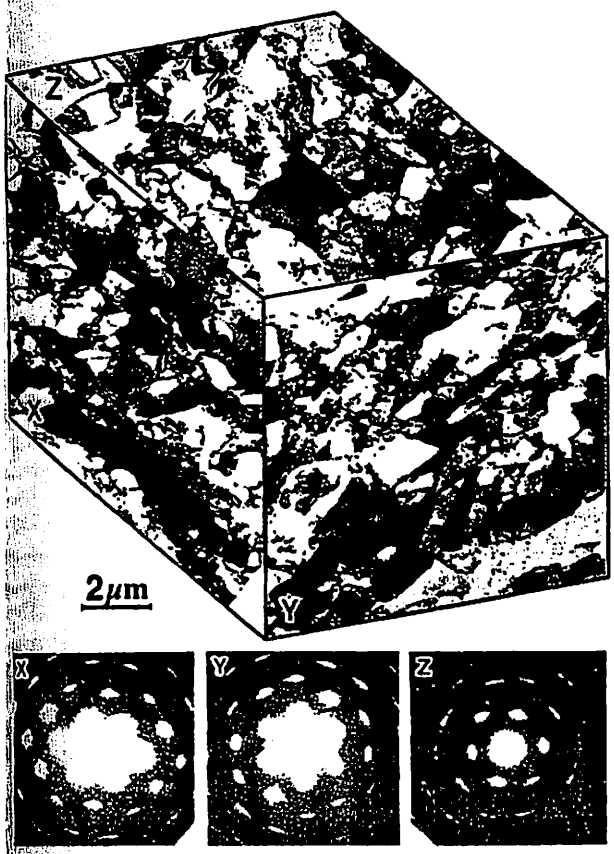

Fig. 2—Microstructure and associated SAED patterns after pressing through route B_A for a total of three passes.

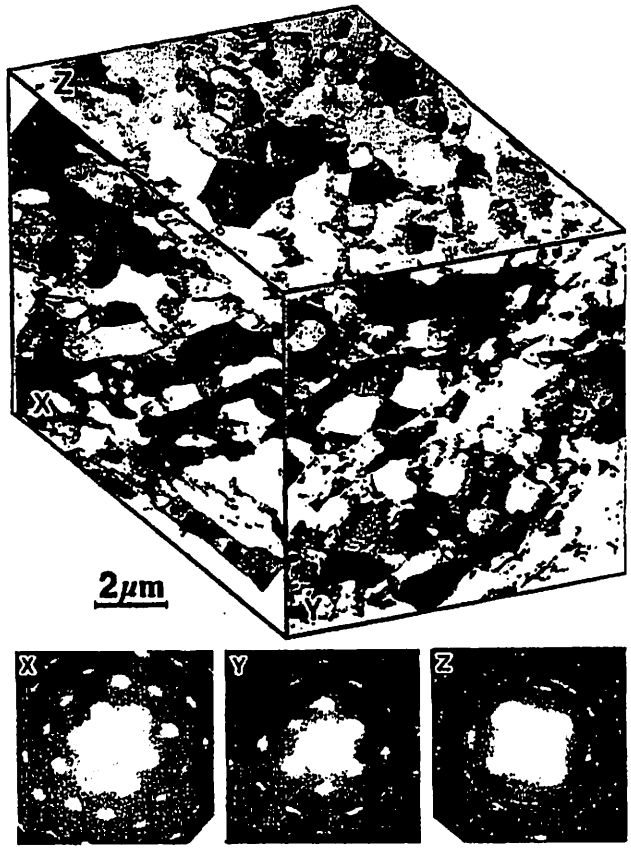

Fig. 3—Microstructure and associated SAED patterns after pressing through route B_A for a total of four passes.

passes in route B_C is sufficient to produce a homogeneous microstructure of equiaxed grains separated by high angle grain boundaries.[16]

Following the ECA pressing, small samples with thicknesses of ~0.5 mm were cut from the centers of the rods with orientations either perpendicular to the longitudinal axes of the rods (the *x* plane), parallel to the side faces at the point of exit from the die (the *y* plane), or parallel to the top surface at the point of exit (the *z* plane); these three orthogonal planes were used also in the earlier experiments for route B_C.[16] Discs with diameters of 3 mm were punched from these samples, ground mechanically, and thinned to perforation using the procedure described earlier.[5] The thinned specimens were examined in a Hitachi H-8100 transmission electron microscope (TEM) operating at 200 kV. Photomicrographs were taken of representative microstructures after tilting to obtain the nearest net patterns. Selected area electron diffraction (SAED) patterns were taken for each condition from regions with diameters of 12.3 μm. Subgrain sizes were estimated directly from the TEM photomicrographs.

Figures 2 and 3 show the microstructures in the *x*, *y*, and *z* planes, together with the appropriate SAED patterns, for the samples tested through three and four passes, respectively.

It is apparent from the SAED patterns in Figure 2 that the microstructure in each plane consists of subgrains separated by low angle grain boundaries. Inspection of the photomicrographs shows that these subgrains are elongated in the *x* and *y* planes but they are fairly equiaxed in the *z* plane. However, there is an important difference between the present observations and those reported earlier on the same material processed through route B_C, because in route B_C the subgrains were replaced by grains having high angle grain boundaries after three passes through the die.[16] Thus, comparing with the earlier data for routes A, B_C, and C, the present microstructure is more similar to route A where subgrains remain after three passes. Despite this difference, the average subgrain size in each plane in Figure 2 is ~1 μm, and this is similar to the subgrain and grain sizes reported earlier for the other processing routes.[16]

The SAED patterns in Figure 3 show that, after a total of four passes, the subgrains and low angle boundaries remain in the *x* and *y* planes, but the diffraction spots are diffused in the *z* plane indicating an increase in the misorientation angles. Inspection of the photomicrographs shows the presence of elongated subgrains in the *x* and *y* planes, but in the *z* plane the structure is evolving more rapidly into an array of equiaxed grains with high angle boundaries. Thus, some subgrain structure remains in route B_A even after four passes through the die, and in this respect the processing route is similar to route A. The earlier observations using route B_C showed that three passes were sufficient to eliminate the subgrain structure and four passes gave a homogeneous microstructure of equiaxed grains with boundaries having high angles of misorientation.[16] By contrast, the present observations using route B_A reveal the

retention of a subgrain structure, with many elongated subgrains, even after four passes through the die.

The results obtained in this investigation provide an explanation for the apparent inconsistency between the data reported by Ferrasse *et al.*[9] and Iwahashi *et al.*[16] Ferrasse *et al.* performed their ECA pressing using route B_A, where evolution into an array of equiaxed grains is very slow, whereas Iwahashi *et al.* pressed using route B_C, where the evolution into an equiaxed grain structure occurs more rapidly. Based on the results available to date for each processing route, it is reasonable to conclude that route B_C is most effective in producing a homogeneous ultrafine-grained structure, route C is intermediate, and routes A and B_A are the least effective.

In summary, (1) the rate of microstructural evolution in ECA pressing depends upon whether the sample is rotated between consecutive pressings; (2) when rotating by 90 deg, the sample may be either rotated alternately in positive and negative directions (route B_A) or rotated each time in the same direction (route B_C); and (3) the experiments show that microstructural evolution, and the development of a homogeneous microstructure of grains separated by high angle boundaries, occurs more rapidly in route B_C than in route B_A.

This work was supported in part by the Light Metals Educational Foundation of Japan, in part by a Grant-in-Aid for Scientific Research from the Ministry of Education, Science, Sports and Culture of Japan, in part by the Japan Society for the Promotion of Science, and in part by the National Science Foundation of the United States under Grant Nos. DMR-9625969 and INT-9602919.

REFERENCES

1. R.Z. Valiev, E.V. Kozlov, Yu.F. Ivanov, J. Lian, A.A. Nazarov, and B. Baudelet: *Acta Metall. Mater.*, 1994, vol. 42, pp. 2467-75.
2. J. Wang, M. Furukawa, Z. Horita, M. Nemoto, R.Z. Valiev, and T.G. Langdon: *Mater. Sci. Eng.*, 1996, vol. A216, pp. 41-46.
3. J. Wang, Y. Iwahashi, Z. Horita, M. Furukawa, M. Nemoto, R.Z. Valiev, and T.G. Langdon: *Acta Mater.*, 1996, vol. 44, pp. 2973-82.
4. M. Furukawa, Z. Horita, M. Nemoto, R.Z. Valiev, and T.G. Langdon: *Acta Mater.*, 1996, vol. 44, pp. 4619-29.
5. Y. Iwahashi, Z. Horita, M. Nemoto, and T.G. Langdon: *Acta Mater.*, 1997, vol. 45, pp. 4733-41.
6. M. Furukawa, Y. Iwahashi, Z. Horita, M. Nemoto, N.K. Tsenev, R.Z. Valiev, and T.G. Langdon: *Acta Mater.*, 1997, vol. 45, pp. 4751-57.
7. M. Mabuchi, H. Iwasaki, K. Yanase, and K. Higashi: *Scripta Mater.*, 1997, vol. 36, pp. 681-86.
8. M. Kawazoe, T. Shibata, T. Mukai, and K. Higashi: *Scripta Mater.*, 1997, vol. 36, pp. 699-705.
9. S. Ferrasse, V.M. Segal, K.T. Hartwig, and R.E. Goforth: *Metall. Mater. Trans. A*, 1997, vol. 28A, pp. 1047-57.
10. S. Ferrasse, V.M. Segal, K.T. Hartwig, and R.E. Goforth: *J. Mater. Res.*, 1997, vol. 12, pp. 1253-61.
11. S.L. Semiatin, V.M. Segal, R.L. Goetz, R.E. Goforth, and T. Hartwig: *Scripta Metall. Mater.*, 1995, vol. 33, pp. 535-40.
12. L.R. Cornwell, K.T. Hartwig, R.E. Goforth, and S.L. Semiatin: *Mater. Characterization*, 1996, vol. 37, pp. 295-300.
13. V.M. Segal, V.I. Reznikov, A.E. Drobyshevskiy, and V.I. Kopylov: *Russ. Metall. (Metally)*, vol. 1, pp. 99-105.
14. V.M. Segal: *Mater. Sci. Eng.*, 1995, vol. A197, pp. 157-64.
15. Y. Iwahashi, J. Wang, Z. Horita, M. Nemoto, and T.G. Langdon: *Scripta Mater.*, 1996, vol. 35, pp. 143-46.
16. Y. Iwahashi, Z. Horita, M. Nemoto, and T.G. Langdon: *Acta Mater.*, 1998, vol. 49, pp. 3317-31.

Proceedings of IMSP '97
Mie University Press

OPTIMIZING THE PROCESSING OF A COMMERCIAL Al-BASED ALLOY FOR HIGH STRAIN RATE SUPERPLASTICITY

Patrick B. Berbon,[†] Minoru Furukawa,[§] Zenji Horita,[‡] Minoru Nemoto,[‡]
Nikolai K. Tsenev,[††] Ruslan Z. Valiev[§§] and Terence G. Langdon[†]

[†]Departments of Materials Science and Mechanical Engineering
University of Southern California
Los Angeles, CA 90089-1453, U.S.A.
[§]Department of Technology, Fukuoka University of Education
Munakata, Fukuoka 811-41, Japan
[‡]Department of Materials Science and Engineering
Kyushu University, Fukuoka 812-81, Japan
[††]Institute of Chemical Technology
Ufa State Petroleum Technical University, Ufa 450062, Russia
[§§]Institute of Physics of Advanced Materials
Ufa State Aviation Technical University, Ufa 450000, Russia

ABSTRACT

Equal-channel angular (ECA) pressing is an experimental procedure which may be used to introduce an ultra-fine grain size into a material through intense plastic straining. In principle, this technique should provide materials which are capable of exhibiting high strain rate superplasticity at relatively low testing temperatures. Experiments were undertaken to determine the feasibility of introducing an ultra-fine grain size and attaining superplastic properties in a commercial Al-Mg-Li-Zr alloy containing a fine dispersion of δ'-Al_3Li and β'-Al_3Zr. The results demonstrate that it is possible, by selecting an appropriate processing route, to achieve a tensile elongation of >1000% in this alloy at testing temperatures of 573 - 623 K and with an imposed strain rate of 1×10^{-2} s^{-1}.

1. INTRODUCTION

Superplasticity, in the form of high tensile elongations prior to failure, may be attained in materials having small grain sizes, typically <10 μm [1]. However, high superplastic elongations are generally confined to a narrow range of strain rates in the vicinity of $\sim 10^{-4}$ - 10^{-3} s^{-1} and these slow rates serve to restrict the use of superplastic forming techniques to applications where production is limited to ~100 - 10,000 units [2]. There is experimental evidence suggesting that a reduction in grain size, by up to one order of magnitude, will both decrease the temperature and increase the strain rate associated with optimum superplastic flow [3,4]. These trends would be beneficial in the superplastic forming industry since a lower operating temperature will reduce tool wear and a faster strain rate has the potential for reducing the forming time and thereby introducing the possibility of the mass production of a large number of components. The present paper describes an attempt to achieve high strain rate superplasticity in a representative commercial aluminum alloy.

2. EXPERIMENTAL MATERIAL AND PROCEDURES

The experiments were conducted using a light-weight high strength commercial Russian alloy designated 01420. This alloy has a chemical composition of Al-5.5% Mg-2.2% Li-0.12% Zr and the development of the alloy was described by Fridlyander *et al.* [5].

The material was received in the form of a hot-rolled plate and it was found by microscopic examination that the as-received grain size was of the order of ~ 400 μm. This large initial grain size precludes any potential for superplasticity in the as-received condition.

In order to introduce an ultra-fine grain size into the Al-Mg-Li-Zr alloy, it was decided to make use of a processing procedure known as equal-channel angular (ECA) pressing. In ECA pressing, a polycrystalline metal is machined and pressed through a special die containing two channels, equal in cross-section, which intersect within the die to give a continuous single passage. This procedure was developed many years ago in order to introduce an intense plastic strain into materials with no change in the cross-sectional area [6] and it is now established as a method for attaining a submicrometer or nanometer grain size [7,8]. In the present experiments, cylindrical samples were cut from the as-received plate, with diameters of either 50 or 20 mm and with lengths in the range of ~ 70 - 100 mm, and these cylinders were pressed through the die in air using an ECA facility in which the angle of intersection of the two channels was 90°. Following pressing, the samples were air cooled and, if required, they were then pressed again through the same die. A relationship is available to estimate the strain introduced into a sample on a single passage through a die [9] and it follows from this relationship that a single passage in the present experiments gives a strain of ~ 1. Initially, ECA pressing was conducted for 4 passes at a temperature of 673 K giving a total strain of ~ 4 but subsequent ECA pressing was conducted where there were 8 passes at 673 K and 4 further passes at 473 K giving a total strain of ~ 12. For convenience, these two ECA pressing procedures are designated Route 1 and Route 2, respectively.

Following ECA pressing, tensile specimens were machined from the samples with a gauge length of 4 mm and a cross-section within the gauge length of 3×2 mm^2. These specimens were pulled in air using an Instron testing machine operating at a constant rate of cross-head displacement and with the testing temperature held constant to within ± 5°C.

The stability of the microstructure after ECA pressing was evaluated by cutting small pieces from the samples, with dimensions of $3 \times 3 \times 4.7$ mm^3, annealing each piece in an argon atmosphere for 1 hour at selected temperatures in the range from 323 to 833 K and then quenching in iced water. Microstructural examination was conducted by preparing discs with a thickness of ~ 200 μm and then mechanically grinding and thinning these discs for examination by transmission electron microscopy (TEM). Selected area electron diffraction (SAED) patterns were recorded from regions of the samples having diameters of 13 μm. The average grain size was determined in each sample by taking TEM photomicrographs and then measuring individually at least 50 different grains for each condition. A procedure was adopted in which SAED patterns were taken systematically along lines of linear traverse of > 100 μm within the TEM and this permitted a qualitative estimate of the relative volume fractions of grains having high and low angles of misorientation.

Additional information is documented elsewhere concerning the procedures and the results obtained on the Al-Mg-Li-Zr alloy [10,11].

3. EXPERIMENTAL RESULTS AND DISCUSSION

Figure 1 shows the microstructures of the alloy and the associated SAED patterns after ECA pressing using (a) Route 1 and (b) Route 2. A detailed description of the microstructure after pressing by Route 1 is given elsewhere [10] but in practice it was found that there was heterogeneity within this material with some areas where the grain boundaries had high angles of misorientation, as indicated by the SAED pattern in Fig. 1(a), and other areas where there were arrays of sub-grain boundaries having low angles of misorientation. This heterogeneity suggests that a strain of ~4 by ECA pressing is insufficient to produce a homogeneous microstructure in this material. It was shown by measurement that there were volume fractions of ~60-70% of grains with high angle boundaries and ~30-40% of grains with low angle boundaries after processing by Route 1. By contrast, there was a homogeneous structure of high angle boundaries after processing by Route 2.

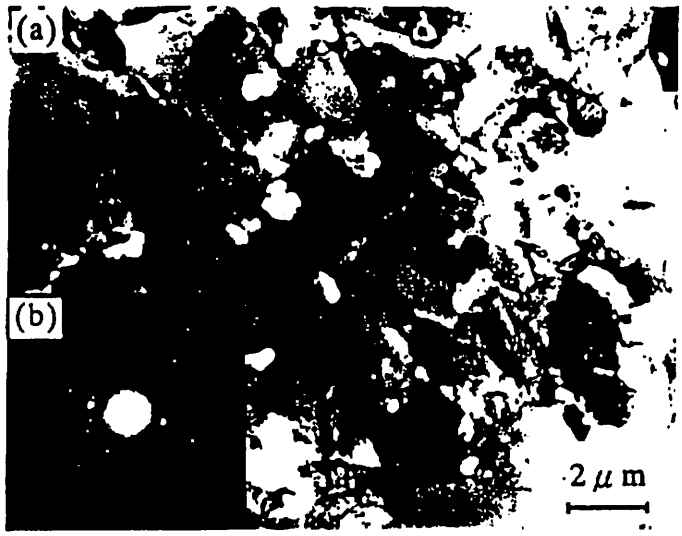

(a)

(b)

Fig. 1 Microstructures after ECA pressing through (a) Route 1 and (b) Route 2.

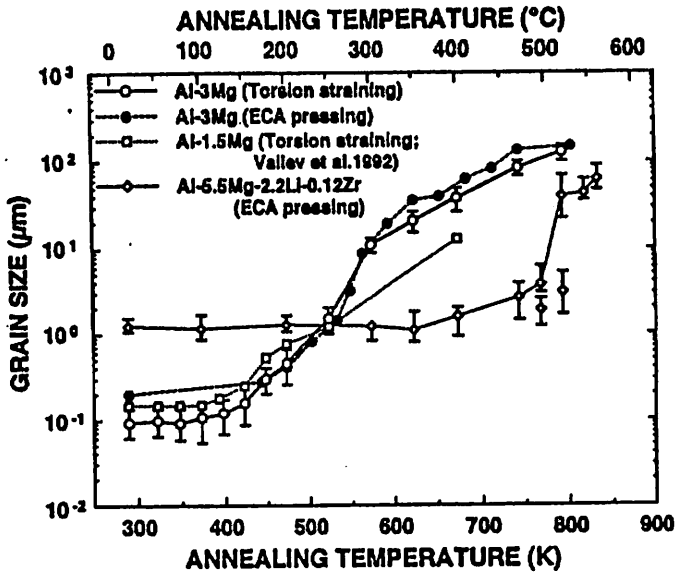

Fig. 2 Average grain size versus annealing temperature, including experimental data for Al-3% Mg after ECA pressing [12] and Al-3% Mg [13] and Al-1.5% Mg [14] after torsion straining.

The average grain size in the Al-Mg-Li-Zr alloy after ECA pressing by Route 1 was ~1.2 μm, and this value applied equally to the areas of grains with high angle boundaries and to the areas of sub-grains with low angle boundaries. An identical grain size of ~1.2 μm was measured also after processing of the alloy by Route 2. Thus, the introduction of a higher strain in the ECA pressing does not lead to an additional refinement of the microstructure but rather it serves to permit an homogenization of the structure and an evolution of the boundaries within those areas containing arrays of sub-grains.

The stability of the microstructure at elevated temperatures was evaluated by annealing samples processed by Route 1 and then measuring the average grain size. The results are plotted in Fig. 2 and, in addition, datum points are included for an Al-3% Mg solid solution alloy after ECA pressing [12] and Al-3% Mg and Al-1.5% Mg solid solution alloys where an intense plastic strain was introduced using the alternative procedure of torsion straining [13,14]. An important conclusion from the work on the Al-Mg solid solution alloys was that an ultra-fine grain size may be introduced, with a typical size of ~0.1 - 0.2 μm, but these very small grain sizes are unstable at temperatures above ~500 K so that grain growth occurs very rapidly. By contrast, the ultra-fine grains introduced into the Al-Mg-Li-Zr alloy used in the present investigation display remarkable stability such that significant grain growth occurs only at temperatures above ~750 K, corresponding to ~0.8 T_m where T_m is the absolute melting temperature of the material. This stability is attributed to the presence of β'-Al_3Zr precipitates in this alloy because these precipitates will be stable at these high temperatures whereas the finer δ'-Al_3Li precipitates will dissolve. Since superplasticity is a diffusion-controlled process, the results in Fig. 2 suggest that the Al-Mg-Li-Zr alloy may be a suitable candidate material for the development of superplasticity at temperatures in the range of ~550 - 700 K: these temperatures are attractive because they avoid problems associated with the depletion of Li and Mg [15-17] at higher temperatures.

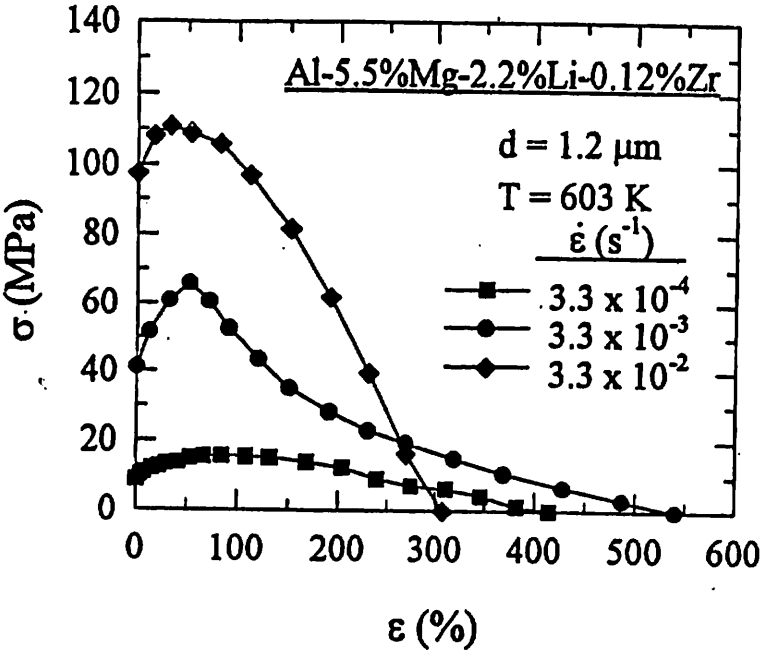

Fig. 3 Stress versus strain after ECA pressing through Route 1.

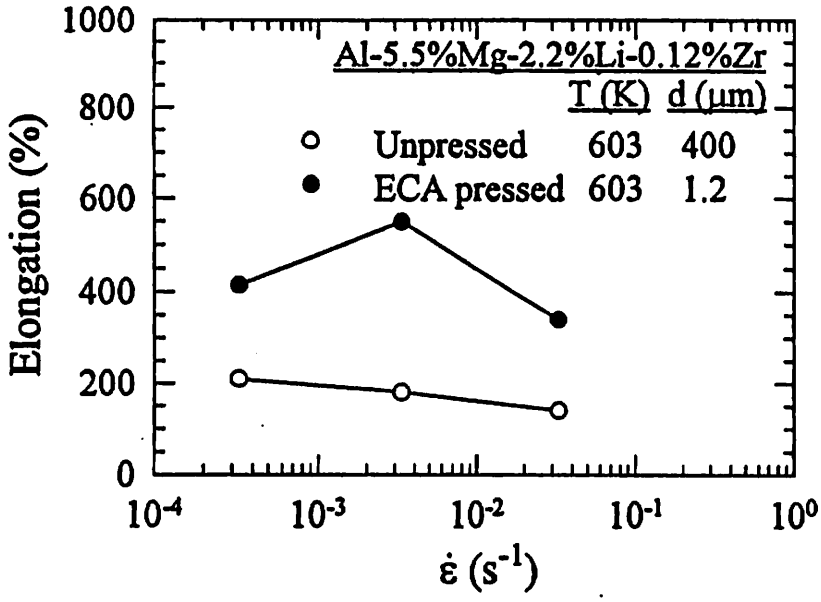

Fig. 4 Elongation versus strain rate after ECA pressing through Route 1 and without ECA pressing.

Figures 3 and 4 show mechanical data obtained on the material subjected to ECA pressing using Route 1: the stress-strain curves are given in Fig. 3 for three samples tested at a temperature of 603 K and at strain rates from 3.3×10^{-4} to 3.3×10^{-2} s^{-1}, respectively, and the total elongations to failure for these three samples are plotted in Fig. 4 together with datum points obtained under the same testing conditions for the Al-Mg-Li-Zr alloy in the as-received and unpressed condition.

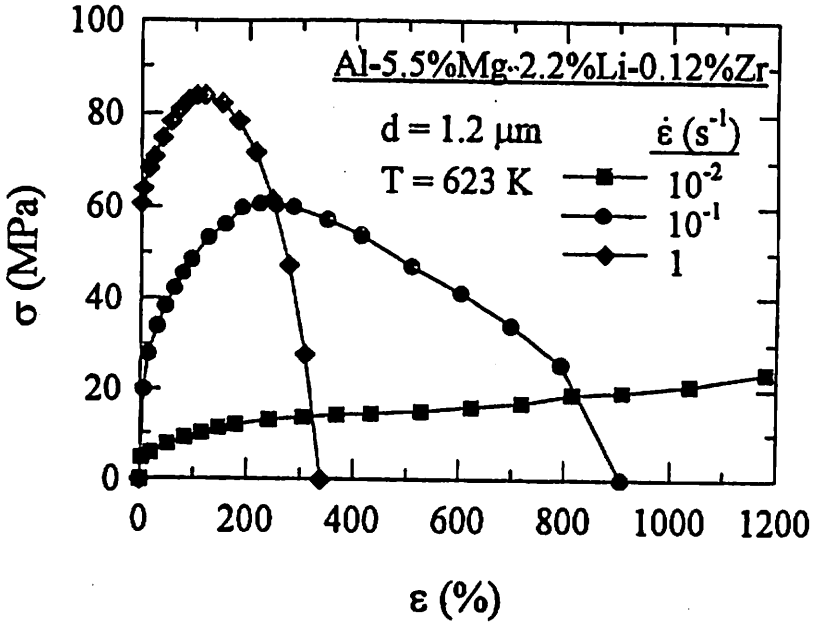

Fig. 5 Stress versus strain after ECA pressing through Route 2.

Further details on the ductility of the Al-Mg-Li-Zr alloy are given elsewhere [11,18], but it is apparent from Fig. 4 that the material subjected to ECA pressing through Route 1 shows substantial ductility, with a maximum elongation of ~550% at a strain rate of 3.3×10^{-3} s^{-1}. Although these results are attractive, they nevertheless fall short of the requirements for a superplastic capability at strain rates within the range of commercial hot working processes.

As already noted, the microstructure after processing to a strain of ~4 through Route 1 was heterogeneous and contained areas of both grains and sub-grains, whereas the microstructure after processing through Route 2 was homogeneous with an array of grains having high angle boundaries and with the same grain size of ~1.2 μm. Therefore, tests were conducted to determine the effect of using a more homogeneous microstructure. The resultant stress-strain curves are shown in Fig. 5 and the variation of elongation with strain rate is given in Fig. 6: it should be noted that these samples were tested at the slightly higher temperature of 623 K and Fig. 6 includes also the three datum points for the unpressed material tested at 603 K.

It is apparent from Fig. 5 that these samples show an initial period of strain hardening followed by strain softening, except for the test conducted at the lowest strain rate of 1×10^{-2} s^{-1} where the test was discontinued without fracture and without the advent of strain softening at a total elongation of 1180%. The appearance of these three specimens after testing, together with other specimens also tested after ECA pressing through Route 2, is illustrated in Fig. 7. High strain rate superplasticity (HSR SP) is normally defined as a high tensile elongation at a strain rate faster than 10^{-2} s^{-1}. Thus, the present set of results provide a remarkable demonstration of the ability to attain HSR SP in a non-superplastic commercial aluminum alloy solely by subjecting the material to ECA pressing in order to introduce an ultra-fine grain size. In Al-based materials, the occurrence of HSR SP has been confined to date to a limited range of metal matrix composites, mechanically alloyed materials and alloys processed using powder metallurgy techniques [19]. These results show the potential for achieving even higher elongations and HSR SP in conventional commercial aluminum alloys.

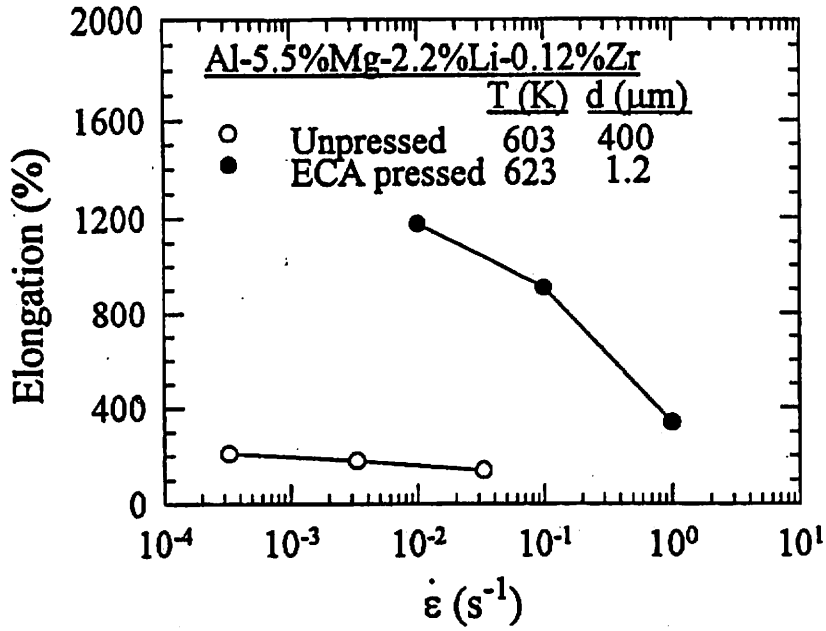

Fig. 6 Elongation versus strain rate after ECA pressing through Route 2 and without ECA pressing.

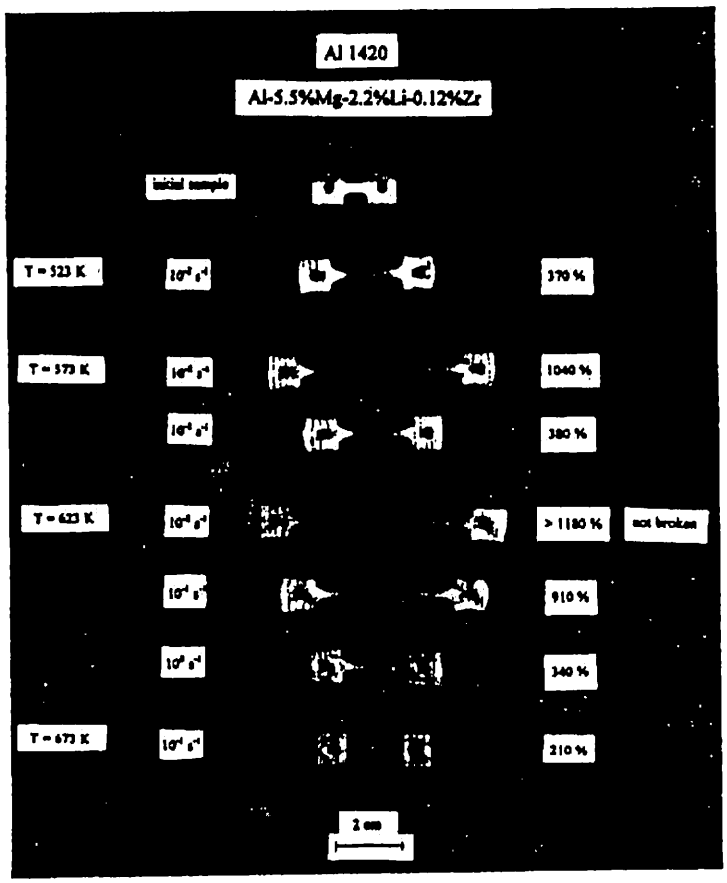

Fig. 7 Appearance of tensile specimens processed using Route 2 and tested at temperatures from 523 to 673 K: there is clear evidence for high strain rate superplasticity at 573 and 623 K.

ACKNOWLEDGEMENTS

This work was supported in part by the Light Metals Educational Foundation of Japan, in part by a Grant-in-Aid for Scientific Research from the Ministry of Education, Science, Sports and Culture of Japan, in part by the National Science Foundation of the United States under Grants No. INT-9602919 and DMR-9625969 and in part by the U.S. Army Research Office under Grants No. DAAH04-96-1-0332 and N68171-96-6-9006.

REFERENCES

1. T.G. Langdon, Metall. Trans., Vol. 13A (1982), p. 689.
2. T.G. Langdon, Recent Advances in Science, Technology and Applications of Zn-Al Alloys (G. Torres-Villaseñor, Y. Zhu and C. Piña-Barba, eds), p. 177. Universidad Autónoma de México, Mexico City (1994).
3. F.A. Mohamed, M.M.I. Ahmed and T.G. Langdon, Metall. Trans., Vol. 8A (1977), p. 933.
4. Y. Ma, M. Furukawa, Z. Horita, M. Nemoto, R.Z. Valiev and T.G. Langdon, Mater. Trans. JIM, Vol. 37 (1996), p. 336.
5. I.N. Fridlyander, V.S. Sandler and T.I. Nikol'skaya, Fiz. Metal. Metalloved., Vol. 32 (1971), p. 767.
6. V.M. Segal, V.I. Reznikov, A.E. Drobyshevskiy and V.I. Kopylov, Metally, Vol. 1 (1981), p. 115 [English translation in Russian Metallurgy, Vol. 1 (1981), p. 99].
7. R.Z. Valiev and N.K. Tsenev, Hot Deformation of Aluminum Alloys (T.G. Langdon, H.D. Merchant, J.G. Morris and M.A. Zaidi, eds), p. 319. The Minerals, Metals and Materials Society, Warrendale, PA (1991).
8. R.Z. Valiev, N.A. Krasilnikov and N.K. Tsenev, Mater. Sci. Engng., Vol. A137 (1991), p. 35.
9. Y. Iwahashi, J. Wang, Z. Horita, M. Nemoto and T.G. Langdon, Scripta Mater., Vol. 35 (1996), p. 143.
10. M. Furukawa, Y. Iwahashi, Z. Horita, M. Nemoto, N.K. Tsenev, R.Z. Valiev and T.G. Langdon, Acta Mater. (in press).
11. M. Furukawa, P.B. Berbon, Z. Horita, M. Nemoto, N.K. Tsenev, R.Z. Valiev and T.G. Langdon, Metall. Mater. Trans. (submitted for publication).
12. J. Wang, Y. Iwahashi, Z. Horita, M. Furukawa, M. Nemoto, R.Z. Valiev and T.G. Langdon, Acta Mater., Vol. 44 (1996), p. 2973.
13. M. Furukawa, Z. Horita, M. Nemoto, R.Z. Valiev and T.G. Langdon, Acta Mater., Vol. 44 (1996), p. 4619.
14. R.Z. Valiev, F. Chmelik, F. Bordeaux, G. Kapelski and B. Baudelet, Scripta Metall., Vol. 27 (1992), p. 855.
15. H. Ueda, A. Matsui, M. Furukawa, Y. Miura and M. Nemoto, J. Japan Inst. Metals, Vol. 49 (1985), p. 562.
16. J.M. Papazian, R.L. Schulte and P.N. Adler, Metall. Trans., Vol. 17A (1986), p. 635.
17. M. Ahmad, Metall. Trans., Vol. 18A (1987), p. 681.
18. P. Berbon, M. Furukawa, Z. Horita, M. Nemoto, N.K. Tsenev, R.Z. Valiev and T.G. Langdon, Mater. Sci. Forum, Vol. 217-222 (1996), p. 1013.
19. K. Higashi, M. Mabuchi and T.G. Langdon, ISIJ Intl., Vol. 36 (1996), p. 1423.

Fabrication of Bulk Ultrafine-Grained Materials through Intense Plastic Straining

PATRICK B. BERBON, NIKOLAI K. TSENEV, RUSLAN Z. VALIEV, MINORU FURUKAWA, ZENJI HORITA, MINORU NEMOTO, and TERENCE G. LANGDON

Ultrafine grain sizes were introduced into samples of an Al-3 pct Mg solid solution alloy and a cast Al-Mg-Li-Zr alloy using the process of equal-channel angular (ECA) pressing. The Al-3 pct Mg alloy exhibited a grain size of ~0.23 μm after pressing at room temperature to a strain of ~4, but there was significant grain growth when the pressed material was heated to temperatures above ~450 K. The Al-Mg-Li-Zr alloy exhibited a grain size of ~1.2 μm, and the microstructure was heterogeneous after pressing to a strain of ~4 at 673 K and homogeneous after pressing to a strain of ~8 at 673 K with an additional strain of ~4 at 473 K. The heterogeneous material exhibited superplastic-like flow, but the homogeneous material exhibited high-strain-rate superplasticity with an elongation of >1000 pct at 623 K at a strain rate of 10^{-2} s^{-1}. It is concluded that a homogeneous microstructure is required, and therefore a high pressing strain, in order to attain high-strain-rate superplasticity (HSR SP) in ultrafine-grained materials.

I. INTRODUCTION

SEVERAL methods are available for the processing of materials with ultrafine grain sizes, including inert gas condensation,[1,2] high-energy ball milling,[3] and sliding wear.[4] These procedures are attractive for producing materials with grain sizes within the nanometer range, but there are disadvantages because some residual porosity remains after fabrication and it is difficult to use these techniques to make large bulk samples. As a consequence of these difficulties, much attention has been given to the alternative procedure of introducing an ultrafine grain size in a material through intense plastic straining.

Torsion straining under a high pressure[5] and equal-channel angular (ECA) pressing,[6] in which a sample is pressed through a die with no change in the cross-sectional area, are two methods currently under investigation for the fabrication of materials with ultrafine grain sizes.[7-11] Although it is possible, in principle, to use these procedures to produce materials within the nanometer range, the grain sizes attained by these techniques are often in the submicrometer range of ~0.1 to 1.0 μm. Despite this possible limitation, however, ECA pressing is an especially attractive procedure because it is a simple process which may be readily adapted for a wide range of materials, the processed samples are free of any porosity, and there is the potential for fabricating large bulk samples which may be subsequently utilized in a wide range of applications.

In the superplastic forming (SPF) industry, for example, it is well established that SPF becomes a viable processing tool only for high-added-value products in medium to low production runs of, typically, ~50 to 5000 pieces.[12] This limitation on SPF technology arises primarily because of the relatively low forming speeds (typically up to ~10^{-3} s^{-1}[13]) and the consequently long forming times (~20 to 30 minutes). However, there is experimental evidence from superplastic alloys that a decrease in grain size will lead both to an increase in the superplastic capability of the material and to the occurrence of optimum superplasticity at faster strain rates.[14] This experimental observation has led to the suggestion that a reduction in grain size from the standard superplastic range of ~1 to 10 μm into the submicrometer range may provide the possibility of attaining superplastic deformation at faster strain rates,[15] thereby potentially expanding the utility of SPF technology so that it becomes a viable process for a much wider range of applications.

In the present article, experiments are described which were designed to provide a useful submicrometer grain size in selected aluminum-based alloys. As will be demonstrated, ECA pressing is a valuable tool for achieving an ultrafine grain size in the submicrometer range, but the subsequent thermal stability of these very small grains depends critically, at least in aluminum alloys, upon the presence of precipitates which are necessary to restrict grain growth at elevated temperatures.

II. EXPERIMENTAL MATERIALS AND PROCEDURES

Initially, experiments were conducted using an Al-3 pct Mg solid solution alloy with an as-received grain size of ~500 μm. Subsequently, the experiments were extended to

PATRICK B. BERBON, Research Assistant, Department of Materials Science, and TERENCE G. LANGDON, Professor, Departments of Materials Science and Mechanical Engineering, are with the University of Southern California, Los Angeles, CA 90089-1453. NIKOLAI K. TSENEV, Senior Scientist, is with the Institute of Chemical Technology, Ufa State Petroleum Technical University, Ufa 450062, Russia. RUSLAN Z. VALIEV, Professor, is with the Institute of Physics of Advanced Materials, Ufa State Aviation Technical University, Ufa 450000, Russia. MINORU FURUKAWA, Associate Professor, is with the Department of Technology, Fukuoka University of Education, Murakata Fukuoka 811-41, Japan. ZENJI HORITA, Associate Professor, and MINORU NEMOTO, Professor, are with the Department of Materials Science and Engineering, Kyushu University, Fukuoka 812-81, Japan.

This article is based on a presentation made in the symposium "Mechanical Behavior of Bulk Nanocrystalline Solids," presented at the 1997 Fall TMS Meeting and Materials Week, September 14–18, 1997, in Indianapolis, Indiana, under the auspices of the Mechanical Metallurgy (SMD), Powder Materials (MDMD), and Chemistry and Physics of Materials (EMPMD/SMD) Committees.

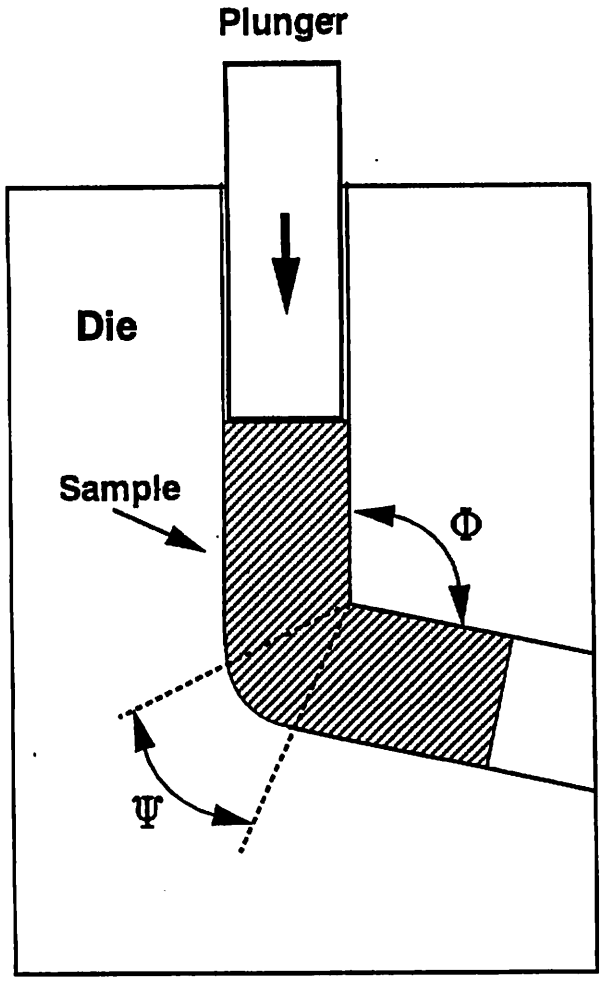

Fig. 1—Schematic illustration of the ECA pressing facility.

include a commercially cast Al-5.5 pct Mg-2.2 pct Li-0.12 pct Zr alloy, designated 01420, with an initial grain size in the hot-rolled condition of ~400 μm. Further details are given elsewhere concerning the processing and properties of the Al-3 pct Mg[11,16,17] and the Al-Mg-Li-Zr[18,19] alloys.

The ECA pressing was conducted using the facility illustrated schematically in Figure 1. Two channels, equal in cross section, intersect within a die. The test sample is machined to fit tightly within the die and it is then pressed through the die using a plunger. The strain imposed on the sample in a single passage through the die is determined by the values of the two angles, Φ and Ψ, shown in Figure 1. Since the cross section of the sample is unchanged by passage through the die, additional pressings may be conducted on the same sample to attain a high strain. It has been shown theoretically,[20] and confirmed experimentally,[21] that the strain associated with a total of N pressings through the die (ε_N) may be expressed as

$$\varepsilon_N = \frac{N}{\sqrt{3}}\left[2\cot\left(\frac{\Phi}{2}+\frac{\Psi}{2}\right)+\Psi\,\mathrm{cosec}\left(\frac{\Phi}{2}+\frac{\Psi}{2}\right)\right] \quad [1]$$

In the present experiments, the die was constructed with Φ = 90 deg and Ψ ≃ 0 deg, so that, from Eq. [1], a strain of ~1 is introduced in each passage through the die.

The Al-3 pct Mg alloy was pressed in air at room temperature for four passes through the die, equivalent to a strain of ~4. The Al-Mg-Li-Zr alloy was pressed in air either at a temperature of 673 K for four passes, to give a strain of ~4, or for eight passes at 673 K and an additional four passes at 473 K, to give a total strain of ~12, with the samples cooled in air between consecutive pressings. For convenience, these two procedures are designated routes 1 and 2, respectively, and it should be noted that the lower temperature of 473 K was selected for the final four passes in route 2 in order to minimize grain growth.

Static annealing experiments were conducted to investigate the stability of the ultrafine grain structures after ECA pressing. Samples were annealed for 1 hour over a range of selected temperatures which were held constant to within ±1 K. Specimens were prepared for examination by transmission electron microscopy (TEM) using the procedure described earlier.[11]

Tensile tests were conducted after ECA pressing by machining specimens with gage sections of 3 × 2 mm² parallel to the longitudinal axis of the pressed samples. All specimens were pulled in air under selected conditions of temperature and strain rate and using an Instron testing machine operating at a constant rate of crosshead displacement. Testing temperatures were held constant to within ±2 K during each test. For comparison purposes, some additional tensile tests were also conducted on the Al-Mg-Li-Zr alloy in the hot-rolled condition without ECA pressing.

III. EXPERIMENTAL RESULTS

A. *Al-3 Pct Mg Alloy*

Figure 2 shows typical examples, at two different magnifications, of the internal structure in the Al-3 pct Mg alloy after ECA pressing at room temperature to a strain of ~4; also included are selected-area electron diffraction (SAED) patterns obtained from regions with a diameter of 1.9 μm. It is apparent from Figure 2, and was confirmed by detailed inspection, that the microstructure was essentially homogeneous in the Al-3 pct Mg alloy in the ECA-pressed condition but the grain boundaries were often poorly delineated, as is evident in Figure 2(b), thereby suggesting that many of the boundaries were in a nonequilibrium configuration.[22,23] The SAED patterns demonstrate that the grain boundaries have high angles of misorientation, and measurements showed that the mean linear intercept grain size in the alloy in this condition was ~0.23 μm.

The stability of the grain structure at elevated temperatures was investigated by annealing a series of samples for 1 hour over a wide range of temperatures up to 803 K. Figure 3 shows the variation of grain size with annealing temperature for the Al-3 pct Mg alloy processed by ECA pressing: data points are included also for the same alloy processed by torsion straining[16] and for the Al-Mg-Li-Zr alloy processed by ECA pressing and discussed in Section III–B. It is apparent from this plot that the grain size of the Al-3 pct Mg alloy increases rapidly at temperatures above ~450 K, such that the grain size is >100 μm at the highest annealing temperatures. The results documented in Figure 3 for the Al-3 pct Mg alloy are also very similar to data

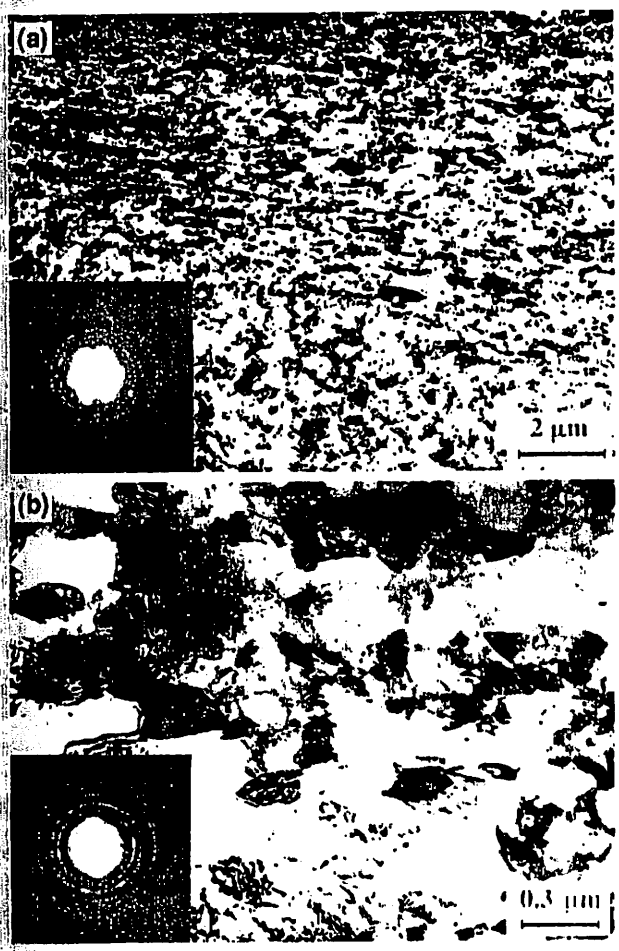

Fig. 2—Representative microstructures in the Al-3 pct Mg alloy after ECA pressing at (*a*) low and (*b*) high magnifications.

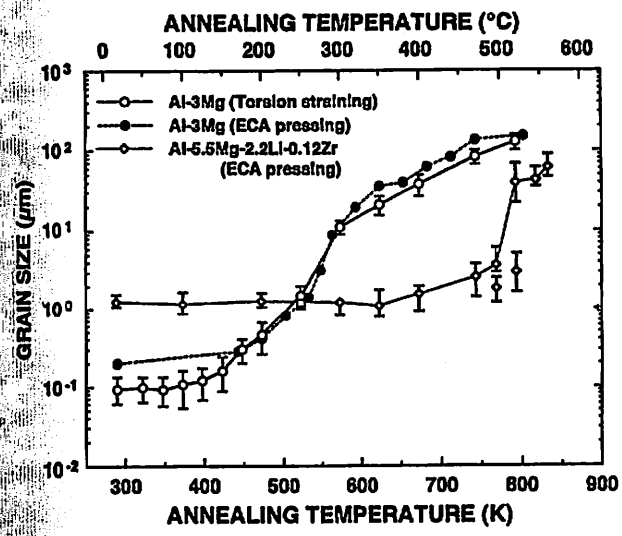

Fig. 3—Variation of grain size with annealing temperature for the Al-3 pct Mg alloy and the Al-Mg-Li-Zr alloy processed by ECA pressing and for an Al-3 pct Mg alloy processed by torsion straining.[16]

reported for an Al-1.5 pct Mg alloy where an ultrafine grain size was introduced by torsion straining.[24]

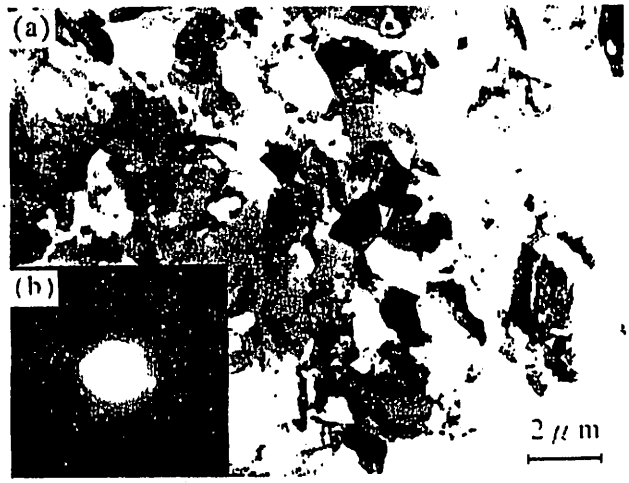

(*a*)

(*b*)

Fig. 4—Representative microstructures in the Al-Mg-Li-Zr alloy after ECA pressing through (*a*) route 1 and (*b*) route 2, respectively.

It is well known that superplasticity is a diffusion-controlled process requiring temperatures on the order of at least ~0.5 T_m, where T_m is the absolute melting temperature of the material.[25] Therefore, the inability to retain an ultrafine grain size at the submicrometer level in the Al-3 pct Mg alloy at temperatures above ~450 K, corresponding to ~0.48 T_m, implies that the submicrometer grain size achieved by ECA pressing will be unstable within the temperature range associated with high superplastic ductilities. These results suggest that it may be preferable to investigate the ECA pressing of an aluminum-based alloy containing precipitates to inhibit grain growth; these experiments are described in Section B.

B. *Al-Mg-Li-Zr Alloy*

The commercial Al-Mg-Li-Zr alloy was subjected to ECA pressing, and Figure 4 shows the microstructures in the alloy and the associated SAED patterns after ECA pressing through (a) route 1 and (b) route 2, respectively. A more detailed description of the processing through route 1 was given earlier,[18,19] and it was reported that the micro-

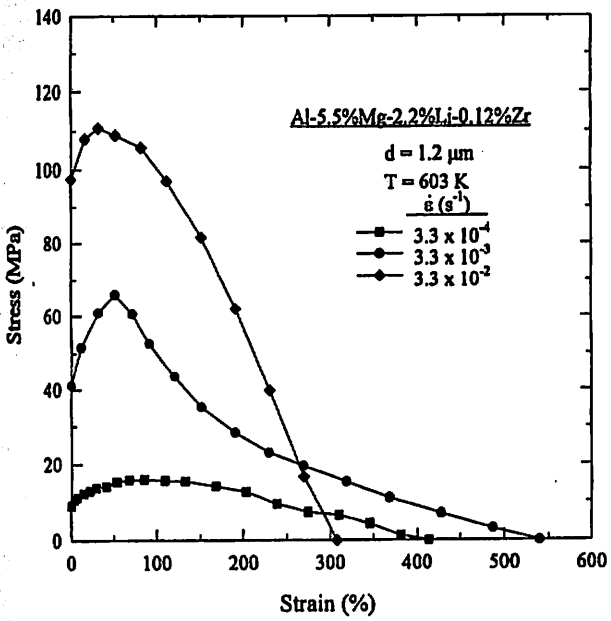

Fig. 5—True stress *vs* strain at 603 K for the Al-Mg-Li-Zr alloy after processing *via* route 1.

structure of this material showed heterogeneity with some areas having arrays of grain boundaries with high angles of misorientation, as in Figure 4(a), and other areas having arrays of subgrain boundaries with low angles of misorientation. Careful measurements revealed that, for this condition with a total strain from ECA pressing of ~4, there was a volume fraction of ~60 to 70 pct of grains with high-angle boundaries and ~30 to 40 pct of subgrains with low-angle boundaries. Despite the difference in boundary misorientations, measurements of the grain size and the subgrain size gave identical values of ~1.2 μm. The presence of marked heterogeneity after processing *via* route 1 suggests that a strain of ~4 in ECA pressing is insufficient to attain a stable homogeneous microstructure in this alloy.

By contrast, careful examination of the alloy processed *via* route 2 to a strain of ~12 revealed a homogeneous microstructure consisting of an array of grains separated by boundaries having high angles of misorientation. The microstructure in this condition is shown in Figure 4(b), and measurements gave a grain size of ~1.2 μm which is identical to the grain size measured after processing *via* route 1. It is reasonable to conclude from these measurements, therefore, that higher strains in ECA pressing permit a homogenization of the microstructure through boundary evolution but with no concomitant refinement in the microstructure. This conclusion is consistent with observations of the evolution of the ultrafine grains and the changes in the boundary misorientations during the ECA pressing of pure Al.[26]

Static annealing experiments were conducted after ECA pressing of the Al-Mg-Li-Zr alloy processed by route 1, and the data points are included in Figure 3. Inspection shows that the commercial Al-Mg-Li-Zr alloy differs from the Al-3 pct Mg solid solution alloy in two important respects. First, the grain size of ~1.2 μm introduced into the Al-Mg-Li-Zr alloy after a strain of ~4 is significantly larger than the grain size of ~0.23 μm obtained by ECA pressing of the Al-3 pct Mg alloy. Second, despite the larger as-pressed grain size in the Al-Mg-Li-Zr alloy, the grain configuration is remarkably stable up to temperatures as high as ~750 K, corresponding to a homologous temperature of ~0.80 T_m. Therefore, processing *via* route 1 leads to an ultrafine grain size which is stable within the anticipated temperature range for superplasticity. As noted earlier,[18] the explanation for the very marked grain stability in the Al-Mg-Li-Zr alloy lies in the stability of the β'-Al_3Zr precipitates at these high temperatures. By contrast, the fine δ'-Al_3Li precipitates are not stable and dissolve at these temperatures.

It is important to note also that the stability of the microstructure at temperatures in the range of ~600 to 700 K has two significant consequences. First, this temperature range is attractive because it avoids the problems of Li and Mg depletion which readily occur in Al-Mg-Li alloys at higher temperatures.[27,28,29] Second, the presence of this very small and stable grain size at high temperatures suggests the potential for fulfilling the well-established need for an SPF capability in Al-Li alloys at temperatures below ~700 K.[30]

Figure 5 shows a plot of the true stress (σ) *vs* the strain (ε) for three samples of the Al-Mg-Li-Zr alloy processed *via* route 1 and tested in tension at an absolute temperature (T) of 603 K and at strain rates ($\dot{\varepsilon}$) from 3.3×10^{-4} to 3.3×10^{-2} s^{-1}; as indicated, the grain size (d) in this condition is 1.2 μm. The three curves in Figure 5 show an initial brief period of strain hardening, which is probably associated with a relaxation of the high internal stresses introduced by the ECA pressing, followed by a period of strain weakening and ultimate failure. It is apparent, from this plot, that high tensile ductilities may be achieved in this alloy after ECA pressing even in the presence of a heterogeneous microstructure *via* route 1: for example, the elongation to failure is ~550 pct at the intermediate strain rate of 3.3×10^{-3} s^{-1}.

Figure 6 shows stress-strain curves obtained on the Al-Mg-Li-Zr alloy after processing through route 2 for a range of strain rates and for testing temperatures of (a) 523, (b) 573, (c) 623, and (d) 673 K, respectively. Inspection shows that the alloy is remarkably ductile in this homogeneous condition. At 523 K, for example, the total ductility of ~620 pct at $\dot{\varepsilon} = 10^{-3}$ s^{-1} is even higher than the ductility achieved with the alloy processed *via* route 1 at the higher testing temperature of 623 K (Figure 5). At 573 K, the highest elongation is ~1040 pct at a strain rate of 10^{-2} s^{-1}, whereas at 623 K the test conducted at a strain rate of 10^{-2} s^{-1} was discontinued without failure at an elongation of 1180 pct. At a testing temperature of 673 K, corresponding to the ECA pressing temperature for the initial eight passes, the elongations are substantially reduced but the flow stresses are increased. Inspection by TEM after tensile testing revealed the occurrence of significant grain growth under dynamic conditions at this temperature.

Based on these limited data, a strain rate of 10^{-2} s^{-1} at a temperature of 623 K appears to be an optimum condition for the development of very high tensile ductility in this alloy. Figure 7 shows the appearance of the microstructure in the sample tested in tension at 623 K to an elongation of 1180 pct without failure. Careful measurements showed

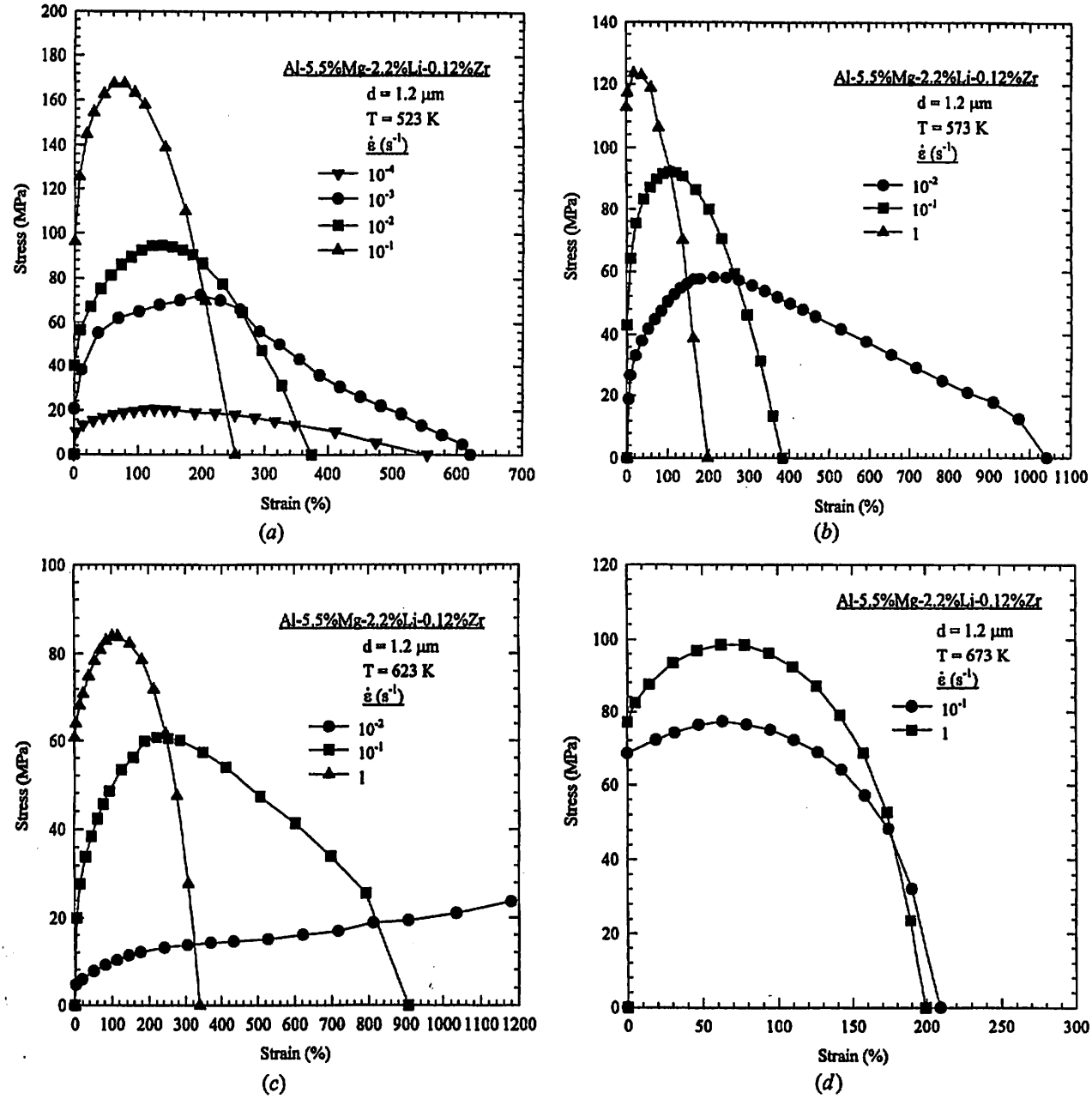

Fig. 6—True stress *vs* strain for the Al-Mg-Li-Zr alloy after processing *via* route 2 at temperatures of (*a*) 523 K, (*b*) 573 K, (*c*) 623 K, and (*d*) 673 K.

there was a very small increase in the grain size in this sample to a value of ~2.0 μm.

Figure 8 provides, for similar testing temperatures in the vicinity of 610 K, a direct comparison of the elongations obtained as a function of strain rate for the unpressed Al-Mg-Li-Zr alloy with a large grain size (open points) and for the two materials subjected to ECA pressing to strains of ~4 (route 1) and ~12 (route 2), respectively. Thus, the unpressed alloy exhibits only modest elongations even at the lowest experimental strain rate, whereas processing *via* route 1 to produce a heterogeneous microstructure gives superplastic-like flow and elongations of up to >500 pct, and processing *via* route 2 to produce a homogeneous microstructure gives exceptionally high elongations to failure and these superplastic elongations occur at very high strain rates.

IV. DISCUSSION

High-strain-rate superplasticity (HSR SP) is defined formally as the occurrence of superplasticity at strain rates faster than 10^{-2} s^{-1}.[31] Therefore, it is clear that the results obtained with the Al-Mg-Li-Zr alloy at a temperature of 623 K after processing *via* route 2, as documented in Figure 8, represent an example of the occurrence of HSR SP in a commercial alloy fabricated by casting. A similar example of HSR SP after ECA pressing has been reported also *in a*

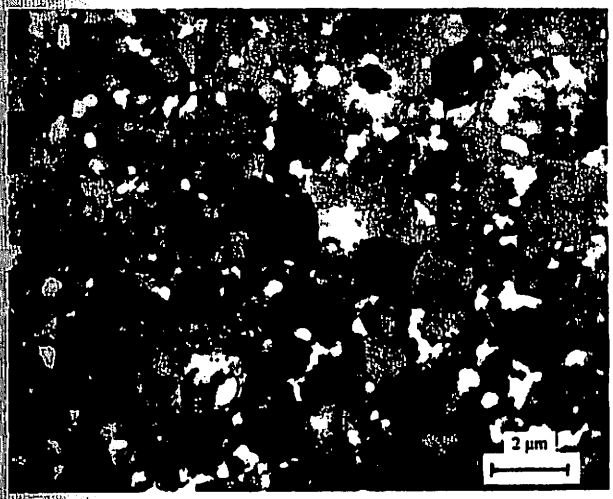

Fig. 7—Microstructure in the Al-Mg-Li-Zr alloy after processing *via* route 2 and pulling to an elongation of 1180 pct without failure at 623 K using a strain rate of 10^{-2} s^{-1}.

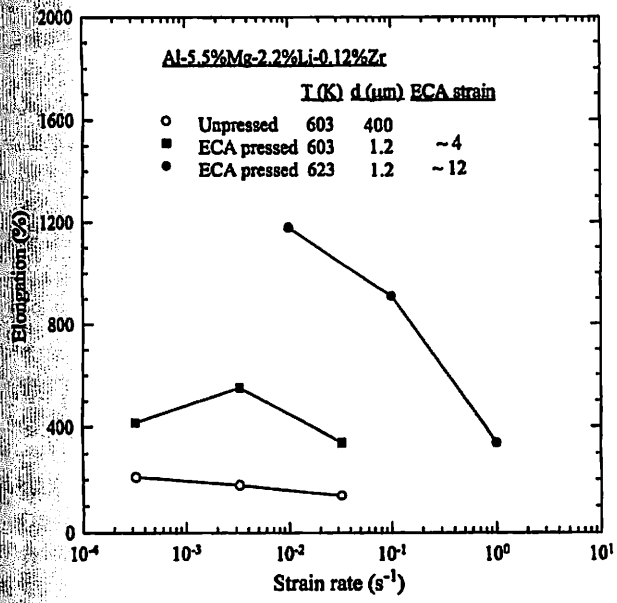

Fig. 8—Elongation *vs* testing strain rate at temperatures in the vicinity of 610 K for the Al-Mg-Li-Zr alloy in the unpressed condition and after ECA pressing *via* route 1 to a strain of ~4 and *via* route 2 to a strain of ~12.

commercially cast Al-2004 alloy known as Supral 100 and containing Al-6 pct Cu-0.4 pct Zr.[32]

These results demonstrate that, contrary to current understanding,[33] HSR SP in Al-based materials is not restricted exclusively to a limited range of metal matrix composites, mechanically alloyed materials, and alloys processed using powder metallurgy techniques. Furthermore, the temperature of 623 K recorded in Figure 8 corresponds to a homologous temperature of only ~0.67 T_m, thereby demonstrating that, contrary to observations in some alloys and metal matrix composites,[34,35] HSR SP is achieved in the Al-Mg-Li-Zr alloy without the occurrence of local melting at the grain boundaries.

An important observation in these experiments is that HSR SP is attained when processing the Al-Mg-Li-Zr alloy to a strain of ~12 (route 2) but the elongations to failure are much lower when the alloy is processed only to a strain of ~4 (route 1). This difference arises because superplasticity occurs by the process of grain boundary sliding,[36] and it is well established that the presence of a reasonably large number of grain boundaries having low angles of misorientation will serve to substantially limit the ability of a material to exhibit high tensile ductilities.[37] Therefore, it is concluded that ECA pressing must always be continued to a sufficiently high strain in order to develop a homogeneous microstructure that will permit a realization of the special mechanical characteristics associated with the presence of an ultrafine grain size. This is particularly true in any attempt to achieve superplastic flow, where the occurrence of grain boundary sliding necessitates the development of an array of boundaries having high angles of misorientation.

V. SUMMARY AND CONCLUSIONS

1. Samples of an Al-3 pct Mg alloy and a commercial Al-Mg-Li-Zr alloy were subjected to ECA pressing in order to attain an ultrafine grain size.
2. The Al-3 pct Mg alloy was pressed at room temperature to a strain of ~4, giving a grain size of ~0.23 μm. Static annealing showed this grain size was unstable at temperatures above ~450 K.
3. The Al-Mg-Li-Zr alloy was pressed either to a strain of ~4 at 673 K (route 1) or to a strain of ~8 at 673 K, and then to an additional strain of ~4 at 473 K, to give a total strain of ~12 (route 2).
4. The Al-Mg-Li-Zr alloy processed *via* route 1 had a heterogeneous microstructure with a grain size of ~1.2 μm. This material exhibited superplastic-like flow at 603 K with an elongation of ~550 pct at a strain rate of ~10^{-3} s^{-1}.
5. The Al-Mg-Li-Zr alloy processed *via* route 2 had a homogeneous microstructure with a grain size of ~1.2 μm. This material exhibited HSR SP, with a maximum elongation of 1180 pct without failure at a temperature of 623 K using a strain rate of 10^{-2} s^{-1}.
6. High-strain-rate superplasticity can be attained in cast alloys by introducing an ultrafine grain size through ECA pressing, but the results demonstrate that it is necessary to press to a sufficiently high strain in order to develop a homogeneous microstructure.

ACKNOWLEDGMENTS

This work was supported in part by the Light Metals Educational Foundation of Japan, in part by a Grant-in-Aid for Scientific Research from the Ministry of Education, Science, Sports and Culture of Japan, in part by the National Science Foundation of the United States under Grant Nos. DMR-9625969 and INT-9602919, and in part by the United States Army Research Office under Grant Nos. DAAH04-96-1-0332 and N68171-96-6-9006.

REFERENCES

1. H. Gleiter: in *Deformation of Polycrystals: Mechanisms and Microstructures* N. Hansen, A. Horsewell, T. Leffers, and H. Lilholt, eds., Risø National Laboratory, Roskilde, Denmark, 1981, pp. 15-21.

2. P.G. Sanders, G.E. Fougere, L.J. Thompson, J.A. Eastman, and J.R. Weertman: *Nanostruct. Mater.*, 1997, vol. 8, pp. 243-52.
3. C.C. Koch and Y.S. Cho: *Nanostruct. Mater.*, 1992, vol. 1, pp. 207-12.
4. D.A. Rigney: *Ann. Rev. Mater. Sci.*, 1988, vol. 18, pp. 141-63.
5. N.A. Smirnova, V.I. Levit, V.I. Pilyugin, R.I. Kuznetsov, L.S. Davydova, and V.A. Sazonova: *Fiz. Met. Metalloved.*, 1986, vol. 61, pp. 1170-77.
6. V.M. Segal, V.I. Reznikov, A.E. Drobyshevskiy, and V.I. Kopylov: *Russ. Metall. (Metally)*, 1981, vol. 1, pp. 99-105.
7. R.Z. Valiev and N.K. Tsenev: in *Hot Deformation of Aluminum Alloys*, T.G. Langdon, H.D. Merchant, J.G. Morris, and M.A. Zaidi, eds., TMS, Warrendale, PA, 1991, pp. 319-29.
8. R.Z. Valiev, N.A. Krasilnikov, and N.K. Tsenev: *Mater. Sci. Eng.*, 1991, vol. A137, pp. 35-40.
9. J. Languillaume, F. Chmelik, G. Kapelski, F. Bordeaux, A.A. Nazarov, G. Cunova, C. Esling, R.Z. Valiev, and B. Baudelet: *Acta Metall. Mater.*, 1993, vol. 41, pp. 2953-62.
10. Z. Horita, D.J. Smith, M. Furukawa, M. Nemoto, R.Z. Valiev, and T.G. Langdon: *J. Mater. Res.*, 1996, vol. 11, pp. 1880-90.
11. J. Wang, Y. Iwahashi, Z. Horita, M. Furukawa, M. Nemoto, R.Z. Valiev, and T.G. Langdon: *Acta Mater.*, 1996, vol. 44, pp. 2973-82.
12. A.J. Barnes: *Mater. Sci. Forum*, 1994, vols. 170–172, pp. 701-14.
13. R. Sawle: in *Superplastic Forming of Structural Alloys*, N.E. Paton and C.H. Hamilton, eds., TMS-AIME, Warrendale, PA, 1982, pp. 307-17.
14. F.A. Mohamed, M.M.I. Ahmed, and T.G. Langdon: *Metall. Trans. A*, 1977, vol. 8A, pp. 933-38.
15. Y. Ma, M. Furukawa, Z. Horita, M. Nemoto, R.Z. Valiev, and T.G. Langdon: *Mater. Trans. JIM*, 1996, vol. 37, pp. 336-39.
16. M. Furukawa, Z. Horita, M. Nemoto, R.Z. Valiev, and T.G. Langdon: *Acta Mater.*, 1996, vol. 44, pp. 4619-29.
17. J. Wang, M. Furukawa, Z. Horita, M. Nemoto, R.Z. Valiev, and T.G. Langdon: *Mater. Sci. Eng.*, 1996, vol. A216, pp. 41-46.
18. M. Furukawa, Y. Iwahashi, Z. Horita, M. Nemoto, N.K. Tsenev, R.Z. Valiev, and T.G. Langdon: *Acta Mater.*, 1997, vol. 45, pp. 4751-57.
19. M. Furukawa, P.B. Berbon, Z. Horita, M. Nemoto, N.K. Tsenev, R.Z. Valiev, and T.G. Langdon: 1998, unpublished research.
20. Y. Iwahashi, J. Wang, Z. Horita, M. Nemoto, and T.G. Langdon: *Scripta Mater.*, 1996, vol. 35, pp. 143-46.
21. Y. Wu and I. Baker: *Scripta Mater.*, 1997, vol. 37, pp. 437-42.
22. R.Z. Valiev, R.Sh. Musalimov, and N.K. Tsenev: *Phys. Status Solidi A*, 1989, vol. 115, pp. 451-57.
23. A.A. Nazarov, A.E. Romanov, and R.Z. Valiev: *Acta Metall. Mater.*, 1993, vol. 41, pp. 1033-40.
24. R.Z. Valiev, F. Chmelik, F. Bordeaux, G. Kapelski, and B. Baudelet: *Scripta Metall. Mater.*, 1992, vol. 27, pp. 855-60.
25. T.G. Langdon: *Metall. Trans. A*, 1982, vol. 13A, pp. 689-701.
26. Y. Iwahashi, Z. Horita, M. Nemoto, and T.G. Langdon: *Acta Mater.*, 1997, vol. 45, pp. 4733-41.
27. H. Ueda, A. Matsui, M. Furukawa, Y. Miura, and M. Nemoto: *J. Jpn. Inst. Met.*, 1985, vol. 49, pp. 562-68.
28. J.M. Papazian, R.L. Schulte, and P.N. Adler: *Metall. Trans. A*, 1986, vol. 17A, pp. 635-43.
29. M. Ahmad: *Metall. Trans. A*, 1987, vol. 18A, pp. 681-89.
30. H.P. Pu, F.C. Liu, and J.C. Huang: *Metall. Mater. Trans. A*, 1995, vol. 26A, pp. 1153-66.
31. K. Higashi, M. Mabuchi, and T.G. Langdon: *Iron Steel Inst. Jpn. Int.*, 1996, vol. 36, pp. 1423-38.
32. R.Z. Valiev, D.A. Salimonenko, N.K. Tsenev, P.B. Berbon, and T.G. Langdon: *Scripta Mater.*, 1997, vol. 37, pp. 1945-50.
33. T.G. Nieh, J. Wadsworth, and O.D. Sherby: *Superplasticity in Metals and Ceramics*, Cambridge University Press, Cambridge, United Kingdom, 1997, pp. 154-67.
34. T.G. Nieh, J. Wadsworth, and T. Imai: *Scripta Metall.*, 1992, vol. 26, pp. 703-08.
35. M. Mabuchi and K. Higashi: *Phil. Mag. Lett.*, 1994, vol. 70, pp. 1-6.
36. T.G. Langdon: *Mater. Sci. Eng.*, 1994, vol. A174, pp. 225-30.
37. R. Crooks, S.J. Hales, and T.R. McNelley: in *Superplasticity and Superplastic Forming*, C.H. Hamilton and N.E. Paton, eds., TMS, Warrendale, PA, 1988, pp. 389-93.

Microstructural Characteristics of Ultrafine-Grained Aluminum Produced Using Equal-Channel Angular Pressing

YOSHINORI IWAHASHI, MINORU FURUKAWA, ZENJI HORITA, MINORU NEMOTO, and TERENCE G. LANGDON

The shearing associated with equal-channel angular (ECA) pressing was examined using optical microscopy. Samples of pure Al with a large grain size were subjected to ECA pressing to different strains and then examined on three orthogonal planes. Samples were pressed without any rotation or with rotations of either 90 or 180 deg between each consecutive pressing. The experimental observations are compared with models which predict the shearing characteristics associated with ECA pressing under different conditions. It is demonstrated that there is good agreement, in terms of both the grain elongation and the shearing within individual grains, between the experimental results and the predictions of the models.

I. INTRODUCTION

THERE is considerable current interest in the processing procedure of equal-channel angular (ECA) pressing in which an intense plastic strain is introduced into a sample through simple shear.[1] It is now established that this procedure provides the capability of producing an ultrafine grain size, in the submicrometer or nanometer range, in large-grained polycrystalline samples.[2,3] To date, there have been numerous reports describing the use of ECA pressing for the fabrication of a wide range of ultrafine-grained materials.[4–17]

Most of the investigations of ECA pressing to date have concentrated primarily on examining the microstructures and properties of selected materials after pressing to a relatively large strain. Recently, an investigation was reported in which transmission electron microscopy (TEM) was used to monitor the microstructural evolution as a function of strain in samples of pure aluminum.[15] However, there have been no similar investigations using optical microscopy.

The present investigation was initiated in order to alleviate this deficiency. Experiments were conducted on pure aluminum with the objective of examining, using optical microscopy, the macroscopic characteristics of ECA pressing as a function of the total imposed strain. The results from these experiments are described in this report and, in addition, it is demonstrated that there is a very good correlation between the experimental observations and the predicted shearing patterns introduced into the samples during the ECA pressing procedure.

YOSHINORI IWAHASHI, formerly Research Assistant with the Department of Materials Science and Engineering, Kyushu University, is Staff Engineer, Mitsubishi Fukahori, Heavy Industries, Ltd., Nagasaki Shipyard and Machinery Works, Munakaka, Nagasaki 851-03, Japan. MINORU FURUKAWA, Associate Professor, is with the Department of Technology, Fukuoka University of Education, Fukuoka 811-41, Japan. ZENJI HORITA, Associate Professor, and MINORU NEMOTO, Professor, are with the Department of Materials Science and Engineering, Kyushu University, Fukuoka 812-81, Japan. TERENCE G. LANGDON, Professor, is with the Departments of Materials Science and Mechanical Engineering, U.S.C., Los Angeles, CA 90089-1453.

This article is based on a presentation made in the symposium "Mechanical Behavior of Bulk Nanocrystalline Solids," presented at the 1997 Fall TMS Meeting and Materials Week, September 14-18, 1997, in Indianapolis, Indiana, under the auspices of the Mechanical Metallurgy (SMD), Powder Materials (MDMD), and Chemistry and Physics of Materials (EMPMD/SMD) Committees.

II. EXPERIMENTAL MATERIAL AND PROCEDURES

The experiments were conducted using samples of aluminum of 99.99 pct purity. An aluminum ingot was rolled into a plate at room temperature and samples were cut for ECA pressing with dimensions of $10 \times 10 \times 75$ mm^3. Each sample was annealed for 1 hour at 773 K and the longitudinal surfaces were prepared for ECA pressing using 800-grit SiC paper. Observations in the unpressed condition revealed an array of equiaxed grains having sizes in the range of ~0.5 to 1.0 mm.

The principles of ECA pressing were described in earlier reports.[8,17] Figure 1 shows a schematic illustration of a section through the ECA pressing facility, with the die consisting of two channels, equal in cross section, which intersect at an angle of Φ. The ECA pressing was conducted by machining each test sample so that it fitted tightly within the vertical channel of the die and then pressing the sample through the die using a plunger.

As indicated in Figure 1, an angle Ψ defines the arc of curvature at the outer point of intersection of the two channels. It has been shown by calculation,[18] and confirmed in model experiments,[19] that the strain accumulated in ECA pressing (ε_N) is given by the expression

$$\varepsilon_N = \frac{N}{\sqrt{3}}\left[2\cot\left(\frac{\Phi}{2}+\frac{\Psi}{2}\right)+\Psi\,\mathrm{cosec}\left(\frac{\Phi}{2}+\frac{\Psi}{2}\right)\right] \quad [1]$$

where N is the number of passages through the die. It is possible to perform repetitive pressings of the same sample to achieve high total strains because the cross section of the sample remains unchanged during passage through the die.

In the present experiments, the die was fabricated from two blocks of SK3 tool steel (Fe-1.0 to 1.1 pct C) held together with large bolts. Each channel had a cross section of 10×10 mm^2 and, as indicated in Figure 1, the experiments were conducted with an ECA pressing die having angles of $\Phi = 90$ deg and $\Psi = 20$ deg. In this condition, it follows from Eq. [1] that a strain of ~1 is introduced into the sample in each passage through the die. All of the

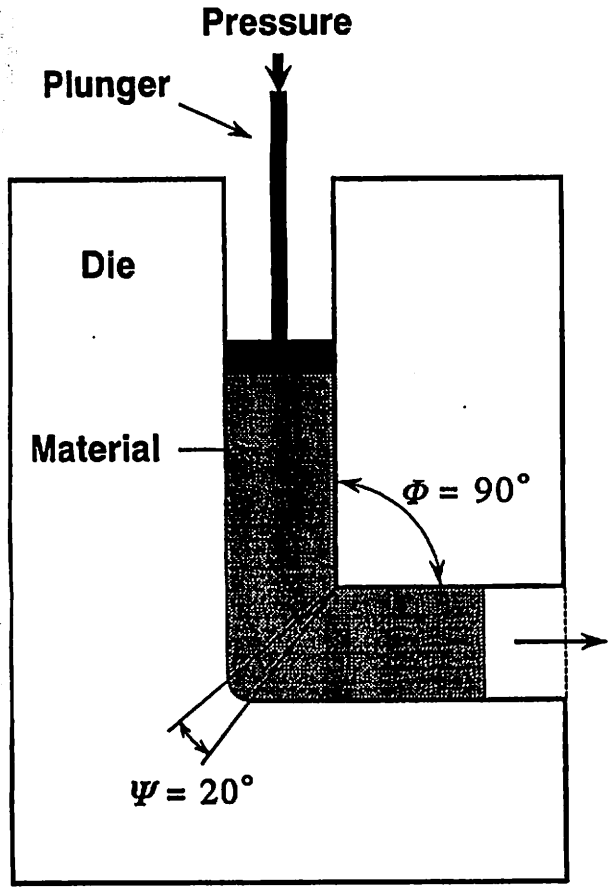

Fig. 1—Schematic illustration of the ECA pressing facility, showing the values used in the present experiments for the two angles Φ and Ψ.

ECA pressings were conducted at room temperature using a pressing speed of ~19 mm s^{-1} and pressures in the range of ~5 to 20 tons. Prior to pressing, samples were coated with a lubricant containing MoS_2.

The samples were pressed using three different processing routes, as illustrated in Figure 2. In route A, the sample is taken through consecutive pressings without any rotation between pressings; in route B, the sample is rotated in the same direction by 90 deg between each consecutive pressing; and in route C, the sample is rotated by 180 deg between each pressing.

Each sample was pressed to a selected number of passages through the die. Following pressing, the surfaces were ground on SiC paper and electropolished at 278 K using a solution of 10 pct $HClO_4$, 20 pct $C_3H_8O_3$, and 70 pct C_2H_5OH, and then the surfaces were anodized for ~40 minutes in a 4 pct $H_2C_2O_4 \cdot 2H_2O$ solution. Samples were examined extensively using an optical microscope, and representative photomicrographs were taken in the three orthogonal planes defined in Figure 3, where *X* is perpendicular to the longitudinal axis of the sample and *Y* and *Z* are the planes parallel to the side faces or to the top face at the point of exit from the die, respectively.

Some selected specimens were also examined using TEM. These specimens were prepared for TEM by cutting discs of 3-mm diameter from the central area of the pressed samples, grinding them on SiC paper to a thickness of

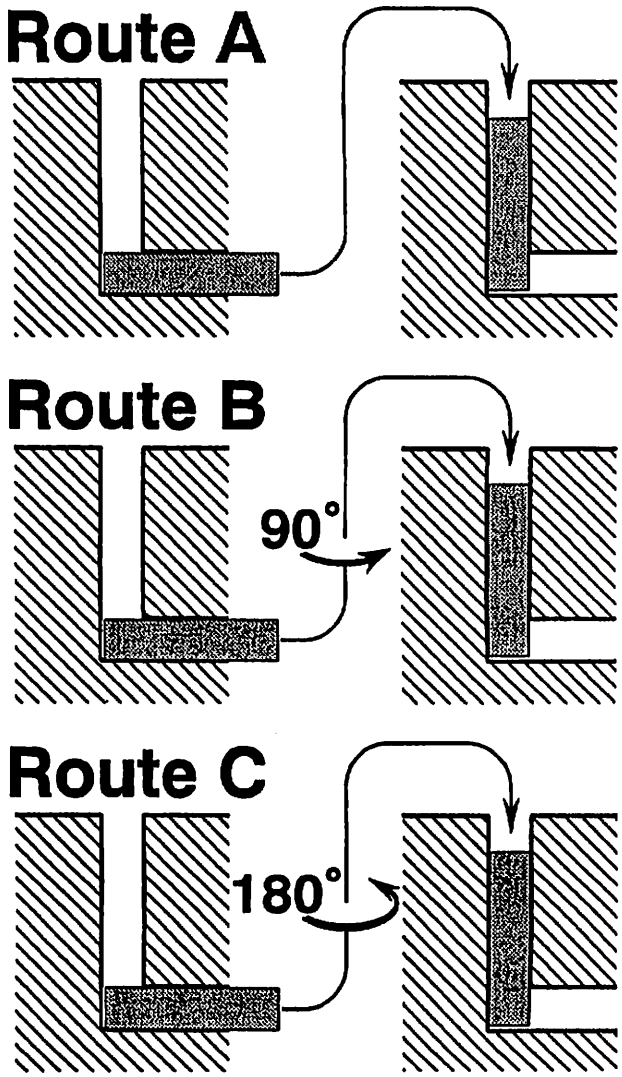

Fig. 2—The three different processing routes used in these experiments: in route A there is no rotation between consecutive pressings, and in routes B and C the samples are rotated by 90 and 180 deg between each pressing, respectively.

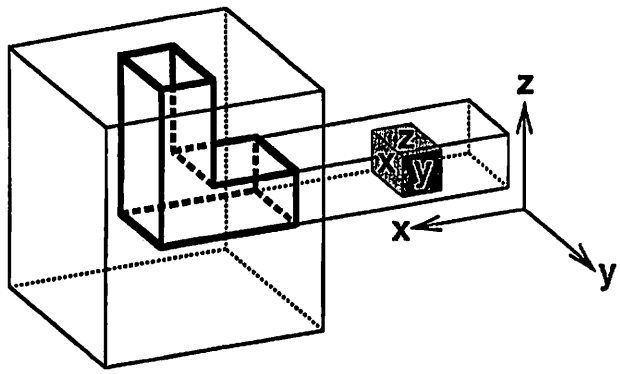

Fig. 3—The three orthogonal planes, *X*, *Y*, and *Z*, examined in these experiments.

~160 mm, and then thinning them to perforation in a twin-jet polishing unit with a solution of 10 pct $HClO_4$, 20 pct

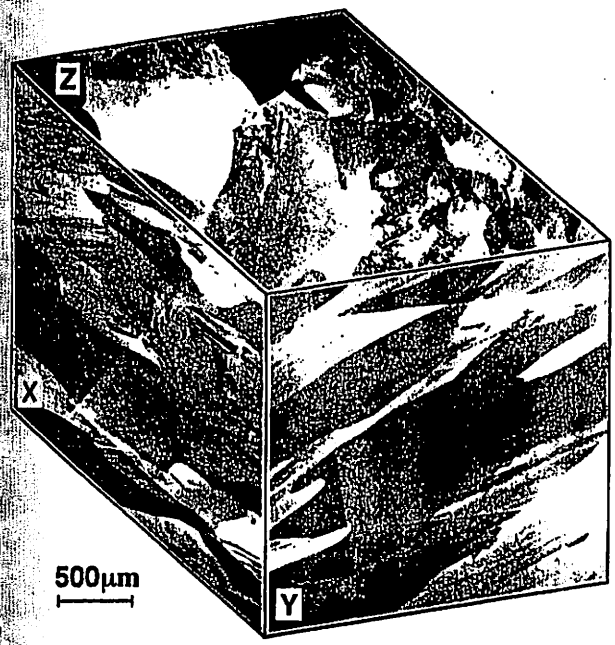

Fig. 4—Microstructures in the *X*, *Y*, and *Z* planes after a single passage through the die.

$C_3H_8O_3$, and 70 pct C_2H_2OH at a temperature of 278 K. The TEM specimens were examined using an Hitachi H-8100 transmission electron microscope operating at 200 kV. Selected-area electron diffraction (SAED) patterns were taken using an aperture size of 12.3 μm.

III. EXPERIMENTAL RESULTS

A. *Single Passage through the Die*

Figure 4 shows the appearance of the microstructures in the optical microscope in the *X*, *Y*, and *Z* planes after a single passage through the die. Detailed inspection of the microstructural characteristics led to several conclusions. In the *X* plane, the grains, which were initially equiaxed, became markedly elongated along the *Y*-axis with a corresponding flattening in the *Z* direction. Within these grains, there was much evidence for shearing in a direction essentially parallel to the *Y*-axis. In the *Y* plane, the grains were elongated parallel to a direction which was inclined, on average, at an angle of ~25 to 30 deg to the *X*-axis.*

*In order to define angles, it is assumed that the positive direction of the selected axis points to the right, and the angles are then given in terms of an anticlockwise rotation from the horizontal. This distinction becomes important in route B, where the sample may be rotated consecutively in either a clockwise or an anticlockwise direction when looking along the longitudinal axis in the direction of pressing. In the present experiments, the samples tested *via* route B were rotated in a clockwise direction between each pressing.

Within the individual grains visible in the *Y* plane, there was evidence for shearing occurring over a range of angles from ~20 to ~70 deg, but primarily with an inclination of approximately 45 deg to the *X*-axis. In the *Z* plane, by contrast, the grains remained relatively equiaxed and essentially unchanged in size, although there was some shearing within the grains approximately parallel to the *Y*-axis.

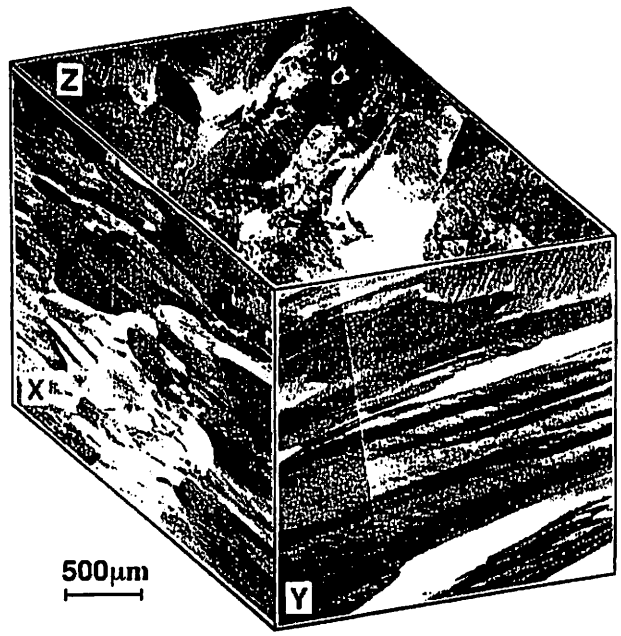

Fig. 5—Microstructures in the *X*, *Y*, and *Z* planes after two passages through the die without rotation (route A).

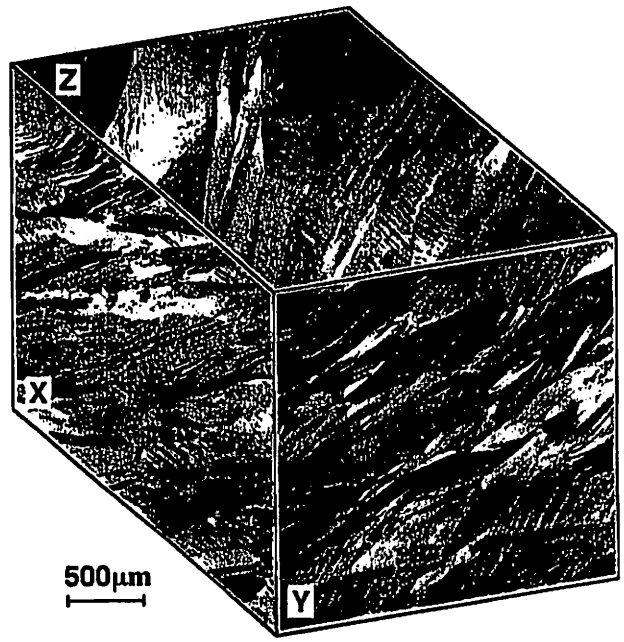

Fig. 6—Microstructures in the *X*, *Y*, and *Z* planes after two passages through the die with rotation of 90 deg (route B).

B. *Two Passages through the Die*

The appearance of the macroscopic microstructures after two passages through the die is given in Figures 5 through 7 for samples subjected to no rotation in route A (Figure 5), a rotation of 90 deg between pressings in route B (Figure 6), and a rotation of 180 deg between pressings in route C (Figure 7), respectively.

In Figure 5, subjected to pressing *via* route A, inspection in the *X* plane revealed that the grains had become even more elongated along the *Y*-axis, and, therefore, flattened

in the *Z* direction, and again there was shearing within the grains parallel to the *Y*-axis. In the *Y* plane, the grains were elongated and lying at an average angle close to ~15 deg to the *X*-axis. Within these grains in the *Y* plane, shearing took place over an angular range of ~20 to 60 deg from the *X*-axis and also at an angle of ~140 deg from the *X*-axis. In the *Z* plane, the grains appeared again to be essentially equiaxed, as in the unpressed material, although there was now more visible evidence for shearing parallel to the *Y*-axis.

Figure 6 shows the microstructures after processing *via* route B. An important observation for this sample was that the grains were elongated and deviated from an equiaxed configuration in all three orthogonal planes. In the *X* plane, the grain boundaries tended to lie approximately at 45 deg to the *Y*-axis and, within the individual grains, there was shearing both parallel to the *Y*-axis and inclined in directions in the range of ~20 to 80 deg from the *Y*-axis. In the *Y* plane, the grain boundaries were oriented in a direction similar to that observed for the boundaries in the *Y* plane in Figure 4 after a single passage through the die, but shearing within the grains was now more visible and lay predominantly at angles inclined at ~30 and ~50 deg to the *X*-axis. In the *Z* plane, the grains were elongated in a manner similar to that observed in the *Y* plane in Figure 4 and, in addition, shearing was visible approximately parallel to the *Y*-axis.

The microstructures after pressing *via* route C are shown in Figure 7. Inspection revealed that the grains were reasonably equiaxed in this condition in each of the three orthogonal planes *X*, *Y*, and *Z*. Shearing was visible in the *X* plane approximately parallel to the *Y*-axis, in the *Y* plane at angles from 20 to 50 deg to the *X*-axis, and in the *Z* plane approximately parallel to the *Y*-axis.

C. *Additional Passages through the Die in Route B*

An experimental investigation reported earlier showed that the microstructure evolves most rapidly into an array of high-angle grain boundaries when the pressing is conducted using route B.[20] Accordingly, additional pressings were performed *via* route B in order to examine the subsequent microstructures.

Figure 8 shows an optical micrograph taken in the *Y* plane after four pressings *via* route B; the *X* and *Z* directions are indicated. In this condition, a large strain of ~4 has been introduced into the sample and it is apparent that the microstructure is now very complex and the grain boundaries are not distinct on the specimen surface. Shearing is visible within the grains but there appear to be no well-defined angular relationships.

In order to obtain more meaningful information on the microstructural characteristics after four pressings, Figure 9 shows a transmission electron micrograph and associated SAED pattern taken in the *Y* plane using the same sample as in Figure 8. It is apparent, from this photomicrograph, that the microstructure consists of an array of small and essentially equiaxed grains, and measurements revealed an average grain size in this condition of ~1.3 μm. The SAED pattern demonstrates that the grain boundaries in this sample are in a high-angle configuration. Therefore, the presence of this ultrafine-grained structure after only four

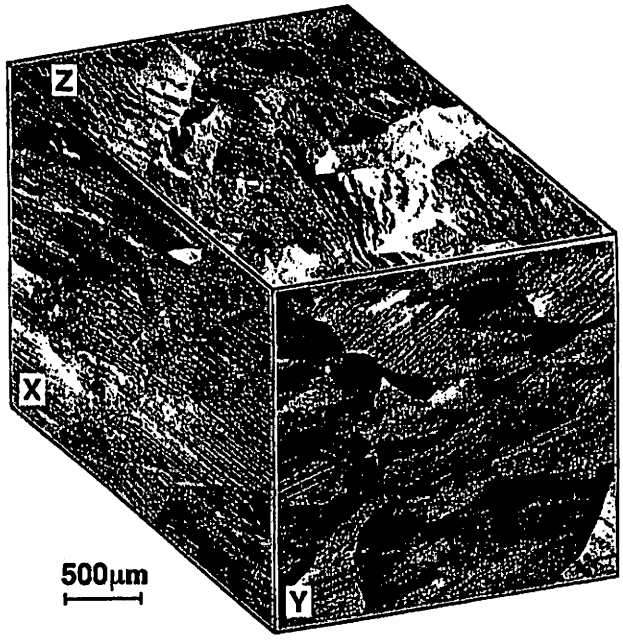

Fig. 7—Microstructures in the *X*, *Y*, and *Z* planes after two passages through the die with rotation of 180 deg (route C).

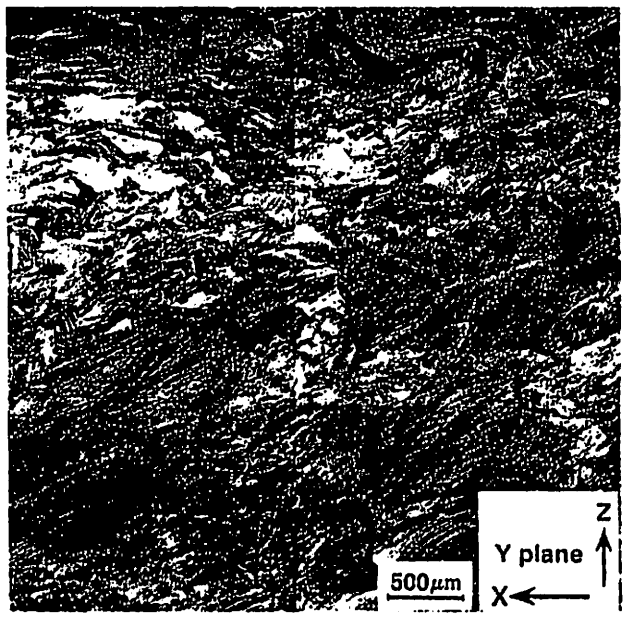

Fig. 8—Microstructure in the *Y* plane after four passages through the die with rotation of 90 deg (route B).

pressings illustrates the potential utility of the ECA pressing procedure.

Figure 10 shows the appearance of the microstructure in the *Y* plane after a total of six pressings *via* route B. The microstructure is again complex, and the grain boundaries are not clearly defined because of the intense straining, but there is some evidence for shearing at an angle of ~30 deg to the *X*-axis.

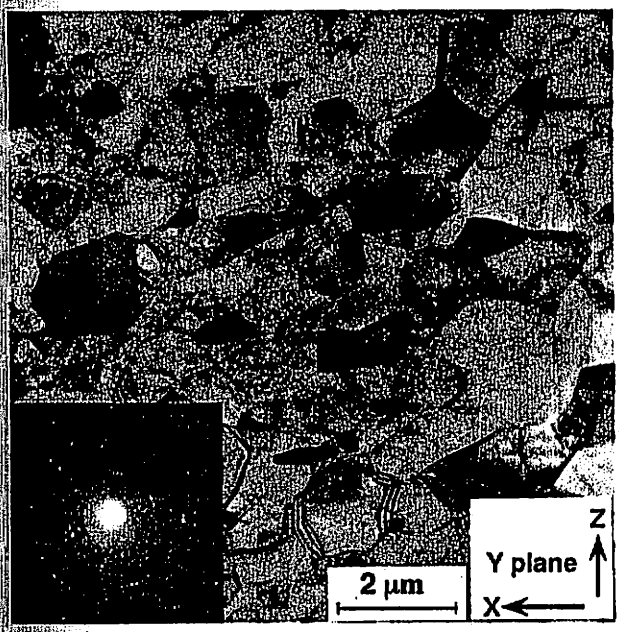

Fig. 9—Microstructure observed in the *Y* plane by TEM, with associated SAED pattern, after four passages through the die with rotation of 90 deg (route B).

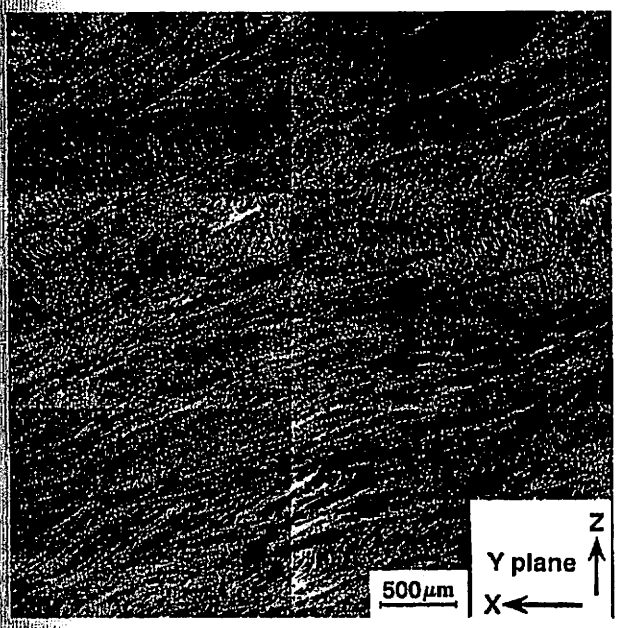

Fig. 10—Microstructure in the *Y* plane after six passages through the die with rotation of 90 deg (route B).

IV. DISCUSSION

The results presented in Section III demonstrate that, when observed at a macroscopic level, the introduction of intense plastic straining through ECA pressing leads to very significant distortions of the large equiaxed grains which are present in the unpressed condition. These results, therefore, supplement the earlier observations reporting the development and evolution of an ultrafine-grained structure during ECA pressing.[15]

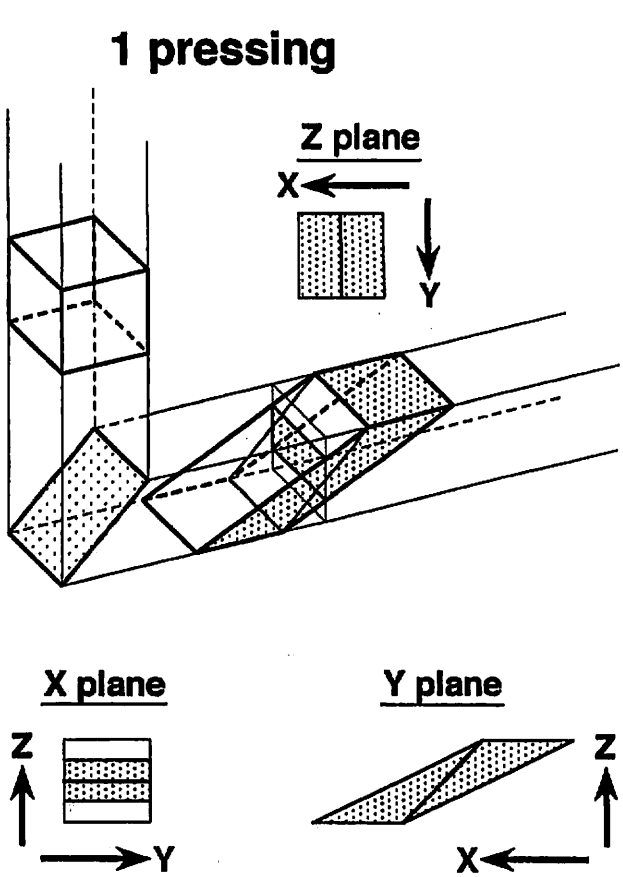

Fig. 11—Schematic illustration of shearing in a single passage through the die, plus the corresponding deformation in the *X*, *Y*, and *Z* planes.

In order to obtain an understanding of the present observations, it is necessary to consider the precise characteristics associated with the shearing introduced on passage through an ECA pressing die.

A. *Shearing for One Pressing*

Figure 11 gives a schematic illustration of the shearing associated with a single passage through the die for the condition where $\Phi = 90$ deg and, for simplicity, $\Psi = 0$ deg.* The cubic element on the left in Figure 11 passes through the theoretical shear plane, shown shaded at left, and is sheared into the rhombohedral shape illustrated within the exit channel of the die. The three inserts depict the consequent deformation, in terms of the macroscopic grain elongation and the associated shearing planes within the individual grains, for observations in the *X*, *Y*, and *Z* planes, respectively.

The predicted behavior in Figure 11 is in good agreement with the experimental observations given in Figure 4 in terms of both the directions associated with the grain boundaries and the predominant shear directions within the

*The present experiments were conducted using $\Psi = 20$ deg, which avoids the problem, revealed by finite-element modeling,[21] that the corner at the intersection of the two channels may not completely fill when friction is present. In practice, it is easier to illustrate the shearing schematically by using a value of $\Psi = 0$ deg.

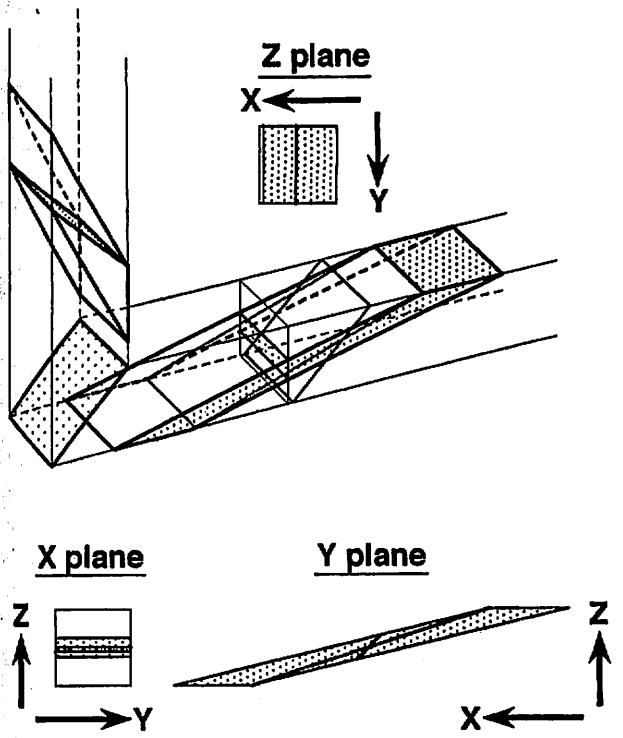

Fig. 12—Schematic illustration of shearing after two passages through the die *via* route A, plus the corresponding deformation in the *X*, *Y*, and *Z* planes.

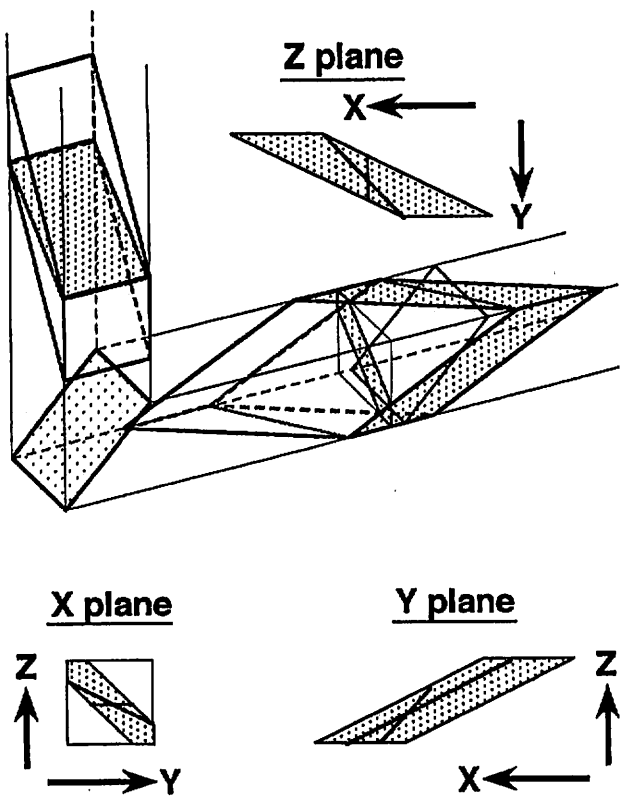

Fig. 13—Schematic illustration of shearing after two passages through the die *via* route B, plus the corresponding deformation in the *X*, *Y*, and *Z* planes.

individual grains. In particular, the experimental observation of grain boundaries in the *Y* plane lying at approximately 25 to 30 deg to the *X*-axis is consistent with the shearing behavior depicted in Figure 11, where the grains become elongated in the *Y* plane at a predicted angle of 27 deg to the *X*-axis. The experimental observations also revealed shearing occurring predominantly at 45 deg to the *X*-axis in the *Y* plane. Again, this is consistent with the expectations from the simple shear depicted in Figure 11 and the additional multiplicity of shearing observed experimentally, over an angular range of ~20 to ~70 deg, is due to the limitations on the crystallographic shear directions in the fcc lattice and the influence of the surrounding grains in maintaining a contiguous structure.

B. *Shearing for Two Pressings*

The effect of two pressings through the die is illustrated schematically in Figures 12, 13, and 14 for pressings conducted *via* routes A, B, and C, respectively.*

*Route B may be further divided into two subcategories, depending upon whether the rotations are +90 deg in the same direction between each pressing or ±90 deg with the direction of rotation alternating between consecutive pressings. The present experiments were conducted using the former route which, for simplicity, is here designated route B.

Figure 12 depicts shearing characteristics which are generally consistent with the experimental observations in Figure 5. In particular, the elongation of grains along the *Y*-axis in the *X* plane is predicted by Figure 12, and the observation in the *Y* plane of elongated grains lying at angles close to ~15 deg to the *X*-axis is consistent with the prediction that the grains elongate in a direction at 14 deg to the *X*-axis. The presence of two distinct shear directions in the *Y* plane in Figure 5 is in agreement with the shearing model in Figure 12 which shows that two shear planes coexist after the second pressing through the die. It is important also to note a characteristic of route A which is evident from the model. Namely, the direction of shearing in the *Y* plane changes with each pressing through the die when using route A, whereas, by contrast, the grains exhibit additional elongation in the *Y* plane as the number of pressings increases.

The shearing model for two pressings *via* route B, depicted in Figure 13, is also consistent with the experimental observations shown in Figure 6. Specifically, the model predicts that the grains are elongated on all three orthogonal planes and that on each plane the individual grains contain two distinct shearing directions.*

*One of the two shearing directions within each grain is transposed by 180 deg in Figure 13 by comparison with the experimental observations because, for convenience in displaying the results pictorially, the hypothetical sample used in the model was rotated by 90 deg in an anticlockwise direction, rather than in a clockwise direction, when looking along the longitudinal axis in the direction of pressing.

Figure 14 depicts the shearing characteristics after two pressings *via* route C. An important characteristic of route C, where there is a rotation of the sample through 180 deg

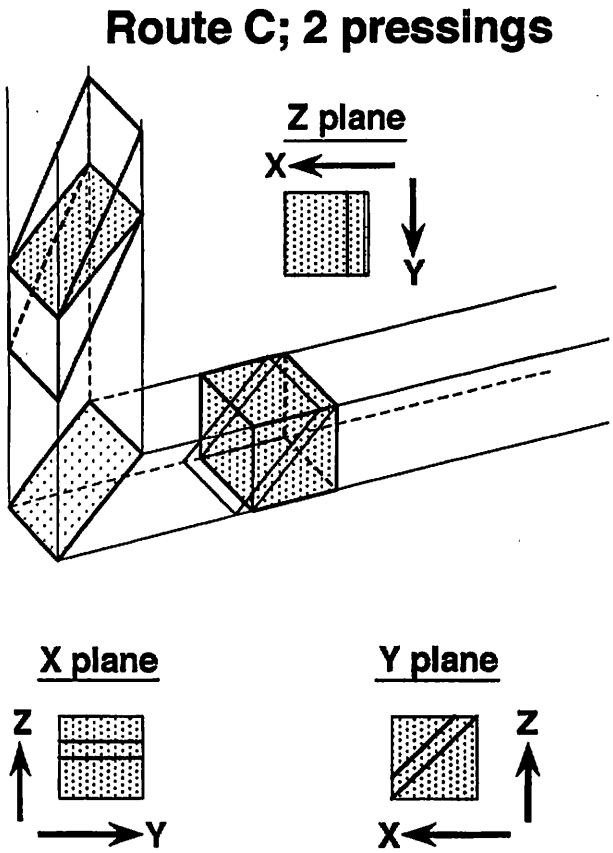

Fig. 14—Schematic illustration of shearing after two passages through the die *via* route C, plus the corresponding deformation in the *X*, *Y*, and *Z* planes.

between consecutive pressings, is that it leads to equiaxed grains after two pressings and each grain then contains a single shear direction. The predictions from the model, as illustrated in Figure 14, are that shearing within the individual grains will occur parallel to the *Y*-axis in the *X* plane, at 45 deg to the *X*-axis in the *Y* plane, and parallel to the *Y*-axis in the *Z* plane. Each of these predictions is consistent with the experimental observations recorded in Figure 7.

C. *Shearing for More Than Two Pressings via Route B*

Since the experimental evidence suggests that route B is preferable for the rapid attainment of an ultrafine-grained structure delineated by boundaries having high angles of misorientation,[20] it is instructive to consider the shearing characteristics associated with additional pressings using route B.

Figure 15 depicts the shearing behavior for three, four, and five pressings *via* route B. There are two important characteristics associated with the use of route B. First, Figure 15 shows that an equiaxed grain configuration is again attained after four pressings through the die.* Second, the shearing direction is different with each pressing, so that there is no single direction of elongation and it is reasonable to assume that, as observed experimentally,[20] this pressing condition will represent an optimum in any attempt to attain an array of ultrafine equiaxed grains. This conclusion is also consistent with the TEM microstructure visible in Figure 9.

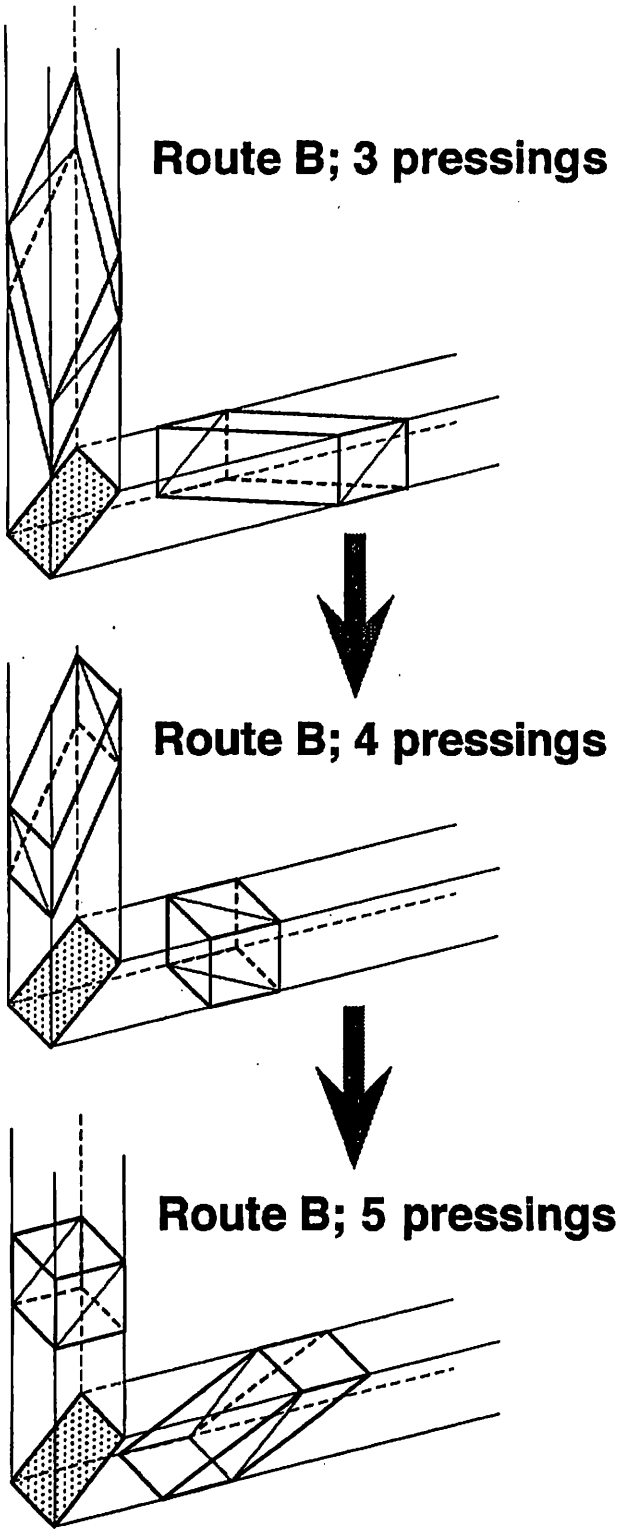

Fig. 15—Schematic illustration of shearing *via* route B after three, four, and five passages through the die.

*In practice, the condition for reaching a macroscopic equiaxed grain configuration in all three orthogonal planes when using route B is given by $N = 4n$, where n is an integer.

V. SUMMARY AND CONCLUSIONS

1. Samples of pure aluminum containing large equiaxed grains were subjected to ECA pressing to different strains at room temperature and then examined in an optical microscope.
2. The deformation was examined in three orthogonal planes of sectioning and for samples pressed either without rotation (route A) or with rotation of either 90 deg (route B) or 180 deg (route C) between consecutive pressings.
3. It is demonstrated that the experimental observations are consistent with models which predict the shearing characteristics for each pressing condition. This consistency includes both the primary direction of grain elongation after each pressing and the nature of the shearing within the grains.

ACKNOWLEDGMENTS

This work was supported in part by the Light Metals Educational Foundation of Japan, in part by a Grant-in-Aid for Scientific Research from the Ministry of Education, Science, Sports and Culture of Japan, in part by the Japan Society for the Promotion of Science, and in part by the National Science Foundation of the United States under Grant Nos. DMR-9625969 and INT-9602919.

REFERENCES

1. V.M. Segal, V.I. Reznikov, A.E. Drobyshevskiy, and V.I. Kopylov: *Russ. Metall. (Metally)*, 1981, vol. 1, pp. 99-105.
2. R.Z. Valiev and N.K. Tsenev: in *Hot Deformation of Aluminum Alloys*, T.G. Langdon, H.D. Merchant, J.G. Morris, and M.A. Zaidi, eds., TMS, Warrendale, PA, 1991, pp. 319-29.
3. R.Z. Valiev, N.A. Krasilnikov, and N.K. Tsenev: *Mater. Sci. Eng.*, 1991, vol. A137, pp. 35-40.
4. R.Z. Valiev, E.V. Kozlov, Yu.F. Ivanov, J. Lian, A.A. Nazarov, and B. Baudelet: *Acta Metall. Mater.*, 1994, vol. 42, pp. 2467-75.
5. S.L. Semiatin, V.M. Segal, R.L. Goetz, R.E. Goforth, and T. Hartwig: *Scripta Metall. Mater.*, 1995, vol. 33, pp. 535-40.
6. V.M. Segal: *Mater. Sci. Eng.*, 1995, vol. A197, pp. 157-64.
7. J. Wang, M. Furukawa, Z. Horita, M. Nemoto, R.Z. Valiev, and T.G. Langdon: *Mater. Sci. Eng.*, 1996, vol. A216, pp. 41-46.
8. J. Wang, Y. Iwahashi, Z. Horita, M. Furukawa, M. Nemoto, R.Z. Valiev, and T.G. Langdon: *Acta Mater.*, 1996, vol. 44, pp. 2973-82.
9. M. Furukawa, Z. Horita, M. Nemoto, R.Z. Valiev, and T.G. Langdon: *Acta Mater.*, 1996, vol. 44, pp. 4619-29.
10. L.R. Cornwell, K.T. Hartwig, R.E. Goforth, and S.L. Semiatin: *Mater. Character.*, 1996, vol. 37, pp. 295-300.
11. M. Mabuchi, H. Iwasaki, K. Yanase, and K. Higashi: *Scripta Metall.*, 1997, vol. 36, pp. 681-86.
12. M. Kawazoe, T. Shibata, T. Mukai, and K. Higashi: *Scripta Metall.*, 1997, vol. 36, pp. 699-705.
13. S. Ferrasse, V.M. Segal, K.T. Hartwig, and R.E. Goforth: *Metall. Mater. Trans. A*, 1997, vol. 28A, pp. 1047-57.
14. S. Ferrasse, V.M. Segal, K.T. Hartwig, and R.E. Goforth: *J. Mater. Res.*, 1997, vol. 12, pp. 1253-61.
15. Y. Iwahashi, Z. Horita, M. Nemoto, and T.G. Langdon: *Acta Mater.*, 1997, vol. 45, pp. 4733-41.
16. M. Furukawa, Y. Iwahashi, Z. Horita, M. Nemoto, N.K. Tsenev, R.Z. Valiev, and T.G. Langdon: *Acta Mater.*, 1997, vol. 45, pp. 4751-57.
17. M. Furukawa, P.B. Berbon, Z. Horita, M. Nemoto, N.K. Tsenev, R.Z. Valiev, and T.G. Langdon: 1998, unpublished research.
18. Y. Iwahashi, J. Wang, Z. Horita, M. Nemoto, and T.G. Langdon: *Scripta Mater.*, 1996, vol. 35, pp. 143-46.
19. Y. Wu and I. Baker: *Scripta Mater.*, 1997, vol. 37, pp. 437-42.
20. Y. Iwahashi, Z. Horita, M. Nemoto, and T.G. Langdon: *Acta Mater.*, in press.
21. P.B. Prangnell, C. Harris, and S.M. Roberts: *Scripta Mater.*, 1997, vol. 37, pp. 983-89.

新しい組織制御法としてのEqual-Channel Angular Pressing(ECAP)

堀田善治* 古川稔**
Terence G. Langdon*** 根本實****

1. ECAP法とは

圧延，線引き，押し出しなどの加工法は，材料を薄くする，細くする，成形するなどが第一目的で，同時に加工硬化や回復・再結晶を利用して組織を制御している．ECAP(Equal-Channel Angular Pressing)法とは，図1に示すように金型中で交差する同じ径の二つの溝孔(Channel)を通して材料を押し出し，曲り角で材料にせん断変形を与えるというきわめて単純なもので，加工前後で材料の断面形状は変わらないから，原理的にプレス回数には制約がなく，バルク状態のままできわめて大きな加工ひずみを加えることができるという塑性加工法である．一種の押し出し法でもあるのでECAE(Equal-Channel Angular Extrusion)法とも呼ばれている．素材の大きさが変わらないという点で従来の圧延や線引きとは全く異なる新しい加工法である．良好な特性がバルク状態のままで得られれば，それから任意の形状に成形でき，素材としての形状や寸法の制約から逃れることができる．

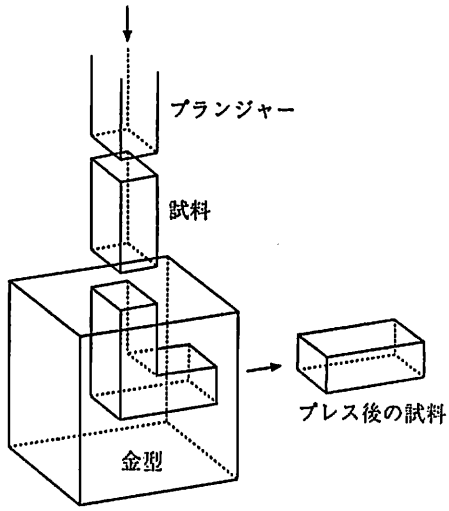

図1 ECAP法の原理(模式図)．

ECAP法はSegalら[1]-[5]によって集合組織制御法として考案され1981年に公表されたが，強加工による結晶粒の超微細化にValievら[6]-[11]が応用して以来世界的に注目されるようになった[12]．金属材料のどの教科書にもあるように，結晶粒の微細化は材料の靭性の向上や超塑性特性の発現には必須の条件である．結晶粒の微細化法にはいろいろあるが，鉄鋼のような相変態が利用できない場合には，強加工-再結晶法が最も良く用いられる．しかし，圧延や押し出し，線引などの通常の加工法では，強加工を与えると材料の厚さや太さが小さくなり，加えられる変形量には現実的な制約がある．一方，ECAP法にはこの制約がなく，動的あるいは静的回復・再結晶を組み合わせると，従来達成できなかった領域まで結晶粒を微細化することができる．最近の研究によりいろいろな材料で超微細粒組織が達成され，延性や超塑性特性が改良されることがわかり，新しい加工プロセスとして期待が高まっている．

* 九州大学助教授；工学部物質科学工学科材料工学教室(〒812-8581 福岡市東区箱崎6-10-1)
** 福岡教育大学助教授；技術科
*** University of Southern California, Professor; Department of Materials Science and Engineering
**** 九州大学教授；工学部物質科学工学科材料工学教室
Equal-Channel Angular Pressing(ECAP): A Novel Method for Microstructural Control; Zenji Horita*, Minoru Furukawa**, T. G. Langdon***, Minoru Nemoto****(*,****Faculty of Engineering, Kyushu University, Fukuoka. **Fukuoka University of Education, Munakata. ***University of Southern California, Los Angeles, CA, USA)
Keywords: *equal-channel angular pressing; ECAP, fine grain, severe deformation, super plasticity, strength, recrystallization*
1998年3月3日受理

2. どのような塑性変形が起こるか

交差する溝孔の曲り角付近の断面を模式的に示したのが図2である．せん断は曲り角のせん断面上でのみ起こり，要素Aはせん断面を通過すると要素Bのように形状が変化する．この図から1回のパスによるせん断ひずみ量はかなり大きいことが容易にわかろう．図3のような一般的な形状の金型でN回押し出した場合の相当ひずみ量は次式で与えられる[13][14]．

$$\varepsilon_N=\frac{N}{\sqrt{3}}\left\{2\cot\left(\frac{\Phi}{2}+\frac{\Psi}{2}\right)+\Psi\,\mathrm{cosec}\left(\frac{\Phi}{2}+\frac{\Psi}{2}\right)\right\} \quad (1)$$

ここでΦは溝孔の交差角，Ψは溝孔の交差点近傍の曲面部の角である．図4は1回押し出した場合のひずみ量εとΦ，Ψの関係を示したもので，ひずみ量はΦに強く依存し，Ψへの依存性は小さいことがわかる．Wuら[15]はモデル実験により材料の流れと式(1)のひずみ量を確かめ，Prangnellら[16]は有限要素法解析により変形が材料内で均一に起こることを示している．図2のように折れ曲がり角Φが90°でΨが0°のときの単純せん断ひずみ量は2，相当ひずみ量にして$2/\sqrt{3}$にも達する．ECAP法では繰り返しプレス回数には原理的に制約がないから，たとえば，N=10のときの相当ひずみ11.5を圧延で達成しようとすると，10万分の1以下の厚さまで薄くしなければならず，ECAP法がいかに有力であるかわかろう．

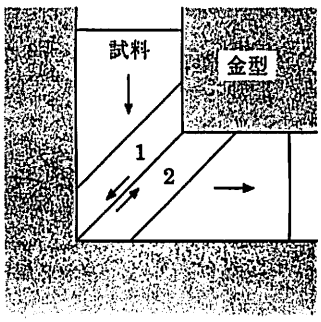

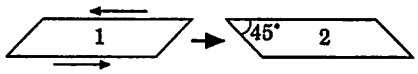

図2　ECAPによるせん断変形．

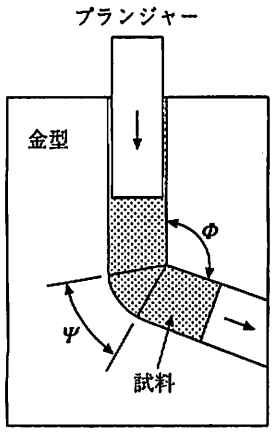

図3　ECAPの一般的な金型．

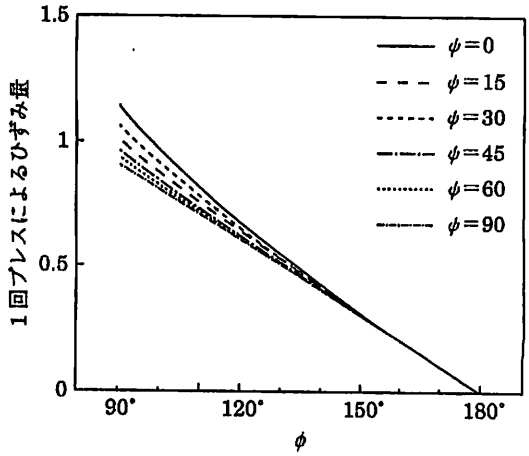

図4　1回のECAPによる相当ひずみ量のϕおよびψによる変化．

3. 加工組織制御の可能性

どのような組織が形成されるかはΦ, Ψ, Nだけではなく，温度，ひずみ速度，せん断方向の組み合わせにも依存する．ECAPでは溝孔の交差面上で単純なせん断変形を受けるから，繰り返しプレス過程で材料を挿入するときの回転のさせ方を変えることによりいろいろなせん断変形を組み合わせることができる[5][17]-[21]．

金型に対して材料を回転させずに挿入して繰り返しプレスするのをRoute A，毎回90°ずつ回転させる場合をRoute B，180°回転させてプレスする場合をRoute Cと定義する．Route Bには90°，0°，90°，0°と回転させるRoute B_Aと90°，180°，270°，360°と回転させるRoute B_Cがある．図5はそれぞれのrouteでどのようなせん断が組み合わされるかをわかりやすく示したもので，Route AとRoute Cではせん断がY面に垂直な面上だけで起こり，Route B_AとRoute B_CではY面とZ面に垂直な面上で三次元的にせん断が組み合わされていることを示している．また，Route B_Cでは3パス目と4パス目のせん断がそれぞれ1パス目，2パス目と同一面上で逆方向に起こっており，Route Cでは2パス目と4パス目のせん断が1パス目と同一面上で逆方向に生じている．Route AとRoute B_Aでは最初のせん断面はその後のパスでせん断されるので，図に示した面が繰り返しプレス後に実際に

観察されるせん断面の方向を表しているわけではないことを注意しておきたい．

図6は，孔の交差角度が90°の場合，1回のプレスによりプレス前の立方体単位がどのように変形するかを模式的に示したもので，変形前の単位立方体を結晶粒とみなすと変形の形態を理解しやすい[20][21]．材料の上面をZ面，側面をY面，押し出し方向に垂直な断面をX面とすると，1回のプレスによりZ面上の粒形は変わらないが，X面ではつぶれ，Y面ではプレス方向と26.6°傾いた方向に伸びる．図7は2回目のプレスを(a) Route A, (b) Route B, (c) Route Cとした場合の形状変化を示している．2回目のプレスによりRoute AではZ面上の粒形は変わらないが，X面ではさらにつぶれ，Y面ではpress方向と14°傾いた方向に伸びる．Route Bでは，Y面，Z面の両方で結晶粒が伸びる．全く対照的にRoute Cでは2回目のプレスにより結晶粒は元の形

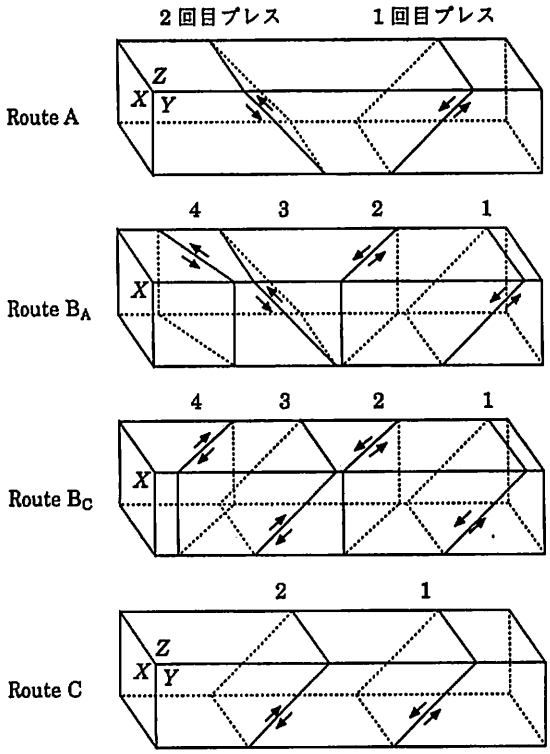

図5　挿入時の試料の回転によるせん断面の組み合わせ．

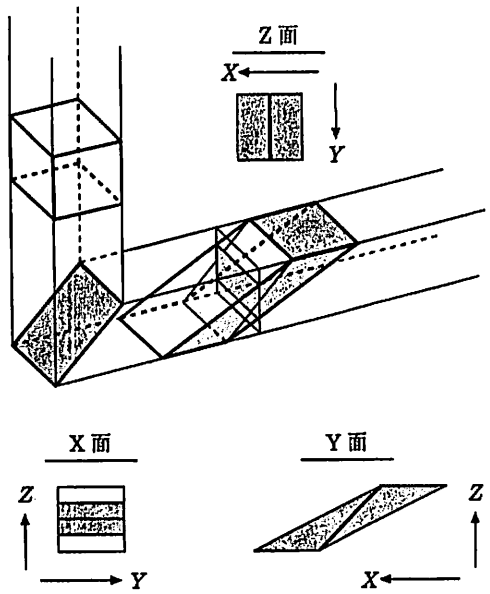

図6　1回のプレスによる立方体単位の形状変化

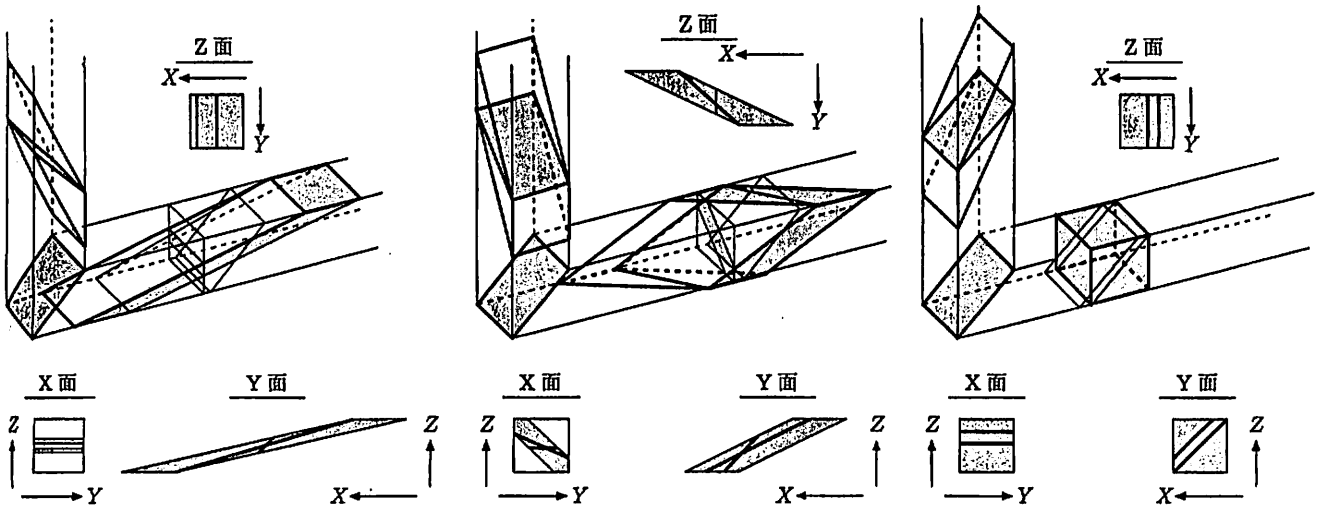

(a) Route A：2回プレス　　(b) Route B：2回プレス　　(c) Route C：2回プレス

図7　2回プレスによる元の立方体単位の形状変化．(a) Route A, (b) Route B, (c) Route C.

に戻る．これは図4に示したように2回目のせん断が1回目と逆方向に起こるためである．Route Bは3回目以降には Route B_A と Route B_C にわかれる．図8は Route B_C での3, 4回目プレスによる結晶粒の形状変化を示している．Route B_C は Route C の三次元合成であるから，4回目のプレスで結晶粒は元の形に戻ることがわかる．

図9は各々の route により結晶粒の形がどのように変化するかをまとめたものである[21]．Route A では Y 面で押し出し方向に組織は伸び，X 面ではつぶれる．Route B_A では Y 面と Z 面の両方で元の結晶粒は押し出し方向に伸びる．したがって，Route A は圧延と類似した集合組織，Route B_A は押し出しや線引と類似した異方性の強い組織になる．もしも2相組織から出発すれば，2相が一方向に伸びたいわゆる *in-situ* 複合組織をつくることができる[22]．一方，Route B_C では粒の形は4回目毎に元に戻り，Route C では2回目毎に元に戻る．したがって，これらの route では加工集合組織は形成されないと考えられる．Route B_C, Route C のように大きなせん断ひずみを加えながらも結晶粒の形を元のままに保てるのが ECAP 法の特徴である．このように，ECAP 法によればせん断方向の組み合わせによっても加工組織を大幅に制御することができ，組織の微細化や均一化を含めて広い応用が期待できる．たとえば，Xiang ら[23]は2024Al-3%Fe-5%Ni(質量%)合金の急冷凝固粉末を冷間静水圧プレス(CIP)後，Route C に相当する方法で 573 K で ECAP することにより 623～723 K で通常の押し出し加工した場合とほぼ同じ密度でより微細な内部組織を達成している．

4. 結晶粒の微細化過程

ECAP 法で強加工と回復・再結晶を組み合わせると結晶粒の微細化が可能となる．ECAP 後に加熱焼鈍して静的に再結晶させ結晶粒を微細化することもできるが，加工中の温度や変形方向を制御することにより動的あるいは連続的に結晶粒を微細化できるのが ECAP 法の特徴である．

図10は室温で1回プレスした 99.99%Al の X, Y, Z 面の透過電子顕微鏡(TEM)組織の立体合成写真で，転位が配列した帯状組織(shear band)が約1 μm 間隔に形成されている[20]．shear band は X 面では底辺にほぼ平行，Y 面では押し出し方向と約45°方向，Z 面では押し出し方向とほぼ垂直に並んでおり，Al 中の{111}すべり面の方向とは一致しないが，図5から予測されるせん断面との交線方向に近い．1パスでの変形は材料中できわめて均一である．図中に示した制限視野電子線回折(SAED)パターン(直径 13.5 μm 領域に対応)はいわゆる net pattern を形成しているが，個々の斑点が円周方向に拡がっていることから，shear band 間には方位差があり，亜結晶粒界となっていることがわかる．図11は Route B_C で4パスした純アルミニウムの組織で，SAED パターンは高角度粒界からなる粒径約 1.2 μm の微細粒になっていることを示している．結晶粒界面は滑らかで，内部には転位がほとんど観察されず，微細粒では ECAP 中に原子拡散がかなり起こっていることを示している．純アルミニウムで通常の強加工-再結晶法により達成できる粒径は 10 μm 程

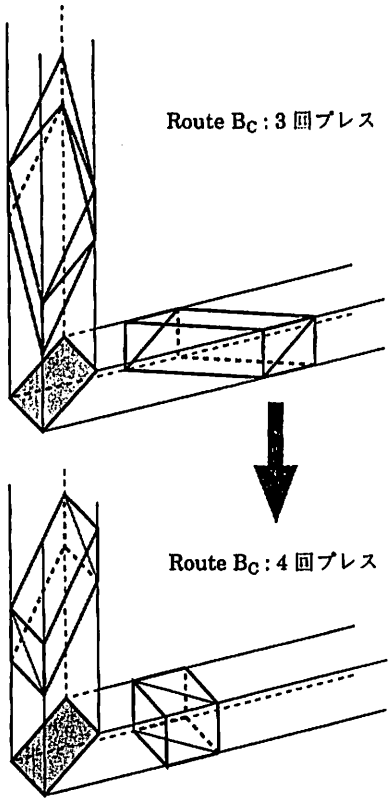

図8　Route B_C で3回および4回プレスしたときの立方体単位の形状変化．

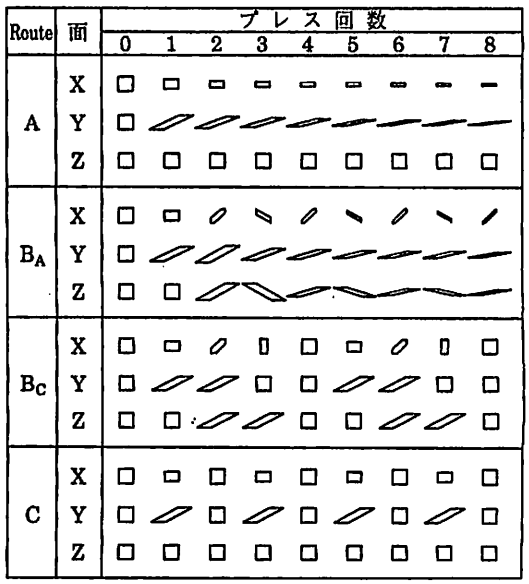

図9　繰り返し ECAP による立方体単位の形状変化．

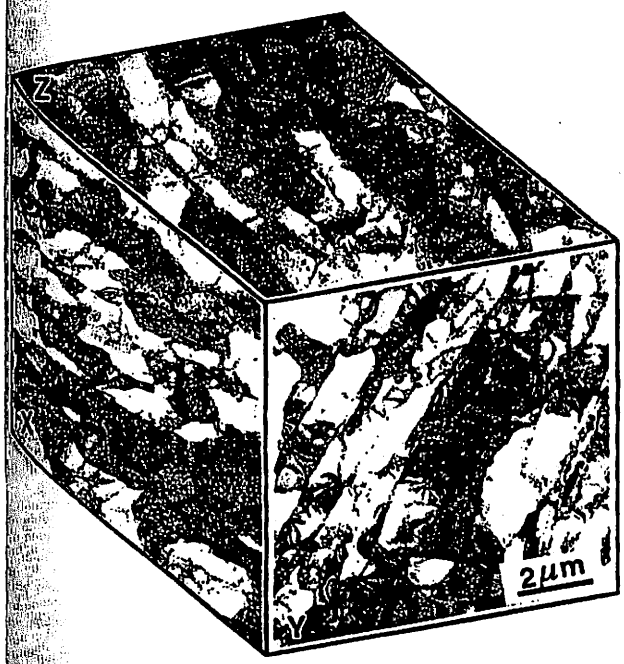

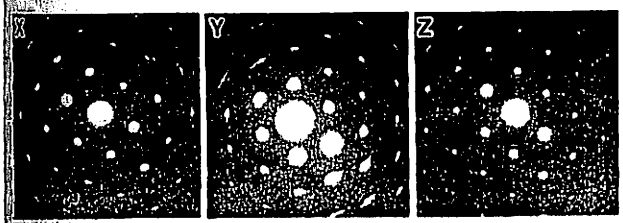

図10　1回パスした99.99%Alの TEM 組織．X, Y, Z 面から観察して立体図に合成．視野制限回折(SAED)パターンはそれぞれの面の直径 13 μm 領域からに対応している．

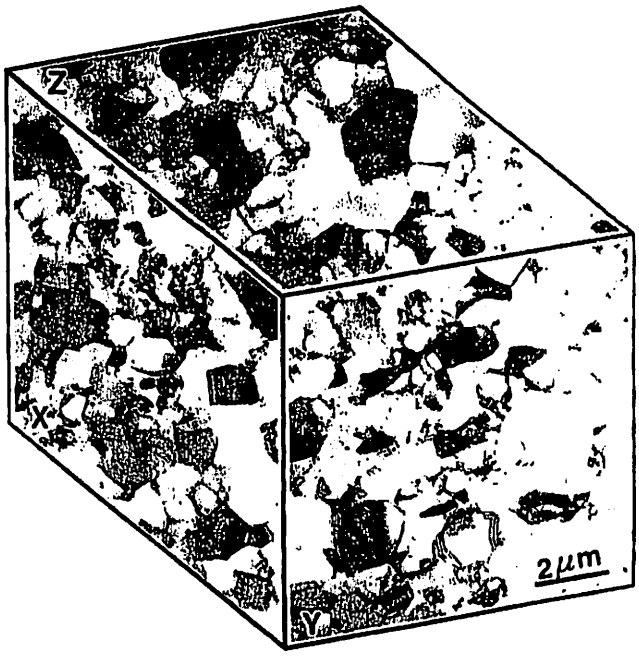

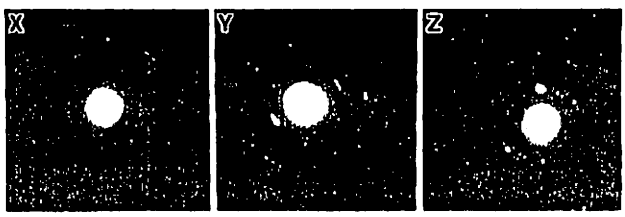

図11　Route B_C で4回パスした99.99%Alの TEM 組織(三次元合成)．

であるので，ECAP 法は結晶粒の微細化にきわめて有効であることがわかる．このように従来の静的再結晶法より結晶粒を大幅に微細化できるのが ECAP 法の特徴である．

図12は ECAP の繰り返しに伴う SAED パターンの斑点の広がりを各 route の各面について調べた結果である[20]．いずれの場合にも ECAP の初期段階で亜結晶粒が形成され，ひずみの増加と共に結晶粒間の方位差が増大し，ついには高角度粒界で構成された微細粒になる．結晶粒間の方位差の増加は連続的と見られることから，結晶粒の微細化は動的連続的再結晶により起こるということができよう．また，図12から亜結晶粒界の傾角の増加傾向が route により異なり，Route B_C で最も早く起こることがわかる．図5に示したように Route B_C では交差する二つの面上での繰り返しせん断が三次元的に組み合わされている．純アルミニウムについて図8における Φ の影響を調べた結果によれば[14]，同じ塑性ひずみ量で比較すると，Φ=90°の場合のひずみ硬化が最大でそれより大きくなるほどひずみ硬化量は小さくなる．実験結果は，一度に大きなせん断変形が起こること，かつ三次元的に起こることが亜結晶粒の傾角の増加に有効であることを示している．具体的な再結晶機構は明らかでないが，高温変形中の動的再結晶過程について提案されているように[24]，アルミニウム中では ECAP の強いせん断変形中に結晶粒回転が促進されている可能性が考えられる．また，強加工により蓄積されたひずみが回復による微細粒の形成を促進し，微細粒化がさらに回復を促進すると考えられる．Prangnell ら[16]は1パスと10パスした99.75%Alをいろいろな温度で焼鈍し，組織の TEM 観察と背面散乱電子線回折(EBSP)解析により，亜結晶粒界は移動速度が小さいため静的焼鈍ではむしろ高温まで残留しやすいことを示している．

このように，99.99%アルミニウムは室温で ECAP 加工しただけで結晶粒が微細化される[16][19][20]．一方，Al-1質量%Mg 合金を室温で6回プレスすると平均 0.45 μm 径，Al-3 質量%Mg 合金を8回プレスすると平均 0.27 μm 径の微細粒が得られる[25]．しかし Al-Mg 合金を室温で ECAP した場合には粒界面や粒内に高密度の転位が残存している．このように，プレスの route，繰り返し数，温度，合金組成などは結晶粒間の方位差の増加の速さと到達粒径をきめる重要な因子である．

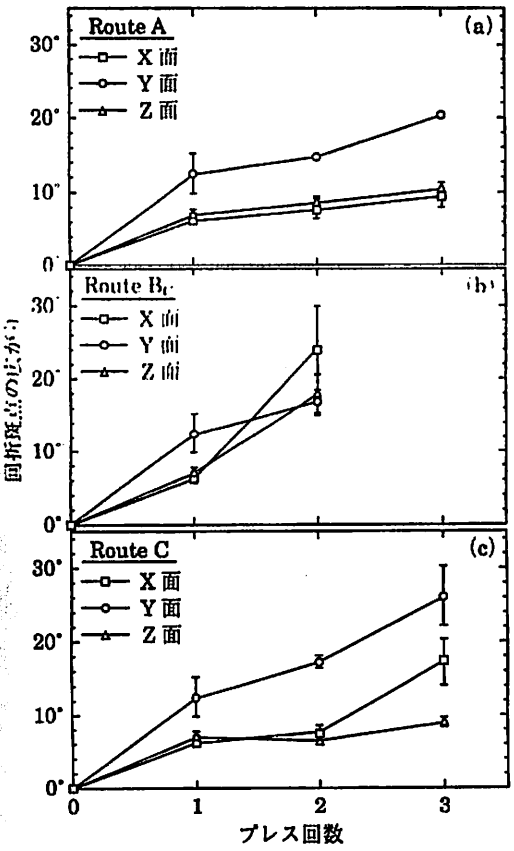

図12　SAED パターン中の回折点の円周方向の広がりのパス回数とプレス route による変化.

5.　高速超塑性の発現

塑性変形が原子の拡散に支配されるとき，応力 σ の下でのひずみ速度 $\dot{\varepsilon}$ は次の構成方程式で与えられる[26].

$$\dot{\varepsilon}=\frac{AGb}{kT}\left(\frac{\sigma-\sigma_0}{G}\right)^n\left(\frac{b}{d}\right)^p D_0 \exp\left(\frac{-Q}{RT}\right) \qquad (2)$$

ここで，A は変形機構に関与する定数，G は剛性率，b はバーガースベクトルの大きさ，k は Boltzmann 定数，T は温度，σ_0 は変形のしきい応力，d は結晶粒径，D_0 は拡散の pre-exponential factor，Q は拡散の活性化エネルギー，R は気体定数，n は応力指数で超塑性変形の場合は 2 程度，p は拡散機構に依存する粒径指数で 2～3 の値をとる．超塑性変形は粒界すべりで起こり，この式から結晶粒径が小さいほど大きなひずみ速度が得られることがわかる．一般に，10^{-2} s^{-1} 以上の初期ひずみ速度で300%以上の伸びがある場合を高ひずみ速度超塑性あるいは高速超塑性と定義し[27]，アルミニウム合金では結晶粒径が 3 μm 以下になるとこの条件が達成される可能性がある[28]．高速超塑性が発現すると超塑性加工を迅速に行えるようになるから工業上の価値は大きい．

超塑性特性は一般に $T_m/2$ 以上の高温で発現する．ここで

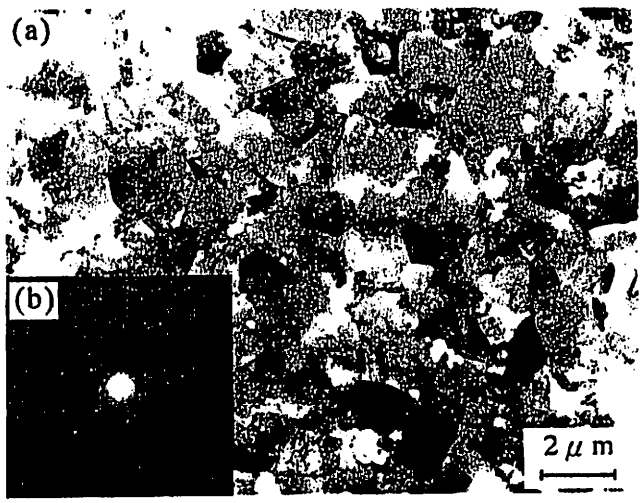

図13　673 K で 8 回パス，さらに 473 K で 4 回パスした Al-5.5%Mg-2.2%Li-0.12%Zr 合金の TEM 組織.

T_m はその材料の融点(K)である．純アルミニウムや純銅[10][29]，Al-Mg 二元系合金[30][31]では微細粒の熱的安定性が低く，高温では粗大化してしまうので超塑性特性は発現しない．ECAP した Al-3%Mg 合金の結晶粒は不安定で，電子顕微鏡観察中に加熱しなくても粒界移動が起こる[31]．超塑性特性の発現には結晶粒の微細化に加えて粒内変形を抑制するための固溶強化と結晶粒界をピン止めし微細粒組織の熱的安定性を高めるための粒子分散あるいは熱的に安定な二相共存組織にする必要がある．

Al-5.5%Mg-2.2%Li-0.12%Zr 合金(1420合金)は Mg と Li により強化され，Al_3Zr の微細分散により結晶粒の粗大化が抑制されている[32]．この1420合金を 673 K で 8 パス，さらに 473 K で 4 パス ECAP 変形すると，図13に示すようにほぼ全域にわたって高傾角粒界からなる平均粒径約 1.2 μm の微細粒となった[33]．図14はこの材料をいろいろな温度と初期ひずみ速度で引張試験した後の試料で，623 K, 1×10^{-2} s^{-1} のひずみ速度で引張試験すると1180%を超える伸びが観察され，1×10^{-1} s^{-1} の高ひずみ速度でも約900%もの伸びが得られることを示している[33][34]．図15は Al-Li 系1420合金についてこれまでに報告されている超塑性特性[35]と比較したもので，従来の加工熱処理材と比較して低温度で著しい高速超塑性が発現していることがわかる．特に，従来の超塑性 Al-Li 合金の多くが粉末冶金法でつくられているのに対して，バルク法であることは特筆できる．また，同じように ECAP 加工した Al-6%Cu-0.4%Zr 合金(Supral 100 A)では平均粒径が約 0.5 μm となり，573 K, 1×10^{-2} s^{-1} のひずみ速度で約970%の超塑性伸びが観測された[33]．これらはいずれも高速超塑性の領域にある．

Al-Mg-Sc 合金は，Mg による固溶強化と整合な Al_3Sc 粒子の微細分散で優れた強度と延性を示すことがすでに知られ

ている[36]-[38]．最近のAl-3%Mg-0.2%Sc合金についての結果によれば[39]，室温で8パスのECAPにより平均粒径約0.2 μmが得られ，673 K, 3.3×10^{-2} s^{-1}での引張変形により1030%の伸びを達成している．各ECAPの間で473 Kで中間焼鈍を加えると伸びは1500%に達しさらに優れた超塑性特性が発現している．ECAP法はMg合金系でも試みられ超塑性特性が発現している[40]．しかし，二相合金のZn-22%Al合金では，ECAPにより各々の相内の結晶粒は微細化されるが混合状態は変わらず，超塑性特性の改善効果は小さい[41]．

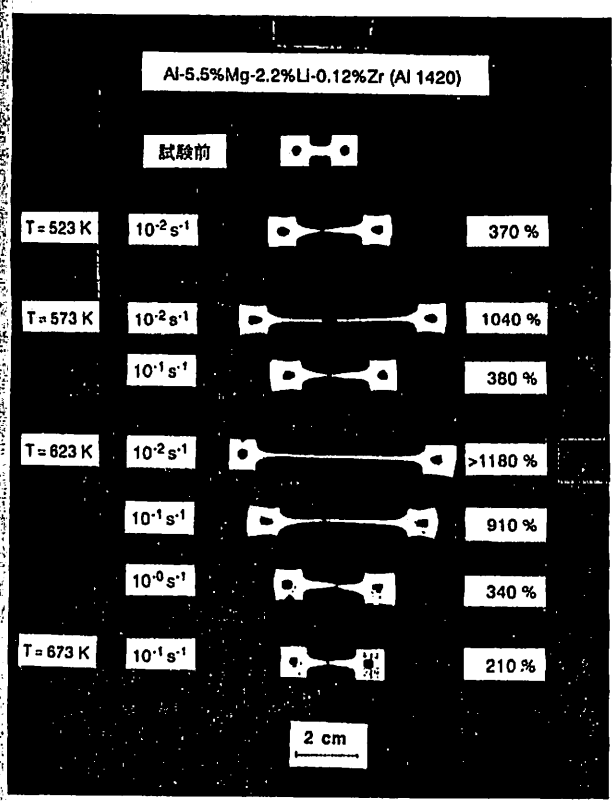

図14　673 Kで8回パス，さらに473 Kで4回パスしたAl-5.5%Mg-2.2%Li-0.12%Zr合金の引張試験による試験片の変形．

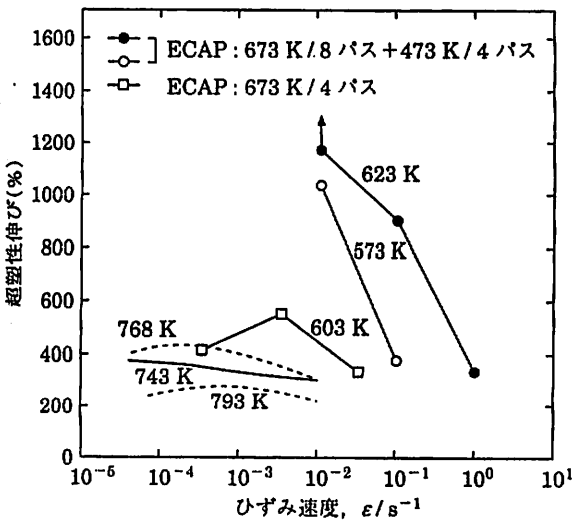

図15　Al-Li系1420合金の超塑性伸びのひずみ速度依存性の比較．

6. 延性の改善

結晶粒の微細化は，延性を損なわない唯一の材料強化法で，高強度材の延性改善には結晶粒の微細化が必須である．Al-Li系合金は，高比強度，高比剛性で次世代の航空機用アルミニウム合金として期待され活発に研究されてきた[32]．ECAPされた1420合金の微細粒組織は高温でも安定なので，ECAP後，粒成長を起こさない程度の高温で再溶体化処理し時効すると硬化させることができる．図16は，熱間圧延材，813 K溶体化・時効材(粗粒材)とECAP後673 Kで溶体化し時効した場合(微細粒材)の強度を伸びに対してプロットしたもので，ECAP材の強度-延性特性が大幅に改善されていることを示している[42]．このようにECAP法は材料の靭性改良にも有効である．Markushevら[43]はAl-Mg-Si系合金の強度と靭性に及ぼすECAPの影響を調べており，Semiatinら[44]はTiAl系金属間化合物のECAPを試み，割れの発生傾向と塑性変形特性との関係を検討している．

7. 結　　言

ECAP法は，コロンブスのたまご的発想で見いだされた独創的な加工法で，結晶粒の微細化法としては従来の強加工-再結晶法の分類に入るが到達結晶粒径はかなり小さく，酸化

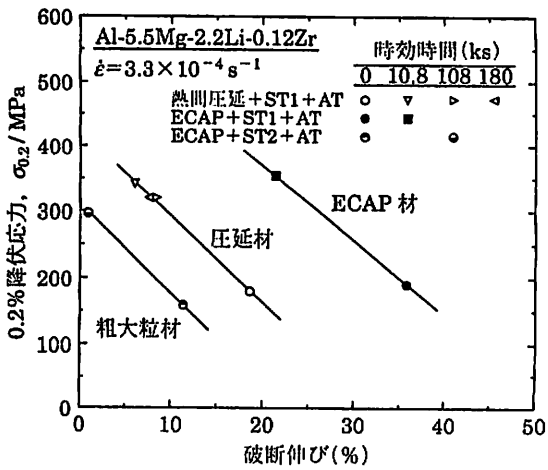

図16　673 Kで4回パスし，673 Kで溶体化後時効処理したAl-5.5%Mg-2.2%Li-0.12%Zr合金の0.2%耐力と伸びの圧延材および高温溶体化処理材(粗大粒材)との比較．

などの汚染がない，残留気孔がない，バルク材が得られるなど物理蒸着法や化学蒸着法，メカニカルアロイング法などの粉末冶金法による結晶粒の微細化にはない多くの特徴がある．すでにECAPしたいくつかの合金で比較的低温，高ひずみ速度で超塑性特性が発現することが知られ，今後の研究でプロセスがより最適化されると，従来の超塑性合金の特性が飛躍的に改善されるだけではなく，新しい超塑性合金も開発される可能性がある．更に材料の強度と靭性の改良法としても有効である．ECAP法はきわめて単純であり，原理的には合金の種類の制約もなく，それだけ応用の可能性は広い．最近の研究により塑性変形機構や結晶粒の微細化機構が明らかになりつつあり，従来にない新しい可能性を持つ組織制御法として大いに期待できる．

共同研究を通して多大な御指導をいただき，多くの資料をご提供くださったR. Z. Valiev教授(Ufa State Aviation Technical University)，ECAP法による超微細粒材料の開発を日米共同研究事業として助成いただいている日本学術振興会と米国科学財団(National Science Foundation)および本稿中の原図の多くを作成された岩橋芳寛氏(現三菱重工㈱)に心から感謝したい．

文　献

(1) V. M. Segal, V. I. Reznikov, A. E. Drobyshevskiy and V. I. Kopylov: Russian Metallurgy-Metally, 1(1981), 99.
(2) V. M. Segal: *Processing Materials for Properties*, Ed. by H. Henein and T. Oki, The Minerals, Metals and Materials Society, Warrendale, PA, (1991), p. 947.
(3) V. M. Segal, R. E. Goforth and K. T. Hartwig: *Processing Materials for Properties*, Ed. by H. Henein and T. Oki, The Minerals, Metals and Materials Society, Warrendale, PA, (1991), p. 971.
(4) V. M. Segal, V. I. Reznikov, V. I. Kopylov, D. A. Pavlik and V. F. Malyshev: *Process of Structure Formation During Plastic Straining, Scientific and Technical Publishing*, Minsk, Belarus, (1994).
(5) V. M. Segal: Mater. Sci. Eng., A197(1995), 157.
(6) R. Z. Abdolov, R. Z. Valiev and N. A. Krasilnikov: Mater. Sci. Lett., 9(1990), 1445.
(7) R. Z. Valiev and N. K. Tsenev: *Hot Deformation of Aluminum Alloys*, Ed. by T. G. Langdon, H. D. Merchant, J. G. Morris and M. A. Zaidi, The Minerals, Metals and Materials Society, Warrendale, PA, (1991), p. 319.
(8) R. Z. Valiev, A. V. Korznikov and R. R. Mulyukov: Mater. Sci. Eng. A168(1993), 141.
(9) N. A. Akhmadeev, N. P. Kobelev, R. R. Mulyukov, Y. M. Soifer and R. Z. Valiev: Acta metall. mater., 41(1993), 1041.
(10) R. Z. Valiev, E. V. Kozlov, Yu F. Ivanov, J. Lian, A. A. Nazarov and B. Baudelet: Acta metall. mater., 42(1994), 2467.
(11) R. Z. Valiev: Mater. Sci. Eng., A234-236(1997), 59.
(12) 堀田善治，王　経涛，古川　稔，根本　實，R. Z. Valiev, Y. Ma, T. G. Langdon：日本金属学会会報，32(1993), 898.
(13) Y. Iwahashi, J. Wang, Z. Horita, M. Nemoto and T. G. Langdon: Scripta Mater., 35(1996), 143.
(14) K. Nakashima, Z. Horita, M. Nemoto and T. G. Langdon: Acta Mater., 46(1997), 1589.
(15) Y. Wu and I. Baker: Scripta Mater., 37(1997), 437.
(16) P. B. Prangnell, C. Harris, S. M. Roberts and F. J. Humphreys: Scripta Mater., 37(1997), 983.
(17) S. Ferasse, V. M. Segal, K. T. Hartwig and R. E. Goforth: J. Mater. Res., 12(1996), 1253.
(18) S. Ferasse, V. M. Segal, K. T. Hartwig and R. E. Goforth: Metall. Mater. Trans., 28A(1997), 1047.
(19) Y. Iwahashi, Z. Horita, M. Nemoto and T. G. Langdon: Acta Mater., 45(1997), 4733.
(20) Y. Iwahashi, M. Furukawa, Z. Horita, M. Nemoto and T. G. Langdon: Metall. Mater. Trans. 29A(1998), 印刷中.
(21) M. Furukawa, Y. Iwahashi, Z. Horita, M. Nemoto and T. G. Langdon: Mater. Sci. Eng., (1998), 投稿中.
(22) V. M. Segal, K. T. Hartwig and R. E. Goforth: Mater. Sci. Eng., A224(1997), 107.
(23) S. Xiang, K. Matsuki, N. Takatsuji, M. Tokizawa, T. Yokote, J. Kusui and K. Yokoe: J. Mater. Sci. Lett., 16(1997), 1725.
(24) T. Sakai, X. Yang and H. Miura: Mater. Sci. Eng., A234-236(1997), 857.
(25) Y. Iwahashi, Z. Horita, M. Nemoto and T. G. Langdon: Metall. Mater. Trans. 29A(1998), 印刷中.
(26) A. K. Mukherjee, J. E. Bird and J. E. Dorn: Trans. ASM, 623(1969), 155.
(27) K. Higashi and M. Mabuchi: Mater. Sci. Forum, 233-234(1997), 155.
(28) K. Higashi, M. Mabuchi and T. G. Langdon: ISIJ Intern., 36(1996), 1423.
(29) Z. Horita, D. J. Smith, M. Nemoto, R. Z. Valiev and T. G. Langdon: J. Mat. Res., 13(1998), 446.
(30) J. Wang, Y. Iwahashi, Z. Horita, M. Furukawa, M. Nemoto, R. Z. Valiev and T. G. Langdon: Acta metall. mater., 44(1996), 2973.
(31) Z. Horita, D. J. Smith, M. Furukawa, M. Nemoto, R. Z. Valiev and T. G. Langdon: J. Mater. Res., 11(1996), 1880.
(32) 古川　稔，美濃康宏，根本　實：日本金属学会会報，23(1984), 172.
(33) P. Berbon, M. Furukawa, Z. Horita, M. Nemoto, N. K. Tsenev, R. Z. Valiev and T. G. Langdon: Mater. Sci. Forum, 217-212(1996), 1013.
(34) P. B. Berbon, N. K. Tsenev, R. Z. Valiev, M. Furukawa, Z. Horita, M. Nemoto and T. G. Langdon: *Advanced Light Alloys and Composite*, Kluwar Press, the Netherland, (1998), 印刷中.
(35) O. B. Makova, V. K. Portnoy and I. I. Novikov: *Aluminium-Lithium*, Ed. by M. Peters and P-J. Winklers, Informationgesellschaft Verlag, Oberursel, (1991), p. 1133.
(36) R. R. Sawtell and C. L. Jensen: Metall. Trans., 21A(1990), 421.
(37) T. G. Nieh, R. Kaibyshev, L. M. Hsiung, N. Nguyen and J. Wadsworth: Scripta Mater., 37(1997), 1011.
(38) L. S. Kramer, W. T. Tack and M. T. Fernandes: Adv. Mater. Proc., 152(1997), 23.
(39) S. Komura, P. B. Berbon, M. Furukawa, Z. Horita, M. Nemoto and T. G. Langdon: Scripta Mater., 38(1998), 1851.
(40) M. Mabuchi, H. Iwasaki and K. Higashi: Mater. Sci. Forum, 243-245(1997), 547.
(41) M. Furukawa, Y. Ma, Z. Horita, M. Nemoto, R. Z. Valiev and T. G. Langdon: Mater. Sci. Eng., A241(1998), 122.
(42) M. Furukawa, P. B. Berbon, Z. Horita, M. Nemoto, N. K. Tsenev, R. Z. Valiev and T. G. Langdon: Metall. Mater. Trans., 29A(1998), 169.
(43) M. V. Markushev, C. C. Bampton, M. Yu. Murashkin and D. A. Hadwick: Mater. Sci. Eng., A234-236(1997), 927.
(44) S. L. Semiatin, V. M. Segal, R. L. Goetz, R. E. Goforth and T. Hartwig: Scripta Metall. Mater., 33(1995), 535.

PHILOSOPHICAL MAGAZINE LETTERS, 1998, VOL. 78, NO. 4, 313–318

Requirements for achieving high-strain-rate superplasticity in cast aluminium alloys

PATRICK B. BERBON†, MINORU FURUKAWA‡, ZENJI HORITA§, MINORU NEMOTO§, NIKOLAI K. TSENEV||, RUSLAN Z. VALIEV¶ and TERENCE G. LANGDON†

† Departments of Materials Science and Mechanical Engineering, University of Southern California, Los Angeles, California 90089-1453, USA
‡ Department of Technology, Fukuoka University of Education, Munakata, Fukuoka 811-41, Japan
§ Department of Materials Science and Engineering. Faculty of Engineering Kyushu University, Fukuoka 812-81, Japan
|| Institute of Chemical Technology, Ufa State Petroleum Technical University, Ufa 450062, Russia
¶ Institute of Physics of Advanced Materials, Ufa State Aviation Technical University, Ufa 450000, Russia

[*Received in final form 1 June 1998 and accepted 19 June 1998*]

ABSTRACT

Equal-channel angular (ECA) pressing has been used to introduce a very small grain size into a commercial cast Al–Mg–Li–Zr alloy. Tensile testing reveals the potential for achieving superplastic ductilities in this alloy at very high strain rates (greater than $10^{-2}\,s^{-1}$) but experiments show that this potential is realized only if a sufficiently high strain is introduced during the ECA pressing such that the microstructure is homogeneous and consists of an array of grains having large-angle grain boundaries.

§ 1. INTRODUCTION

Superplastic forming is an industrial process in which the high tensile ductility of a superplastic sheet metal is used to form a complex shape (Barnes 1994). This procedure is employed extensively for the fabrication of low volumes of high-value components but there has been no extension into mass production because the forming is conducted at the relatively slow strain rates associated with optimum superplastic ductility, typically up to about 10^{-3}–$10^{-2}\,s^{-1}$ (Langdon 1982), and the forming times are consequently very long (about 20–30 min).

There have been several recent reports of the occurrence of high-strain-rate (HSR) superplasticity (SP) in aluminium-based materials where high tensile elongations are achieved at strain rates above $10^{-2}\,s^{-1}$ (Higashi *et al.* 1996). However, these reports have been restricted to date to a limited range of metal matrix composites, mechanically alloyed materials and alloys fabricated using powder metallurgy procedures (Nieh *et al.* 1997) and there have been no reports of HSR SP in conventional commercial aluminium alloys processed by casting.

Experiments on superplastic materials have demonstrated that a decrease in grain size leads both to an increase in the elongations to failure and to the occurrence of these higher elongations at faster strain rates (Mohamed *et al.* 1977) This well established trend led to the suggestion that it may be possible to achieve HSR SP in

0950–0839/98 $12.00

conventional cast materials by making a very substantial reduction in the grain size using a procedure such as, for example, equal-channel angular (ECA) pressing (Ma *et al.* 1996). Some preliminary experiments on a commercial Al–Mg–Li–Zr alloy subjected to ECA pressing revealed a potential for superplastic-like flow at high strain rates (Furukawa *et al.* 1998a) and very recently HSR SP was achieved in this alloy, and in an Al–Cu–Zr alloy also, with high tensile ductilities up to strain rates of about $10^{-1}\,s^{-1}$ (Valiev *et al.* 1997). This paper reports further experiments which were designed to delineate the precise requirements for attaining HSR SP when using ECA pressing for the grain refinement of cast aluminium-based alloys.

§ 2. Experimental material and procedures

The experiments were conducted using a Russian light-weight high-strength alloy fabricated by casting and having the commercial designation of 01420; the alloy has a fabricated composition of Al–5.5 wt% Mg–2.2 wt% Li–0.12 wt% Zr and contains a fine dispersion of δ'-Al_3Li and β'-Al_3Zr precipitates. This alloy was selected initially because of the well established need to develop a superplastic forming capability in Al–Li alloys at relatively low temperatures, of the order of 600–700 K, where there is negligible Li and Mg depletion (Pu *et al.* 1995). The experimental alloy was received in a hot-rolled non-superplastic condition with an initial grain size of $\sim 400\,\mu m$ and grain refinement was achieved using ECA pressing.

The ECA pressing procedure was developed several years ago as a method of metal working by simple shear (Segal *et al.* 1981) and subsequently it was reported that ECA pressing may be used to attain submicrometer or nanometer grain sizes in metals (Valiev *et al.* 1991, Valiev and Tsenev 1991). The principle of ECA pressing is illustrated schematically by the section through a pressing die shown in figure 1. Two channels of equal cross-section intersect within the die at an angle of Φ and there is an additional angle Ψ defining the arc of curvature at the outer point of intersection of the two channels. A test sample is machined to fit within the channel and it is pressed through the die with a plunger. It has been shown from first principles (Iwahashi *et al.* 1996), and confirmed in model experiments (Wu and Baker 1997), that the strain ε_N accumulated in ECA pressing is given by

$$\varepsilon_N = \frac{N}{3^{1/2}}\left[2\cot\left(\frac{\Phi}{2}+\frac{\Psi}{2}\right)+\Psi\,\mathrm{cosec}\left(\frac{\Phi}{2}+\frac{\Psi}{2}\right)\right],$$

where N is the number of passages through the die. Since the cross-section of the sample remains unchanged after a single passage through the die, repetitive pressings of the same sample may be undertaken in order to achieve high total strains.

Samples were machined in the form of cylinders having diameters of either 50 or 20 mm and with corresponding lengths of ~100 or ~70 mm respectively. The ECA pressing was conducted in air at selected elevated temperatures with the samples cooled in air between consecutive pressings. In the present experiments, the angles associated with the die were $\Phi = 90°$ and $\Psi = 0°$ so that a single pressing gave a strain of about unity. Two sets of experiments were undertaken using pressing routes 1 or 2. In route 1, each sample was pressed for four passes through the die at a temperature of 673 K giving a total strain of about four; in route 2, the samples were pressed for eight passes at 673 K and four additional passes at 473 K to give a total strain of about 12, with the lower temperature selected for the final passes in order to minimize grain growth.

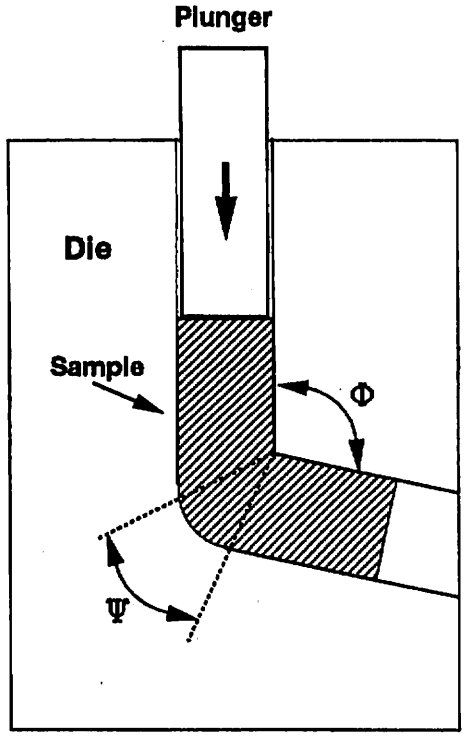

Figure 1. The principle of equal-channel angular pressing.

The potential for superplastic forming was evaluated by machining tensile specimens parallel to the longitudinal axes of the ECA-pressed samples with gauge lengths of 4 mm and gauge cross-sections of 3 mm × 2 mm. These specimens were pulled in air in a testing machine operating at a constant rate of cross-head displacement at selected elevated temperatures from 523 to 673 K, with the temperature held constant during each test to within ±2 K. Small discs of some samples were prepared for inspection by transmission electron microscopy (TEM) using a standard preparation procedure for Al-based alloys (Wang *et al.* 1996).

§ 3. Experimental results and discussion

Inspection of samples by TEM after ECA pressing by route 1 revealed a heterogeneous microstructure consisting of areas of reasonably equiaxed grains separated by large-angle boundaries interspersed with areas of subgrains where the boundaries were at small angles of misorientation. Measurements revealed an average grain size of ~1.2 μm and the volume fractions were estimated as ~60–70% of grains with large-angle boundaries and ~30–40% of grains with small-angle suboundaries; further information on the nature of the microstructure in this condition has been given elsewhere (Furukawa *et al.* 1997, 1998a). Tensile experiments on these samples demonstrated a possible potential for high superplastic ductilities but the maximum recorded elongation at a temperature of 603 K was only ~550% when using a strain rate of $3.3 \times 10^{-3}\,s^{-1}$ and the elongation to failure dropped to ~340% when the strain rate was increased to $3.3 \times 10^{-2}\,s^{-1}$. This microstructural condition appears, therefore, to achieve only partially the anticipated superplasticity at high strain rates.

Figure 2 shows a representative microstructure within the alloy after ECA pressing through route 2. Very careful examination by TEM, combined with inspection of the associated diffraction patterns, revealed a homogeneous structure of equiaxed

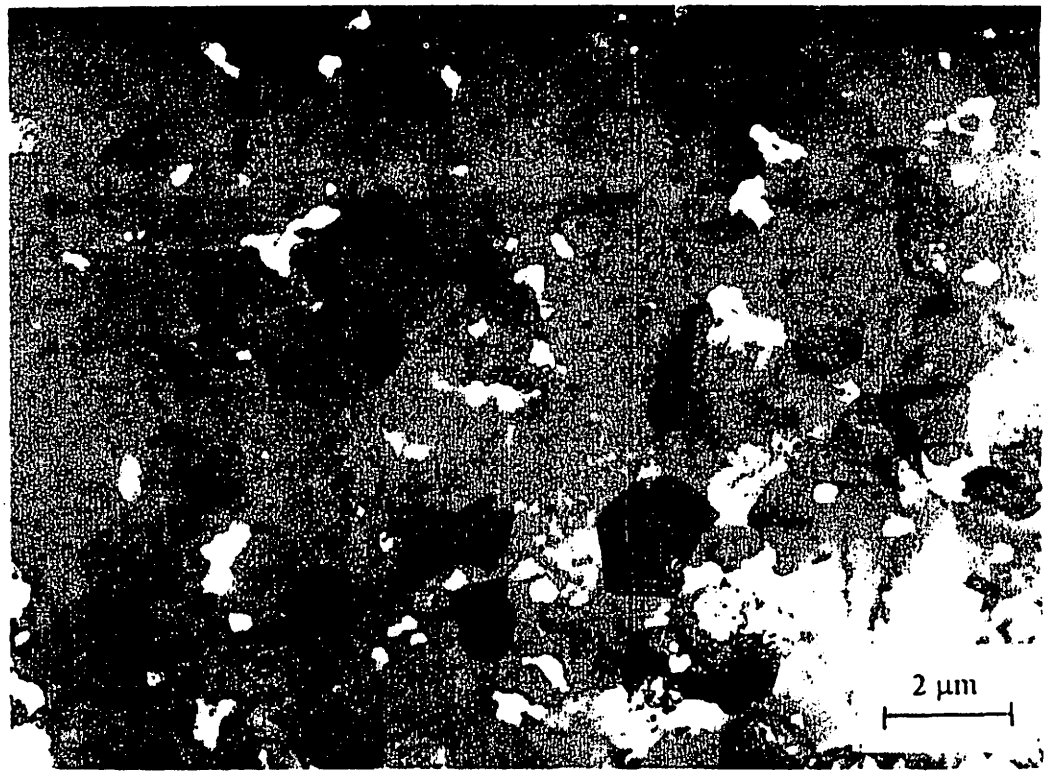

Figure 2. Microstructure in the Al–Mg–Li–Zr alloy after ECA pressing through route 2.

grains with an average grain size of $\sim 1.2\,\mu m$ which was identical with the samples pressed through route 1 but with all the grain boundaries now having large misorientation angles. It was observed also, as is evident in figure 2, that many of the grain boundaries exhibited a non-uniform contrast which is typical of the high-energy non-equilibrium boundaries introduced through intense plastic straining (Valiev *et al.* 1993, Horita *et al.* 1996, 1998).

Several specimens processed through route 2 were pulled in tension at relatively high strain rates and the appearance of these specimens after testing is recorded in figure 3; the upper specimen is untested. It is apparent from figure 3 that some of these specimens exhibit extremely high tensile ductilities, with a maximum elongation of 1180% without failure in a sample pulled at an initial strain rate of $1 \times 10^{-2}\,s^{-1}$ at 623 K and an elongation to failure of 1040% at the same strain rate at 573 K. The uniform deformation of this and other specimens and the absence of visible macroscopic necking within the gauge lengths confirm the occurrence of superplastic deformation in these samples. In addition, the strain rates associated with these superplastic ductilities are remarkably high, including an elongation of 340% achieved at 623 K with a strain rate of $1\,s^{-1}$. Industrial superplastic forming operations are performed at strain rates up to $\sim 10^{-2}\,s^{-1}$ and these operations generally require strains of the order of 300–400% (Dressel 1995, Wisbey and Kearns 1995). Therefore, the present results confirm the potential both for introducing ultrafine grain sizes with consequent superplastic ductilities into nominally non-superplastic commercial cast alloys and for utilizing these alloys in superplastic forming operations at strain rates up to two orders of magnitude faster than employed in current practice.

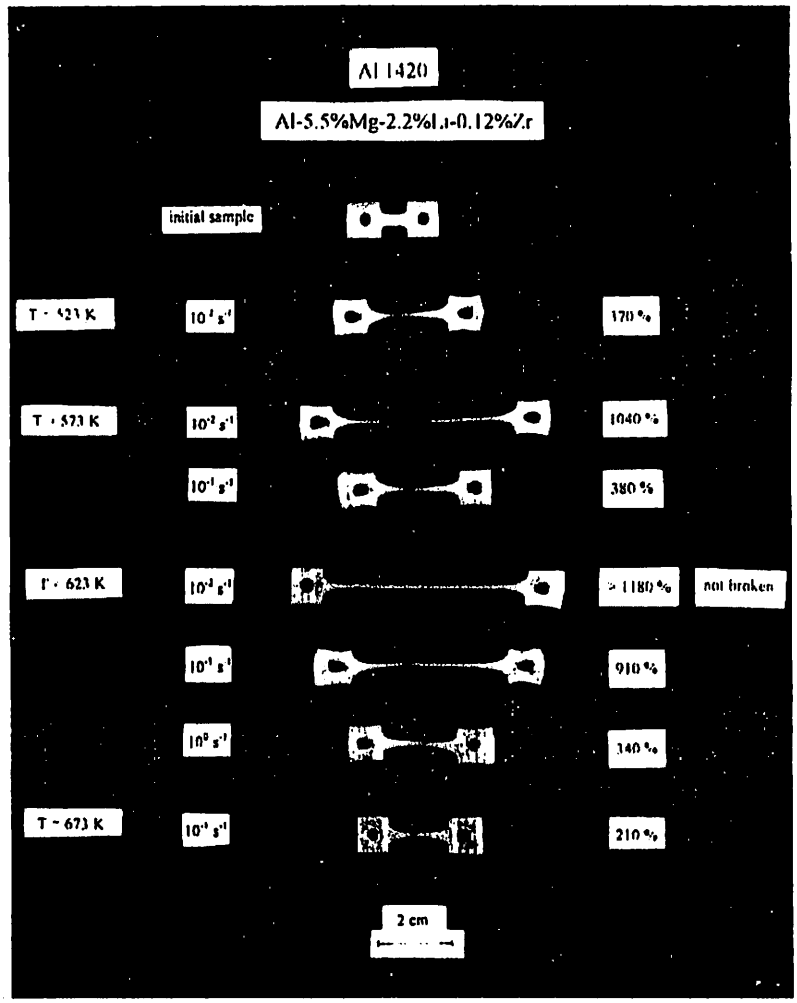

Figure 3. Examples of tensile ductility in samples pulled at high strain rates at elevated temperatures.

The experimental results reveal that ECA pressing through route 1 to a total strain of about four is insufficient to maximize the superplastic capabilities of this alloy whereas pressing through route 2 to a strain of ~ 12 leads to very high tensile ductilities at fast strain rates. Current evidence suggests that grain-boundary sliding is capable of accounting for all the deformation occurring under superplastic conditions (Langdon 1994) and, since small-angle grain boundaries are not conducive to easy sliding, it is concluded that pressing through route 1 fails to achieve the very high tensile ductilities because of the heterogeneity in the microstructure and especially the presence of many small-angle sub-boundaries. It is concluded that the development of HSR SP in commercial aluminium-based alloys requires the introduction by ECA pressing of a sufficiently high strain such that the microstructure evolves into an array of reasonably equiaxed grains separated by large-angle grain boundaries.

Earlier experiments showed that the mechanical properties of ECA pressed materials were dependent upon the temperature of pressing and therefore upon the nature of any relaxation of internal stresses which may take place during the straining process (Furukawa *et al.* 1998b). The present results extend this work by demonstrating that the mechanical properties, and especially the attainment of HSR SP, are

dependent also upon the precise nature of the microstructure introduced during the ECA pressing. In particular, it is possible to utilize ECA pressing to achieve SP at high strain rates in non-superplastic cast alloys but care must be exercised to ensure that the pressing is continued to a sufficiently high total strain.

ACKNOWLEDGEMENTS

This work was supported in part by the Light Metals Educational Foundation of Japan, in part by a Grant-in-Aid for Scientific Research from the Ministry of Education, Science, Sports and Culture of Japan, in part by the Japan Society for the Promotion of Science, in part by the National Science Foundation of the USA under grants DMR-9625969 and INT-9602919 and in part by the US Army Research Office under grants DAAH04-96-1-0332 and N68171-96-6-9006.

REFERENCES

BARNES, A. J., 1994, *Mater. Sci. Forum*, **170–172**, 701.

DRESSEL, C. F., 1995, *Superplasticity: 60 Years after Pearson*, edited by N. Ridley (London Institute of Materials), p. 359.

FURUKAWA, M. , BERBON, P. B., HORITA, Z., NEMOTO, M., TSENEV, N. K., VALIEV, R. Z., and LANGDON, T. G., 1998a, *Metall. Mater. Trans.* A, **29**, 169.

FURUKAWA, M., HORITA, Z., NEMOTO, M., VALIEV, R. Z., and LANGDON, T. G., 1998b, *Phil. Mag.* A, **78**, 203.

FURUKAWA, M., IWAHASHI, Y., HORITA, Z., NEMOTO, M., TSENEV, N. K., VALIEV, R. Z., and LANGDON, T. G., 1997, *Acta Mater.*, **45**, 4751.

HIGASHI, K., MABUCHI, M., and LANGDON T. G., 1996, *ISIJ Int.*, **36**, 1423.

HORITA, Z., SMITH, D. J., FURUKAWA, M., NEMOTO, M., VALIEV, R. Z., and LANGDON, T. G., 1996, *J. Mater. Res.*, **11**, 1880.

HORITA, Z., SMITH, D. J., NEMOTO, M., VALIEV, R.Z., and LANGDON, T. G., 1998, *J. Mater. Res.*, **13**, 446.

IWAHASHI, Y., WANG, J., HORITA, Z., NEMOTO, M., and LANGDON, T. G., 1996, *Scripta Mater.*, **35**, 143.

LANGDON, T. G., 1982, *Metall. Trans.* A, **13**, 689; 1994, *Mater. Sci. Engng*, **A174**, 225.

MA, Y, FURUKAWA, M., HORITA, Z., NEMOTO, M., VALIEV, R. Z., and LANGDON, T. G., 1996, *Mater. Trans. Japan Inst. Metals*, **37**, 336.

MOHAMED, F. A., AHMED, M. M. I., and LANGDON, T. G., 1977, *Metall. Trans.* A, **8**, 933.

NIEH, T. G., WADSWORTH, J., and SHERBY, O. D., 1997, *Superplasticity in Metals and Ceramics* (Cambridge University Press), pp. 154–188.

PU, H. P., LIU, F. C., and HUANG, J. C., 1995, *Metall. Mater. Trans.* A, **26**, 1153.

SEGAL, V. M., REZNIKOV, V. L., DROBYSHEVSKIY, A. E., and KOPYLOV, V. I., 1981, *Russ. Metall. (Metally)*, **1**, 99.

VALIEV, R. Z., KORZNIKOV, A. V., and MULYUKOV, R. R., 1993, *Mater. Sci. Engng*, **A168**, 141.

VALIEV, R. Z., KRASILNIKOV, N. A., and TSENEV, N. K., 1991, *Mater. Sci. Engng*, **A137**, 35.

VALIEV, R. Z., SALIMONENKO, D. A., TSENEV, N. K., BERBON, P.B., and LANGDON, T. G., 1997, *Scripta mater.*, **37**, 1945.

VALIEV, R. Z., and TSENEV, N. K., 1991, *Hot Deformation of Aluminium Alloys*, edited by T. G. Langdon, H. D. Merchant, J. G. Morris and M. A. Zaidi (Warrendale, Pennsylvania: Minerals, Metals and Materials Society), p. 319.

WANG, J., IWAHASHI, Y., HORITA, Z., FURUKAWA, M., NEMOTO, M., VALIEV, R. Z., and LANGDON, T. G., 1996, *Acta mater.*, **44**, 2973.

WISBEY, A., and KEARNS, M. W., 1995, *Superplasticity: 60 Years after Pearson*, edited by N. Ridley (London: Institute of Material), p. 305.

WU, Y., and BAKER, I., 1997, *Scripta mater.*, **37**, 437.

PROCESSING OF ALUMINUM ALLOYS

FOR HIGH STRAIN RATE SUPERPLASTICITY

Patrick B. Berbon,[1] Minoru Furukawa,[2] Zenji Horita,[3] Minoru Nemoto,[3]
Nikolai K. Tsenev,[4] Ruslan Z. Valiev[5] and Terence G. Langdon[1]

[1]Departments of Materials Science and Mechanical Engineering
University of Southern California, Los Angeles, CA 90089-1453, U.S.A.
[2]Department of Technology, Fukuoka University of Education
Munakata, Fukuoka 811-41, Japan
[3]Department of Materials Science and Engineering, Faculty of Engineering
Kyushu University, Fukuoka 812-81, Japan
[4]Institute of Chemical Technology
Ufa State Petroleum Technical University, Ufa 450062, Russia
[5]Institute of Physics of Advanced Materials
Ufa State Aviation Technical University, Ufa 450000, Russia

Abstract

Equal-channel angular (ECA) pressing is a processing procedure in which substantial microstructural refinement may be introduced into a material through intense plastic shearing. This paper describes an investigation of the effects of ECA pressing on an Al-Mg solid solution alloy and on a commercial aluminum alloy fabricated by casting. The results demonstrate the potential both for producing a very small grain size and for achieving superplastic tensile ductilities of up to $>1000\%$ at high strain rates ($\geq 10^{-2}$ s^{-1}).

Hot Deformation of Aluminum Alloys II
Edited by T.R. Bieler, L.A. Lalli, and S.R. MacEwen
The Minerals, Metals & Materials Society, 1998

Introduction

Superplasticity refers to the ability of a polycrystalline material to exhibit a very high elongation when pulled in tension. Under optimum conditions, materials having a potential for superplastic flow usually exhibit maximum ductility at strain rates of the order of $\sim 10^{-3}$ - 10^{-2} s^{-1} and there are very substantial decreases in the elongations to failure at both higher and lower strain rates [1].

The occurrence of superplasticity provides the possibility of making use of this process for the fabrication of complex parts in the procedure known as superplastic forming. Because of the nature of the superplastic process, this forming is usually conducted at the strain rates corresponding to optimum superplastic flow so that the forming times are fairly slow and of the order of ~20 - 30 minutes. This forming rate is sufficiently slow that it precludes the mass production of large numbers of identical components for use in, for example, the automotive industry and superplastic forming is therefore restricted instead to the fabrication of high-value components in more limited applications such as the aerospace and architectural industries.

The possibility of achieving high strain rate superplasticity (HSR SP) was first reported by Nieh *et al.* [2] in experiments conducted on an Al-2124 matrix alloy reinforced with SiC whiskers. In these experiments, a maximum elongation of ~300% was achieved at the very high strain rate of 3.3×10^{-1} s^{-1} and there was only a relatively minor decrease in the elongations to failure at even faster strain rates. These unusual results led to the initiation of several major investigations into the properties and characteristics of HSR SP in a range of materials: much of this work was summarized in a recent review [3] and there are now numerous reports of HSR SP in a range of metal matrix composites, mechanically alloyed materials and in alloys fabricated using powder metallurgy procedures [4]. As a result of this very substantial activity, HSR SP has been defined formally, in a standard designated JIS H7007 by the Japanese Standards Association, as the advent of high superplastic-like elongations at strain rates at or above 10^{-2} s^{-1} [3].

In conventional superplastic alloys, there is experimental evidence showing that a reduction in grain size leads to higher elongations to failure and, in addition, these higher elongations occur at faster strain rates [5]. This observation led to the development of the proposal that it may be possible to achieve a superplastic forming capability at high strain rates in conventional materials by making a substantial reduction in the grain size [6]. It is therefore necessary to consider possible procedures for achieving an ultrafine grain size.

Several methods are currently under investigation for the processing of materials with ultrafine grain sizes, including inert gas condensation [7,8], high energy ball milling [9] and sliding wear [10]. However, these methods have the disadvantage that some residual porosity remains within the materials after fabrication so that the procedures may not be appropriate for subsequent use in superplastic forming operations. An alternative procedure is to refine the microstructure through intense plastic straining using the procedures of torsion straining under a high pressure [11] or equal-channel angular (ECA) pressing [12,13]. Of these two procedures, ECA pressing is an especially attractive processing route because a sample is pressed through a die with no change in the cross-sectional area, thereby permitting the possibility of fabricating large bulk samples in a fully-dense condition. There are several reports of the use of ECA pressing in order to produce ultrafine-grained structures in Al-based and Mg-based alloys [14-16] and the present investigation was conducted in order to determine the feasibility of using this procedure to attain HSR SP in aluminum alloys.

The principle of ECA pressing

The ECA pressing was conducted using a facility which is illustrated schematically in Fig. 1. The facility consists of a die which has two channels, equal in cross-section, intersecting at an angle of Φ. A second angle, Ψ, defines the outer arc of curvature at the point of intersection of the two channels. Prior to pressing, the test sample is machined so that it fits within the die and it is then pressed through the die using a plunger. It is apparent that the sample exiting from the die has the same cross-section as the original sample. Therefore, repetitive pressings may be conducted in order to achieve high total strains.

In practice, the strain imposed on a single passage through the die is determined exclusively by the magnitudes of the two angles, Φ and Ψ. It can be shown that the strain, ε_N, associated with a total of N passages through the die may be expressed by a relationship of the form [17]

$$\varepsilon_N = \frac{N}{\sqrt{3}} \left[2 \cot\left(\frac{\Phi}{2} + \frac{\Psi}{2}\right) + \Psi \operatorname{cosec}\left(\frac{\Phi}{2} + \frac{\Psi}{2}\right) \right] \qquad (1)$$

Model experiments have been conducted in which layered billets of colored plasticine were pressed through a die of plexiglass and these have shown that equation (1) provides an accurate representation of the strain introduced during the ECA pressing procedure except at the sample edges where there are friction effects [18]. The implications of eqn. (1) are illustrated in Fig. 2 where ε_1, corresponding to a single passage through the die and N = 1, is plotted as a function of the angle between the two channels, Φ, for values of Ψ from 0° to 90°. The present experiments were conducted using a die having $\Phi = 90°$ and $\Psi \simeq 0°$ and therefore it follows from eqn. (1) and Fig. 2 that a strain of ~ 1 is introduced on each passage of the sample through the ECA die.

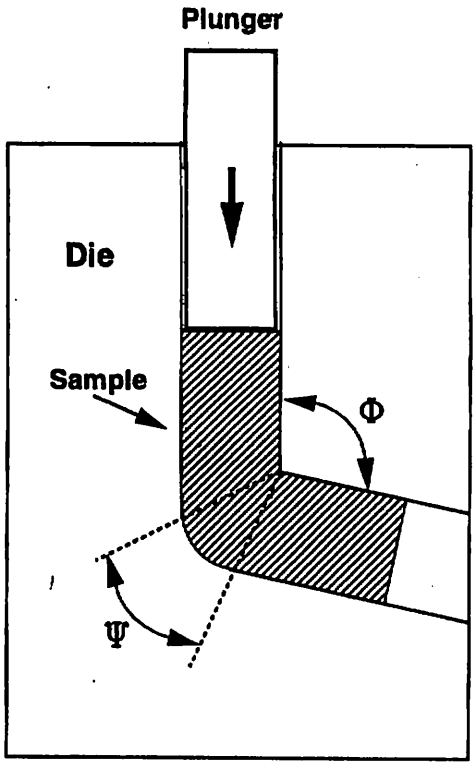

Figure 1 - ECA pressing facility.

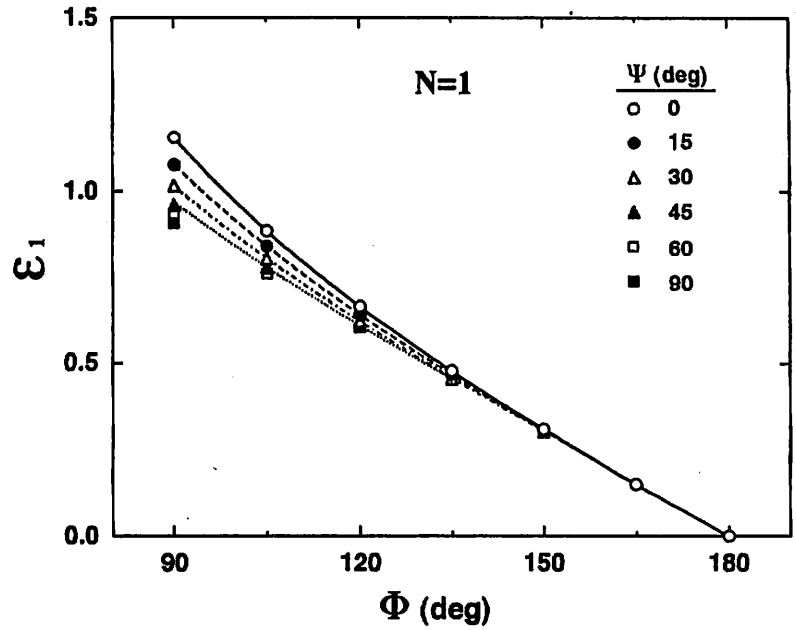

Figure 2 - Strain introduced in a single passage through the die as a function of the angles Φ and Ψ.

Experimental materials and procedures

The experiments were conducted using two different materials, an Al-Mg solid solution alloy and a commercial Al-Mg-Li-Zr alloy.

An Al-3% Mg solid solution alloy was obtained in a hot rolled condition with an initial grain size of $\sim 500\ \mu m$. The alloy was subjected to ECA pressing at room temperature to a total of four passes through the die, equivalent to a strain of ~ 4. Further details concerning this material are given elsewhere [19-21].

A commercial cast Al-5.5% Mg-2.2% Li-0.12% Zr alloy was received in a hot rolled condition with a grain size of $\sim 400\ \mu m$: this material is a Russian light-weight high strength alloy with the designation of 01420 [22]. The Al-Mg-Li-Zr alloy was pressed under two different conditions designated routes 1 and 2, respectively. In route 1, samples were pressed in air at a temperature of 673 K for a total of four passes to give a strain of ~ 4. In route 2, the samples were again pressed in air but to a total of 8 passes at 673 K and a further 4 passes at 473 K, thereby introducing a total strain of ~ 12. In each processing route, the samples were cooled in air between consecutive pressings. In route 2, the lower temperature of 473 K was used for the final pressings in at attempt to minimize any grain growth which may occur at these elevated temperatures. Further details concerning this material are given elsewhere [23,24].

Following ECA pressing, both materials were subjected to static annealing experiments in which small samples were annealed for 1 hour over a selected range of temperatures, with the temperature held constant to within ± 1 K. Selected specimens were also examined by transmission electron microscopy (TEM) using the preparation procedure described elsewhere [19]. Tensile tests were conducted after ECA pressing using specimens in which the gauge

lengths were parallel to the longitudinal axes of the samples after pressing. For the tensile tests, samples were pulled in air using an Instron testing machine operating at a constant rate of cross-head displacement and with the temperatures controlled to within ± 2 K during each separate test. For comparison purposes, some tensile tests were also conducted on samples of the Al-Mg-Li-Zr alloy in the as-received hot rolled condition without subsequent ECA pressing.

Experimental results

Figure 3 shows the microstructure in the Al-3% Mg alloy after ECA pressing, together with a selected area electron diffraction (SAED) pattern obtained from a region having a diameter of 1.9 μm. Detailed inspection showed that the microstructure was essentially homogeneous in this alloy after ECA pressing at room temperature to a strain of ~ 4 and the SAED pattern demonstrates that the grain boundaries have high angles of misorientation. The mean linear intercept grain size in this condition was measured as ~ 0.23 μm. More detailed inspection showed that the grain boundaries were generally poorly delineated suggesting that, as in Al-Mg alloys subjected to intense plastic straining in torsion [25], they are in high energy non-equilibrium configurations [26,27].

These results demonstrate the potential for attaining an ultrafine grain size in the Al-3% Mg alloy but it is important to determine the stability of this structure since any attempts to achieve a superplastic condition will necessitate the testing of samples at temperatures of the order of $\sim 0.5\ T_m$ or higher, where T_m is the absolute melting temperature [1]. The effect of annealing for 1 hour at different elevated temperatures is illustrated in Fig. 4, where the four photomicrographs correspond to annealing temperatures of (a) 443 K, (b) 503 K, (c) 533 K and (d) 563 K, respectively. It is apparent from inspection of Fig. 4 that there is an increase in the average grain size with increasing temperature, there is the development of a duplex structure of unrecrystallized and recrystallized grains, and as the grains grow there is a corresponding evolution in the nature of the grain boundaries into a more equilibrated structure. The recrystallization occurring in these samples is a direct consequence both of thermal activation and of the initial non-equilibrium nature of the microstructure in the material; this process has been designated continuous static recrystallization [28].

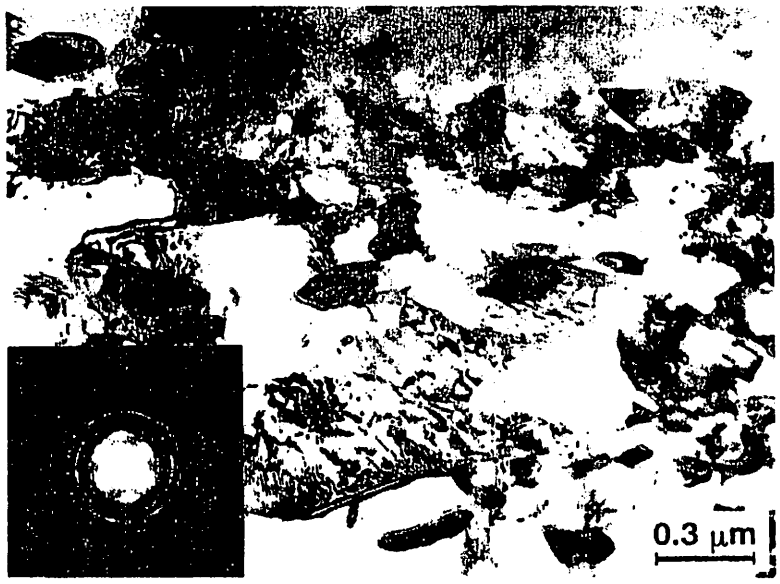

Figure 3 - Microstructure of the Al-3% Mg alloy after ECA pressing.

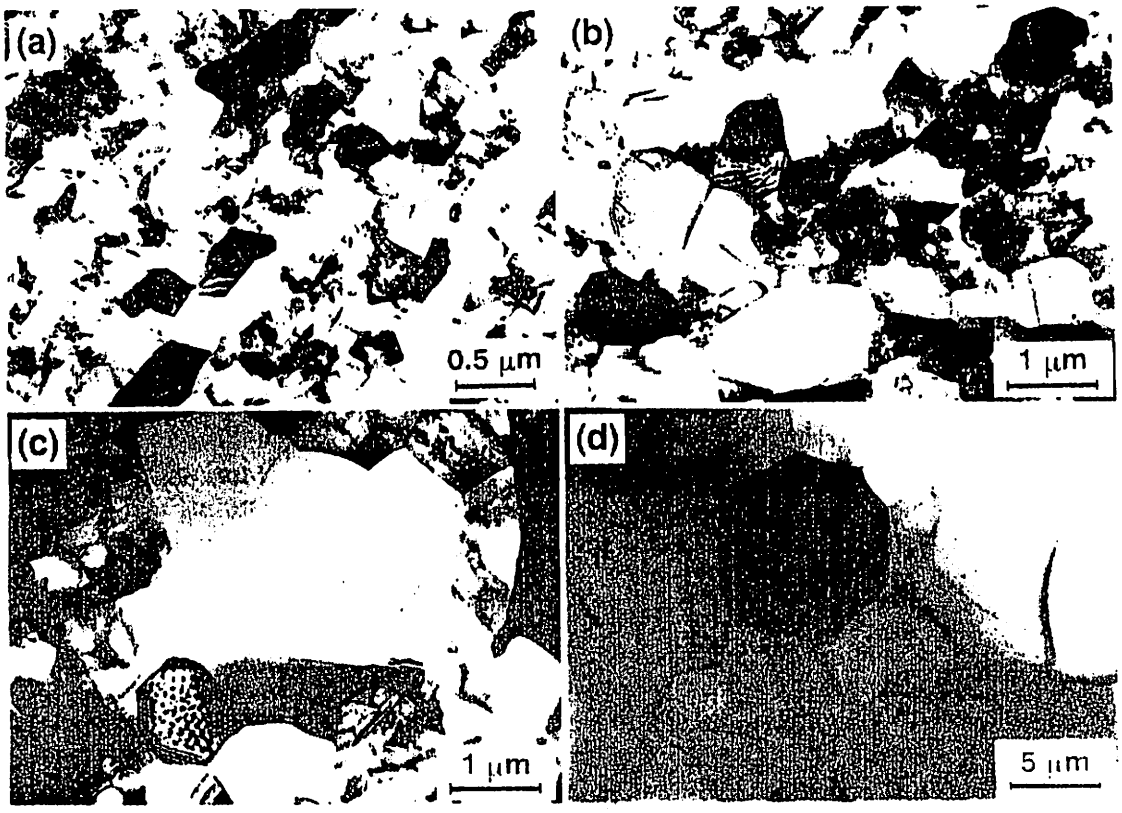

Figure 4 - Microstructures in the Al-3% Mg alloy after annealing for 1 hour at (a) 443 K, (b) 503 K, (c) 533 K and (d) 563 K, respectively.

As noted earlier, the Al-Mg-Li-Zr alloy was subjected to two different ECA processing conditions which are designated routes 1 and 2. Figures 5 and 6 show typical microstructures and the associated SAED patterns after processing of this alloy through routes 1 and 2, respectively.

Careful inspection after processing via route 1 showed that the microstructure was heterogeneous and consisted of areas where there were grain boundaries with high angles of misorientation, as in Fig. 5, and other areas where the boundaries were in low angles of misorientation. Measurements showed that the volume fraction of grains with high angle boundaries was ~60-70% and the remaining volume of ~30-40% contained low angle sub-boundaries. Measurements showed also that the average grain size and the sub-grain size were essentially identical at ~1.2 μm. It is clear from these observations that route 1 and a strain of ~4 is not capable of providing a stable homogeneous microstructure.

By contrast, the microstructure was homogeneous after processing through route 2 to a strain of ~12 and all of the boundaries exhibited high angles of misorientation. It is well-established that the boundary misorientation angles increase with increasing numbers of pressings in ECA pressing, and therefore with increasing strain [29], and these results demonstrate that a strain of ~12 is sufficient to attain an array of high angle boundaries in the Al-Mg-Li-Zr alloy. Measurements revealed an average grain size of ~1.2 μm and this value is identical to the recorded grain size after processing through route 1. Therefore, additional pressings to a higher strain serve only to permit an evolution of the microstructure with no corresponding refinement to smaller grain sizes.

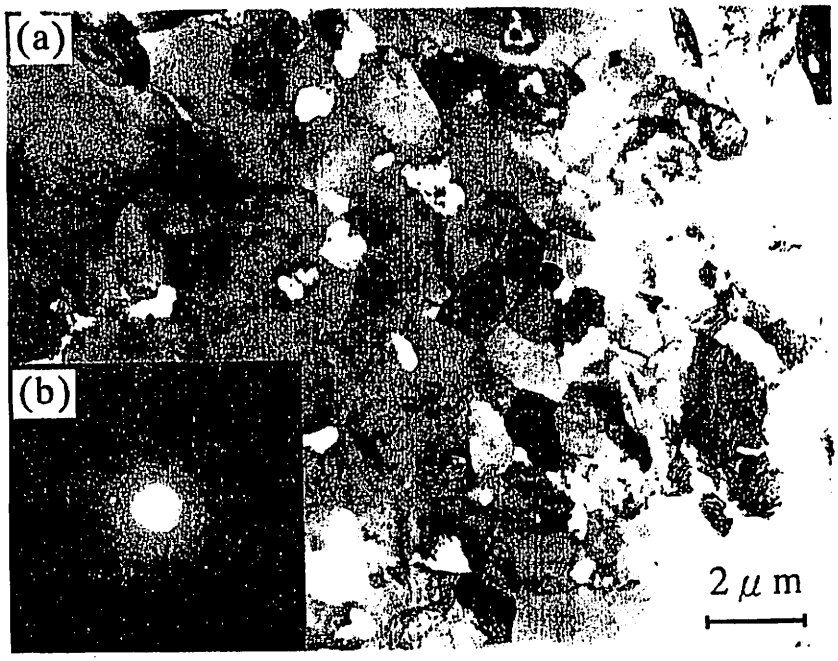

Figure 5 - Microstructure of the Al-Mg-Li-Zr alloy after processing through route 1.

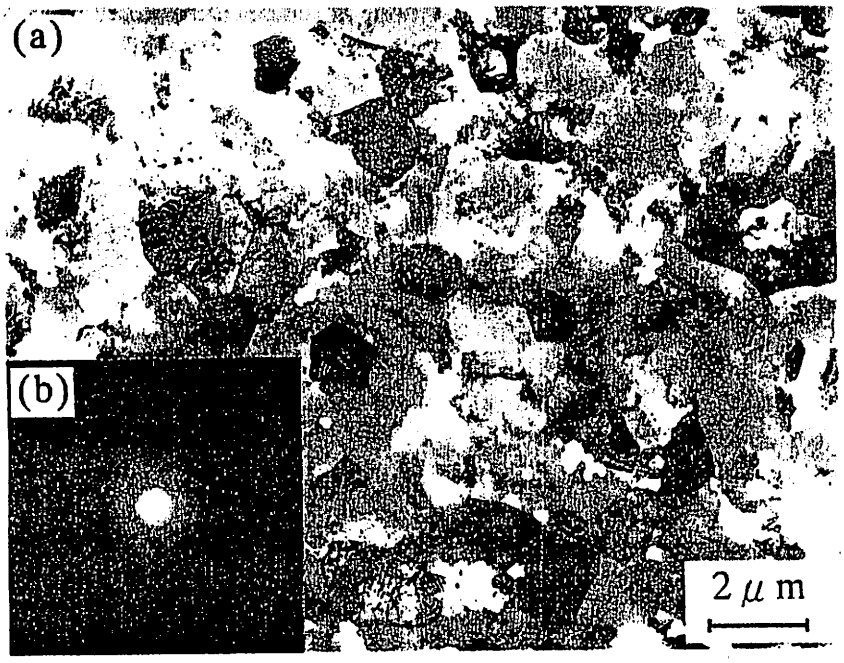

Figure 6 - Microstructure of the Al-Mg-Li-Zr alloy after processing through route 2.

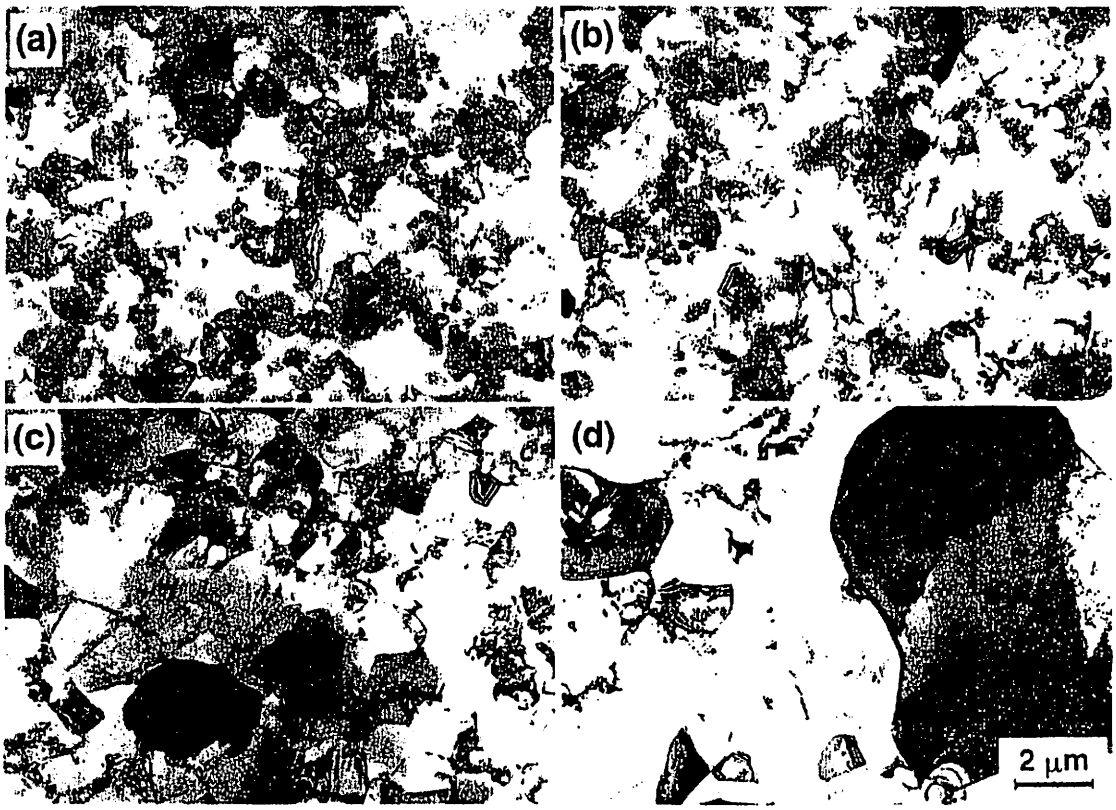

Figure 7 - Microstructures in the Al-Mg-Li-Zr alloy after pressing through route 1 and annealing for 1 hour at (a) 473 K, (b) 573 K, (c) 673 K and (d) 793 K, respectively.

Figure 7 shows the effect of static annealing of the Al-Mg-Li-Zr alloy, where the microstructures are the result of annealing of 1 hour at temperatures of (a) 473 K, (b) 573 K, (c) 673 K and (d) 793 K, respectively. It is apparent that, by comparison with the annealed microstructures shown in Fig. 4 for the Al-3% Mg alloy, grain growth is significantly inhibited in this material so that the grains remain small even at temperatures as high as 673 K, as shown in Fig. 7(c). Furthermore, this inhibition occurs despite the fact that the initial as-pressed grain size is larger by a factor of ~ 5. This grain stability is attributed to the presence of β'-Al_3Zr precipitates which are stable at these high temperatures.

The grain size stability of these two materials is compared directly in Fig. 8. Thus, the Al-3% Mg alloy exhibits fairly rapid grain growth at temperatures above ~ 500 K whereas the commercial Al-Mg-Li-Zr alloy retains essentially the same grain size of ~ 1.2 μm up to temperatures close to 700 K. At the very highest annealing temperatures, in the vicinity of 800 K, it is apparent that both materials exhibit very substantial grain growth and grain sizes of ~ 100 μm after annealing for 1 hour.

Tensile tests were conducted on samples processed through routes 1 and route 2. Figure 9 shows an example of the stress-strain curves for specimens processed via route 1 having a grain size, d, of 1.2 μm and pulled to failure at an absolute temperature, T, of 603 K using initial strain rates, $\dot{\varepsilon}$, from 3.3×10^{-4} to 3.3×10^{-2} s^{-1}. The three curves exhibit an initial strain hardening, probably associated with a relaxation of the high internal stresses associated with the ECA pressing, and then a strain weakening and ultimate failure. These plots show the potential for superplastic deformation with recorded elongations to failure of up to $\sim 550\%$.

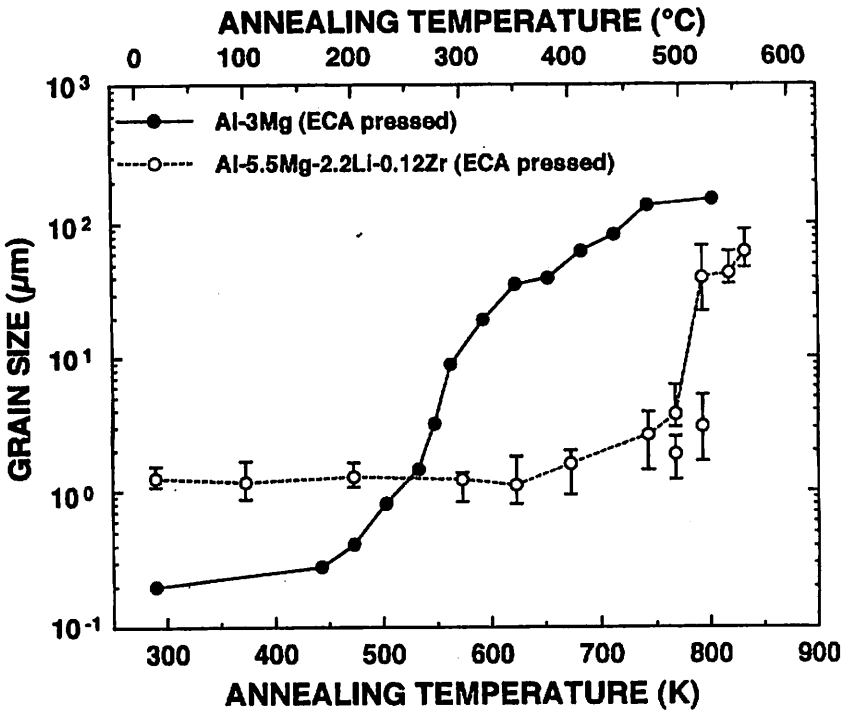

Figure 8 - Grain size versus annealing temperature for static annealing treatments of 1 hour on the Al-3% Mg alloy and the commercial Al-Mg-Li-Zr alloy.

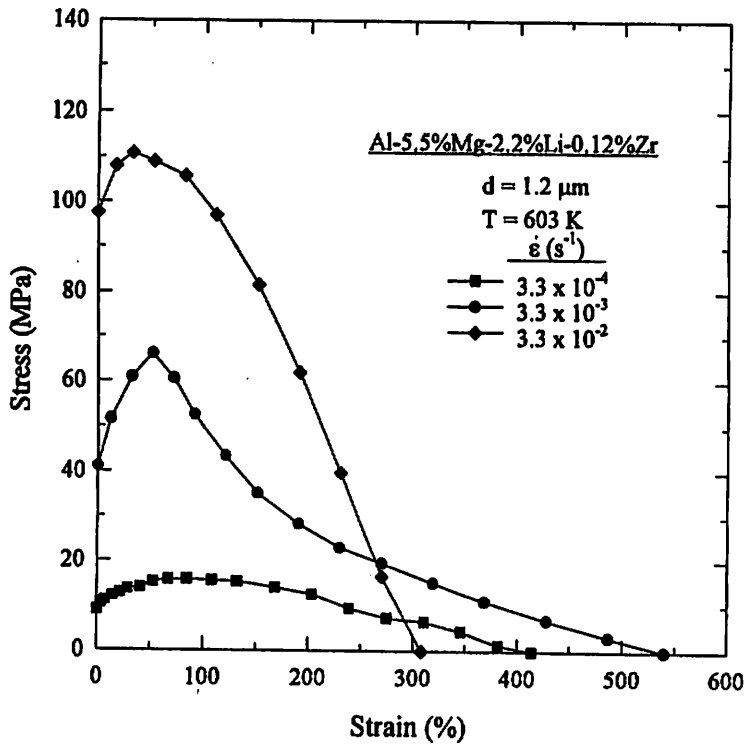

Figure 9 - True stress versus strain for the Al-Mg-Li-Zr alloy after processing via route 1.

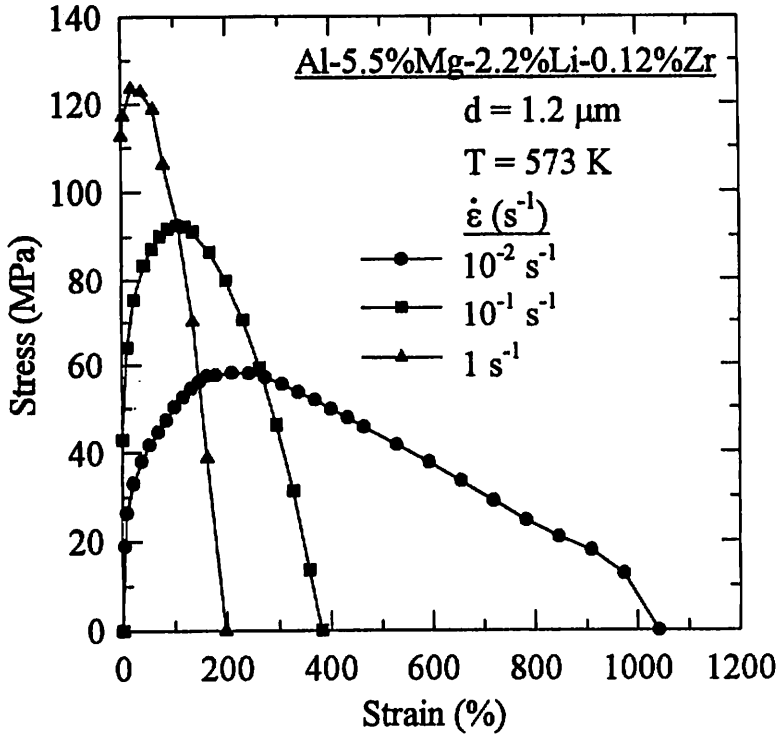

Figure 10 - True stress versus strain for the Al-Mg-Li-Zr alloy tested at 573 K after processing via route 2.

Similar plots are shown in Figs 10 and 11 for samples processed through route 2 and tested at temperatures of 573 and 623 K, respectively. These plots reveal the potential for remarkably high ductilities at rapid strain rates, including an elongation to failure of ~1040% at 573 K with an initial strain rate of 10^{-2} s^{-1} and an elongation of 1180% without failure at 623 K with an initial strain rate of 10^{-2} s^{-1}: the latter test was terminated without ultimate failure of the specimen and it clearly reveals the potential for HSR SP in this alloy after ECA pressing. This tendency is further confirmed by noting that the elongations to failure at 623 K are 910% and 340% for tests conducted with initial strain rates of 10^{-1} and 1 s^{-1}, respectively. These elongations obtained on the cast Al-Mg-Li-Zr alloy after ECA pressing exceed the tabulated data for Al-based materials exhibiting HSR SP and prepared using mechanical alloying and powder metallurgy procedures [3].

Figure 12 shows the appearance of the two specimens exhibiting the highest elongations at a testing temperature of 623 K: the top specimen shows the untested configuration. Inspection shows that both specimens pull out in a very uniform manner, without any necking within the gauge length, thereby confirming the advent of superplastic flow under these testing conditions.

A comparison of Figs 9 and 11, which represent almost identical testing temperatures, shows that the ductility is greatly enhanced by ECA pressing to a strain of ~12 (route 2) rather than to a strain of ~4 (route 1). This difference is attributed to the presence of a homogeneous array of high angle grain boundaries when using processing route 2.

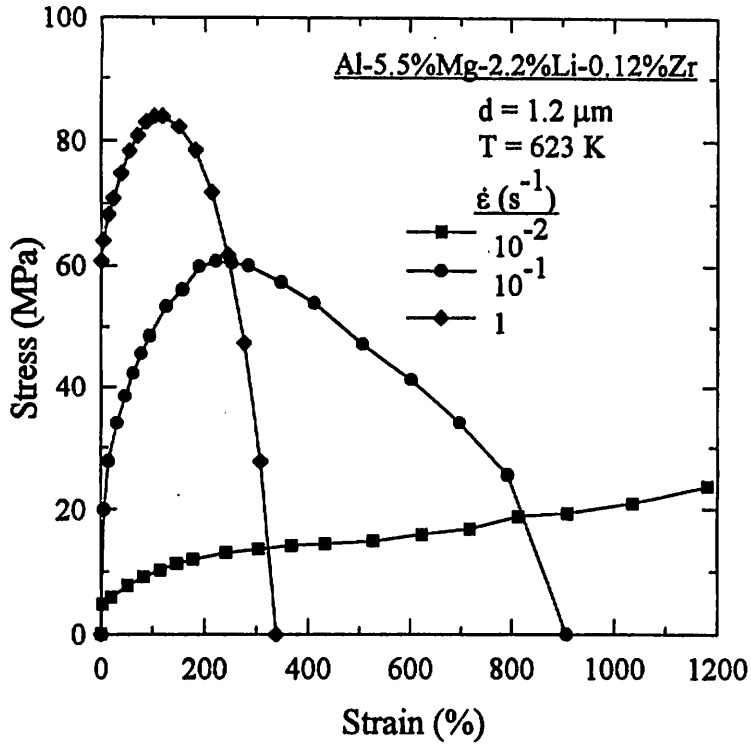

Figure 11 - True stress versus strain for the Al-Mg-Li-Zr alloy tested at 623 K after processing via route 2.

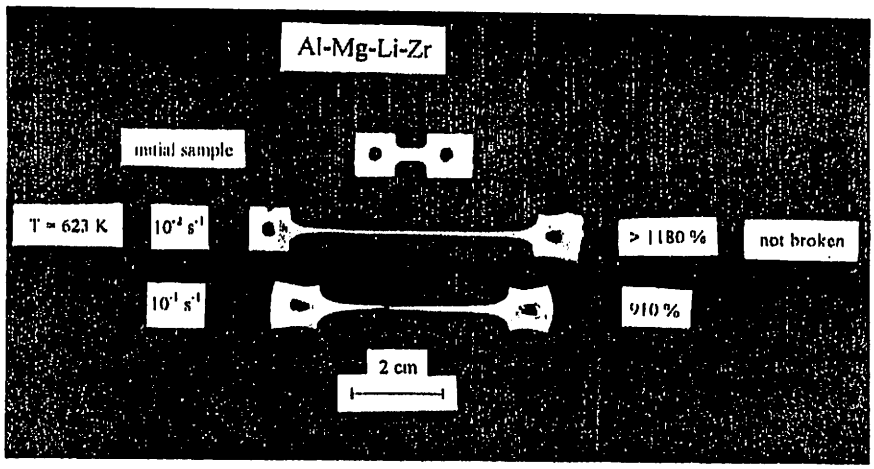

Figure 12 - Appearance of two specimens processed via route 2 and tested in tension at 623 K: the upper specimen is untested.

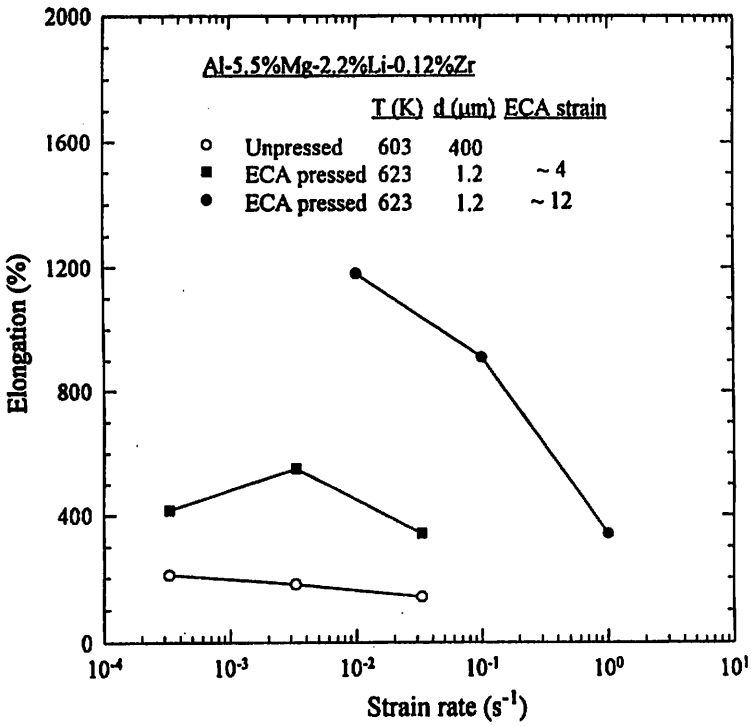

Figure 13 - Elongation versus strain rate for tests conducted at similar testing temperatures using samples without ECA pressing and after ECA pressing via route 1 (strain ~4) and route 2 (strain ~12), respectively.

A direct comparison of the elongations is shown in Fig. 13 for tests conducted at similar temperatures in the vicinity of 610 K. In the unpressed condition, with an initial grain size of ~400 μm, the tensile ductilities are low in the strain rate range from ~10^{-4} to 10^{-1} s^{-1}, but pressing through route 1 gives reasonable ductility and the appearance of limited superplastic-like flow and pressing through route 2 gives exceptionally high elongations to failure even at the highest testing strain rate of 1 s^{-1}.

It is apparent from these results that ECA pressing is an effective tool for introducing an ultrafine grain size for subsequent HSR SP in tensile testing but, because superplasticity occurs by grain boundary sliding [30], high angle grain boundaries are an important prerequisite for the occurrence of significant sliding and this necessitates continuing the ECA pressing to a total strain which is sufficiently high that the microstructure consists of a homogeneous array of high angle boundaries. In the present experiments on the commercial Al-Mg-Li-Zr alloy, this condition is achieved with a strain of ~12 but not with a strain of ~4.

Summary and conclusions

1. The process of equal-channel angular (ECA) pressing can be used to produce ultrafine grain sizes in Al-based alloys, but the subsequent stability of these grains at elevated temperatures

requires the presence of precipitates to inhibit grain growth. Experiments show that an Al-3% Mg alloy exhibits rapid grain growth at temperatures above ~500 K whereas a commercial Al-Mg-Li-Zr alloy exhibits a relatively stable grain size up to temperatures as high as ~700 K.

2. High strain rate superplasticity (HSR SP) can be attained in the cast Al-Mg-Li-Zr alloy provided the ECA pressing is continued to a sufficiently high strain that the microstructure is homogeneous and consists of an array of high angle grain boundaries.

Acknowledgements

This work was supported in part by the Light Metals Educational Foundation of Japan, in part by a Grant-in-Aid for Scientific Research from the Ministry of Education, Science, Sports and Culture of Japan, in part by the Japan Society for the Promotion of Science, in part by the National Science Foundation of the United States under Grants No. DMR-9625969 and INT-9602919 and in part by the U.S. Army Research Office under Grants No. DAAH04-96-1-0332 and N68171-96-6-9006.

References

1. T.G. Langdon, "The Mechanical Properties of Superplastic Materials," Metall. Trans., 13A (1982) 689-701.
2. T.G. Nieh, C.A. Henshall and J. Wadsworth, "Superplasticity at High Strain Rates in a SiC Whisker Reinforced Al Alloy," Scripta Metall., 18 (1984) 1405-1408.
3. K. Higashi, M. Mabuchi and T.G. Langdon, "High-Strain-Rate Superplasticity in Metallic Materials and the Potential for Ceramic Materials," ISIJ Intl., 36 (1996) 1423-1438.
4. T.G. Nieh, J. Wadsworth and O.D. Sherby, Superplasticity in Metals and Ceramics (Cambridge, England: Cambridge University Press, 1997), 154-188.
5. F.A. Mohamed, M.M.I. Ahmed and T.G. Langdon, "Factors Influencing Ductility in the Superplastic Zn-22 Pct Al Eutectoid," Metall. Trans., 8A (1977) 933-938.
6. Y. Ma, M. Furukawa, Z. Horita, M. Nemoto, R.Z. Valiev and T.G. Langdon, "Significance of Microstructural Control for Superplastic Deformation and Forming," Mater. Trans. JIM, 37 (1996) 336-339.
7. H. Gleiter, "Materials with Ultra-fine Grain Sizes," in Deformation of Polycrystals: Mechanisms and Microstructures, ed. N. Hansen, A. Horsewell, T. Leffers and H. Lilholt (Roskilde, Denmark: Risø National Laboratory, 1981), 15-21.
8. P.G. Sanders, G.E. Fougere, L.J. Thompson, J.A. Eastman and J.R. Weertman, "Improvements in the Synthesis and Compaction of Nanocrystalline Materials," Nanostruct. Mater., 8 (1997) 243-252.
9. C.C. Koch and Y.S. Cho, "Nanocrystals by High Energy Ball Milling," Nanostruct. Mater., 1 (1992) 207-212.
10. D.A. Rigney, "Sliding Wear of Metals," Ann. Rev. Mater. Sci., 18 (1988) 141-163.
11. N.A. Smirnova, V.I. Levit, V.I. Pilyugin, R.I. Kuznetsov, L.S. Davydova and V.A. Sazonova, "Evolution of Structure of f.c.c. Single Crystals During Strong Plastic Deformation," Fiz. Metal. Metalloved., 61 (1986) 1170-1177.
12. V.M. Segal, V.I. Reznikov, A.E. Drobyshevskiy and V.I. Kopylov, "Plastic Working of Metals by Simple Shear," Russian Metallurgy (Metally), 1 (1981) 99-105.
13. V.M. Segal, V.I. Reznikov, V.I. Kopylov, D.A. Pavlik and V.F. Malyshev, Process of Structure Formation During Plastic Straining (Minsk, Belarus: Science and Technical Publishing, 1994).

14. R.Z. Valiev and N.K. Tsenev, "Structure and Superplasticity of Al-based Submicron Grained Alloys," in Hot Deformation of Aluminum Alloys, ed. T.G. Langdon, H.D. Merchant, J.G. Morris and M.A. Zaidi (Warrendale, PA: The Minerals, Metals and Materials Society, 1991), 319-329.
15. R.Z. Valiev, N.A. Krasilnikov and N.K. Tsenev, "Plastic Deformation of Alloys with Submicron-grained Structure," Mater. Sci. Engng, A137 (1991) 35-40.
16. R.Z. Valiev, A.V. Korznikov and R.R. Mulyukov, "Structure and Properties of Ultrafine-grained Materials Produced by Severe Plastic Deformation," Mater. Sci. Engng, A168 (1993) 141-148.
17. Y. Iwahashi, J. Wang, Z. Horita, M. Nemoto and T.G. Langdon, "Principle of Equal-Channel Angular Pressing for the Processing of Ultra-fine Grained Materials," Scripta Mater., 35 (1996) 143-146.
18. Y. Wu and I. Baker, "An Experimental Study of Equal Channel Angular Extrusion," Scripta Mater., 37 (1997) 437-441.
19. J. Wang, Y. Iwahashi, Z. Horita, M. Furukawa, M. Nemoto, R.Z. Valiev and T.G. Langdon, "An Investigation of Microstructural Stability in an Al-Mg Alloy with Submicrometer Grain Size," Acta Mater., 44 (1996) 2973-2982.
20. M. Furukawa, Z. Horita, M. Nemoto, R.Z. Valiev and T.G. Langdon, "Microhardness Measurements and the Hall-Petch Relationship in an Al-Mg Alloy with Submicrometer Grain Size," Acta Mater., 44 (1996) 4619-4629.
21. J. Wang, M. Furukawa, Z. Horita, M. Nemoto, R.Z. Valiev and T.G. Langdon, "Enhanced Grain Growth in an Al-Mg Alloy with Ultrafine Grain Size," Mater. Sci. Engng, A216 (1996) 41-46.
22. I.N. Fridlyander, V.S. Sandler and T.I. Nikol'skaya, "Investigation of the Ageing of Aluminium-Magnesium-Lithium Alloys," Fiz. Metal. Metalloved, 32 (1971) 767-774.
23. M. Furukawa, Y. Iwahashi, Z. Horita, M. Nemoto, N.K. Tsenev, R.Z. Valiev and T.G. Langdon, "Structural Evolution and the Hall-Petch Relationship in an Al-Mg-Li-Zr Alloy with Ultra-fine Grain Size," Acta Mater., 45 (1997) 4751-4757.
24. M. Furukawa, P.B. Berbon, Z. Horita, M. Nemoto, N.K. Tsenev, R.Z. Valiev and T.G. Langdon, "Age Hardening and the Potential for Superplasticity in a Fine-grained Al-Mg-Li-Zr Alloy," Metall. Trans., in press.
25. Z. Horita, D.J. Smith, M. Furukawa, M. Nemoto, R.Z. Valiev and T.G. Langdon, "An Investigation of Grain Boundaries in Submicrometer-grained Al-Mg Solid Solution Alloys Using High-Resolution Electron Microscopy," J. Mater. Res., 11 (1996) 1880-1890.
26. R.Z. Valiev, R.Sh. Musalimov and N.K. Tsenev, "The Non-Equilibrium State of Grain Boundaries and the Grain Boundary Precipitations in Aluminium Alloys," Phys. Stat. Sol. (a), 115 (1989) 451-457.
27. A.A. Nazarov, A.E. Romanov and R.Z. Valiev, "On the Structure, Stress Fields and Energy of Nonequilibrium Grain Boundaries," Acta Metall. Mater., 41 (1993) 1033-1040.
28. M. Furukawa, Z. Horita, M. Nemoto, R.Z. Valiev and T.G. Langdon, "Recrystallization in Ultrafine-grained Materials with Non-Equilibrium Grain Boundaries," Proceedings of ReX'96: The Third International Conference on Recrystallization and Related Phenomena, ed. T.R. McNelley (Monterey, CA: Monterey Institute of Advanced Studies, 1997), 149-160.
29. Y. Iwahashi, Z. Horita, M. Nemoto and T.G. Langdon, "An Investigation of Microstructural Evolution During Equal-Channel Angular Pressing," Acta Mater., 45 (1997) 4733-4741.
30. T.G. Langdon, "An Evaluation of the Strain Contributed by Grain Boundary Sliding in Superplasticity," Mater. Sci. Engng, A174 (1994) 225-230.

SUPERPLASTICITY IN AN ULTRAFINE-GRAINED Al-Mg-Sc ALLOY PRODUCED BY EQUAL-CHANNEL ANGULAR PRESSING

Shogo Komura,[1] Patrick B. Berbon,[2] Atsushi Utsunomiya,[1] Minoru Furukawa,[3] Zenji Horita,[1] Minoru Nemoto[1] and Terence G. Langdon[2]

[1]Department of Materials Science and Engineering, Faculty of Engineering
Kyushu University, Fukuoka 812-81, Japan
[2]Departments of Materials Science and Mechanical Engineering
University of Southern California, Los Angeles, CA 90089-1453, U.S.A.
[3]Department of Technology, Fukuoka University of Education
Munakata, Fukuoka 811-41, Japan

Abstract

An Al-3% Mg-0.2% Sc alloy was subjected to equal-channel angular (ECA) pressing to produce a grain size of ~0.2 μm. Static annealing experiments showed that it was possible to retain a very small grain size at temperatures up to 673 K for an annealing time of 1 hour. Large tensile ductilities were observed after ECA pressing, including elongations of >600% and >1000% when testing with an initial strain rate of 3.3×10^{-2} s^{-1} at temperatures of 573 and 673 K, respectively. The results demonstrate the potential for using a scandium addition in Al-based alloys in order to retain an ultrafine grain size at elevated temperatures and thereby to achieve superplastic ductilities.

Hot Deformation of Aluminum Alloys II
Edited by T.R. Bieler, L.A. Lalli, and S.R. MacEwen
The Minerals, Metals & Materials Society, 1998

Introduction

Superplasticity refers to the capability of some materials for exhibiting very large elongations when pulled in tension [1]. It is now well-established that there are two important requirements in order to achieve superplasticity in polycrystalline metals [2]. First, superplasticity occurs by the process of grain boundary sliding in which strain is achieved by the relative displacements of adjacent grains [3] and this means in practice that the grain size of the material must be very small. Typical grain sizes in superplastic alloys are of the order of ~1 – 10 μm. Second, superplasticity occurs by a diffusion-controlled process and this requires a sufficiently high temperature so that diffusion is reasonably rapid. In practice, superplastic ductilities are generally observed at temperatures above ~0.5 T_m, where T_m is the absolute melting temperature of the material.

For most superplastic metals, the grain size is generally ~1 – 5 μm and optimum superplasticity occurs at a strain rate in the vicinity of ~10^{-3} s^{-1} with a strain rate sensitivtiy, m, which is usually close to ~0.5. This behavior is designated region II and in practice the superplastic effect is lost at slower and faster strain rates in the two regions of behavior designated regions I and III. Since superplasticity occurs over a narrow range of strain rates, superplastic forming operations in industry are restricted to relatively low strain rates so that the forming times are fairly long (typically, up to ~30 minutes).

A possible procedure for achieving high tensile ductility at faster strain rates, and thereby improving the superplastic forming capability, is to decrease the grain size to within the submicrometer or nanometer level. Experiments on the Zn-22% Al eutectoid alloy have shown that a decrease in grain size has the potential for both increasing the total elongations to failure and achieving these high elongations at faster strain rates [4]. However, it is usually difficult in practice to reduce the grain size within a polycrystalline matrix to a size less than ~1 μm.

Attention has been focussed recently on a new procedure for grain refinement known as equal-channel angular (ECA) pressing. This procedure was originally developed as a method of working metals in simple shear [5] and subsequently it was reported that ECA pressing may be used to produce ultrafine grain sizes in polycrystalline materials [6,7]. Therefore, there is a potential for using this procedure to achieve an ultrafine grain size and it is possible, in addition, that the material may exhibit superplasticity at reasonably rapid strain rates. Very recent experiments on Al-Mg-Li-Zr and Al-Cu-Zr alloys have confirmed this possibility with grain sizes of ~1 μm and reported elongations of >1000% and >600% when testing at an initial strain of 1 x 10^{-2} s^{-1} for these two alloys, respectively [8].

The present investigation was initiated in order to examine the ECA pressing of an Al-3% Mg alloy containing an addition of 0.2% Sc. Scandium was selected as the addition because it is well known that the presence of dilute amounts of scandium in aluminum-based alloys leads to enhanced properties including increased strength and a significant inhibition in grain growth and recrystallization [9,10]. Furthermore, there is experimental evidence for high tensile ductilities (>1000%) in an Al-4% Mg alloy containing 0.5% Sc thereby demonstrating the superplastic potential in Al-Mg alloys with Sc additions [11]. As will be demonstrated, the Al-3% Mg-0.2% Sc alloy used in the present investigation exhibited a submicrometer grain size after ECA pressing and subsequent tensile testing

gave elongations to failure of up to >1000% when testing at 673 K with an initial strain rate of 3.3×10^{-2} s^{-1}.

Experimental material and procedures

The experiments were conducted using an alloy of Al–3% Mg–0.2% Sc. The material was prepared by arc melting, in an Ar atmosphere, Al of 99.99% purity and 3 wt % Sc of 99.999% purity to form an Al–3% Sc alloy. This material was then remelted with additional Al and 3 wt % Mg to give the required Al–3% Mg–0.2% Sc alloy. The molten alloy was cast into a steel mold to form a small ingot with dimensions of 17 x 55 x 120 mm^3 and the ingot was then homogenized in air for one day at a temperature of 743 K. Approximately 1 mm was removed from each surface of the ingot by grinding and the ingot was cut into three bars each having dimensions of 15 x 15 x 120 mm^3. These bars were swaged to provide the alloy in the form of rods with a diameter of 10 mm. The rods were cut to lengths of ~60 mm and they were then annealed for 1 hour in air at 883 K. Inspection by optical microscopy after annealing revealed a grain size of ~200 μm.

Each rod was subjected to ECA pressing using the procedure illustrated schematically in Fig. 1. In ECA pressing the sample, which is typically in the form of a rod, is pressed through a die using a plunger. In the present experiments, the die was made from a solid block of high strength tool steel and it contained a single channel, circular in cross–section, which passed through the die in an L–shaped configuration. Two angles are generally used to define the precise nature of the ECA pressing configuration. In the

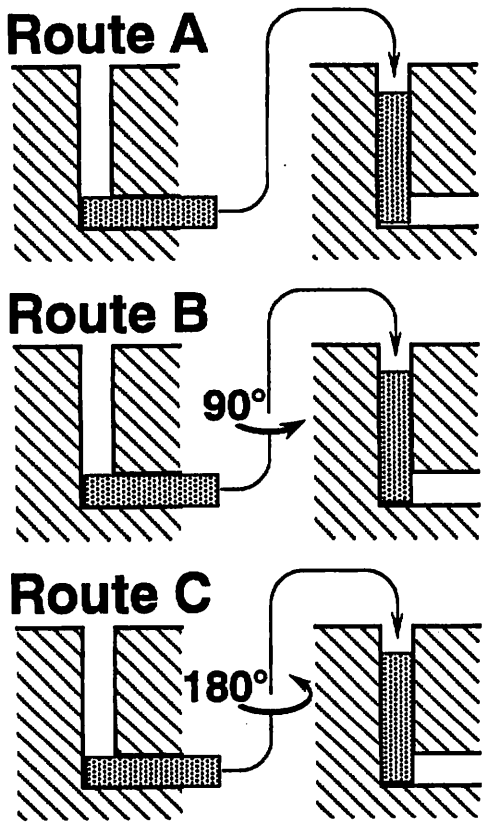

Figure 1 – Schematic illustration of ECA pressing and different processing routes.

present experiments, the angle of intersection between the two separate parts of the channel was $\phi = 90°$ and the angle defining the outer arc of curvature at the point of intersection was $\psi = 90°$. All pressings were conducted in air at ambient temperature for a total of 8 passes through the die and with no additional annealing during the pressing procedure. Three distinct processing routes are illustrated in Fig. 1. However, it was shown earlier, in experiments on pure Al, that a homogeneous equilibrium microstructure, consisting of an array of grains having high angle grain boundaries, is achieved most readily when the sample is rotated by 90° in the same direction between each separate passage through the die [12] and the same procedure was used in these experiments. This processing technique is designated route B in Fig. 1 and the associated shearing characteristics are described in detail elsewhere [13].

It can be shown from first principles that the total strain accrued in a sample on passage through an ECA pressing die depends upon the values of the two angles, ϕ and ψ [14]. For the present experiments, the values of ϕ and ψ lead to a calculated strain of ~1 on each separate passage through the die, giving a total strain of ~8 after 8 passes. Model experiments have confirmed the validity of the method used to estimate the strain except in the presence of frictional effects at the walls of the channel [15]. In these experiments, frictional effects were reduced by using a molybdenum disulfide lubricant.

After the ECA pressing, several bars were sliced perpendicular to the longitudinal axis to give a number of small pieces having thicknesses of ~0.4 mm. These specimens were used to investigate the stability of the as-pressed microstructure by statically annealing for 1 hour in an argon atmosphere at selected temperatures in the range from 373 to 773 K.

Following ECA pressing through 8 passes, tensile specimens were machined from the samples with cross-sections of 1×3 mm^2 and gauge lengths of 4 mm. The machining was conducted so that the gauge length of each sample lay parallel to the longitudinal axis after pressing. Tensile tests were conducted using an Instron testing machine operating at a constant rate of cross-head displacement and with initial strain rates from 3.3×10^{-4} to 3.3×10^{-2} s^{-1}. These tests were performed in air at temperatures from 523 to 723 K with the temperature controlled to within ±2 K during each test and with the variation of load with strain recorded continuously on a strip-chart recorder. The yield stresses were estimated from the 0.2% offsets for each separate curve.

Samples were examined by transmission electron microscopy (TEM) after ECA pressing and also after static annealing. Discs were prepared having diameters of 3 mm and thicknesses of ~0.15 mm and these discs were then thinned to perforation using a twin-jet electropolishing unit with a mixture of 10% $HClO_4$, 20% $C_3H_8O_3$ and 70% C_2H_5OH at a temperature of 278 K. Specimens were prepared for TEM from within the gauge lengths after tensile testing using a focused ion beam facility (Hitachi FB-2000). All microstructural observations were made using an Hitachi H-8100 transmission electron microscope operating at 200 kV. Selected area electron diffraction (SAED) patterns were taken from regions of the samples using, except where noted otherwise, a diameter of 12.3 μm.

For comparison purposes, some additional experiments were also conducted using an Al-3% Mg solid solution alloy with an initial unpressed grain size of ~500 μm. Further details concerning the ECA pressing and the characteristics of this material were given in earlier reports [16-18].

Microstructural observations after ECA pressing

Figure 2 shows examples of the microstructure after ECA pressing for (a) an Al–3% Mg alloy subjected to ECA pressing at room temperature for a total of 8 passes and (b) the Al–3% Mg–0.2% Sc alloy after ECA pressing for a total of 8 passes: the SAED patterns are also included for both of these microstructures.

Inspection of the SAED pattern in Fig. 2(b) shows that the microstructure for the Al–Mg–Sc alloy in this field of view contains boundaries having high angles of misorientation and it is apparent that there is an array of essentially equiaxed grains. However, careful inspection of a large area of the Al–Mg–Sc sample revealed a heterogeneous microstructure consisting of some regions with grains separated by boundaries having high angles of misorientation and some regions with subgrains separated by boundaries having low angles of misorientation. This lack of homogeneity, and the presence of regions of both grains and subgrains, is similar also to observations reported earlier for an Al–Mg–Li–Zr alloy subjected to ECA pressing to a strain of ~3.7 at a temperature of 673 K [19] but it contrasts with the Al–3% Mg solid solution alloy where the microstructure is homogeneous after 8 passes through the ECA die at room temperature. Thus, the microstructure shown in Fig. 2(a) is representative of the grain boundary configurations in this alloy.

It was estimated from detailed inspection that the Al–Mg–Sc alloy contained, after 8 passes through the die, a volume fraction of the order of ~10% of subgrains with low angle boundaries and ~90% of grains with high angle boundaries. The average grain size in this alloy was estimated as ~0.2 μm from an examination of several different areas containing both subgrains and grains. As with the Al–Mg–Li–Zr alloy investigated earlier [19], the measured average subgrain size was essentially identical to the measured average grain size.

An important conclusion from these observations is that the grain size attained in the Al–Mg–Sc alloy (~0.2 μm) is, within the experimental accuracy, identical to the reported grain size for the Al–3% Mg alloy after ECA pressing at room temperature (~0.2 μm) [17]. Recent experiments have shown that the equilibrium grain size attained by ECA pressing depends, at least in part, upon the rate of recovery in the material [20]. In pure Al, for example, the equilibrium grain size was measured as ~1 μm after ECA pressing at room temperature for 4 passes [12,21] and in a commercial Al–Mg–Li–Zr alloy the equilibrium grain size was reported as ~1.2 μm after pressing to a strain of ~3.7 at a temperature of 673 K [19]. Based on the present results, where the Al–3% Mg alloy and the Al–3% Mg–0.2% Sc alloy both have essentially identical equilibrium grain sizes, it is reasonable to conclude that the presence of 0.2 wt % Sc in the Al–3% Mg alloy has no significant effect on either the overall recovery rate or the magnitude of the stacking fault energy of the material.

Inspection of Fig. 2 shows also that the Al–Mg alloy and the Al–Mg–Sc alloy both contain grain boundaries which are relatively poorly delineated and appear to represent the transitions between grains or grain fragments. These boundaries are generally characterized as non–equilibrium boundaries [22,23] and they are typical of the boundaries observed in ultrafine–grained materials fabricated using intense plastic straining techniques [7,24–26].

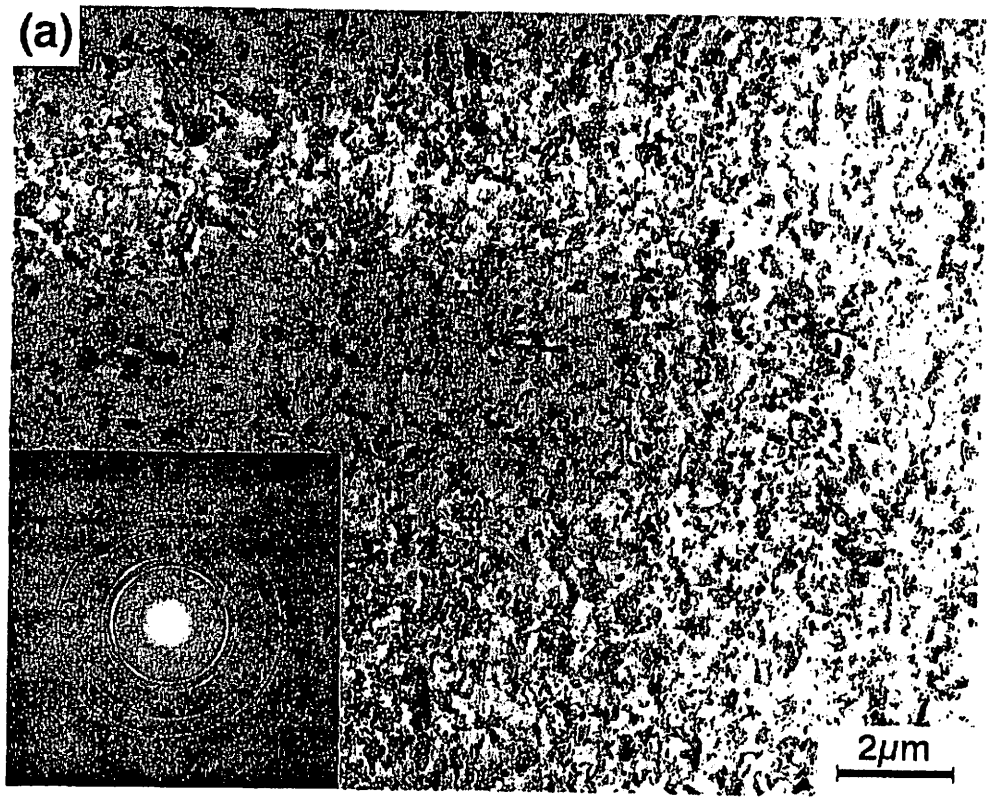

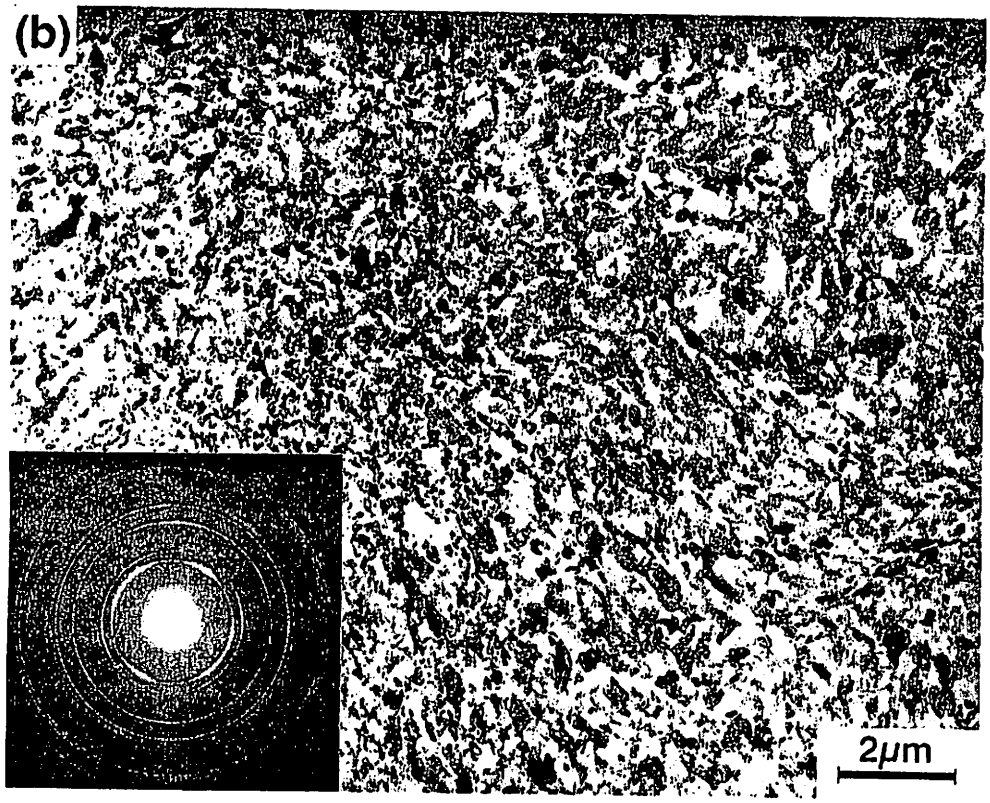

Figure 2 – Microstructures after ECA pressing for (a) Al–3% Mg alloy and (b) Al–3% Mg–0.2% Sc alloy.

Microstructural observations after static annealing

Several specimens were subjected to static annealing for periods of 1 hour at different temperatures up to 773 K and Fig. 3 shows examples of the microstructures after annealing for the Al–3% Mg alloy (on the left) and the Al–3% Mg–0.2% Sc alloy (on the right).

A detailed description of the microstructural evolution which occurs on annealing of the Al–3% Mg alloy was given earlier [17]. Briefly, this alloy exhibited little or no grain growth up to temperatures of ~500 K but at temperatures in the range of ~500 – 560 K there was a duplex structure of very small unrecrystallized grains and larger recrystallized grains and at temperatures above ~560 K the material was essntially fully recrystallized and there was a uniform distribution of grains separated by high angle grain boundaries. Ultimately, at temperatures above ~750 K, the grains grew to reach average sizes of >100 μm. These observations of substantial grain growth at elevated temperatures suggest that the Al–3% Mg alloy is not a suitable candidate material for the development of a superplastic forming capability. It is therefore important to examine methods by which an ultrafine grain size may be retained at temperatures higher than ~500 K.

It is apparent from inspection of the microstructures given in Fig. 3 for the Al–Mg–Sc alloy (on the right) that the structure remains almost the same as in the ECA-pressed condition after annealing at 473 K. It is also apparent that there is only a minor increase in the average grain size at annealing temperatures of 573 and 673 K although careful inspection revealed that some of the grain boundaries became better defined after annealing at these higher temperatures suggesting a gradual evolution into a more equilibrated configuration. Furthermore, and unlike the Al–3% Mg solid solution alloy, the grain size of the Al–Mg–Sc alloy remains in the ~1 – 2 μm range even after annealing at a temperature of 723 K. At the highest annealing temperature of 773 K, it was found that there were some regions containing reasonably large grains; an example of these large grains may be seen in the microstructure shown at the bottom right in Fig. 3.

These observations demonstrate that the very fine grain size is remarkably stable in the Al–3% Mg alloy when 0.2 wt % Sc is introduced. The grain stability inherent in the Al–Mg alloy through the introduction of scandium is evident from the direct comparison shown in Fig. 4 which plots the average grain size versus the annealing temperature for the Al–3% Mg alloy [17,18] and for the Al–3% Mg–0.2% Sc alloy. Thus, the Al–Mg–Sc alloy retains a grain size of <3 μm up to the highest annealing temperature of 773 K whereas the Al–3% Mg alloy exhibits grain growth to sizes of >100 μm in the absence of the scandium additive.

The stability of the grain structure by the addition of dilute amounts of scandium may be attributed to the introduction of fine coherent Al_3Sc precipitates which serve both to strengthen the matrix alloy and to inhibit recrystallization [9,27,28]. These precipitates are thermally stable up to temperatures close to the melting point of the alloy and therefore they are exceptionally effective in inhibiting the movement of grain boundaries and in suppressing grain growth. For example, it is well documented that the presence of small amounts of Sc in aluminum-based alloys can increase the recrystallization temperature to >600°C [9] which is higher than the normal temperature for the solution heat treatment of aluminum alloys in industrial applications.

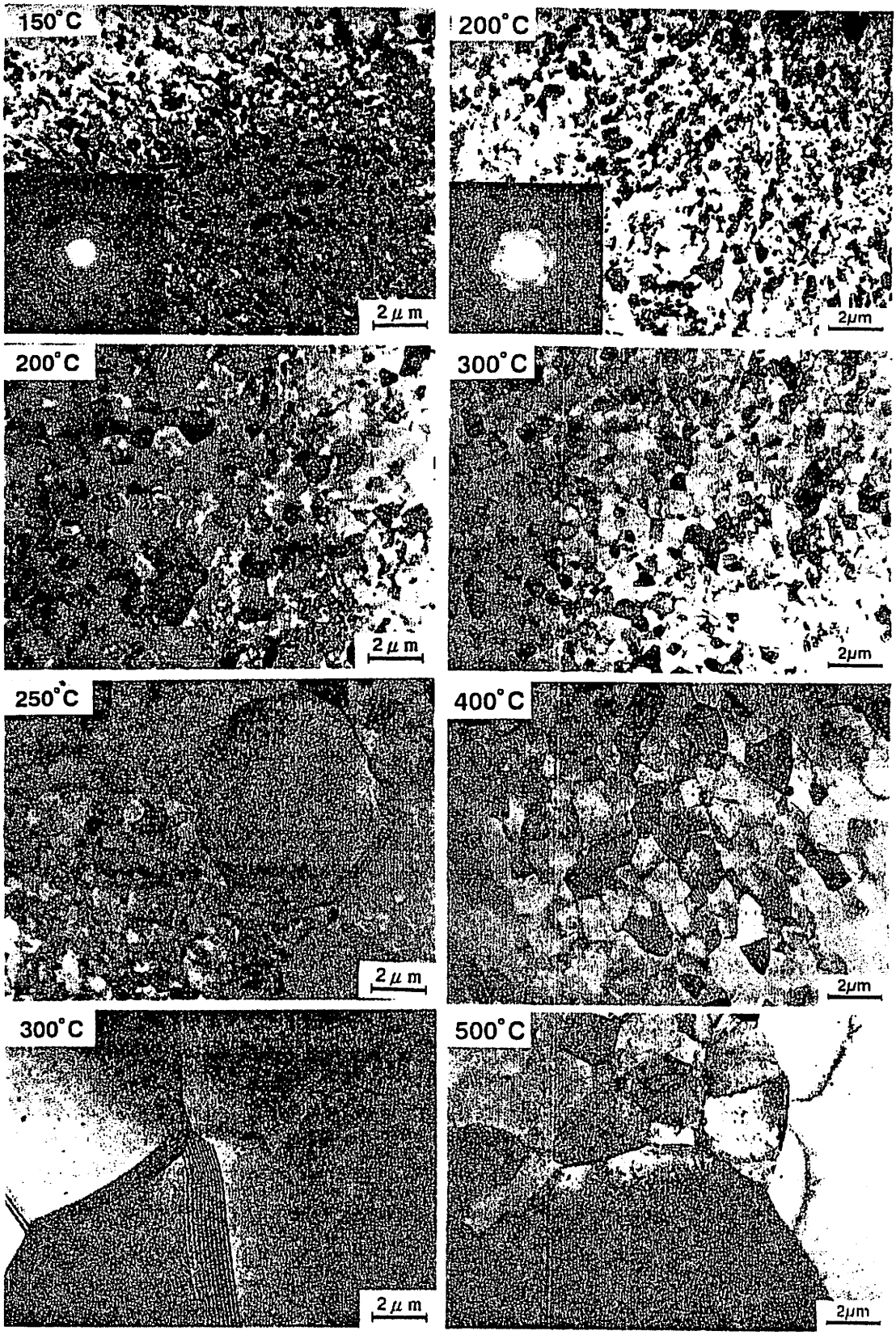

Figure 3 – Microstructures after static annealing for 1 hour for Al–3% Mg alloy (on left) and Al–3% Mg–0.2% Sc alloy (on right).

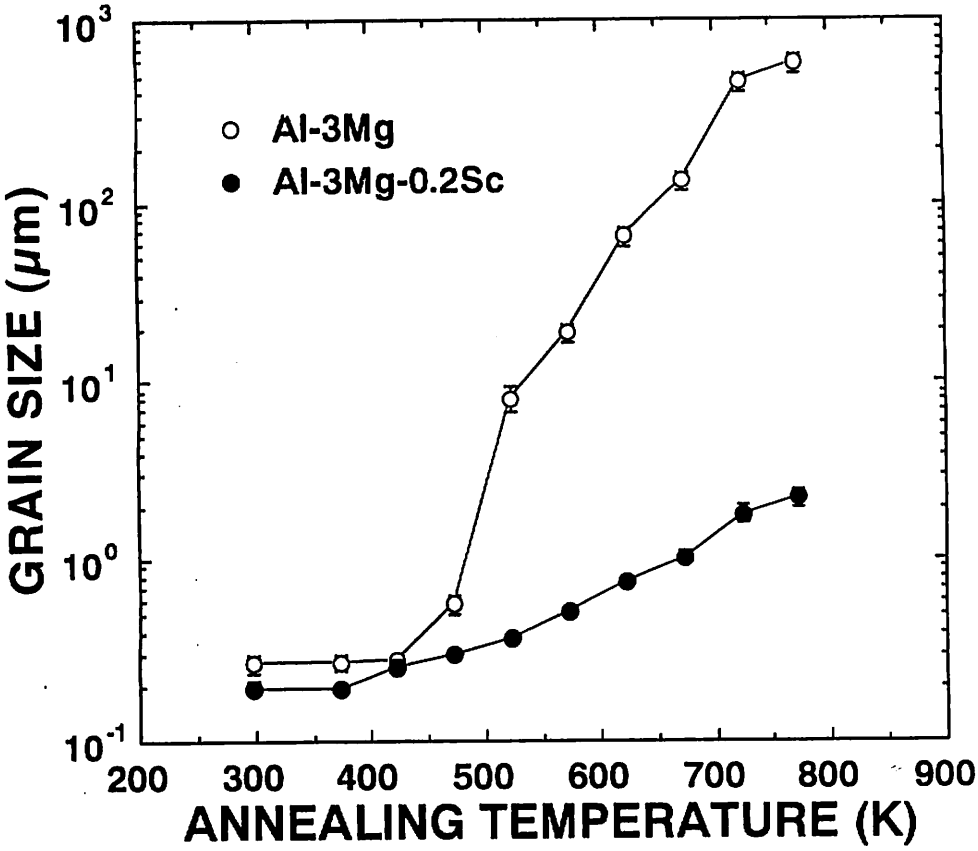

Figure 4 – Grain size versus annealing temperature for Al–3% Mg and for Al–3% Mg–0.2% Sc.

Stress–strain behavior of the Al–Mg–Sc alloy

The requirement for the realization of high strain rate superplasticity is good tensile ductility and superplastic elongations to failure at strain rates faster than 10^{-2} s^{-1} [29]. Therefore, tensile testing of the Al–Mg–Sc alloy was conducted after ECA pressing but without any subsequent annealing.

Typical stress–strain curves are shown in Fig. 5 for two tests conducted under the same conditions of an initial strain rate of 3.3×10^{-2} s^{-1} and at the two temperatures of 573 and 673 K. Inspection shows that both curves exhibit an initial period of strain hardening and then subsequent softening leading ultimately to failure of the samples. The yield stresses for these two curves, corresponding to the 0.2% offsets, were estimated as ~31 and ~12 MPa at the testing temperatures of 573 and 673 K, respectively.

It is apparent from Fig. 5 that the two ECA–pressed specimens exhibit substantial ductility even at this rapid strain rate, with elongations to failure of ~610% and ~1030% at the two temperatures of 573 and 673 K, respectively. These results therefore demonstrate the capability of achieving superplastic behavior in the Al–Mg–Sc alloy at high strain rates.

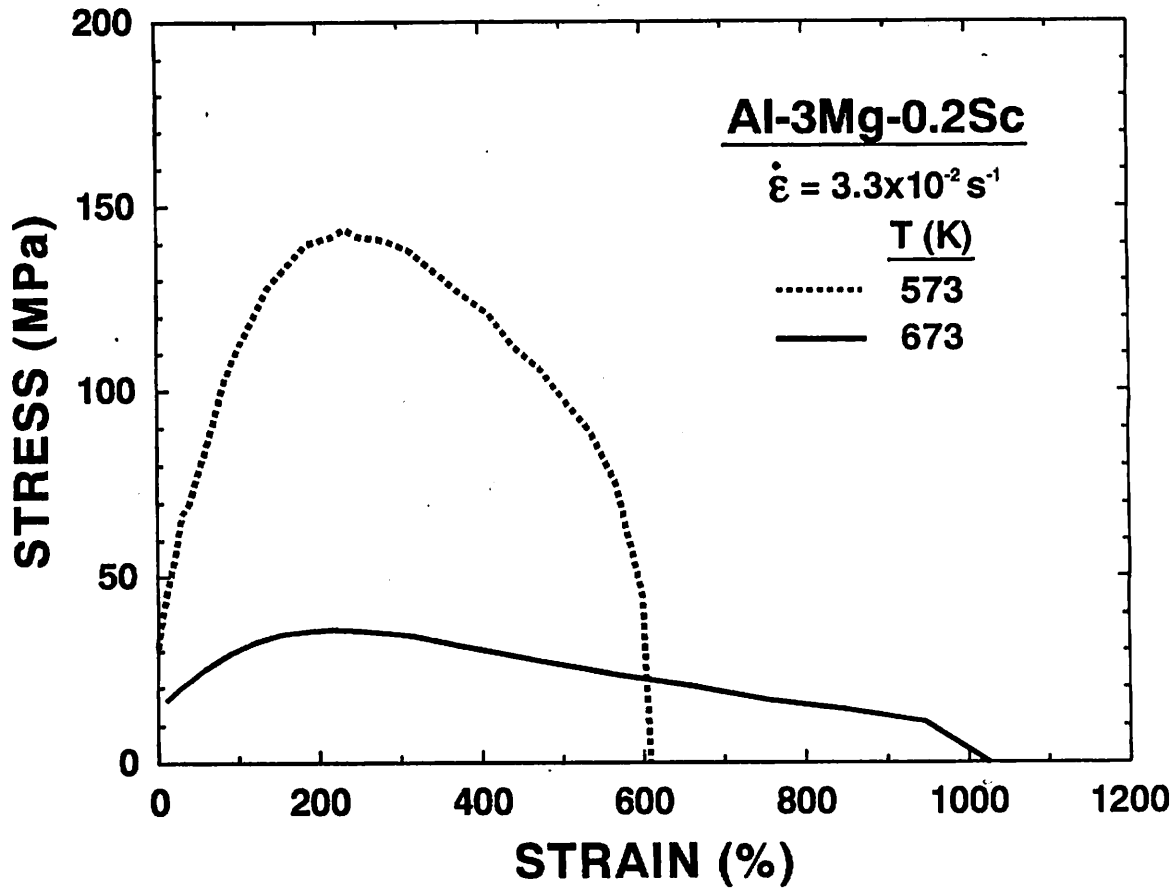

Figure 5 – True stress versus strain for Al–3% Mg–0.2% Sc specimens tested with an initial strain rate of 3.3 x 10^{-2} s^{-1}.

Elongation as a function of strain rate

To examine the ductility in more detail, and to provide a direct comparison with earlier work, Fig. 6 shows a plot of the elongation to failure versus strain rate for the Al–3% Mg–0.2% Sc alloy used in the present investigation and for an Al–4% Mg–0.5% Sc alloy tested earlier by Sawtell and Jensen [11]: the vertical arrows in Fig. 6 denote tests which were discontinued without failure at elongations of 1020%.

Inspection of Fig. 6 shows that the ductilities achieved in the present experiments, when compared at similar strain rates and testing temperatures, tend to be slightly higher than those reported in the earlier investigation by Sawtell and Jensen [11]. However, both investigations demonstrate high tensile ductility at strain rates of 10^{-2} s^{-1}.

For comparison purposes, additional tests were conducted using specimens of the Al–3% Mg–0.2% Sc alloy subjected to annealing for 1 hour at 853 K but without any ECA pressing. These unpressed samples were tested at an initial strain rate of 3.3 x 10^{-2} s^{-1} at the two temperatures of 573 and 673 K and they gave elongations to failure of only 97% and 150%, respectively. These results therefore serve to demonstrate the importance of ECA pressing in introducing an ultrafine grain size in order to achieve high strain rate superplasticity.

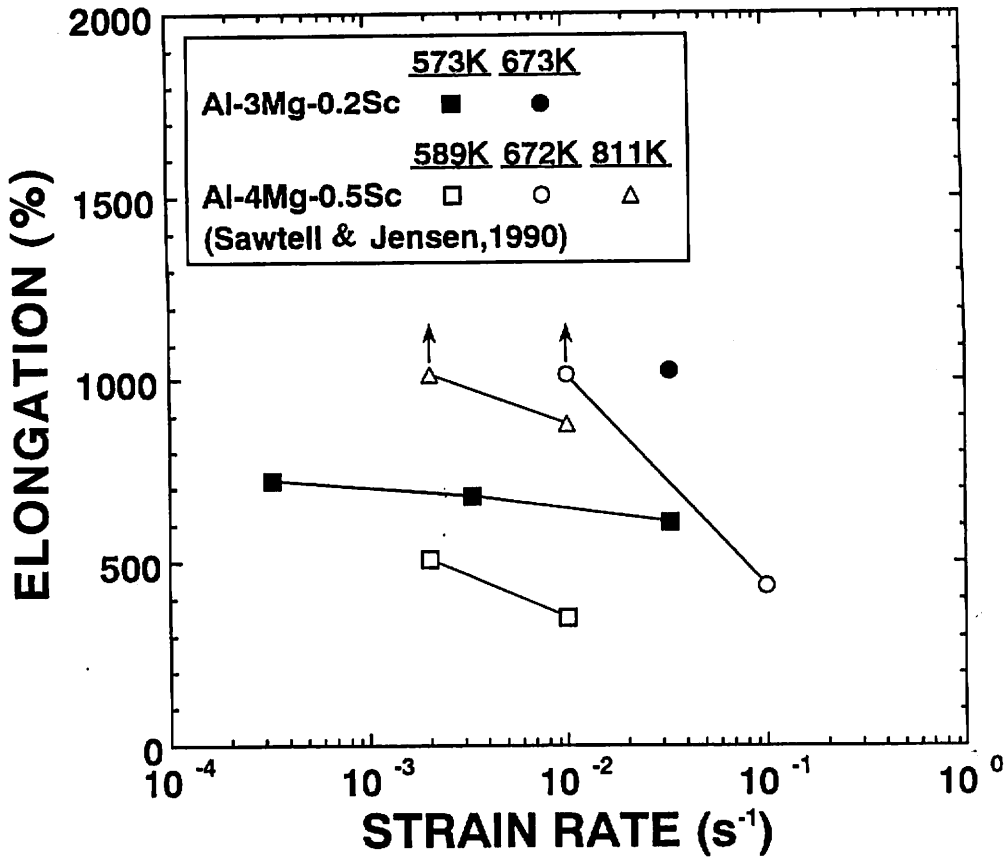

Figure 6 – Elongation to failure versus strain rate for Al–3% Mg–0.2% Sc specimens and for Al–4% Mg–0.5% Sc [11].

Microstructure of the Al–Mg–Sc alloy after tensile testing

Figure 7 shows two representative microstructures taken from the specimen pulled to failure at 673 K with an initial strain rate of 3.3×10^{-2} s^{-1}: these photomicrographs were taken (a) within the grip section of the sample in an area located behind the pinning point and (b) within the gauge length in an area very near to the point of failure, respectively. As indicated in Fig. 7(b), the tensile axis is horizontal for the photomicrograph taken within the gauge length.

Inspection of Fig. 7 shows that some grain growth occurs after testing at a temperature of 673 K. In the grip section, the average grain size was measured as ~1 μm which is consistent, at this temperature, with the grain growth data shown earlier in Fig. 4. Within the gauge length, however, the grain growth was more extensive and the average grain size was measured as ~4 μm. The grains were essentially equiaxed in the grips and also within the gauge length, thereby showing an absence of any obvious elongation of the grains along the tensile axis. There was evidence for the formation of some cavitation within the gauge length under these testing conditions and several very small cavities are visible at the triple junctions near the upper edge of Fig. 7(b). Inspection of a large area of this sample showed evidence for the growth of some cavities to form cracks along the grain boundaries.

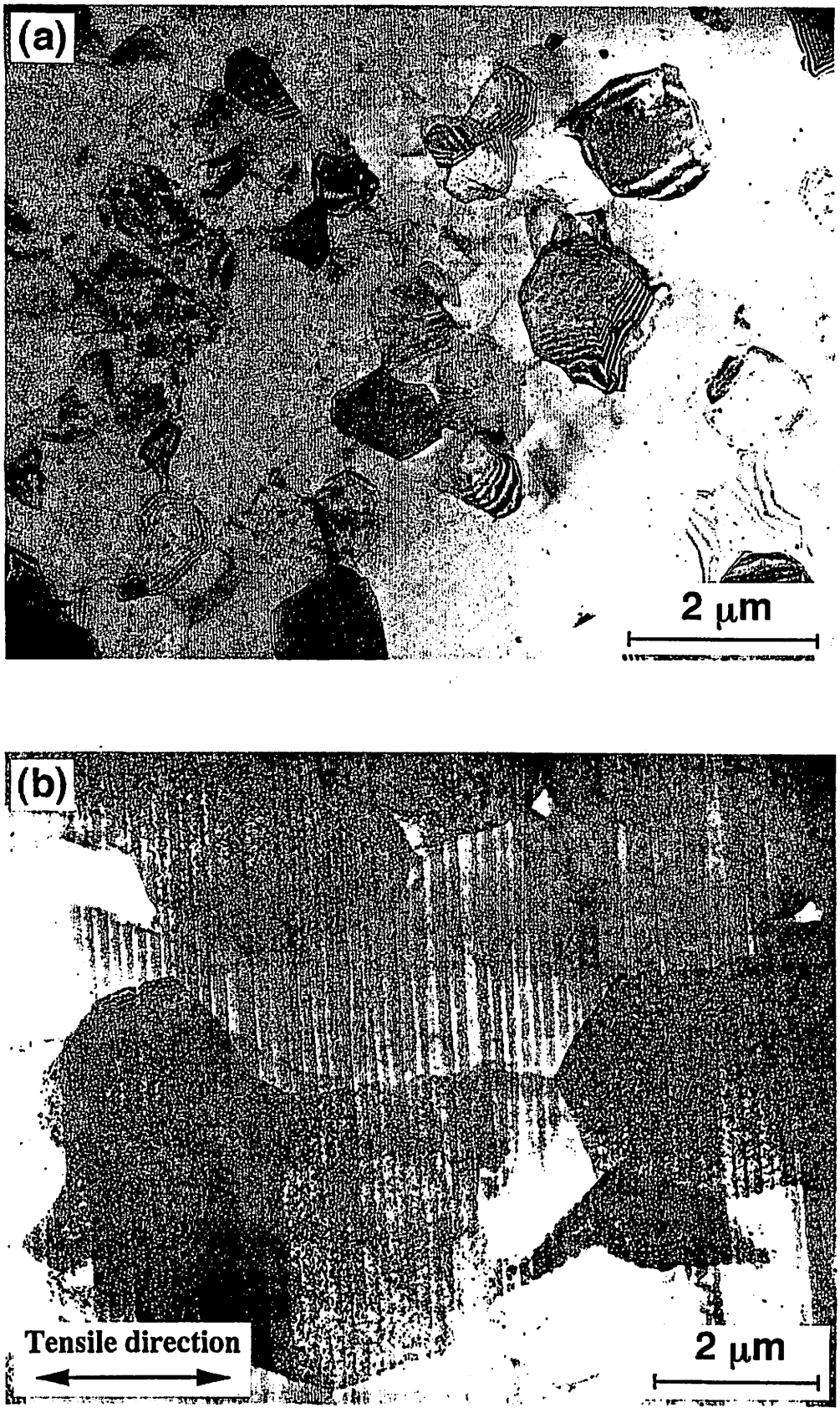

Figure 7 – Microstructures after tensile testing with an initial strain rate of 3.3 x 10^{-2} s^{-1} at 673 K: (a) within grips, (b) within gauge length.

Summary and conclusions

1. The presence of 0.2% Sc in an Al–3% Mg alloy is very beneficial for retaining an ultrafine grain size after ECA pressing. In these experiments, the measured average grain size after ECA pressing was ~0.2 μm.

2. High strain rate superplasticity was achieved in the Al–3% Mg–0.2% Sc alloy with a tensile elongation of >1000% when testing at a temperature of 673 K with an initial strain rate of 3.3×10^{-2} s^{-1}.

Acknowledgements

This work was supported in part by the Light Metals Educational Foundation of Japan, in part by a Grant-in-Aid for Scientific Research from the Ministry of Education, Science, Sports and Culture of Japan, in part by the Japan Society for the Promotion of Science and in part by the National Science Foundation of the United States under Grants No. DMR-9625969 and INT-9602919.

References

1. A.H. Chokshi, A.K. Mukherjee and T.G. Langdon, "Superplasticity in Advanced Materials," Mater. Sci. Eng., R10 (1993) 237–274.
2. T.G. Langdon, "The Mechanical Properties of Superplastic Materials," Metall. Trans., 13A (1982) 689–701.
3. T.G. Langdon, "An Evaluation of the Strain Contributed by Grain Boundary Sliding in Superplasticity," Mater. Sci. Eng., A174 (1994) 225–230.
4. F.A. Mohamed, M.M.I. Ahmed and T.G. Langdon, "Factors Influencing Ductility in the Superplastic Zn–22 Pct Al Eutectoid," Metall. Trans., 8A (1977) 933–938.
5. V.M. Segal, V.I. Reznikov, A.E. Drobyshevskiy and V.I. Kopylov, "Plastic Working of Metals by Simple Shear," Russian Metallurgy (Metally) 1 (1981) 99–105.
6. R.Z. Valiev and N.K. Tsenev, "Structure and Superplasticity of Al-based Submicron Grained Alloys," in Hot Deformation of Aluminum Alloys, ed. T.G. Langdon, H.D. Merchant, J.G. Morris and M.A. Zaidi (Warrendale, PA: The Minerals, Metals and Materials Society, 1991), 319–329.
7. R.Z. Valiev, N.A. Krasilnikov and N.K. Tsenev, "Plastic Deformation of Alloys with Submicron-grained Structure," Mater. Sci. Eng., A137 (1991) 35–40.
8. R.Z. Valiev, D.A. Salimonenko, N.K. Tsenev, P.B. Berbon and T.G. Langdon, "Observations of High Strain Rate Superplasticity in Commercial Aluminum Alloys with Ultrafine Grain Sizes," Scripta Mater., 37 (1997) 1945–1950.
9. L.S. Kramer, W.T. Tack and M.T. Fernandes, "Scandium in Aluminum Alloys," Adv. Mater. Proc., 152 (10) (1997) 23–24.
10. T.G. Nieh, R. Kaibyshev, L.M. Hsiung, N. Nguyen and J. Wadsworth, "Subgrain Formation and Evolution During Deformation of an Al–Mg–Sc Alloy at Elevated Temperatures," Scripta Mater., 38 (1997) 1011–1016.
11. R.R. Sawtell and C.L. Jensen, "Mechanical Properties and Microstructures of Al–Mg–Sc Alloys," Metall. Trans., 21A (1990) 421–430.
12. Y. Iwahashi, Z. Horita, M. Nemoto and T.G. Langdon, "The Process of Grain Refinement in Equal-Channel Angular Pressing," Acta Mater., in press.
13. M. Furukawa, Y. Iwahashi, Z. Horita, M. Nemoto and T.G. Langdon, "The Shearing Characteristics Associated with Equal-Channel Angular Pressing," Mater. Sci. Eng., submitted for publication.

14. Y. Iwahashi, J. Wang, Z. Horita, M. Nemoto and T.G. Langdon, "Principle of Equal-Channel Angular Pressing for the Processing of Ultra-fine Grained Materials," Scripta Mater., 35 (1996) 143-146,
15. Y. Wu and I. Baker, "An Experimental Study of Equal Channel Angular Extrusion," Scripta Mater., 37 (1997) 437-441.
16. J. Wang, Z. Horita, M. Furukawa, M. Nemoto, N.K. Tsenev, R.Z. Valiev, Y. Ma and T.G. Langdon, "An Investigation of Ductility and Microstructural Evolution in an Al-3% Mg Alloy with Submicron Grain Size," J. Mater. Res., 8 (1993) 2810-2818.
17. J. Wang, Y. Iwahashi, Z. Horita, M. Furukawa, M. Nemoto, R.Z. Valiev and T.G. Langdon, "An Investigation of Microstructural Stability in an Al-Mg Alloy with Submicrometer Grain Size," Acta Mater., 44 (1996) 2973-2982.
18. M. Furukawa, Z. Horita, M. Nemoto and T.G. Langdon, "Microhardness Measurements and the Hall-Petch Relationship in an Al-Mg Alloy with Submicrometer Grain Size," Acta Mater., 44 (1996) 4619-4629.
19. M. Furukawa, Y. Iwahashi, Z. Horita, M. Nemoto, N.K. Tsenev, R.Z. Valiev and T.G. Langdon, "Structural Evolution and the Hall-Petch Relationship in an Al-Mg-Li-Zr Alloy with Ultra-fine Grain Size," Acta Mater., 45 (1997) 4751-4757.
20. Y. Iwahashi, Z. Horita, M. Nemoto and T.G. Langdon, "Factors Influencing the Equilibrium Grain Size in Equal-Channel Angular Pressing: Role of Mg Additions to Aluminum," Metall. Mater. Trans., submitted for publication.
21. Y. Iwahashi, Z. Horita, M. Nemoto and T.G. Langdon, "An Investigation of Microstructural Evolution During Equal-Channel Angular Pressing," Acta Mater., 45 (1997) 4733-4741.
22. R.Z. Valiev, R.Sh. Musalimov and N.K. Tsenev, "The Non-Equilibrium State of Grain Boundaries and the Grain Boundary Precipitations in Aluminium Alloys," Phys. Stat. Sol. (a), 115 (1989) 451-457.
23. A.A. Nazarov, A.E. Romanov and R.Z. Valiev, "On the Strcture, Stress Fields and Energy of Nonequilibrium Grain Boundaries," Acta Metall. Mater., 41 (1993) 1033-1040.
24. R.Z. Valiev, F. Chmelik, F. Bordeaux, G. Kapelski and B. Baudelet, "The Hall-Petch Relationship in Submicro-Grained Al-1.5% Mg Alloy," Scripta Metall. Mater., 27 (1992) 855-860.
25. R.Z. Valiev, A.V. Korznikov and R.R. Mulyukov, "Structure and Properties of Ultrafine-Grained Materials Produced by Severe Plastic Deformation," Mater. Sci. Eng., A168 (1993) 141-148.
26. Z. Horita, D.J. Smith, M. Furukawa, M. Nemoto, R.Z. Valiev and T.G. Langdon, "An Investigation of Grain Boundaries in Submicrometer-Grained Al-Mg Solid Solution Alloys Using High-Resolution Electron Microscopy," J. Mater. Res., 11 (1996) 1880-1890.
27. M.E. Drits, S.G. Pavlenko, L.S. Toropova, Yu.G. Bykov and L.B. Ber., "Mechanism of the Influence of Scandium in Increasing the Strength and Thermal Stability of Alloys of the Al-Mg System," Soviet Phys. Doklady, 26 (1981) 344-346.
28. N. Blake and M.A. Hopkins, "Constitution and Age Hardening of Al-Sc Alloys," J. Mater. Sci., 20 (1985) 2861-2867.
29. K. Higashi, M. Mabuchi and T.G. Langdon, "High-Strain-Rate Superplasticity in Metallic Materials and the Potential for Ceramic Materials," ISIJ Intl., 36 (1996) 1423-1438.